ERDC/CHL TR-03-5

Coastal and Hydraulics Laboratory

US Army Corps
of Engineers®
Engineer Research and
Development Center

Monitoring Completed Navigation Projects Program

Monitoring Dredged Material Disposal at Mouth of Columbia River, Washington/Oregon, USA

Joseph Z. Gailani, Jarrell W. Smith, Nicholas C. Kraus, David D. McGee, Edward B. Hands, Charles J. Mayers, Hans R. Moritz, Heidi P. Moritz, Mark D. Siipola, Daryl B. Slocum, Mark R. Byrnes, Feng Li, Terence L. Dibble, William H. Hollings, Christian R. Lund, Charles K. Sollitt, and David R. Standley

July 2003

Monitoring Completed Navigation Projects Program

ERDC/CHL TR-03-5
July 2003

Monitoring Dredged Material Disposal at Mouth of Columbia River, Washington/Oregon, USA

Joseph Z. Gailani, Jarrell W. Smith, Nicholas C. Kraus, David D. McGee, Edward B. Hands, and Charles J. Mayers

Coastal and Hydraulics Laboratory
U.S. Army Engineer Research and Development Center
3909 Halls Ferry Road
Vicksburg, MS 39180-6199

Hans R. Moritz, Heidi P. Moritz, and Mark D. Siipola

U.S. Army Engineer District, Portland
P. O. Box 2946
Portland, OR 97208-2946

Daryl B. Slocum

SonTek, Inc.
6937 Nancy Ridge Drive, No. A
San Diego, CA 92121

Mark R. Byrnes and Feng Li

Applied Coastal Research and Engineering, Inc.
766 Falmouth Road, Suite A-1
Mashpee, MA 02649

Terence L. Dibble, William H. Hollings, Christian R. Lund, Charles K. Sollitt, and David R. Standley

O. H. Hinsdale Wave Research Laboratory
Oregon State University
Corvallis, OR 97330

Final report

Prepared for U.S. Army Corps of Engineers
Washington, DC 20314-1000

Under MCNP Work Unit 11M12

ABSTRACT: The entrance channel at the Mouth of the Columbia River requires annual dredging of 3 to 5 million cu m (3.9 to 6.5 million cu yd) of fine-to-medium sand to maintain the navigation channel at the authorized depth. The sandy dredged material is placed in EPA-approved Ocean Dredged Material Disposal Sites (ODMDS). Exceedance of ODMDS capacity at the Mouth of the Columbia River creates two operational problems for the Portland District: (a) The overall footprint of disposed dredged material extends beyond the existing ODMDS formally permitted boundaries by as much as 915 m (3,000 ft) in some cases, and (b) dredged material within the ODMDS has accumulated to such an aerial and vertical extent that adverse sea conditions are created. In some cases, mounds rise 18.3 to 21.4 m (60 to 70 ft) above surrounding bathymetry. Mariners report that the ODMDS mounds cause waves to steepen and/or break in the vicinity of the sites, and that these wave conditions are hazardous to navigation.

The objectives of the MCNP monitoring at the Mouth of the Columbia River were to: (a) Analyze existing data to document historic bathymetric response at the Mouth of the Columbia River entrance and the ODMDS due to anthropogenic and environmental conditions at the Mouth of the Columbia River; (b) monitor selected Mouth of the Columbia River ODMDS locations to observe bathymetric response with respect to dredging disposal operations and the forcing environment; (c) explain qualitatively and quantitatively the rates of sediment dispersion at the Mouth of the Columbia River ODMDS, and relate observed sediment dispersion of ODMDS citing and management practice; (d) assess the suitability of new USACE Dredging Research Program sediment fate models (STFATE, LTFATE, and MDFATE) and RCPWAVE, and synthetically-generated input data from HPDPRE, HPDSIM, and ADCIRC for predicting sediment dispersion in the environment off the Mouth of the Columbia River; and (e) develop a standardized method for data collection and management that can be used by other Corps District offices using as ODMDS.

The FATE models had previously suffered from a lack of quality field data for their calibration and verification. As the new MCNP data were being acquired and processed, enhancements to the FATE models were incorporated to ensure these models would accurately predict the ultimate disposition of future dredged material disposal at such exceedingly energic locations. Finally, predictive techniques for determining sediment transport processes under both waves and currents were developed to assess the movement of disposed material at the Mouth of the Columbia River for assessing capacity and to determine the useful life of the ODMDS.

The MCNP Mouth of the Columbia River study approach consisted of the execution of four fundamental tasks: (a) a regional coastal processes analysis, (b) oceanographic field data collection and analysis, (c) state-of-the-art numerical modeling, and (d) a comprehensive analysis of sediment transport processes.

Contents

List of Figures

List of Tables

Conversion Factors, Non-SI to SI Units of Measurement

Non-SI units of measurement used in this report can be converted to SI units as follows:

Multiply	By	To Obtain
acres	4,046.873	square meters
cubic feet	0.02831685	cubic meters
cubic yards	0.7645549	cubic meters
feet	0.3048	meters
inches	0.0254	meters
inches	25.4	millimeters
miles (US statute)	1.609347	kilometers
ounces	0.02834952	kilograms
pounds (mass)	0.4535924	kilograms
pounds (force) per foot	14.5939	newtons per meter
pounds (force) per square inch	0.006894757	megapascals
pounds (force) per square foot	47.88026	pascals
square miles	2.589998	square kilometers
tons (2,000 pounds, mass)	907.1847	kilograms
yards	0.9144	meters

Preface

The studies reported herein were conducted as part of the Monitoring Completed Navigation Projects (MCNP) Program (formerly Monitoring Completed Coastal Projects (MCCP) Program. Work was conducted under MCNP Work Unit No. 11M12, "Mouth of the Columbia River (MCR)," during the time period October 1994 – September 1999. Overall program management of the MCNP is provided by Headquarters, U.S. Army Corps of Engineers (HQUSACE). The Coastal and Hydraulics Laboratory (CHL), U.S. Army Engineer Research and Development Center (ERDC), Vicksburg, MS, is responsible for technical and data management, and support for HQUSACE review and technology transfer. Program Monitors for the MCNP Program are Messrs. Barry W. Holliday, Charles B. Chesnutt, and David B. Wingerd, HQUSACE. MCNP Program Managers during the conduct of this MCNP MCR study were Ms. Carolyn M. Holmes and Messrs. E. Clarke McNair and Robert R. Bottin.

The objectives of this MCNP monitoring at the MCR are to supplement other studies by the U.S. Army Engineer District, Portland, by (a) analyzing existing data to document historic bathymetric response at the MCR entrance and the ocean dredge material disposal sites (ODMDS) due to anthropogenic and environmental conditions at the MCR, (b) monitoring selected MCR ODMDS locations to observe bathymetric response with respect to dredging disposal operations and the forcing environment, (c) explaining qualitatively and quantitatively the rates of sediment dispersion at the MCR ODMDS, and relate observed sediment dispersion to ODMDS siting and management practice, (d) assessing the suitability of new USACE Dredging Research Program sediment fate models (Short-Term Fate (STFATE), Long-Term Fate (LTFATE), and Multiple Dump Fate (FATE)), Regional Coastal Processes Wave (RCPWAVE) model, and synthetically-generated input data from Height Period Direction Preliminary (HPDPRE) wave model, Height Period Direction Simulation (HPDSIM) wave model, and Advanced Circulation (ADCIRC) hydrodynamic circulation model for predicting sediment dispersion in the environment off the MCR, and (e) developing a standardized method for data collection and management that can be used by other Corps District offices using an ODMDS.

The studies reported herein that were funded by the MCNP were conducted by Drs. Joseph Z. Gailani and Nicholas C. Kraus, and Messrs. Edward B. Hands, Charles J. Mayers, David D. McGehee, and Jarrell W. Smith, CHL; Ms. Heidi P. Moritz, and Messrs. Hans R. Moritz and Mark D. Siipola, Portland District;

Dr. Daryl B. Slocum, SonTek, Inc., San Diego, CA; Drs. Mark R. Byrnes and Feng Li, Applied Coastal Research and Engineering, Inc., Mashpee, MA; and Drs. Terence L. Dibble, William H. Hollings, Christian R. Lund, Charles K. Sollitt, and David R. Standley, O. H. Hinsdale Wave Research Laboratory, Oregon State University, Corvallis, OR. Other supplemental studies that contributed significantly to this investigation were conducted by the Portland District, and by the U.S. Environmental Protection Agency, Region 10. This work was performed under the general supervision of Dr. James R. Houston, former Director, CHL; Mr. Thomas W. Richardson, Director, CHL; Mr. Bruce A. Ebersole, Chief, Coastal Processes Branch, CHL; and Mr. William L. Preslan, former Chief, Prototype Measurement and Analysis Branch, CHL. Drs. Michelle Thevenot (deceased) and Nichols C. Kraus were the Principal Investigators for this MCNP work unit. The MCNP Team Member from the Portland District was Ms. Moritz. This report was compiled by Dr. Lyndell Z. Hales and Ms. Donna L. Richey, CHL.

COL John W. Morris III, EN, was Commander and Executive Director of ERDC. Dr. James R. Houston was Director.

1 Introduction

Monitoring Completed Navigation Projects (MCNP) Program

The goal of the Monitoring Completed Navigation Projects (MCNP) Program (formerly the Monitoring Completed Coastal Projects Program) is the advancement of coastal and hydraulic engineering technology. The program is designed to determine how well projects are accomplishing their purposes and how well they are resisting attacks by their physical environment. These determinations, combined with concepts and understanding already available, will lead to (a) the creation of more accurate and economical engineering solutions to coastal and hydraulic problems, (b) strengthening and improving design criteria and methodology, (c) improving construction practices and cost-effectiveness, and (d) improving operation and maintenance techniques. Additionally, the monitoring program will identify where current technology is inadequate or where additional research is required.

To develop direction for the program, the U.S. Army Corps of Engineers (USACE) established an ad hoc committee of engineers and scientists. The committee formulated the objectives of the program, developed its operation philosophy, recommended funding levels, and established criteria and procedures for project selection. A significant result of their efforts was a prioritized listing of problem areas to be addressed. This is essentially a listing of the areas of interest of the program.

Corps offices are invited to nominate projects for inclusion in the monitoring program as funds become available. The MCNP Program is governed by Engineer Regulation 1110-2-8151 (Headquarters, U.S. Army Corps of Engineers (HQUSACE) 1977). A selection committee reviews and prioritizes the nominated projects based on criteria established in the regulation. The prioritized list is reviewed by the Program Monitors at HQUSACE. Final selection is based on this prioritized list, national priorities, and the availability of funding.

The overall monitoring program is under the management of the Coastal and Hydraulics Laboratory (CHL), U.S. Army Engineer Research and Development Center (ERDC), with guidance from HQUSACE. An individual monitoring project is a cooperative effort between the submitting District and/or Division office and CHL. Development of monitoring plans, and conduct of data collection and analyses, are dependent upon the combined resources of CHL and the District and/or Division.

Mouth of Columbia River (MCR) Navigation Project [1]

The Columbia River is the largest river on the west coast of the United States, draining an area of about 670,000 km^2 (259,000 square miles)[2] and extending some 1,930 km (1,200 miles) from British Columbia before entering the Pacific Ocean as the boundary between the states of Washington and Oregon (Figure 1) (McManus 1972). Average annual discharge of the Columbia River is about 216 km^3 per year (52 $miles^3$ per year), more than twice the combined discharges of all other rivers in California, Oregon, and Washington (Barnes et al. 1972; Komar and Li 1991). Peak discharges of 21,000 m^3 per sec (742,000 ft^3 per sec) occur in May and June as the result of snowmelt, whereas minimum flows of 3,000 m^3 per sec (106,000 ft^3 per sec) occur in August and September (Neal 1972). It is the major source of sediment to the northwest continental shelf (Sternberg 1986). Suspended sediment discharge from the river is about 1 to 2 $\times$ 10^{13} g per year (1 to 2 $\times$ 10^7 tons per year), and bed-load discharge is estimated to be on the order of 10^{12} g per year (10^6 tons per year) (Karlin 1980). Gross and Nelson (1966) estimate that the Columbia River discharges 10^4 times more sediment to the northwest continental shelf than all other sources combined.

Rapid and continual adjustments in channel configuration and shoaling patterns at the Columbia River mouth have caused navigation problems since its discovery in 1792. It was decided that structural control was needed to maintain safe navigation through the entrance area, so in April 1885 construction on the south jetty started. Nearly 10 years later (October 1895), a 7.2-km- (4.5-mile-) long jetty was completed from Point Adams in a northwesterly direction (Lockett 1967). Although a general improvement in navigation was achieved, shoals began to form along both sides of the jetty, causing renewed shoaling problems at the entrance. When the 12.2-m- (40-ft-) deep mean low water (mlw) entrance project was adopted in 1905, it was recommended that the south jetty be extended 3.4 km (2.1 mile) in a westerly direction. The extension and rehabilitation of the south jetty were completed in 1913, giving the structure a total length of 10.6 km (6.6 miles) (Lockett 1967; Komar and Li 1991). Construction of the north jetty began in 1913 as a component of the 12.2-m- (40-ft-) deep mlw entrance project. When completed in 1917, the structure extended 3.9 km (6.6 miles) in a southwesterly direction from Cape Disappointment (Lockett 1967).

Since 1905, a program of regular dredging has been established to provide safe navigation in support of commerce. However, early dredging operations often were not able to achieve project dimensions (Lockett 1967). Starting in 1953, a concerted effort was made to attain project dimensions. Dredged material was initially disposed in about 18-m (60-ft) water depth south and west of the entrance, until it was suspected that much of the sediment disposed at this site was ending up back in the channel. Thence, an alternate dredge disposal site was used seaward of the ebb shoal in about 36-m (120-ft) water depth. Periodically the jetties have been improved and the authorized channel dimensions increased.

[1] This section is extracted essentially verbatim from Byrnes and Li (2001).

[2] A table of factors for converting non-SI units of measurement to SI units is presented on page xiii.

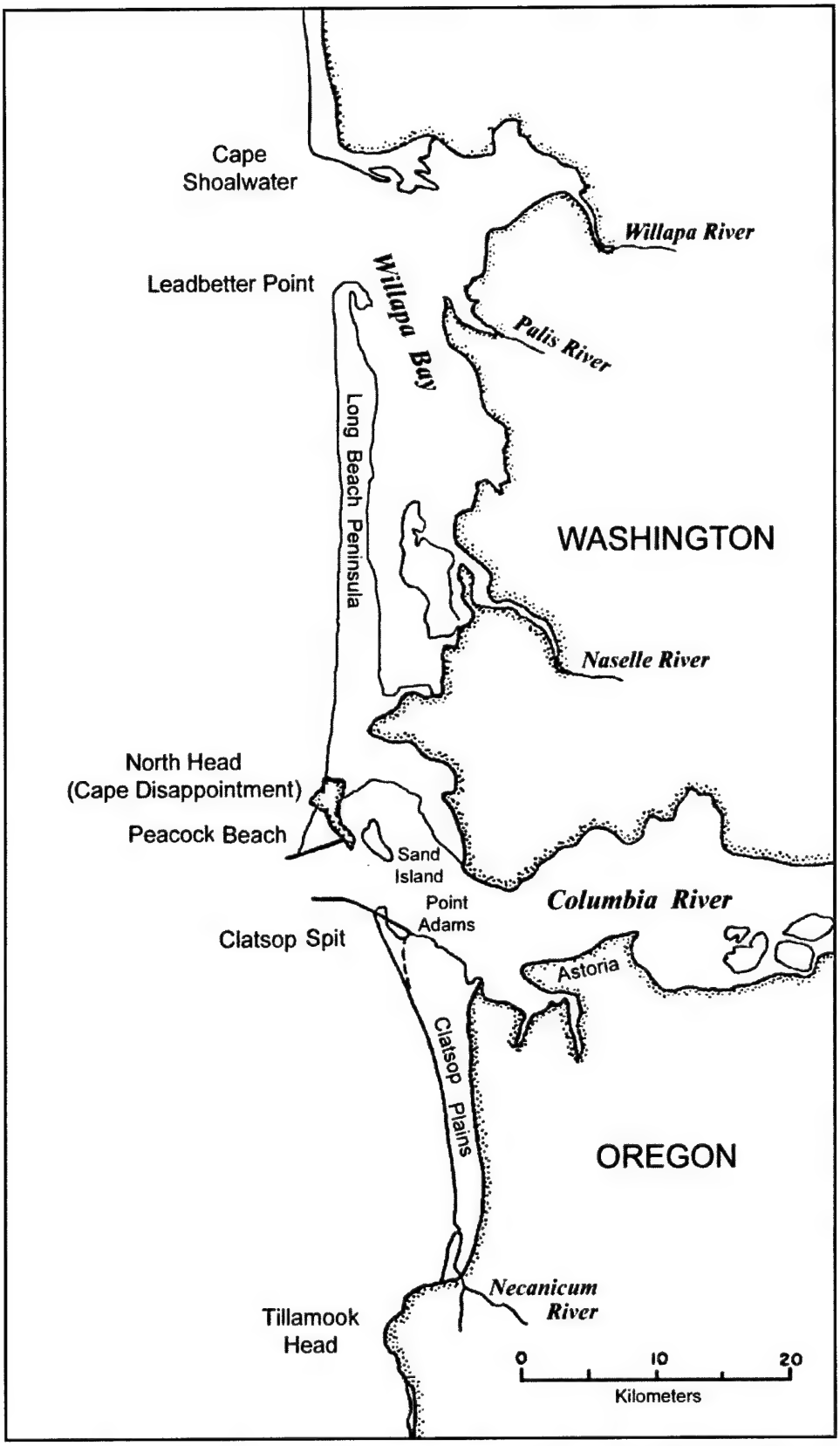

Figure 1. Washington and Oregon coasts north and south of MCR (after Byrnes and Li 2001)

The Mouth of the Columbia River (MCR) entrance channel was deepened to 14.6 m (48 ft) mlw in 1956. The channel was further deepened to its present authorized depth of 16.8 m (55 ft) mlw in 1984. The authorized deep-draft navigation project (Rivers and Harbor Act of 1984, 1905, 1954; Public Law 98-63) provides for a 9.7-km- (6-mile-) long, 805-m (2,640-ft-) wide channel through the jettied entrance and across the Columbia River bar. The northerly inbound 610 m (2,000 ft) of the channel was deepened to 16.8 m (55 ft) mlw (plus 1.5 m (5 ft) for overdredging), while the southerly outbound 195 m (640 ft) of the channel remains at 14.6 m (48 ft) mlw (plus 1.5 m (5 ft) for overdredging). Approximately 27 million cu m (million cu m) (35 million cu yd (million cu yd)) of material were placed in offshore disposal sites between 1988 and 1994, and maintenance dredging is not expected to decrease in the foreseeable future (USAED, Portland, 1995a).

Problem Statement[1]

In its present configuration, the entrance channel at the MCR requires annual dredging of 3 to 5 million cu m (3.9 to 6.5 million cu yd) of fine-to-medium sand to maintain the navigation channel at the authorized depth. The sandy dredged material is placed in Environmental Protection Agency (EPA) approved ocean dredged material disposal sites (ODMDS) (Figure 2). Dredging at the MCR is performed by hopper dredge. The use of open water sites for disposal of material dredged from the MCR became regular after 1945 and continues to the present time.

Prior to 1977, all ocean disposal sites were described only by approximate locations. Before EPA designation, the location of the disposal sites was not precisely specified, and the placement of dredged material within the disposal sites was not strictly controlled. In January 1977, disposal sites A, B, E, and F received interim designations when EPA issued the final Ocean Dumping Regulations (40 CFR 228) (dashed lines in Figure 2). The interim designations were extended by the EPA several times since promulgation of the CFR. An environmental impact statement for final designation of the four sites was finalized in February 1983. Formal boundaries for the present ODMDS at the MCR were designated by EPA in 1986 (solid lines in Figure 2). The annual volume of dredged material placed at the MCR ODMDS between 1956 and 1997 is summarized in Table 1.

ODMDS A and B have been the primary locations where the MCR dredged material has been placed. These two ODMDS are located on the westward boundary of the ebb-tidal shoal, and are economical (in terms of haul distance) for disposal of sediments dredged from both the outer and inner bars at the MCR. Since 1992, ODMDS B has received most of the MCR dredged material as concerns arose that sediments deposited in ODMDS A were accumulating, creating an adverse wave climate, and might migrate northward back into the entrance channel.

[1] This section is extracted from U.S. Army Engineer District, Portland (1995a), and U.S. Army Engineer District, Portland/U.S. Environmental Protection Agency, Region 10 (1997) (USAED, Portland/USEPA 1997).

ODMDS E and F have been used as secondary disposal sites for sediments dredged from the entrance channel at the MCR. The use of ODMDS E is partially in response to a 1979 request from the Washington Department of Ecology to enhance sand by-passing and retard erosion of the coastal beaches north of the MCR. Beginning in 1988, the volume of dredged material placed in ODMDS E was restricted to 0.77 million cu m per year (1 million cu yd per year) to prevent dredged material accumulation (mounding) and limit transport of placed dredged material back into the MCR channel. ODMDS F has been used only recently, motivated by the need for disposal of sediments from locations other than the MCR, and additional site capacity requirements.

Since 1986, dredged material placed within the designated ODMDS boundaries has accumulated at a rate much faster than the U.S. Army Engineer District, Portland, had anticipated when the disposal sites were formally designated. ODMDS, which were intended to be moderately dispersive and have 20-year life cycles, reached capacity within 10 years of initial operation. ODMDS capacity can roughly be defined as that quantity of material that can be placed within the legally designated disposal site without extending beyond the site boundaries or interfering with navigation (Poindexter-Rollings 1990).

Exceedence of ODMDS capacity at the MCR creates two operational problems for the Portland District:

a. The overall footprint of disposed dredged material extends beyond the existing ODMDS formally permitted boundaries by as much 915 m (3,000 ft) in some cases.

b. Dredged material within the ODMDS has accumulated to such an areal and vertical extent that adverse sea conditions are created. In some cases, mounds rise 18.3-21.3 m (60-70 ft) above surrounding bathymetry. Mariners report that the ODMDS mounds cause waves to steepen and/or break in the vicinity of the sites, and that these wave conditions are hazardous to navigation.

The issue of accumulated dredged material extending outside of the formal ODMDS boundaries has been resolved by obtaining regulatory agency approval for temporary site expansion. This is only a short-term solution to the site capacity problem, and does not reliably address the issue of avoiding hazardous navigation conditions. The rate at which placed dredged material accumulates within or outside of an ODMDS, and the maximum mound height that can be attained before safe navigation is affected, must be ascertained. ODMDS expansions require extensive regulatory coordination, are very time consuming, and are exceedingly costly.

Obtaining regulatory approval for a new permanent ODMDS requires significant investment, up to a half-million dollars or more per disposal site. Section 103 of the Marine Protection, Research, and Sanctuaries Act of 1972 (Ocean Dumping Act) and subsequent amendments thereto, and Section 404 of the Clean Water Act of 1977 and subsequent amendments thereto, require that field-verified, state-of- the-art procedures be used for the assessment of possible physical impacts due to the operation of proposed ODMDS. Recent operational performance of the ODMDS at the MCR indicates that existing site selection

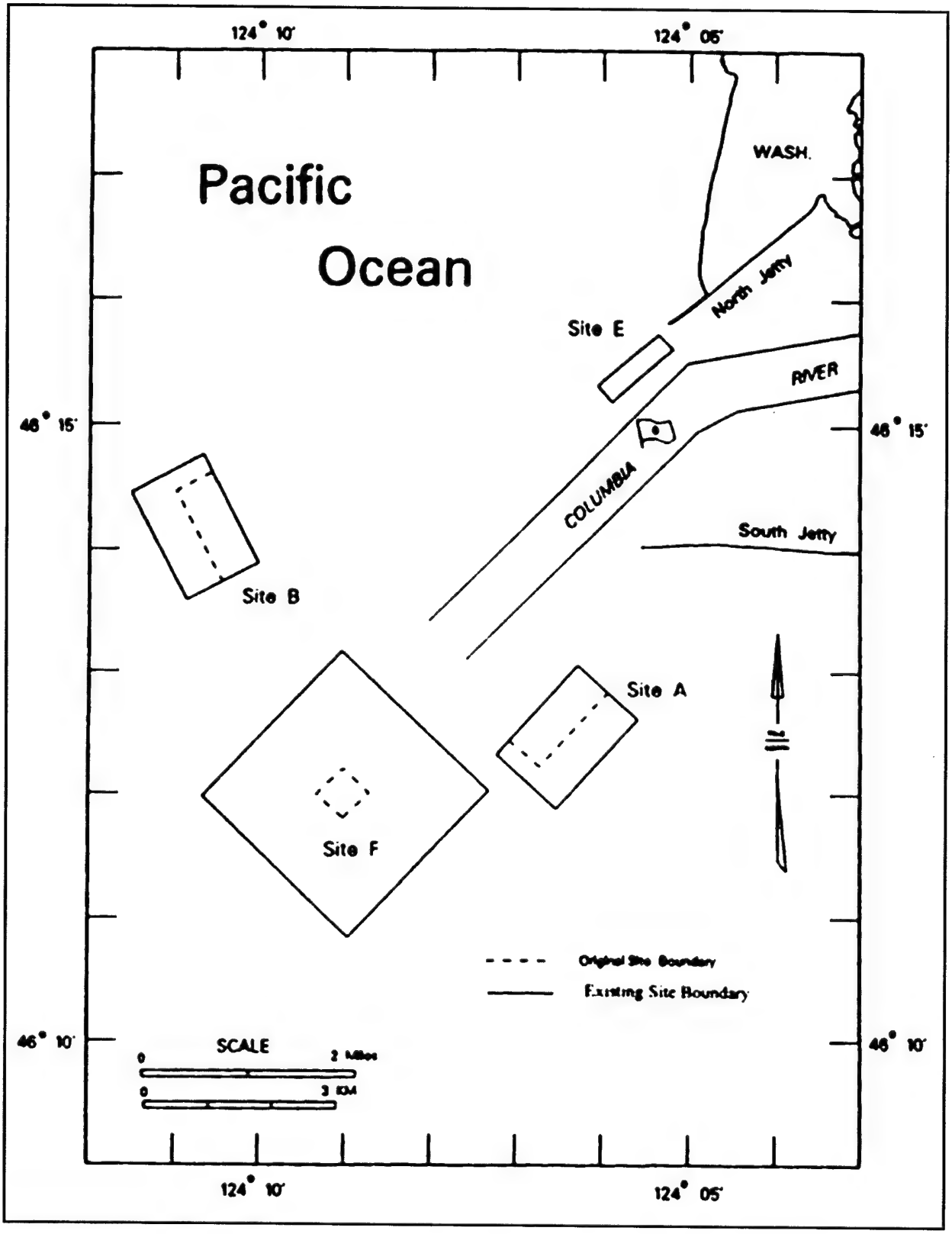

Figure 2. MCR ocean dredged material disposal sites (ODMDS) (Dashed lines = original site boundaries; solid lines = existing site boundaries) (after USAED, Portland, 1995a)

Table 1
Dredged Material Disposed at Mouth of Columbia River, 1956 - 1997
Source: U.S. Army Corps of Engineers, Portland District (1998)

Disposal Site	A	B	C*	D*	E	F	G	Total cubic yards
Fiscal Year	cy	cy	cy	cy	cy	cy	cy	cy
1956	12,096,000	1,296,000	504,000	504,000	0	0	0	14,400,000
1957	1,605,643	1,221,307	422,071	838,428	0	0	0	4,087,449
1958	6,135	2,274,704	0	326,753	0	0	0	2,607,592
1959	0	1,914,964	0	661,021	0	0	0	2,575,985
1960	0	1,927,206	0	612,636	0	0	0	2,539,844
1961	0	1,837,879	0	297,066	0	0	0	2,134,945
1962	0	2,322,256	2,838	632,618	0	0	0	2,957,712
1963	0	1,725,851	724,630	234,735	0	0	0	2,685,216
1964	0	514,900	1,459,186	683,151	0	0	0	2,657,237
1965	0	675,921	1,205,090	1,606,671	0	0	0	3,487,682
1966	0	2,010,673	29,891	2,437,451	0	215,002	0	4,693,017
1967	0	1,463,573	1,067	354,700	0	422,066	0	2,241,406
1968	0	1,919,199	0	109,592	0	0	0	2,028,791
1969	0	2,021,562	0	89,042	0	0	0	2,110,604
1970	0	1,489,795	0	3,060	0	0	0	1,492,855
1971	51,047	1,439,042	13,816	241,689	0	0	0	1,745,596
1972	12,995	2,579,688	0	287,646	0	1,886	0	2,882,215
1973	0	3,051,662	0	409,640	291,439	3,060	0	3,755,801
1974	0	994,059	0	506,711	2,168,543	29,123	0	3,698,436
1975	0	333,462	0	895,594	4,886,792	27,539	0	6,143,387
1976	2,574	1,017,100	0	758,743	4,257,150	53,250	602,895	6,691,712
1977	2,867,393	1,868,579	0	710,373	3,678,429	0	0	9,124,774
1978	3,060	187,704	0	312,635	3,925,986	0	0	4,429,385
1979	0	116,502	0	158,466	4,930,840	0	0	5,205,808
1980	11,142	118,686	0	0	2,675,722	0	0	2,805,550
1981	2,254,321	9,180	0	0	3,042,896	0	0	5,306,397
1982	971,209	12,240	0	0	3,086,514	0	0	4,069,963
1983	1,124,466	199,969	0	0	606,218	0	0	1,930,653
1984	4,080,853	3,864,247	0	0	969,600	0	0	8,914,700
1985	1,326,150	2,068,927	0	0	4,126,429	0	0	7,521,506
1986	2,037,455	3,387,376	0	0	2,926,412	0	0	8,351,243
1987	1,593,550	1,209,358	0	0	1,183,050	0	0	3,985,958
1988	1,447,240	4,533,756	0	0	478,864	0	0	6,459,860
1989	647,458	3,456,285	0	0	568,522	2,030,954	0	6,703,219
1990	2,729,358	1,119,663	0	0	507,201	0	0	4,356,222
1991	1,486,938	1,956,570	0	0	380,142	0	0	3,823,650
1992	874,700	2,888,028	0	0	796,198	0	0	4,558,926
1993	0	1,629,208	0	0	988,208	2,288,431	0	4,905,847
1994	406,924	1,002,668	0	0	397,621	1,500,407	0	3,309,620
1995	0	2,480,664	0	0	988,547	0	0	3,469,211
1996	0	1,693,145	0	0	726,336	2,205,113	0	4,624,594
1997	0	326,824	0	0	1,171,246	174,883	0	1,672,953
Totals	37,618,611	68,160,384	4,362,591	13,672,421	49,778,905	8,776,831	602,895	183,147,521
Volume of sediment placed in Ocean Dredged Material Disposal Sites for 1956-1997 (cy)								*169,475,100*

Annual Avg	ODMDS A	ODMDS B	ODMDS E	ODMDS F
1990-1997	687,490	1,637,096	744,437	771,104

Annual avg for	
1990-1997	3,840,128
1985-1989	6,375,070
1977-1985	5,478,748
1956-1976	3,696,071

Note 1: ODMDSs receive *interim* designation in 1977.
Note 2: Final designation of ODMDSs in 1986.
Note 3: * Estuarine disposal site

methods are unreliable in terms of providing candidate sites with sufficient long-term capacity. If existing ODMDS selection methods are unreliable, any expensive redesignation process could still result in unacceptable future conditions.

The key to successful ODMDS designation is knowing a priori (or reliably predicting) the ultimate fate of dredged material placed at the disposal site. Until recently, estimating the fate of dredged material (sediments) placed on ambient bathymetry was determined by one of three procedures:

a. Indirect observation by comparison of consecutive hydrographic surveys (hindcast).

b. Direct point measurement of sediment transport potential through field monitoring (nowcast).

c. Estimated point prediction of sediment transport potential by empirical methods (forecast).

All of these sediment fate prediction methods possess a high degree of uncertainty when applied to complex large-scale conditions, and do not provide the flexibility of addressing rapidly changing scenarios. These methods also do not address the need for reliable life-cycle ODMDS management. This is especially true with point estimate methods that assume equal transport potential for all sediment within a given area, despite the ambient bathymetry and accumulation pattern of placed dredged material. The sediment fate estimates have been used at the MCR in various studies to obtain formal ODMDS designation (Sternberg et al. 1977; Roy et al.1979, 1982; Sherwood 1989). The lack of operational efficiency of the MCR ODMDS due to rapid sediment mounding requires that improved sediment fate numerical simulation technology be used in future disposal site designation processes.

Objectives of MCNP Monitoring at MCR

The objectives of the MCNP monitoring at the MCR are to:

a. Analyze existing data to document historic bathymetric response at the MCR entrance and the ODMDS due to anthropogenic and environmental conditions at the MCR.

b. Monitor selected MCR ODMDS locations to observe bathymetric response with respect to dredging disposal operations and the forcing environment.

c. Explain qualitatively and quantitatively the rates of sediment dispersion at the MCR ODMDS, and relate observed sediment dispersion to ODMDS siting and management practice.

d. Assess the suitability of new USACE Dredging Research Program sediment fate models including Short-Term FATE (STFATE), Long-Term FATE (LTFATE), and Multiple-Dump FATE (MDFATE), Regional Coastal Processes WAVE (RCPWAVE) model, and synthetically-generated input data from Height Period Direction PREliminary (HPDPRE) wave model, Height Period Direction SIMulation (HPDSIM)

wave model, and Advanced CIRCulation (ADCIRC) hydrodynamic circulation model for predicting sediment dispersion in the environment off the MCR.

e. Develop a standardized method for data collection and management that can be used by other Corps District offices using an ODMDS.

Study Approach

The inherent nature of an MCNP monitoring program implies that an extensive observational and data acquisition effort will be sustained for a significant period of time (3 to 5 years) to acquire new knowledge pertaining to the phenomena of interest. New field data were obtained by developing and placing four instrumentation tripods at pertinent locations on the ODMDS for three different critical deployment periods. While these new oceanographic forcing data and new hydrographic surveys were being obtained at the MCR, existing data sets and bathymetric surveys were studied and analyzed to formulate an understanding of the processes that have resulted in the existing condition at the ODMDS. These existing data and surveys provided guidance regarding regional sediment transport dynamics associated with natural processes. They also were used as input to wave and sediment fate numerical simulation models for estimating amplification of wave climate resulting from existing disposal mound geometry, and for deducing the ultimate disposition of material previously placed at the ODMDS.

The FATE models had previously suffered from a lack of quality field data for their calibration and verification. As the new MCNP data were being acquired and processed, enhancements to the FATE models were incorporated to ensure these models would accurately predict the ultimate disposition of future dredged material disposal at such exceedingly energetic locations. Finally, predictive techniques for determining sediment transport process under both waves and currents were developed to assess the movement of disposed material at the MCR for assessing capacity and to determine the useful life of the ODMDS. These techniques will assist in crucial decision-making for the management of dredged materials at navigation channels and harbors, including mound dispersal, channel infilling, and protective cap erosion.

The MCNP MCR study approach consisted of the execution of four fundamental tasks: (a) a regional coastal processes analysis, (b) oceanographic field data collection and analysis, (c) state-of-the-art numerical modeling, and (d) a comprehensive analysis of sediment transport processes.

Regional processes

There are data supporting net northward transport of sediment in the vicinity of the MCR. The erosion of beach and shoreface sand south of the south jetty may be related to blocking by the entrance jetties of southward-directed littoral material. However, this erosion could be related to a combination of factors, including reflection of waves arriving from southwest storms by the south jetty,

causing large oblique angles to enhance southward sand movement and produce erosion. Detailed shoreline and bathymetric change analyses for the MCR and adjacent shelf and shoreline environments were conducted. Primary interest was sediment transport associated with wind- and wave-induced currents. Historical data sets included shoreline position from U.S. Coast and Geodetic Survey (USC&GS) maps, and bathymetry data from the USACE and the USC&GS. The analysis time period was from 1868 to 1994. Bathymetric surface models were developed for four historical time periods to evaluate regional sediment transport dynamics. Patterns of deposition and erosion relative to engineering activities were quantified to establish a framework upon which management strategies could be developed for dredged material disposal practices.

Field data collection and analysis

The USACE relies on accurate data about the dynamic ocean to fulfill its mission of designing, building, and maintaining coastal projects. The traditional platform for this work is a research vessel or barge, an approach that is appropriate if sea conditions are relatively mild. However, there are times and places where conditions can render this form of deployment unsafe, logistically difficult, or economically unfeasible. For some locations such as the MCR, dangerously energetic surf is normal. Here, the USACE contracted with Oregon State University to design, construct, deploy, and retrieve four data collection open frame tripod platforms for the acquisition of necessary environmental data pertaining to conditions at the MCR ODMDS.

Each of the four tripod platforms was outfitted with Doppler wave and current sensors, temperature, pressure, and salinity sensors, and Optical Backscatter Sensors (OBS) that measure suspended sediment concentrations. The three deployment periods were (a) Deployment 1: 19 August – 09 October 1997, (b) Deployment 2: 15 April – 24 August 1998, and (c) Deployment 3: 27 November 1998 – 01 March 1999. The four tripod platforms were located at Sites B1, B2, E, and M (Figure 3). A profile across the MCR ebb-tidal shoal shows the elevation of each tripod platform (Figure 4).

USACE also developed techniques for using helicopters to accomplish the data collection mission. While not actually used for data acquisition at the MCR, this methodology will be exceedingly useful for future long-term management of ODMDS nationwide.

Numerical modeling

The USACE Dredging Research Program (DRP) developed several sediment fate numerical simulation models (STFATE, LTFATE, MDFATE, HPDPRE, HPDSIM, and ADCIRC) to enhance and improve the reliability of long-term site management of ODMDS. The numerical simulation modeling objectives of this MCNP monitoring at the MCR were all accomplished and included; (a) verifying the applicability of the DRP numerical models for the evaluation of ODMDS, (b) assessing the data collection needs for site evaluation by the DRP models, (c) identifying the capabilities and limitations of the DRP models, and

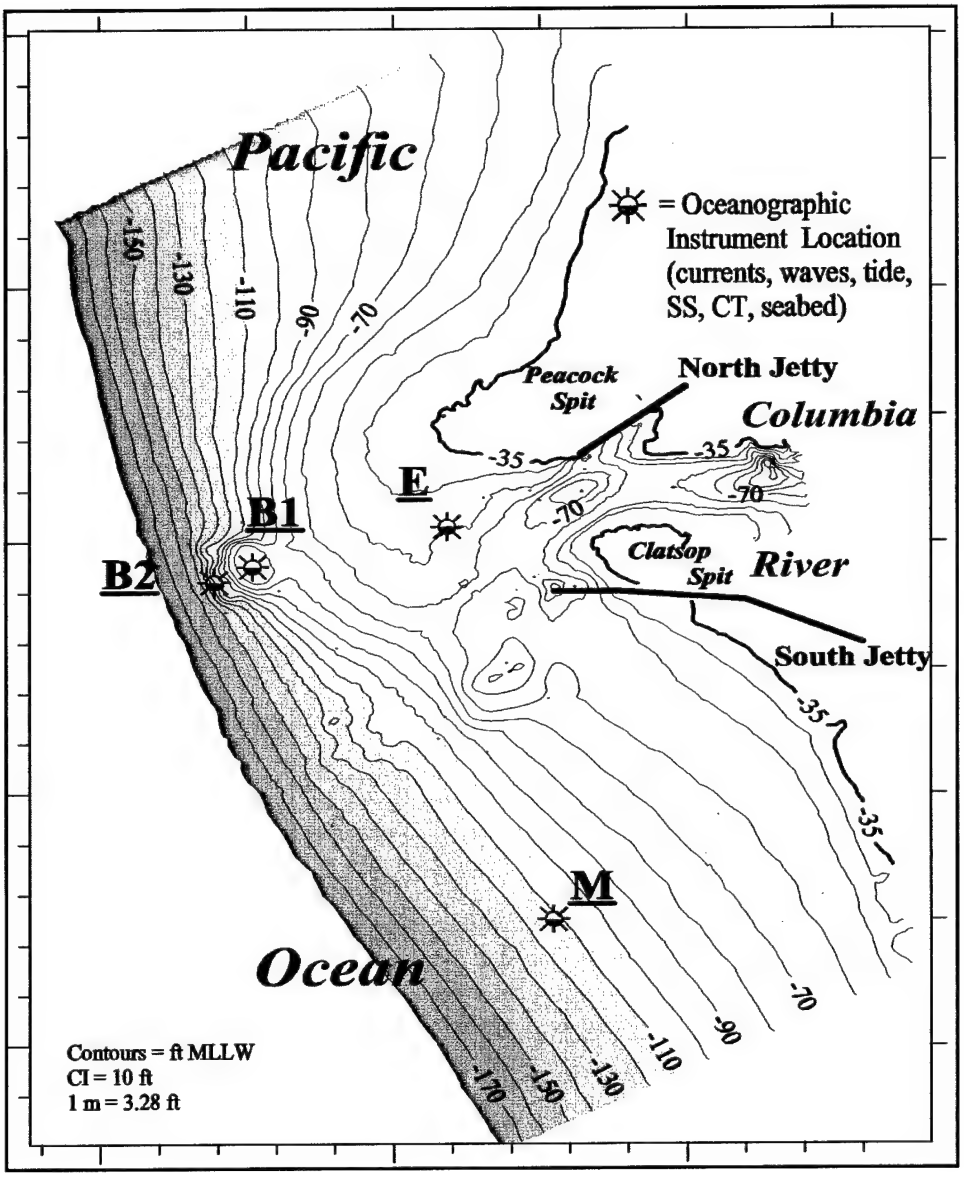

Figure 3. MCR and location of four tripod instrumentation platform sites (after Moritz et al. 2000)

(d) developing a systematic methodology for the application of the DRP models at other Corps districts. A wave transformation numerical simulation model (RCPWAVE) was also applied at the MCR to ascertain the extent of wave height amplification and resulting hazards to navigation by the MCR ODMDS. Attaining the numerical simulation modeling objectives of verification and accuracy determination of the DRP-developed fate models significantly contributed to attaining the MCNP study objectives of development of a standardized method for data collection and ODMDS management that can be used by other Corps District offices. The very high quality field data obtained during this MCNP monitoring provided the opportunity to better understand sediment suspension and seabed change under highly energetic oceanographic process of combined waves and currents. Studies are summarized in the following paragraphs.

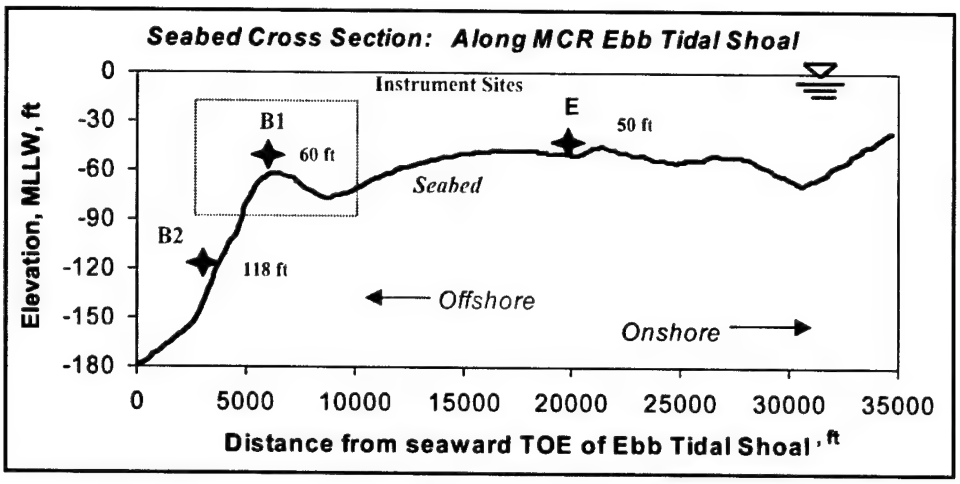

Figure 4. Location of instrumentation Sites E, B1, and B2 on a profile across MCR ebb-tidal shoal (after Moritz et al. 2000)

Sediment suspension at MCR. Seabed sediment suspension due to the presence of waves and currents at the MCR was investigated. Relevant data were measured at ODMDS B, instrumentation tripod platform Site B1 (Figure 3), 6 km (3.7 miles) offshore of the MCR in a water depth of 18.3 m (60 ft) with seabed sediment composed of fine to medium sand. The analyses addressed the effect on bottom sediment (sand) when waves and currents interact along the seabed of an ebb-tidal shoal. Special considerations included (a) assessing the modification of waves by current, (b) describing the spectral relationship between bottom current and peak sediment suspension, and (c) investigating wave group effects.

Oceanographic processes and seabed change at MCR. Oceanographic processes at the MCR were correlated with seabed changes that occurred at ODMDS Sites B1, B2, and E during Deployment 1 (19 August – 22 September 1997) by the Oregon State University data acquisition phase of the MCNP study. Based on the textural variation of bottom sediment at the MCR, both suspended and bed-load aspects of sediment transport were measured to fully describe sediment response vs. environmental forcing.

Effect of ODMDS A and B on wave climate (1994 bathymetry). The presence of large underwater mounds at the existing MCR ODMDS exacerbates wave amplification to the point of breaking, and adversely impacts marine safety with resulting hazards to navigation. The numerical simulation wave model RCPWAVE was used to predict behavior of waves as they are shoaled, refracted, and diffracted by the bathymetry that the waves pass over. RCPWAVE was used to compare the MCR wave climate due to the present (1994) ODMDS bathymetry with the wave climate due to past (1985) bathymetry before prominent mounds were formed at the ODMDS.

FATE model simulations at ODMDS B (1994 bathymetry). Early in 1995, the Portland District was considering limiting most of ocean dredged material disposal operations at the MCR to ODMDS B for the 1995 dredging season. To avoid placement of dredged material at ODMDS A and F, approximately 3.3 million cu m (4.3 million cu yd) of sandy dredged material were assumed to be placed at ODMDS B during 1995. STFATE was used to predict

the bathymetric distribution (footprint) of dredged material after it had passed through the water column, on an individual dump (disposal vessel load) basis. The model accounted for various disposal vessel, water column, and dredged material parameters. LTFATE and MDFATE were used to predict the bathymetry at the MCR ODMDS B resulting from a series of dumps and to simulate long-term change (sediment transport) of the resultant bathymetry. MDFATE can be used to simulate a disposal operation that could extend over a year and consist of hundreds of dumps. The model accounted for the overall disposal operation and environmental parameters such as waves, tides, and currents. Waves and currents were incorporated to account for the sediment transport processes affecting the short- and long-term fate of the dredged material placed in open water. The reason for using MDFATE was to provide realistic estimates of aggregate mound formation at ODMDS B. Two disposal scenarios were assessed using LTFATE and MDFATE.

FATE model and RCPWAVE model simulations at ODMDS F (1995 bathymetry). In 1996, the MCR ODMDS A, B, and E could accept only limited amounts of dredged material. Excluding ODMDS F, the total capacity of the MCR ODMDS could decrease to 0.77 million cu m per year (1 million cu yd per year) after 1997. The annual volume of sediment dredged from the MCR project and placed in ODMDS varied from 3.1-3.8 million cu m per year (4-5 million cu yd per year). Given the capacity limitations on the MCR ODMDS, ODMDS F would be expected to receive as much as 3.1 million cu m per year (4 million cu yd per year) after 1996. To confidently rely on ODMDS F to handle present and future MCR dredging disposal requirements, the capacity of ODMDS F (for 1996 and beyond) was assessed with respect to impacts on navigation. Two disposal scenarios were assessed. Predicted changes in wave height at ODMDS F in 1996 due to mound formation resulting from disposal Scenario 2 since the 1995 baseline condition were evaluated by RCPWAVE.

FATE model and RCPWAVE model simulations at expanded ODMDS B and E (1996 bathymetry). During site assessment studies in 1966, the only feasible option for providing an additional 2.3-3.1 million cu m per year (3-4 million cu yd per year) disposal capacity for the MCR navigation project was to temporarily expand existing ODMDS. The expanded ODMDS would be used for dredged material placement until which time new ODMDS were formally designated. As a conservative estimate, the expanded sites were expected to be utilized for 5 years, beginning in 1997. STFATE simulations were conducted for the disposal of dredged material from two types of hopper dredges; (a) a split-hull hopper dredge (*Newport*), and (b) a multiple bottom door hopper dredge (*Essayons*). The long-term fate of dredged material to be placed within the expanded ODMDS B and E was assessed using LTFATE and MDFATE. Transport of sediment off the dredged material mounds was simulated for a period of 1 year. Changes in wave height at the MCR due to bathymetric changes mounding) at the expanded ODMDS B and E were estimated using RCPWAVE. The mounded configuration accounted for 15.3 million cu m (20 million cu yd) of dredged material placed within the expanded ODMDS B and E. To permit disposal of this volume of material without negatively affecting the wave environment due to mounding, it was recommended that the site's boundaries be significantly expanded beyond the initially proposed configuration.

FATE model simulations at expanded ODMDS E (1998 bathymetry). FATE model simulations of dredged material deposited at ODMDS E located near the north jetty and adjacent to the navigation channel were conducted using 1998 bathymetry. Environmental data from Deployment 2 (15 April-24 August 1998) was utilized. Since one of the governing parameters in an efficient dredging disposal program is minimization of the haul distance for the dredge, disposal sites such as ODMDS E can be advantageous. In contrast to the more oceanward sites, ODMDS E is believed to be current- rather than wave-dominated and has been very dispersive in past disposal operations. The energetic dispersiveness of the site, however, also represented an extreme test of the robustness of the DRP FATE models. This study addressed a predictive 2-month application of the FATE models at ODMDS E using oceanographic data that were collected at the same time as the dredge disposal operation. The DRP FATE models (STFATE, LTFATE, and MDFATE) were all found to be applicable at a high-energy, current-dominated site. To correctly simulate the sediment deposition on the seabed, the current profile for both the STFATE and LTFATE model applications required modifications from the full depth-averaged current profile typically used.

Analysis of sediment transport processes, ODMDS B, E, and M

Predictive techniques for determining environmental conditions and sediment transport processes under both waves and currents were developed to assess the movement of disposed material at the MCR ODMDS B and E. These techniques assisted in determining crucial information for the management of dredged materials at navigation channels and harbors, with implications pertaining to mound dispersal, channel infilling, and protective cap erosion. The potential transport climate at proposed ODMDS M was also analyzed. Processes controlling the transport of sands at ODMDS are complex, and potentially include widely variable environmental conditions and both temporal and spatial variations in the characteristics of sediments. Three methods of estimating sediment transport by waves and currents (van Rijn; Wikramanayake and Madsen; Ackers and White) were applied at MCR ODMDS locations to evaluate the capabilities of available sediment modeling technologies. To estimate the long-term sediment transport climate, a 12-year synthetic database of wave and current conditions was developed from combined field measurements and numerical modeling. The sediment transport methods were then applied to the 12-year period of the developed database. The estimated sediment transport indicated significant variability in annual transport and a predominant transport direction to the north at ODMDS B and E. Conclusions from this work can be separated into three categories: (a) management of ODMDS, (b) observations from data collection, and (c) indications from sediment transport modeling. Methods verified with the MCR data can be applied with greater confidence to other ODMDS that have similar sediment characteristics and environmental conditions.

2 MCR Site Description

The Columbia River enters the Pacific Ocean as the boundary between the States of Washington and Oregon (Figure 1).

Bathymetry of Region

Since 1945, about 153 million cu m (200 million cu yd) of sandy material has been dredged at the MCR, and about 60 percent of this material has been placed in ODMDS where water depths are less than 18.3 m (60 ft). This has resulted in mounding and shoal regions off the river mouth, with underwater bathymetric contours being aligned nonparallel with the general coastline (Figure 5). Refraction and diffraction of waves around the ODMDS causes large steepening of the waves in the lee of the mounds. Since the Columbia River is the largest river on the Pacific coast of the United States, its riverine currents are very large. Thus, the MCR region also is characterized as an area with exceptionally strong surface gravity waves and riverine current interactions. This wave/current interaction causes large steepening of the waves. These two phenomena combine to create wave conditions that are exceedingly hazardous to navigation.

Currents at the MCR tend to be aligned with the seabed contours during normal climatic conditions. Since the direction of currents at the MCR is nominally controlled by the local geometry, the current direction at the northern perimeter of the MCR is different from that at the western and southern perimeter. Likewise, the magnitude of currents at the MCR is based on the relative location with respect to the river plume since the river's flow has a significantly pronounced effect on the orientation of the ebb-tidal (outer) shoal at the MCR.

Currents at the MCR tend to become less aligned with the ambient bathymetry during storm conditions, when wind-driven currents dominate and can produce flows perpendicular to the MCR bathymetry contours depending upon the wind direction with respect to the river plume. This flow perpendicular to the bathymetric contours probably produces the most pronounced transport of bottom sediments at the MCR (USAED, Portland, 1995b). The closer a current measurement is to the seabed, the more parallel the current is aligned with the bathymetric contours.

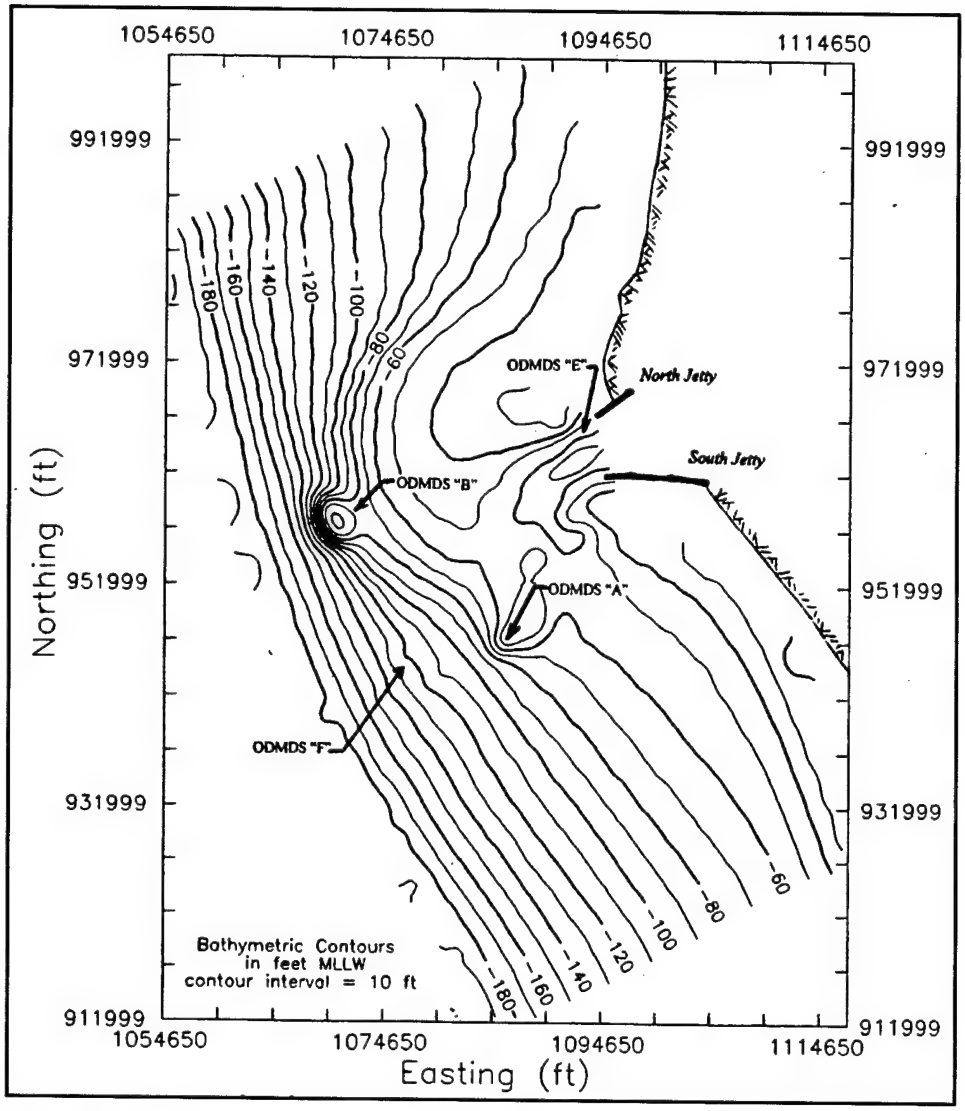

Figure 5. Regional bathymetry at MCR, 1994 survey (after USAED, Portland, 1995a)

Sediment Characteristics[1]

The type and median grain size of dredged materials historically placed at the MCR ODMDS has been typically poorly-graded sand with d_{50} = 0.18-0.33 mm.[2] The grain size of the dredged materials placed at the ODMDS depends upon where the materials were dredged. Seasonal changes in sediment texture at the MCR and vicinity have been described by Sternberg et al. (1977), and Roy et al. (1982). The sediments that characterize the Columbia River entrance area during all seasons have been categorized as either Factor 1 (0.21-0.25 mm) or Factor 2 (0.18-0.20 mm) sizes. Factor 3 (0.13-0.15 mm) sediment has been observed at the MCR channel, but is more common during the summer than winter. It has

[1] This section is extracted essentially verbatim from U.S. Army Engineer District, Portland (1995a).

[2] Sediment grain diameter is typically given in metric units (mm).

been observed that winter storms winnow the silt fraction (finer than 0.062 mm) from sediments between the entrance and the outer edge of the tidal delta, including ODMDS B. The seaward advance of Factor 2 sediments has been observed to occur with onset of the spring freshet (high river discharge). The silt size fraction returns to the MCR sediments in the spring (April) and increases markedly through the summer. The area offshore of the tidal delta deeper than 18-30 m (60-100 ft) is believed to receive sediments from the nearshore area during the summer.

Dredged material removed from the inner bar (Factor 1 and 2) and placed in the MCR ODMDS is characteristically different from the ambient seafloor sediments on the nearshore shelf (Factor 3). The distinction is based on textural and mineralogical properties of in situ sediments and the placed dredged material.

Bathymetric mounding of placed dredged material offers a secondary means of identifying disposed sediments and estimating transport rates for the dumped material. Sediments dredged from the outer shoal of the entrance channel are texturally identical (Factor 3) to the modern marine sands characteristic of the nearshore shelf and the natural sediments at ODMDS A, B, and F (Borgeld 1978). Consequently, the ambient seafloor sediments and any dumped Factor 3 sediments will behave similarly. Coarser estuarine sediments (Factor 1) will behave differently from the ambient sediments at the ODMDS (Factor 3) and will tend to remain at the disposal site. The outer limit of natural sedimentation due to river bed-load transport on the tidal delta has been defined as the seaward limit of Factor 3 sediment (0.13-0.15 mm). ODMDS B is identifiable in terms of the seafloor sediment size and percent fine-grain material (Figure 6), due to the dumped dredged material being coarser than the ambient sediment at these sites (Siipola 1992).

For ODMDS B and similar water depths of 30.5-39.6 m (100-130 ft), sediments coarser than 0.18 mm are relatively stable and apparently move slowly northward at 0.4 km per year (0.25 miles per year) as bed load under the influence of the winter nearshore circulation regime. Sediments finer than 0.18 mm are frequently resuspended throughout the year and move as suspended load toward the north (Borgeld 1978).

Sediments dredged from the Columbia River navigation channel and deposited at ODMDS B and E are characterized as having a median grain size, d_{50}, of 0.13-0.35 mm. On average, the silt/clay (sediment diameter less than 0.062 mm) content of the dredged material amounts to 3 percent of the volume of dredged material. The outer bar portion of the MCR navigation channel has been found to contain finer sands (d_{50} = 0.19 mm) than the inner bar portion of the MCR navigation channel (d_{50} = 0.25 mm). Variation in sand grain sizes along the navigation channel results in layering of the disposal mound as loads of material from different origins are placed on the mound. If substantial differences in sediment characteristics exist, the sediment transport potential may vary significantly with exposure of the multiple layers of sediment within the mound.

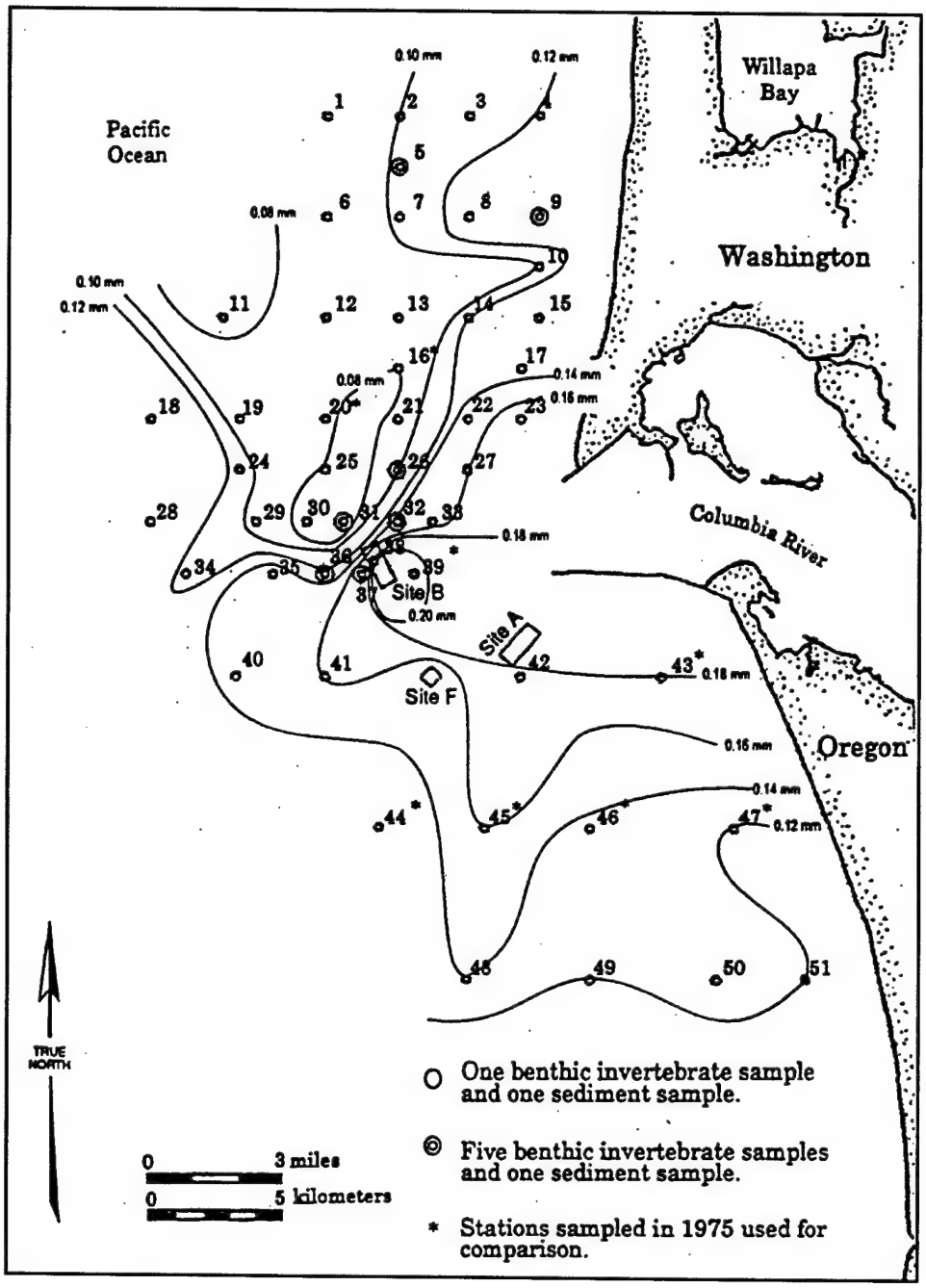

Figure 6. Mean gram size (mm) offshore from MCR, July 1992 (after USAED, Portland, 1995a)

Sediments on the ebb shoal in the vicinity of the ODMDS B and E are characterized as having median grain sizes in the range of 0.06-0.12 mm, somewhat finer than the sediments dredged from the navigation channel. In addition, a larger percentage of clays and silts (as much as 40 percent) exist in the deeper water adjacent to ODMDS B.

ODMDS Descriptions and Limitations[1]

Annually, 2.1-3.5 million cu m (2.8-4.6 million cu yd) of sediments are dredged from the 9.7-km- (6-mile-) long MCR channel and placed in EPA designated ODMDS. Unexpected mounding has been experienced at ODMDS A and B to the point that disposal quantity limitation and site expansion management options have been coordinated with regional resource agencies and implemented (Siipola and Braun 1995). Consistent annual bathymetric surveys at the ODMDS have been conducted since 1983. Since 1992, ODMDS surveys have been conducted twice annually, before and after the dredging season (April-May to September-October). The semiannual surveying of the ODMDS is necessary to ensure that the Corps does not unintentionally worsen the mounding problem or place dredge material outside the limited ODMDS boundaries.

ODMDS A

Prior to formal designation as an interim ocean disposal site in 1977, about 21.4 million cu m (28 million cu yd) of dredged sediment had been placed within or in vicinity of Site A (1904 to 1976). The average annual volume of dredged material placed in Site A between 1945-1958 was 1.2 million cu m per year (1.6 million cu yd per year). About 49 percent of the dredged material placed at Site A during this time 10.5 million cu m (13.7 million cu yd) occurred within a 2-year period (1956-57) and resulted in rapid mounding. Consequently, use of Site A was discontinued from 1959 to 1971.

A small volume of dredged material was placed at Site A during 1971-1976. Based on a 1975 MCR bathymetry survey, there was little indication of dredged material mounding at Site A as a result of the 1956-57 high volume disposal (Sternberg et al. 1979). Apparently, much of the dredged material placed at Site A during 1956-57 had been dispersed during the period 1958-1975. This would infer a maximum dispersion rate of 612,000 cu m per year (800,000 cu yd per year) or 10.5 million cu m per 17 years (13.7 million cu yd 17 years), assuming all dredged material placed during 1956-57 was dispersed out of Site A by 1975. It is likely that a lesser amount of dispersion took place, since there was some indication of mounding in the 1975 survey. The fact that most of the dredged material placed at Site A during 1956-57 had dispersed within a 20-year time frame likely contributed to consideration of Site A as an interim site in 1977.

At the time of final ODMDS designation in 1986, Site A was not considered to have a mounding problem. The assessment was based on MCR bathymetry surveys conducted in 1975 and 1978. Between 1977 and 1991, approximately 17.2 million cu m (22.5 million cu yd) of dredged material was placed within ODMDS A boundaries, an average of 1.2 million cu m per year (1.6 million cu yd per year) (20 percent of which was placed by contractor-operated split-hull hopper dredges. Based on a 1985 survey, mounding of dredged material ODMDS A was beginning to occur. By 1992, significant mounding of dredged material was reported within ODMDS A.

[1] This section is extracted essentially verbatim from USAED, Portland (1998).

In 1993 ODMDS A was expanded and placement of dredged material within that site was restricted to a maximum of 1.1 million cu m (1.5 million cu yd) annually. Only the western one-third of this site was used, and only during the summer months when nearshore currents are believed to flow southward (Siipola and Braun 1995). Even though ODMDS A was expanded in 1993, the site has received only 312,000 cu m (408,000 cu yd) of dredged material since then. In May 1993 mounding at ODMDS A, due to dredged material placement, reached -11 m (-36 ft) mean low low water (mllw). The mound was 11 m (36 ft) high relative to the 1981 bathymetry. Instances of steepened, amplified, and breaking wave conditions in the vicinity of ODMDS A were reported by navigation vessels transiting the MCR entrance channel. The wave effects were attributed to the mound at ODMDS A. Consequently, the disposal of dredged material at ODMDS A has not occurred since 1994. Between May 1993 and July 1997, the maximum mound height at ODMDS A was reduced by 4.6 m (15 ft), from 11 m (36 ft) to 6.4 m (21 ft), about 1.2 m per year (4 ft per year), through sediment dissipation by waves and currents (Siipoal and Braun 1995). In 1997, the minimum bottom elevation within ODMDS A remained at -12.8 m (-42 ft mllw).

The height and areal coverage of the dredged material mound dramatically increased between 1981 and 1995. In 1995, the dredged material mound at ODMDS A was 7.6 m (25 ft) high and extended 460 m (1,500 ft) beyond the site boundaries, with respect to the 1981 bathymetry. The total volume gain associated with bathymetric change at ODMDS A between 1981-1995 was calculated to be 11.8 million cu m (15.4 million cu yd) (based on differencing of 1981 and 1995 surveys). The actual volume of dredged material placed in ODMDS A during 1981-95 was estimated to be 16 million cu m (21 million cu yd) (Portland District dredge logs). Based on the preceding data, approximately 26 percent of the dredged material placed at ODMDS A of 4.2 million cu m (5.5 million cu yd) cannot be accounted using bathymetric survey calculations. This volume underestimate could be the result of: (a) an average vertical survey error of 0.5 m (1.7 ft) (which is possible), (b) consistent over-reporting of dredged volumes in the logs (unlikely), or (c) transport of placed dredged material out of ODMDS A and vicinity to an apron thickness undetectable by surveys (likely). It is likely that ODMDS A is somewhat dispersive, but not to a sufficient level to handle to consistent dredged material disposal exceeding 275,000 cu m per year (360,000 cu yd per year) (4.2 million cu m (5.5 million cu yd) placed over 15 years). The net direction of dredged material dispersion at ODMDS A appears to be northward toward the MCR entrance channel.

Although there appears to be a moderate rate of dispersion at ODMDS A, this site is considered to be nondispersive with respect to the amount of dredged material that has been historically placed there during active site use (1.2 million cu m per year (1.6 million cu yd per year). Placement of dredged material in ODMDS A is currently restricted, due to the present mounding and potentially related adverse wave shoaling effects upon navigation. ODMDS A is near its capacity to handle additional dredged material disposal. If dredged material disposal at ODMDS A were indefinitely restricted, the dredged material mound would be dispersed out of the site boundaries within 20-40 years from 1995. This conclusion was based on the estimated range in dispersion rate at ODMDS A: 360,000 cu yd per year (1981-95) to 612,000 cu m per year

(800,000 cu yd per year) (1958-1975). It is assumed that the dispersion rate for ODMDS A is 275,000 cu m per year (360,000 cu yd per year).

ODMDS B

Prior to formal designation as an interim ocean disposal site in 1977, approximately 26 million cu m (34 million cu yd) of dredged sediment had been placed within or in vicinity of Site B (1945 to 1975). The year-to-year volume of dredged material placed at Site B during this time period was fairly consistent with the average annual disposal volume of 1.4 million cu m per year (1.8 million cu yd per year).

Based on the1975 MCR bathymetry survey, the accumulation of dredged material placed at Site B had resulted in a mound about 6.1 m (20 ft) high with respect to the 1945 bathymetric condition (Sternberg et al. 1979). The accumulation of dredged material placed at Site B represented a shoaling rate of 0.20 m per year (0.67 ft per year) between 1945 and 1975. In 1975, bathymetry within Site B varied between 24-43 m (80-140 ft) mllw. Given that the observed shoaling rate due to dredged material disposal during 1945-75 was less than 0.3 m per year (1 ft per year) and that water depths in Site B were for the most part greater than 69 m (90 ft), continued use of Site B was not considered to present a problem to navigation. This finding likely contributed to consideration of Site B as an interim site.

At the time of formal ODMDS designation in 1986, Site B was not considered to have a mounding problem, and continued use of Site B was not considered to present a problem to navigation. This assessment was based on a 1978 MCR bathymetry survey. Between 1977 and 1991, approximately 18.5 million cu m (24.2 million cu yd) of dredged material was placed within the ODMDS B boundaries, an average of 1.3 million cu m per year (1.7 million cu yd per year), 50 percent of which was placed by contractor-operated split-hull hopper dredges. In 1992, significant mounding of dredged material was reported within ODMDS B.

In 1993 ODMDS B was expanded, and the site was divided into six 610-m × 610-m (2,000-ft × 2,000-ft) cells. Dredged material disposal was managed by designating specific cells available for placement each year. Since 1993, dredged material placement has been restricted to the deeper portion of ODMDS B (the three westernmost cells) to avoid placement on the mound that had formed within the interim site boundaries. In September 1994, mounding at ODMDS B due to dredged material placement reached -14.6 m (-48 ft) mllw. The dredged material mound had accumulated over 21 m (70 ft) in height relative to the 1981 bathymetry (Siipola and Braun 1995). Instances of steepened, amplified, and breaking wave conditions in the vicinity of ODMDS B also were reported by navigation vessels transiting the MCR entrance channel. These wave effects were attributed to the mound at ODMDS B. To minimize potential interference with navigation, the mound at ODMDS B was reduced 1.5-3.0 m (5-10 ft) by dredging the top from -14.6 m (-48 ft) mllw to -16.2 m (-53 ft) mllw. The material was placed in the three westernmost cells of the ODMDS. Between fall 1994 and summer 1997, the highest mound elevation at ODMDS B (located in the eastern half of

the site) was further reduced by 2.1 m (7 ft), from -16.2 m (-53 ft) mllw to -18.3 m (-60 ft) mllw through sediment dissipation by waves and currents. The reduction in mound height represents an erosion rate of about 0.6 m per year (2 ft per year), applicable for the top of the mound at ODMDS B. The equivalent volume of annual erosion was estimated to be 230,000 cu m per year (300,000 cu yd per year) (USAED, Portland/USEPA 1997). This "erosion effect" at ODMDS B is considered to be confined to the shallow area of the site near the top of the dredged material mound.

In 1997, the dredged material mound at ODMDS B was 16.8 m (55 ft) high and extended more that 1,760 m (2,500 ft) beyond the site boundaries, with respect to the 1981 bathymetric condition. Prior to 1981, the accumulation of dredged material previously placed at ODMDS B had formed a mound approximately 6.1 m (20 ft) high, with respect to the 1945 bathymetry (Sternberg et al. 1977). The total volume gain associated with bathymetric change at ODMDS B between 1981-1997 was calculated to be 28.8 million cu m (37.6 million cu yd). This volume estimate was based on survey differencing. According to the Portland District dredge logs, the actual volume of dredged material placed in ODMDS B during 1981-97 was estimated to be 24.1 million cu m (31.5 million cu yd). Based on that data, approximately 19 percent more material appears to be on the seabed than was placed at ODMDS B. This volume overestimate could be the result of (a) an average vertical survey error of 0.5 m (1.7 ft) (possible), (b) consistent under-reporting of dredged volumes in the logs (unlikely), or (c) a regionwide accumulation of sediment due to natural processes (possible). In either case, ODMDS B is not considered to be a dispersive site, with respect to the volume of dredged material placed of 1.4 million cu m per year (1.8 million cu yd per year) for 1990-1996).

During 1993-1996, much of the dredged material that would have been placed at ODMDS B was diverted to ODMDS F to prevent further mounding at site B. Additional disposal within the 1993 boundaries of ODMDS B has been limited since 1996 due to potential mounding effects on waves and navigation. In FY 1997, only 254,000 cu m (332,000 cu yd) was placed in the western one-fourth of ODMDS B (relative to the 1993 site boundaries) to avoid wave amplification due to mounding. Due to the reliance on ODMDS B as a primary disposal site (52.2 million cu m (68.2 million cu yd) placed at this site since 1956), ODMDS B was temporarily expanded in 1997 (USAED, Portland/USEPA 1997). The 1997 expanded boundary of ODMDS B was intended to provide more than sufficient disposal capacity for a 3-5 year period while providing for the operational flexibility of disposal at nearshore depths of 15.2-21.3 m (50-70 ft) and offshore depths of 49-61 m (160-200 ft). A utilization plan for the 1997 expanded ODMDS B was developed to minimize benthic impacts.

ODMDS E

Because ODMDS E is 305 m (1,000 ft) north of the MCR entrance channel, this site has typically been used during early summer or fall when the littoral transport of material from the site is thought to be northward toward Peacock Spit, and away from the MCR entrance channel. Between 1988-1996, the volume of dredged material placed at ODMDS E was restricted to a maximum of

0.77 million cu m (1 million cu yd) annually. This was done to prevent overloading the site (creating a mounding condition or facilitating the transport of placed dredged material back into the navigation channel) due to the small ODMDS boundaries. It is estimated that placement of 0.77 million cu m (1 million cu yd) within the original ODMDS E boundary would have resulted in a mound 1-1.2 m (3-4 ft) in height.

There was a lack of accumulation of dredged material at ODMDS E from 1990 to 1997. Only the eastern one-fourth of ODMDS E appears to have accumulated any sediment, and this localized accumulation is within the detection limit of bathymetric surveys of 0.3 m (1 ft). Most of ODMDS E (1986 boundaries) has experienced a net decrease in seabed elevation. The seabed within the western one-half of ODMDS E has eroded by 0.6 m (2 ft) or more between 1990 and 1997. The total volume loss associated with bathymetric change at ODMDS E between 1990-1997 was calculated to be -237,000 cu m (-310,000 cu yd) (based on survey differencing). According to the Portland District dredge logs, the actual volume of dredged material placed in ODMDS E (1986 boundaries) during 1990-97 was estimated to be 3.9 million cu m (5.1 million cu yd). Based on the preceding data, none of the material that was placed at ODMDS E appears to have accumulated on the seabed. The total ODMDS E volume loss of 4.1 million cu m (5.4 million cu yd) between 1990-97 could be the result of (a) an average vertical survey error of -11 m (-36 ft) (impossible), (b) consistent under-reporting of dredged volumes in the logs (unlikely), or (c) a regionwide transport or erosion of sediment due to natural processes (likely). The dredged material placed at ODMDS E each year appears to be completely transported out of the site by the following year. This indicates that ODMDS E appears to be a highly dispersive site. Based on the survey data, the dispersive capacity within the 1986 boundary of ODMDS E is considered to be about 0.77 million cu m per year (1 million cu yd per year).

Due to the high dispersion rate observed at ODMDS E, its close proximity to the MCR entrance channel (short haul distance), reliance on the site as a primary disposal site (38.2 million cu m (50 million cu yd) placed since 1956), and the potential for dredged material placed at ODMDS E to be reintroduced into the littoral environment of the Washington coast, ODMDS E was temporarily expanded in 1997 (USAED, Portland/USEPA 1997). The 1997 boundary of expanded ODMDS E was intended to maximize the site's dispersion of dredged material. A site utilization plan for the 1997 expanded ODMDS B was developed to minimize navigation impacts (USACE/USEPA 1997). The dispersive capacity for the entire 1997 expanded boundary of ODMDS E was estimated to be 0.77-2.7 million cu m per year (1.0-3.5 million cu yd per year).

Approximately 382,000 cu m (500,000 cu yd) of dredged material was placed within the original boundaries of ODMDS E during June-August 1997, and 306,000 cu m (400,000 cu yd) of dredged material was placed within the expanded area of ODMDS E. Immediately following dredged material disposal in August 1997, a 1.0-1.2 m (3-4 ft) accumulation (mound) was observed on the seabed within ODMDS E. During the ensuing fall, winter, and spring, the accumulated (placed) material was dispersed. Between May 1997 and May 1998, there was little accumulation of placed dredged material within expanded

ODMDS E, despite placement of 689,000 cu m (900,000 cu yd) during the 1997 dredging season.

ODMDS F

Prior to 1989, ODMDS F was rarely used for the disposal of sediments dredged from the MCR due to established preferences for utilizing ODMDS A, B, and E. Additional factors that discouraged the aggressive use of ODMDS F are that the site lies directly in the path of vessels approaching the MCR navigation channel, and that ODMDS F is located at the bar pilot transfer area. The presence of two dredges simultaneously operating in ODMDS F was perceived to be detrimental to safe navigation at the MCR entrance. In 1992, it became apparent that ODMDS F must be used more extensively to avert additional mounding (due to dredged material disposal) at ODMDS A and B. Due to the small areal extent (as originally designated in 1986), ODMDS F was expanded by a factor of 30-fold in 1993. The Portland District has minimized the interference of dredging disposal activities with shipping and commerce at ODMDS F by allowing only one dredge to utilize the disposal site during a given disposal season.

In 1993, the expanded ODMDS F was divided into 16 cells 610-m × 610-m (2,000-ft × 2,000-ft) cells. ODMDS F is surrounded by a 305-m (1,000-ft) buffer zone. Placement of dredged material is not permitted within or outside the buffer zone. Dredged material disposal is managed by designating a limited number of cells available for placement each year. Beginning in 1993, ODMDS F has been used more extensively to reduce the amount of dredged material placed in ODMDS A and B.

Recent active use of ODMDS F formally began in 1989. The recent placement of dredged material at ODMD F has resulted in multiple mounds 2.4-3.7 m (8-12 ft) high distributed throughout the southeastern half of ODMDS F. The total volume gain associated with bathymetric change at ODMDS F between 1981-1997 was calculated to be 8.4 million cu m (11 million cu yd), based on survey differencing. The actual volume of dredged material placed in ODMDS F during 1981-97 was estimated to be 6.4 million cu m (8.3 million cu yd) (Portland District dredge logs). Based on these data, approximately 9 percent more material appears to be on the seabed than was placed at ODMDS F. This volume overestimate could be the result of (a) an average vertical survey error of 0.2 m (0.6 ft) (likely), (b) consistent under-reporting of dredged volumes in the logs (unlikely), or (c) a regionwide accumulation of sediment due to natural processes (possible).

In either case, ODMDS F is not considered to be a dispersive site with respect to the volume of dredged material placed at the site per year of 707,000 cu m per year (924,000 cu yd per year). This finding corroborates with previous investigations (Siipola, Emmett, and Hinton 1993; USAED, Portland/ USEPA 1997) that stated that dredged material placed at site F is not subject to significant annual dispersal.

The capacity of ODMSD F to handle additional dredged material disposal beyond 1997 is limited to 7.7 million cu m (10 million cu yd) (USAED,

Portland/USEPA 1997). If more than 7.7 million cu m (10 million cu yd) is placed at ODMDS F, the resultant dredged material mound could adversely affect the wave environment at the approaches to the MCR entrance channel. After 1997, dredged material placement in ODMDS F will be restricted to the northwestern one-half of the site. The southeastern one-half of ODMDS F is effectively filled, based on the limiting mound height of 3.0-4.6 m (10-15 ft) for the onset of adverse wave conditions.

ODMDS Management[1]

The transition in ODMDS management at the MCR is characterized by three important shifts in USACE and USEPA policy.

MCR ocean dredging disposal before 1977

Prior to 1977, ODMDS at the MCR were sited only in terms of approximate location and areal configuration. Placement of dredged material within the ODMDS was governed by the need to minimize navigational impact from dumped dredged material being transported back into the navigation channel. Mounding did not appear to be a major concern due to the spatial variability of dredged material disposal within a given site. The site boundaries were not fixed and it was not required to place material strictly within the disposal site. The operational flexibility of disposal site boundaries and vessel control during material placement resulted in a higher degree of dredged material dispersal during placement than at present. Prior to 1977, dredged material was placed over a wider areal expanse than the configuration of the ODMDS indicate (Soderlind 1995).[2]

MCR ocean dredging disposal: 1977 to 1986

Between 1977 and 1986, management of the ODMDS at the MCR was characterized by the transition from unregulated dredged material disposal to a regulated program. In January 1977, active ocean disposal sites at the MCR received interim designations as such when EPA issued the final Marine Protection Research and Sanctuaries Act (MPRSA 1972) and associated regulations (40 CFR 228). The exact position for each of the interim ocean disposal sites was fixed by specification of the corner coordinates by EPA to abide by the rules of the MPRSA. The interim ocean disposal sites received final designation in August 1986. The final EPA approved configuration for each ODMDS was governed by the requirement to minimize the benthic area of impact due to open water disposal of dredged sediments. The areal size of the designated ODMDS at the MCR was based on the following:

---

[1] This section is extracted essentially verbatim from USAED, Portland/USEPA (1997).

[2] Soderlind, K. (1995). Memorandum for Record to PE-HY, U.S. Army Engineer District, Portland.

a. *ODMDS length.* Average dumping run for one dump = (disposal vessel speed while dumping) × (time to empty disposal vessel).

b. *ODMDS width.* Average turn during one dump = disposal vessel turning radius while dumping.

c. *ODMDS long axis orientation.* Preferential approach heading during dredged material disposal (site orientation is set by disposal vessel operators, and is based on dumping efficiency and vessel seakeeping due to incident wave direction).

Prior to the 1980s, sediment dredged at the MCR and placed in ODMDS was accomplished using government hopper dredges. Government hopper dredges utilize a series of doors located on the hull bottom to gradually release dredged material from the vessel. Contractor hopper dredges normally used at the MCR are split-hull vessels. Dredged material released from a split-hull hopper dredge is rapidly placed on the seabed, in a manner much more quickly (efficiently) than bottom-door hopper dredges. While the use of split-hull hopper dredges reduces the time required for material disposal, split-hull dredges reduce the horizontal dispersal of dumped dredged material on the seabed while increasing the vertical extent of accumulation per dump. After 1980, approximately half of the material dredged at the MCR was accomplished using contractor split-hull hopper dredges.

Beginning in 1981, ocean disposal site management was somewhat effective in restricting placement of dredged material within the designated disposal sites. At this time, placement of dredged material within the ocean disposal sites was done randomly at some radius from an assigned disposal coordinate or buoy. Efficiency-oriented dredging contractors most likely placed dredged material on the extreme channel side of the disposal area (or buoy location) to shorten the haul distance. This could have enhanced the accumulation of dredged material over a small area.

MCR ocean dredging disposal: 1987 to present (1997)

After final EPA approval of the MCR ODMDS in 1986, disposal site management became increasingly proactive in the year-to-year operation of ODMDS. Disposal site management has been progressively improved and enhanced in order to maximize site capacity utilization of the EPA designated ODMDS. The unintended consequence of using the areally-restricted ODMDS has been the creation of potentially adverse impacts to navigation at the MCR by mounding of placed dredged material.

In 1990, accurate navigation and positioning control became available for hopper dredges operating on the open coast. This was possible with the installation of shore-based microwave towers that were used to determine the ship's position through electronic trilateration. The ship's position was known to several meters accuracy on a real-time basis. Hence, the hopper dredges could reliably place dredged material within the assigned ODMDS locations during all

times of operation (Soderlind 1995).[1] Instead of placing material within some marginal radius from a predetermined location, hopper dredges could return to the exact assigned dump coordinate (ODMDS centroid) and place dredged material within a very limited area. The rapid accumulation of dredged material within ODMDS A and B (formation of high mounds) during the late 1980s and early 1990s is attributed to three factors:

a. The restriction of dredged material disposal within small EPA designated ODMDS rather than in large unconfined areas, and in a dispersive manner of placement.

b. Increased use of split-hull hopper dredges which tend to enhance the vertical extent of dredged material placed on the seabed within the ODMDS.

c. The improvement of ODMDS navigation in 1990 allowing for precise positioning control during disposal and repeated dumping at the same location.

Due to rapid accumulation of dredged material (mounding problems) at ODMDS A and B, those two ODMDS and ODMDS F were expanded in 1992 (Figure 2, solid lines). The temporary expansion of ODMDS A, B, and F were coordinated with regional resource agencies and special management options were implemented (Siipola and Braun 1995). The 1992 temporary expansion of the MCR ODMDS was intended to "buy time" until additional studies could be completed and final expanded or new ODMDS could be designated. Despite the temporary site expansions, mounding has continued to be problematic at these sites. Beginning in 1995, placement of additional material at ODMDS A was restricted, and placement at ODMDS B was limited to 1.5 million cu m (2 million cu yd) per year. By 1997, dredged material disposal within the existing ODMDS B boundaries will be highly limited in terms of the location, timing, and volume of dredged material placed at this site.

Seasonal and Extreme Event Hydrodynamics[2]

Physical processes in the coastal waters near the Columbia River mouth (MCR) result from an interaction of seasonal and extreme event hydrodynamics such as regional oceanic circulation, astronomical tidal currents, and nearshore estuary or river currents as affected by meteorological events. These processes in turn act on sediments to produce the bathymetric condition observed at any particular time. Time scales for these processes range from seconds for wind generated waves to months for seasonal weather patterns to years for large-scale events such as El Nino. One of the direct effects of physical processes near the MCR is on the transport of ODMDS sediments.

---

[1] Soderlind (1995), op. cit., p. 25.

[2] This section is extracted essentially verbatim from USAED, Portland (1995a) and USAED, Portland/USEPA (1997).

Regional oceanic circulation

Mean circulation of the continental shelf waters of Washington and Oregon is subject to seasonal reversal, being northward during winter and southward during summer. On time scales of several days, coastal circulation can be highly variable in direction and speed with fluctuations correlating with changes in sea level and the alongshore component of wind (Huyer and Smith 1977). The alongshore component of flow is substantially stronger and more responsive to changes in wind conditions than is the onshore-offshore component. Fluctuations in the mean alongshore circulation appear to be coherent over distances of 200 km (125 miles) and are independent of depth in both phase and magnitude to at least 20 m (66 ft) depth (Huyer and Smith 1977). The magnitude of such fluctuations decreases rapidly with distance offshore. Currents averaged over very long periods (e.g., longer than 50 days) correlate better with sea level changes than with winds to depths of 36.6 m (120 ft). By 76.2-m (250-ft) depth, the influence of both sea level and winds appears to be substantially diminished and other processes such as tides, large scale circulation, and internal waves control the current regime.

Regional circulation along the Washington and Oregon coasts has been characterized in terms of two seasonal current regimes (Bourke and Glenne 1971). The California current is a broad, slow, shallow southward flowing current that attains maximum strength during the summer when surface winds are consistently from the north- northwest. It flows offshore as a diffuse band about 483 km (300 miles) wide with an average speed of 10.4 cm per sec (0.34 ft per sec) toward the south. The Davidson current is a northward flowing current attaining speeds of 27.4-45.8 cm per sec (0.9-1.5 ft per sec) over extensive distances. The current develops off of the Oregon-Washington coast in September, becomes well established in January, and has a minimum width of about 80 km (50 miles). The Davidson current diminishes towards the spring and disappears by May (Bourke and Glenne 1971).

The transition from the winter circulation regime to the spring or summer regime is abrupt, occurring only in about a week during a strong northerly wind event. The transition is the result of a large cumulative offshore transport of water caused by local wind stress and the establishment of strong offshore density gradients in the shelf waters. Upwelling is associated with the spring current transition and continues into July or August. The offshore density gradients are associated with the persistent southward surface current of the summer oceanographic season. Maximum current speeds during summer can approach 40 cm per sec. The combined offshore transport due to upwelling and southward surface flow cause the Columbia River discharge and its associated suspended sediments to form a plume in the surface waters that extends southward and offshore in the summer.

During summer, a strong vertical gradient (shear) in alongshore current can be found in the lower half of the flow over the middle and outer shelf. The mean alongshore current is weak near the bottom and strongly southward at the surface. Current reversal during the summer seldom occurs. Maximum speeds occur over the midshelf about 16 km (10 miles) offshore during June when the southward flow is reinforced by strong northerly winds. The transition between

summer and winter nearshore circulation is gradual. The offshore shear zone between the northward flowing outer shelf waters and the nearshore southward flow expands upward and shoreward under the influence of fall and winter southeasterly winds until the winter regime of northward flow is re-established throughout the water column (Sobey 1977).

In general, there are three environmental seasons near the Columbia River mouth (Borgeld 1978). These seasons are briefly defined as:

a. *Winter*--characterized by high flow in the Columbia River, caused by high rainfall in the coast ranges and a winter oceanic regime along the Oregon-Washington continental shelf. The winter season is tentatively defined as December-March.

b. *Spring*--characterized by the highest flow of the Columbia River, caused by snowmelt in the higher elevations of the catchment basin, and the onset of the upwelling regime along the continental shelf. The spring season is tentatively defined as April-June.

c. *Summer*--characterized by low flow of the Columbia River and the summer shelf circulation regime. The summer season is tentatively defined as July-November.

Based upon results of a seabed drifter study, the annualized mean flow of the inner shelf waters has been estimated to be in a northerly direction. Seabed drifters released between the 36.5- and 91.4-m- (120- and 300-ft-) contours drift northward at 1-3 cm per sec (0.03-0.10 ft per sec), either parallel to the shelf contours or with a very slight offshore component.

Astronomical tidal currents

Simulated tides and currents. Tidal currents arise as a result of astronomical tides. The tidal environment at the MCR was simulated using the five primary tidal constituents generated from the Advanced Circulation- (ADCIRC-) derived database for the eastern North Pacific coast (Hench et al. 1994). ADCIRC is a three-dimensional (3-D) finite-element model developed under the DRP to simulate hydrodynamic circulation (tides) along shelves and coasts. (At the MCR, ADCIRC was operated in a two-dimensional (2-D) mode.) The time series shown in the top of Figure 7 represents a simulated equilibrium (generic) tide at ODMDS B for 1 year. An equilibrium tide is harmonically correct to the actual case, but is not referenced to a specific date or time. The bottom graph shown in Figure 7 is a detailed view for the first 350 hr (2 weeks) of the top graph. Depth-averaged tidal currents (u,v) shown in Figure 8 were similarly produced using the ADCIRC constituent database. These data were used to simulate water level and current fluctuations for the MDFATE application described in Chapter 5.

Note the extent of the simulated tidal elevations shown in Figure 7. The actual mean range at the MCR is 2 m (6.5 ft), the spring tide range is about 2.6 m (8.5 ft), and the extreme range is 4.3 m (14.0 ft). The maximum tidal range for the simulated tide shown in Figure 7 is 4.6 m (15 ft), or about 0.3 m (1 ft) larger

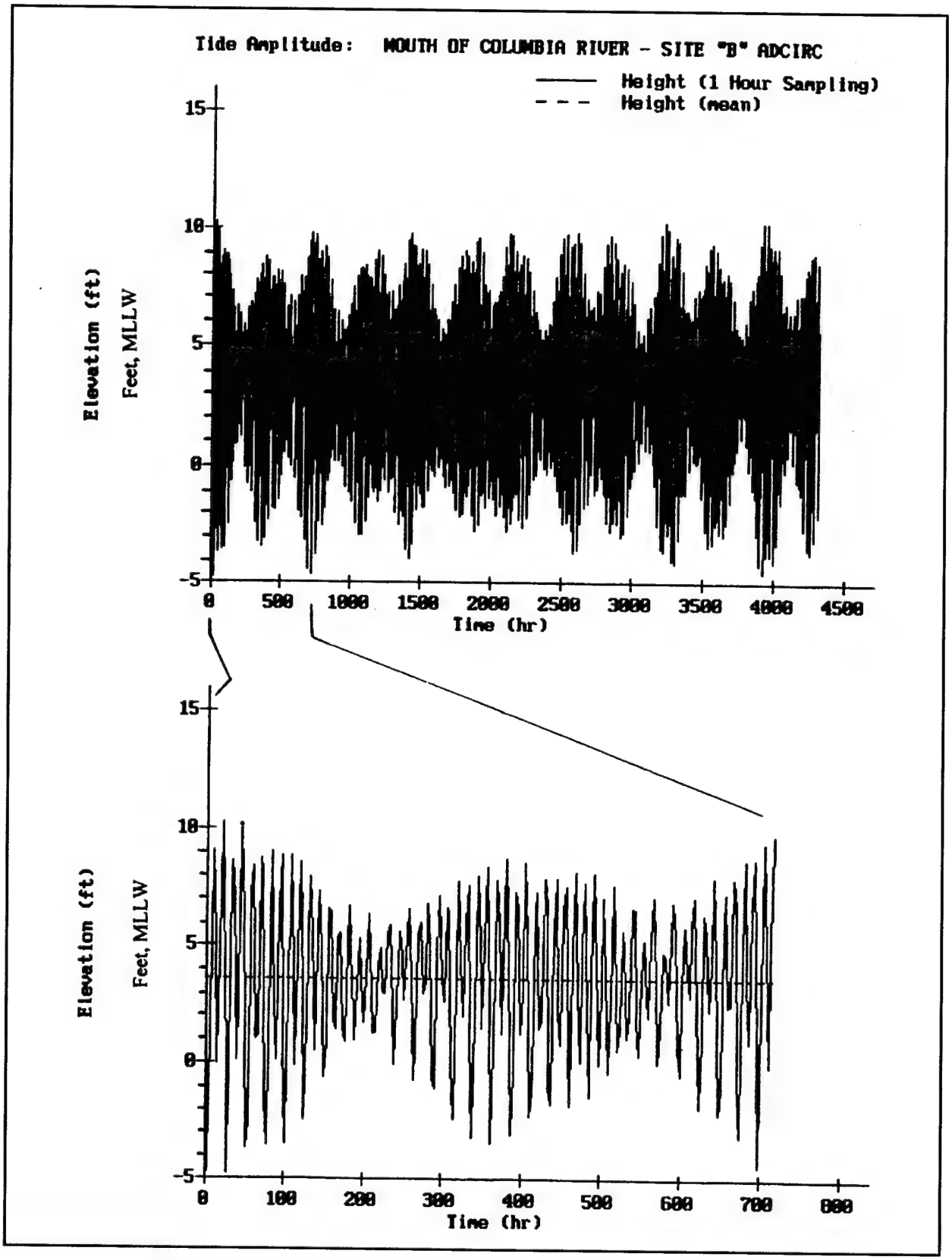

Figure 7. ADCIRC-simulated equilibrium tidal elevation for ODMDS B for 6 months (top), and for 2 weeks (bottom) (after USAED, Portland, 1995a)

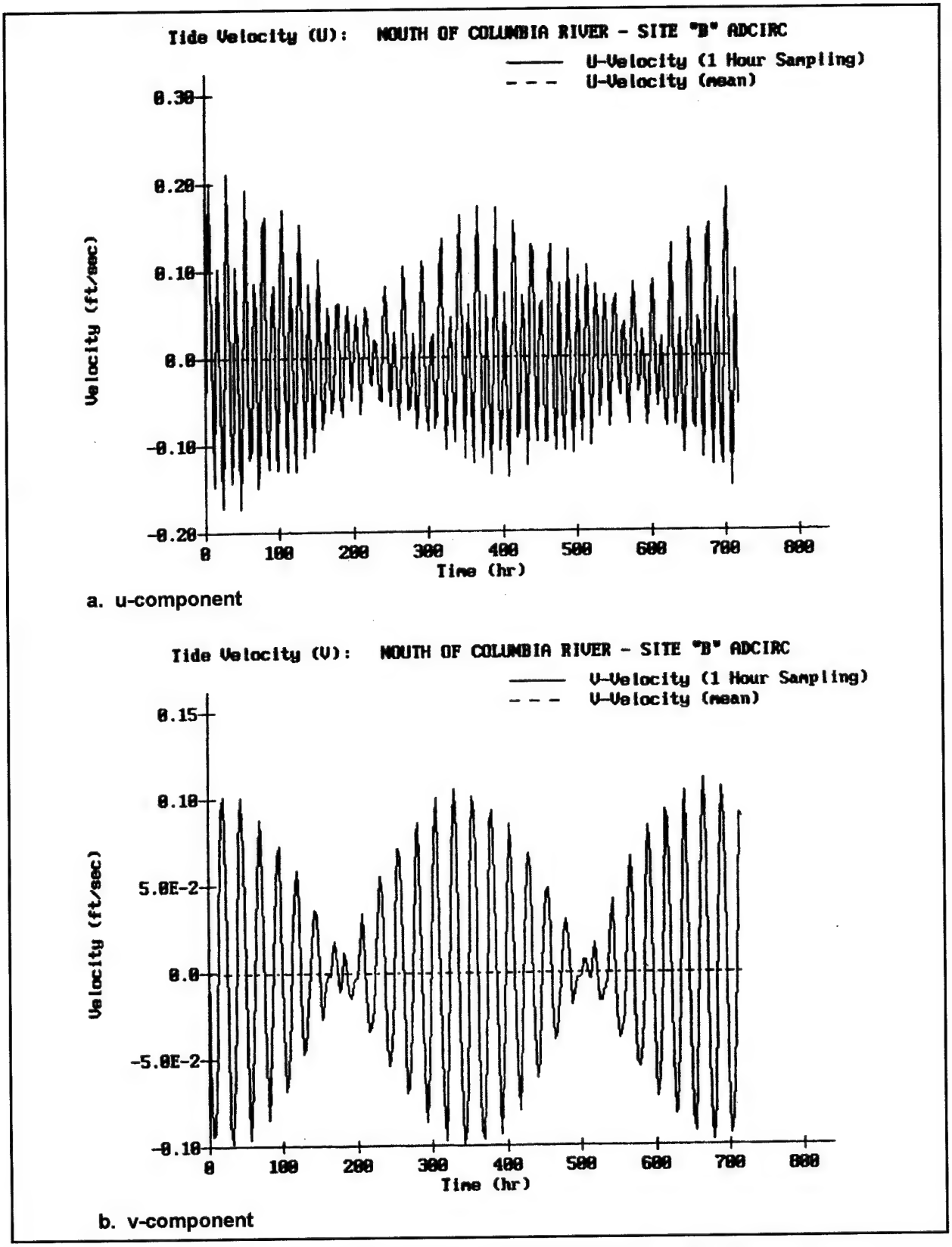

Figure 8. Simulated depth-averaged tidal currents for ODMDS B (after USAED, Portland, 1995a)

than the maximum reported range for the MCR. This is considered sufficiently adequate in terms of the input used in the DRP fate models.

The tidal currents of Figure 8 simulated by the ADCIRC model accounts only for the open coast component, based on the approach and passage of the tidal wave. The estuarine tidal current generated by flood and ebb flow from the Columbia River estuary is not included in these ADCIRC-predicted tidal currents. The u-component (x, or east-west) for the ADCIRC-simulated tidal currents at ODMDS B shown in Figure 8 slightly dominates the v-component (y, or north-south) and displays some onshore residual. The maximum +u is 6.1 cm per sec (0.2 ft per sec), the maximum -u is -4.6 cm per sec (-0.15 ft per sec). The v-component is symmetric at 3.1 cm per sec (0.1 ft per sec) and -3.1 cm per sec (-.1 ft per sec) (no residual) and is composed of only a diurnal signal. The u-component is composed of a mixed signal (diurnal and semidiurnal). Based on Figure 8, the phasing of the v-component lags the u-component by approximately 15 percent through a 2-week tidal cycle.

Comparison of actual tides and simulated tides. The actual tidal signal for jetty A located at river mile 3 was reproduced using 11 primary constituents based on a 235-day observation period in 1981. The resulting time series shown in the top of Figure 9 represents the actual equilibrium (generic) tide at jetty A for 1 month. The corresponding simulated tidal signal for ODMDS B is shown in the bottom of Figure 9. Assuming that the tidal signal at ODMDS B should be equivalent to jetty A, the simulated tide exceeds the actual case. The predicted high and low spring tide is approximately 0.3 m (1 ft) higher and 0.5 m (1.5 ft lower), respectively, than the actual case. The predicted highest high during neap tide is 0.3 m (1 ft) higher for the predicted case.

Fairly good agreement between simulated and actual cases is found when comparing the lowest low during neap tidal conditions. The ADCIRC-simulated tidal signal is about 10-20 percent higher than the actual case, for defining the magnitude of the tidal envelope. The phasing for the predicted and actual tidal signals corresponds fairly well overall, although there appears to be a shift for the semidiurnal component. In all cases, the constituent amplitude for the ADCIRC tide is larger than the actual tide at jetty A.

Nearshore estuary and river currents

Near the MCR, estuarine circulation exerts its influence, tending to draw nearbottom marine waters into the estuary while discharging low salinity waters at the surface. For example, at 21.4-m (70-ft) depth near ODMDS A, mean bottom currents flowed eastward at slightly more than 1 cm per sec (0.03 ft per sec) during June, based on seabed drifter results. This onshore circulation pattern has been documented to extend 9.7 km (6 miles) offshore by observing that seabed drifters released offshore MCR tend to enter the estuary and ground at Clatsop Spit (Morse et al. 1968). General observations made at the Columbia River lightship indicate a seasonally variable nontidal current induced by a combination of river discharge and shelf nearshore current regimes. The set of nontidal currents created by the river flow changes from 235 deg N during

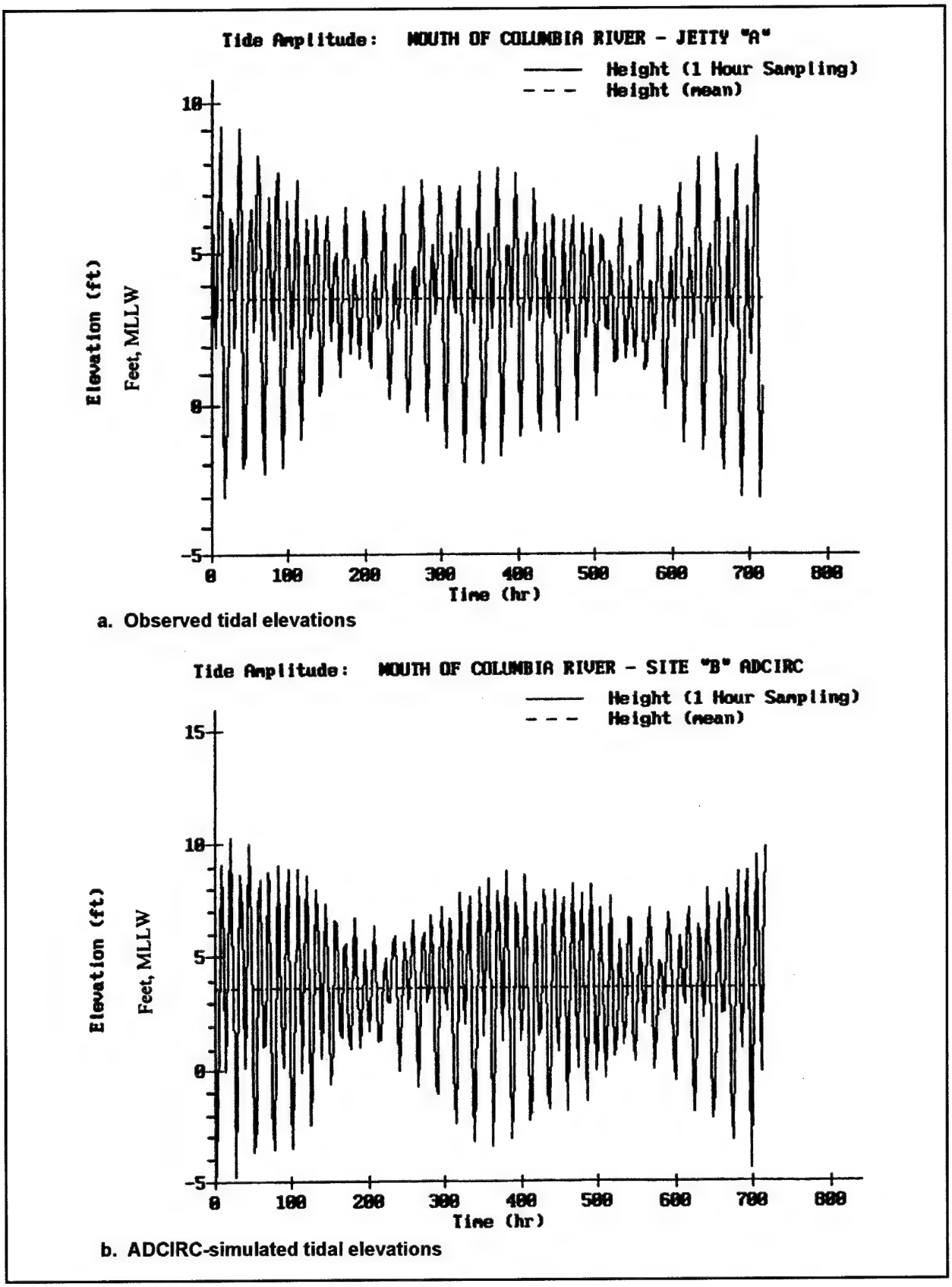

Figure 9. Observed and simulated tidal elevations near MCR (after USAED, Portland, 1995a)

February-October to 295 deg N from October-February in response to the seasonal shift in the regional current pattern.

The nontidal current speed at the MCR lightship ranged between a monthly average of 15 cm per sec (0.5 ft per sec) in March to 39 cm per sec (1.3 ft per sec) in June. During periods of high river discharge, the combined tidal and nontidal current can exceed 104 cm per sec (3.4 ft per sec) at 225 deg N. The greatest surface current speed observed at the MCR lightship was 180 cm per sec (5.9 ft per sec). As a comparison, the surface currents measured at the channel entrance between the north and south jetties were 300 cm per sec (9.8 ft per sec) on ebb and 120 cm per sec (3.9 ft per sec) on flood during June 1959 (USACE 1960). In September 1959, the surface currents at the same location had changed to 240 cm per sec (7.9 ft per sec) on ebb and 180 cm per sec (5.9 ft per sec) on flood.

Within the estuary, ebb flow in the northern portion of the river entrance is seaward, both at the surface and seabed. During flood tide, salt water tends to intrude along the southern side of the river channel. Consequently, sediments tend to enter the estuary with the marine waters through the southern portion of the mouth during flood tide. Sediments tend to exit the entrance through the northern part of the channel and are carried offshore during the ebb-tidal flow, when middepth ebb currents can exceed 183 cm per sec (6 ft per sec) in the entrance channel (USAED, Portland, 1960; Sternberg et al. 1979).

To assess the bathymetric impacts and transportability of dredged material placed within the expanded ODMDS boundaries, the current regime at each site must be sufficiently defined. Sediment transport is governed by the current regime observed at a given location. In addition to currents, the presence of waves (sea and swell) increases the potential for currents to transport sediments along the seabed. The current regimes between ODMDS B and E are completely different due to these sites being situated at different locations with respect to the Columbia River estuary outflow. Before any attempt can be made to quantify short- or long-term sediment behavior at a given ODMDS, that site's current regime must be adequately described. Considerable effort has been expended by the Portland District to resolve the current environments at ODMDS B and E (USAED, Portland/USEPA 1997).

ODMDS B. This disposal site is located about 6.4 km (4 miles) west (off-shore) and 3.2 km (2 miles) north of the entrance to the Columbia River estuary. Sediment transport at ODMDS B is believed affected by waves as much as currents. The currents observed at this site are controlled by seasonal coastal circulation, ebb and flood flows from the Columbia River estuary (plume), astro-nomical tides, and ocean currents. The currents in the upper 18.3 m (60 ft) of the water column at ODMDS B tend to be affected more by the Columbia River plume than by other processes. The currents in the lower part of the water column at ODMDS B tend to be dominated by seasonal coastal circulation and astronomical tidal flow. The tidal current ellipse for ODMDS B (middepth) is shown in Figure 10a (Sternberg et al. 1979). Currents are defined in terms of the direction which flow is heading toward. Generally, the flow at ODMDS B is directed toward the south-southwest during ebb tide and north-northeast during flood tide. Seasonal changes in the overall current environment at ODMDS B

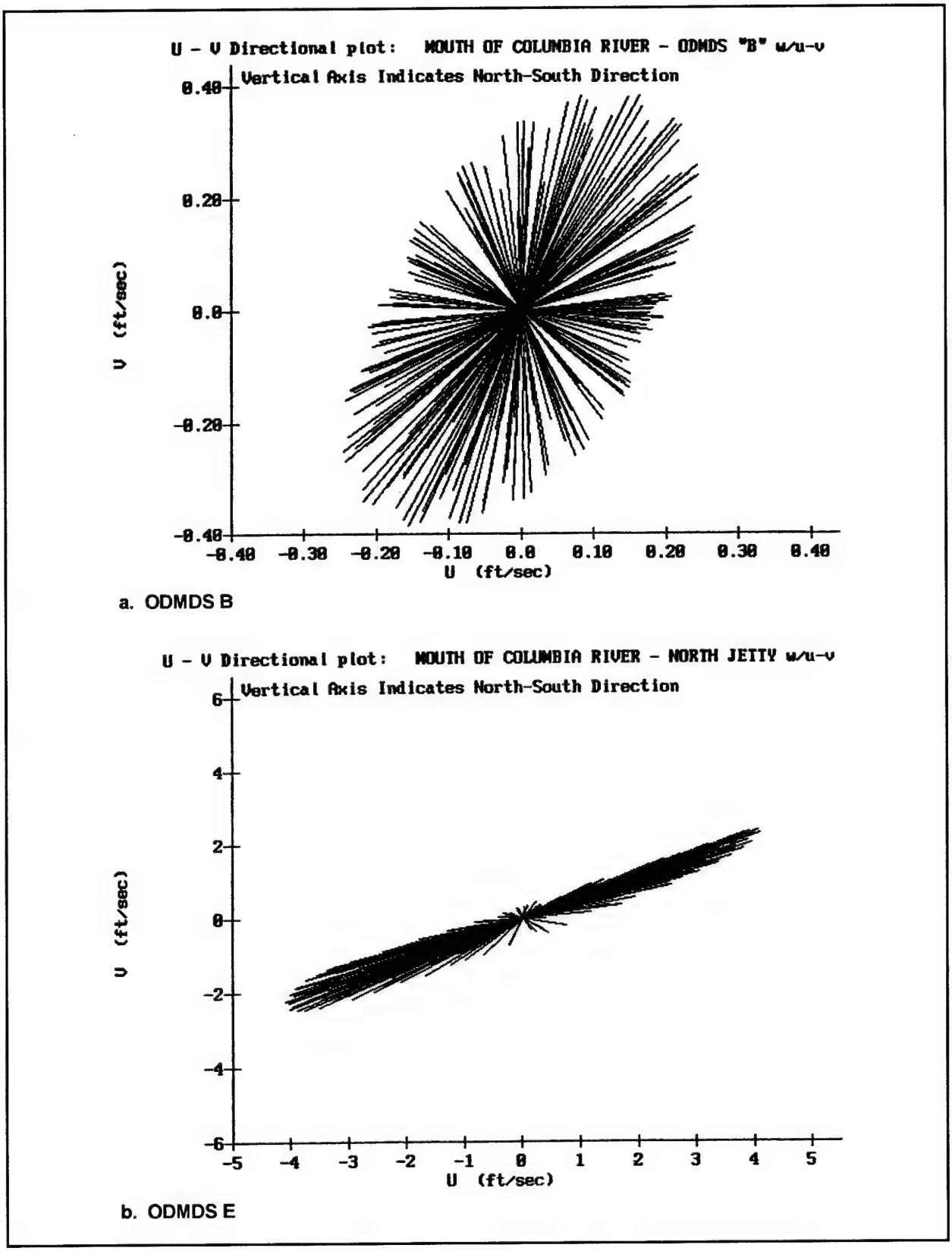

Figure 10. Tidal current ellipses for ODMDS B (top) and ODMDS E (bottom) (after USAED, Portland/USEPA 1997)

are due to changes in coastal circulation, which is expressed as a seasonally averaged residual current (residual current). The residual current at ODMDS B is described in terms of a winter-spring and summer-fall seasonal average (Sternberg et al. 1979).

Seasonal Residual Current at ODMDS B

Spring residual coastal current = 2.7 cm per sec (0.09 ft per sec) at 320 deg N during April-June

Summer residual coastal current = 18.3 cm per sec (0.60 ft per sec) at 213 deg N during July-October

Winter residual coastal current = 29.3 cm per sec (0.96 ft per sec) at 294 deg N during November-March

At ODMDS B, the magnitude of the seasonal residual current is at times equivalent to or greater than the tidal currents. Net sediment transport observed at ODMDS B is most likely influenced by the residual current speed and direction. The total current at middepth observed at ODMDS B is obtained by adding the appropriate residual current to the tidal ellipse.

ODMDS E. This disposal site is located in the entrance to the Columbia River estuary. Sediment transport at ODMDS E is believed dominated by currents. The currents observed throughout the water column at this site are controlled by the ebb and flood tidal flow associated with riverine flow of the Columbia river and the exchange of the estuary's tidal prism with adjacent ocean waters. Generally, the flow at ODMDS E is directed southwest during ebb tide and northeast during flood tide. Current speeds are high. At middepth, currents can exceed 152 cm per sec (5 ft per sec). The tidal current ellipse for ODMDS E (at middepth) is shown in the bottom part of Figure 10 (Sternberg et al. 1979). Seasonal changes in the overall current environment at ODMDS E are due to changes in coastal circulation, which is expressed as a seasonally averaged residual current. The residual current at ODMDS E is described in terms of a winter-spring and summer-fall seasonal average.

Seasonal Residual Current at ODMDS E

Winter-spring residual coastal current = 35 cm per sec (1.16 ft per sec) at 315 deg N during November-June

Summer-fall residual coastal current = 35 cm per sec (1.16 ft per sec) at 225 deg N during July-October

Although the magnitude to the tidal currents (Figure 10) at ODMDS E is much greater than the seasonally averaged (residual) currents, net sediment transport observed at ODMDS E may be heavily influenced by the residual current in speed and direction. The total current at middepth observed at ODMDS E is obtained by adding the appropriate residual current to the tidal ellipse.

Seasonal and Extreme Event Waves[1]

Measured Coastal Data Information Program (CDIP) wave data

Measured wave data (time series) have been obtained for the region near the MCR by National Oceanic and Atmospheric Administration (NOAA), and by the Coastal Data Information Program (CDIP) since 1979. (CDIP is operated by the University of California, Scripps Institution of Oceanography, La Jolla, CA, with funding by the California Department of Boating and Waterways, and by USACE.) In some cases, the wave data are limited to wave height and period parameters only. Other data sets contain wave height, period, direction, and spectral parameters.

The CDIP 1992 wave data set was selected as representative of nearshore wave conditions for the MCR. The CDIP station location is about 9.7 km (6 miles) north of the project. The 1992 data set had a more continuous period of record than any of the other CDIP wave year records. This CDIP data file did not include the wave direction parameter. The CDIP time series data were recorded at a variable time interval, usually centered on a 3- or 6-hr nominal value.

The USAEC Wave Information Study (WIS) has developed a technique for generating a simulated wave database for any length of time desired by using a finite length of record of measured wave data to compute a matrix of coefficient multipliers. Direct comparison of the measured wave data to WIS simulated wave data for the same time period is necessary to ascertain the accuracy of the WIS simulated data. To facilitate direct comparison of the measured wave data to the synthetically generated (WIS) wave data, the CDIP wave time series was resampled at a constant 3-hr interval. The resampling algorithm used a piece-wise linear interpolation scheme. The resampled CDIP wave time series is shown in the top of Figure 11 for wave height, and in the top of Figure 12 for wave period.

Simulated WIS wave data

A synthetic time series for the annualized wave environment at the MCR was generated using a PC program Height Period and Direction SIMulation (HPDSIM) developed under the DRP (Borgman and Scheffner 1991). The program uses a finite length wave record to compute a matrix of coefficient multipliers that can be used to generate arbitrarily long time sequences of simulated wave data which preserve the primary statistical properties of the source finite data set. The wave height, period, and direction for the synthetic data set are based upon the 20-year WIS sta 22, Phase III database (Jenson and Hubertz 1989). WIS sta 22 is located offshore and south of Clatsop Spit in Oregon about 9.7 km (6 miles) south of the MCR.

[1] This section is extracted essentially verbatim from USAED, Portland (1995a).

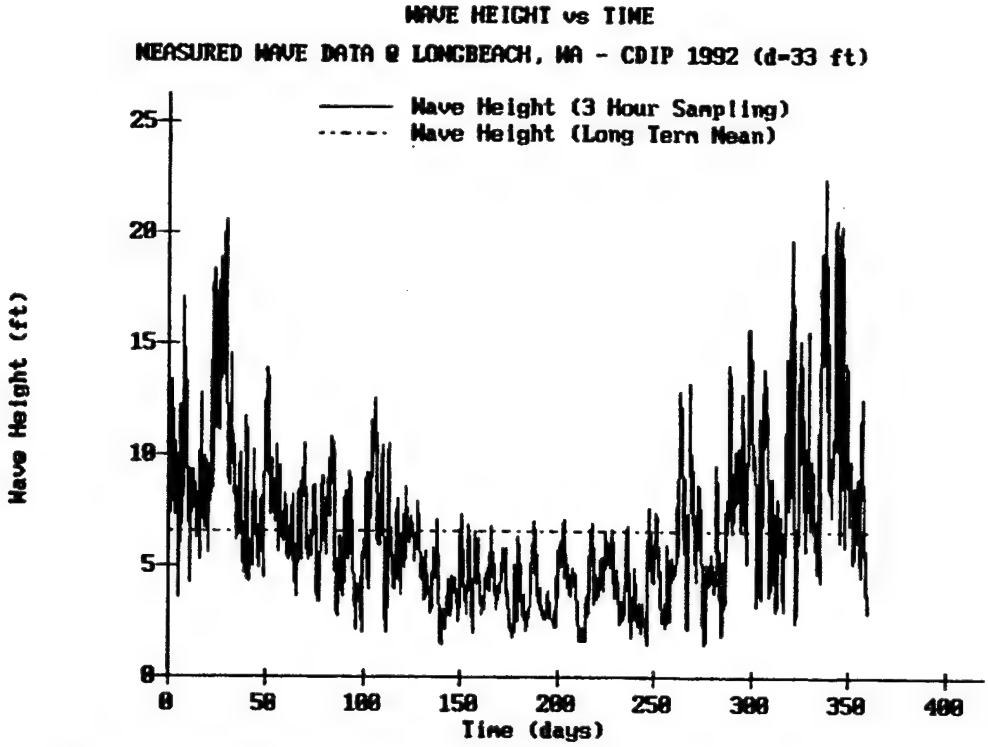

a. Measured wave height

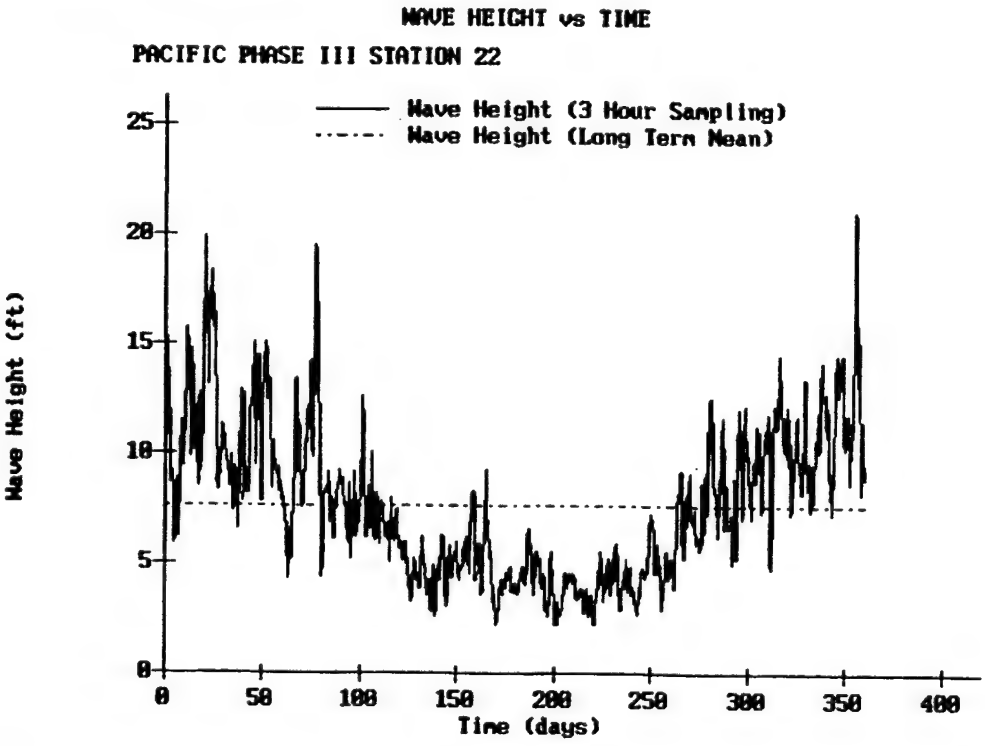

b. Simulated wave height

Figure 11. Measured CDIP wave height near MCR, and simulated wave height near MCR (after USAED, Portland, 1995a)

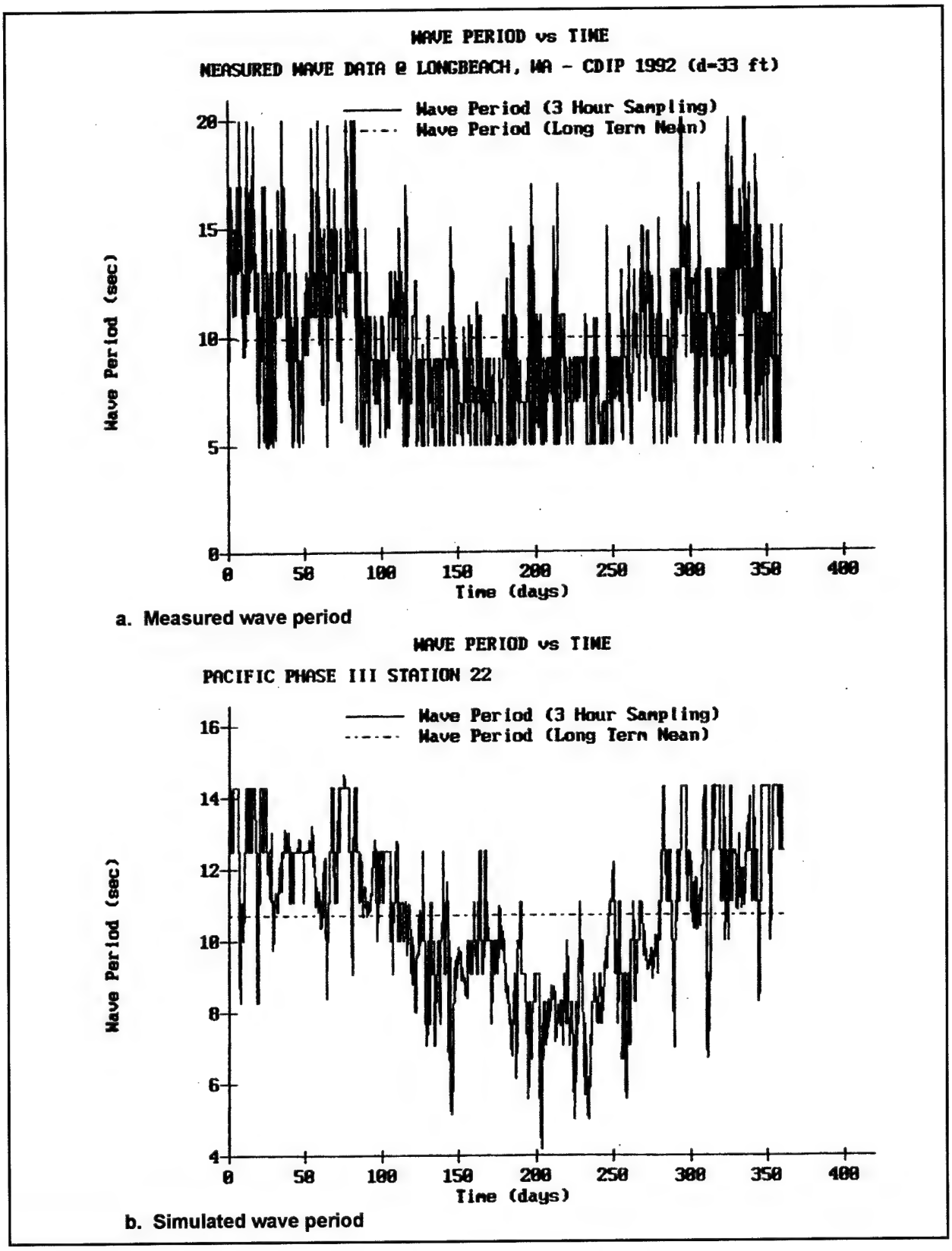

Figure 12. Measured CDIP wave period near MCR, and simulated wave period near MCR (after USAED, Portland, 1995a)

Seasonal WIS parameters for sta 22. Summary seasonal statistics for sta 22 are:

Shoreline azimuth = 158 deg N.

Water depth = 10.1 m (33 ft) mllw

$H_{1/3}$ = average annual significant wave height = 2.4 m (7.87 ft)

σ_h = annual standard deviation of $H_{1/3}$ = 1.1 m (3.61 ft)

T_s = wave period (associated with $H_{1/3}$) = 11 sec

σ_T = annual standard deviation of T_s = 2.5 sec

Most frequent wave direction band = 218 deg N.

Extreme Event WIS parameters for sta 22. Summary extreme event statistics for sta 22 are:

Maximum $H_{1/3}$ = 7.1 m (23.2 ft)

Maximum T_s = 16.7 sec

Direction associated with maximum $H_{1/3}$ = 233 deg N.

An example of the simulated wave environment (l-year duration, time = 0 corresponds to January 1) is shown in the bottom of Figures 11 and 12. Note that the waves are more severe during the late fall, winter, and early spring than other times of the year. The maximum and minimum wave heights for the synthetic wave year were about 6.4 m (21 ft) and0.8 m (2.5 ft), respectively. The average wave height was 2.3 m (7.6 ft). The maximum and minimum wave periods were 14.5 sec and 4 sec, respectively. The average wave period for the synthetic time series was 11 sec. The higher wave periods for the WIS data set appear to be truncated at 14.5 sec. It has long been observed that large waves in the northwest Pacific have periods that exceed 20 sec. The effect of wave period upon sediment mobility will dictate whether the apparent underprediction of wave period by the WIS data requires improvement for purposes of using WIS-based time series in the DRP sediment fate models.

Comparison of measured CDIP to simulated WIS wave data

The wave height time series for the two data sets (Figure 11) are well correlated, both in terms of seasonality and magnitude. The maximum wave height for the CDIP data is 6.7 m (22 ft), about 0.3 m (1 ft) higher than the synthetic WIS data set. The average wave height for the CDIP data set is 2.0 m (6.5 ft), about 0.3 m (1.1 ft) lower than the WIS data set.

The seasonality of wave period time series for the CDIP data set is somewhat coherent with the WIS wave period time series. The CDIP wave period is truncated below 5 sec due to attenuation of smaller period waves in gauge water depth of 10.1 m (33 ft).

The WIS wave period is truncated above 14.5 sec due to the method of resolving peak spectral wave period. The wave environment in the Pacific Northwest is characterized by a bimodal spectrum. There is typically a dominant wave period associated with locally generated sea (T_{sea}) that is different from the dominant period associated with swell (T_{swell}). Swell wave periods typically exceed 18 sec, whereas locally generated waves rarely exceed 15 sec. In the case of this synthetic data set for WIS Phase III sta 22, the peak spectral period assigned to the WIS database was based upon the locally generated seas. This is why the WIS wave period shown in the bottom of Figure 12 is truncated at 14.5 sec. The reported wave height is based on the root-mean-square (rms) value of (H_{sea} and H_{swell}) (Jenson and Hubertz 1989).

The maximum wave period for the CDIP data is 20 sec, 5.5 sec larger than for the WIS data. The mean value for CDIP wave period is 10 sec, 1 sec lower than for the WIS data. It appears that the variability of the CDIP wave period is in the higher end, whereas the variability of the WIS wave period is in the lower end. Although the maximum wave period and wave height for the 1992 CDIP data are greater than for the WIS data, the persistence of the WIS data is biased toward the higher values of wave period. The persistence of the WIS time series affects both the average values for wave height and period (i.e., the average WIS parameters are slightly higher than the observed CDIP parameters).

Need for additional wave data

The initial assessment of the synthetically generated wave data for the MCR indicates fairly good agreement with measured wave data obtained along the open coast for the 1992 wave year. The most important parameter, wave height, is matched very well between the two data sets. Wave period is not matched as well, especially for the larger wave periods where the WIS data falls 28 percent short of the measure CDIP values (due to the WIS being based on T_{sea}). The fact that the CDIP wave data was obtained along the open coast away from the direct influence of MCR requires additional prototype measurement for waves in the vicinity of the MCR ODMDS to resolve the uncertainty due to the MCR influences upon incoming waves. Influences include not only complex river current interactions with incident waves, but also high bathymetric gradients. The focus of wave data collection for this MCNP study is not to investigate the interactions of bathymetry and current upon waves, but to collect wave data that accurately reflect the average, seasonal, and extreme conditions present at the ODMDS under investigation. Only then can the DRP models be rigorously applied with certainty.

The requirement for these supplemental measured wave data (and other oceanographic phenomena) provided the impetus for the development and construction of four instrumented tripod platforms by Oregon State University (OSU) (Lund et al. 1999). These platforms were deployed and retrieved over four different time periods by OSU during the conduct of this MCNP study.

3 Regional Processes[1]

While there is a preponderance of data supporting net northward transport of sediment in the vicinity of the MCR, Lockett (1967) suggests that erosion of beach and shoreface sand south of the south jetty is related to blocking by the entrance jetties of southward-directed littoral material. Substantial sand deposition north of the north jetty (Peacock Beach) is used to support this contention as well. However, Komar and Li (1991) propose that erosion south of the entrance is related to a combination of factors, including blocking of southward-directed Columbia River sediment and reflection of waves arriving from southwest storms by the south jetty, causing large oblique angles to enhance southward sand movement and produce erosion.

Byrnes and Li (2001) performed detailed shoreline and bathymetric change analyses for the MCR and adjacent shelf and shoreline environments. Their primary interest was sediment transport associated with wind- and wave-induced currents. Data sources and potential error estimates, methodology of processing and analysis, and results are presented. Bathymetric surface models were developed for four historical time periods to evaluate regional sediment transport dynamics. Patterns of deposition and erosion relative to engineering activities were quantified to establish a framework upon which management strategies could be developed for dredged material disposal practices.

Data Sources

Two data sources were used for compiling shoreline and bathymetry measurements. National Ocean Service (NOS) T- and H-sheets provided the foundation upon which regional nearshore and coastal change analyses were determined; however, USACE hydrographic surveys were essential for filling gaps near the MCR in 1935. In addition, recent bathymetric surveys (1988 and 1994) at the Columbia River mouth represent the only data sets for making long-term comparisons of change. Methods used for compiling and analyzing historical data sets are described in Byrnes and Hiland (1994a, 1994b).

[1] Chapter 3 was written by Mark R. Byrnes and Feng Li, Applied Coastal Research and Engineering, Inc., Mashpee, MA (Byrnes and Li 2001).

Shoreline position

Three primary open coast shoreline surveys were conducted by the USC&GS (predecessor to NOS) in 1868/74, 1926, and 1948/57 for the area between Willapa Bay, WA, and Tillamook Head, OR (Table 2). The 1868/74 and 1926 surveys were completed as field surveys using standard planetable techniques, whereas the final survey was interpreted from aerial photography (1948/57). The 1935/36 survey was compiled for the estuarine shoreline of the lower Columbia River. Although the 1935/36 data were not used for quantifying shoreline position change, the data were used as the upland boundary for developing the 1926/35 bathymetric surface.

Table 2
Summary of Shoreline Source Data Characteristics for Coast Between Tillamook Head, OR, and Leadbetter Point, WA

Date	Data Source	Comments and Map Numbers
1868/74	USC&GS Topographic Maps(1:10,000)	First regional shoreline survey throughout study area using standard planetable surveying techniques; 1868 - seaward coast of Clatsop Spit east to Astoria, OR (T-sheets 1112 and 1123); 1869 - seaward coast of Peacock Spit east towards Megler, WA (T-sheets 1138, 1139a, and 1139b); 1871 - Leadbetter Point, WA (T-1261); 1872 - northern Long Beach Peninsula, WA (T-1293); 1873 - southern Long Beach Peninsula, WA (T-1341a, T-1341b); 1874 - Clatsop Plains to Tillamook Head, OR (T-sheets 1381a, 1381b, 1382b)
1926	USC&GS Topographic Maps1:10,000 (T-4250, T-4264)1:20,000 (T-4226, 4227, 4251, 4252)	Second regional shoreline survey along seaward coast of study area using standard planetable surveying techniques; Tillamook Head, OR, north to the Columbia River entrance (T-sheets 4226, 4227, 4250, 4264); Peacock Spit to Leadbetter Point, WA (T-sheets 4251 and 4252).
1935/36	USC&GS Topographic Maps1:5,000 (T-6383a, 6383b)1:10,000 (T-6480, 6481a, 6483a, 6483b, 6521b)	Topographic survey of interior shoreline for lower reaches of Columbia River from Astoria, OR, seaward to jettied river mouth between Peacock Spit, WA, and Clatsop Spit, OR; 1935 - T-sheets 6383a, 6383b, 6480, 6481a, 6483a, 6483b; 1936 - T-6521b.
July 1948/ August 1957	USC&GS Topographic Maps (1:10,000)	All maps produced from interpreted aerial photography; July 1948 - southern Clatsop Plains, just north of Tillamook Head, OR (T-10650); July 1950 - northern Long Beach Peninsula, at and just south of Leadbetter Point, WA (T-9637N, 9637S, 9634S); June 1955 - seaward extent of Peacock Spit next to the north entrance jetty (T-10344) and interior shoreline from Hammond, OR, seaward to the entrance jetties (T-10341, 10346, 10347, 10354, 10355, 10360); July 1957 - Clatsop Plains north to Long Beach Peninsula (T-10340, 10345, 10352, 10353, 10359, 10649) and middle Long Beach Peninsula (about 4.8 km (3 miles) of shoreline interpreted using USC&GS photography by Washington State Department of Ecology, Shorelands Program)

When determining shoreline position change, all data contain inherent errors associated with field and laboratory compilation procedures. These errors should be quantified to gage the significance of measurements used for research, engineering applications, and management decisions. Table 3 summarizes estimates of potential error for the shoreline data sets used in this study. Because these

Table 3
Estimates of Potential Error Associated with Shoreline Position Surveys

Traditional Engineering Field Surveys (1868/74, and 1926/35)		
Location of rodded points	±1 m	
Location of plane table	±2 to 3 m	
Interpretation of high-water shoreline position at rodded points	±3 to 4 m	
Error due to sketching between rodded points	up to ±5 m	
Cartographic Errors (all maps for this study)	**Map Scale**	
	1:10,000	**1:20,000**
Inaccurate location of control points on map relative to true field location	up to ±3 m	up to ±6 m
Placement of shoreline on map	±5 m	±10 m
Line width for representing shoreline	±3 m	±6 m
Digitizer error	±1 m	±2 m
Operator error	±1 m	±2 m
Aerial Surveys (1948/57)	**Map Scale**	
	1:10,000	**1:20,000**
Delineating high-water shoreline position	±5 m	±10 m

Sources: Shalowitz 1964; Ellis 1978; Anders and Byrnes 1991; Crowell et al. 1991.

individual errors are considered to represent standard deviations, root-mean-square (rms) error estimates are calculated as a realistic assessment of combined potential errors.

Positional errors for each shoreline can be calculated using the information in Table 2; however, change analysis requires comparing two shorelines from the same geographic area but different time periods. Table 4 is a summary of potential errors associated with change analyses computed for the specific time periods. As expected, maximum positional errors are associated with the oldest shorelines (±18.1 m (±59 ft) for 1868/74 to 1926), but most change estimates for the study area document shoreline advance or retreat greater than these values.

Table 4
Maximum Root-Mean-Square (rms) Potential Error for Shoreline Change Data, Adjacent to Mouth of Columbia River, WA/OR

Date	**1926**	**1948/57**
1868/74	±18.1[1]	±12.9
	(±0.3)[2]	(±0.1)
1926		±17.3
		(±0.5)

[1] Magnitude of potential error associated with high-water shoreline position change (m)
[2] Rate of potential error associated with high-water shoreline position change (m/year).

Bathymetry

Seafloor elevation measurements collected during historical hydrographic surveys are used to identify changes in nearshore bathymetry for quantifying sediment transport trends relative to natural processes and engineering activities. Three USC&GS bathymetry data sets and three USACE surveys were used to document seafloor changes between 1868/77 and 1994. Temporal comparisons were made for a 25-km (15.1-mile) coastal segment from 12 km (7.5 miles) north of the Columbia River entrance along Long Beach Peninsula to 6 km (3.7 miles) south of Point Adams along Clatsop Plains. Data extend offshore to about the 70-m- (230-ft-) depth contour at 12 km (7.5 miles) and into the lower estuary to a line between Grays Point and Tongue Point. The survey sets

consist of digital data compiled by the National Geophysical Data Center (NGDC) and analog information (maps) that had to be compiled in-house using standardized digitizing procedures (Byrnes and Hiland 1994b). The 1935 USACE entrance survey was compiled from a map containing a linear paper coordinate system with its origin at the Cape Disappointment Light. Ten local triangulation stations (coordinates obtained from USC&GS maps) located on the map were used to register the bathymetry data to a geographic coordinate system for comparison with USC&GS data sets. A spatial overlay was made with the 1935/36 USC&GS shoreline survey as a quality control check for positional accuracy of registered data; coincident points overlayed very well.

The earliest USC&GS survey was conducted in 1868/77 (Table 5). Nearshore data were registered in units of feet (0 to 18) and fathoms (greater than 18 ft). The density of points was good, but shoals shallower than 1.8 m (6 ft) mllw typically were not surveyed, presumably for safe navigation reasons. The offshore survey recorded few depths along a survey line, and longshore spacings of lines were about 3.5 km (2.2 miles) apart. Regardless, the nearshore depth values appear reasonable and, for the most part, compared well with more recent surveys. Most of the recent surveys were available as digital data; however, the 1935 USACE map and a couple of 1958 maps had to be digitized for incorporation in the data base. The 1988 and 1994 data sets were completed by the USACE as ebb-shoal surveys. They cover a slightly different area, so part of the 1988 survey was combined with the 1994 survey to create a composite surface for comparison with historical data sets.

Table 5
Summary of Bathymetry Source Data Characteristics for Area Between Tillamook Head, OR, and Long Beach Peninsula, WA

Date	Data Source	Comments and Map Numbers
1868/77	USC&GS Hydrographic Sheets 1:20,000 (H-1018 and H-1019) 1:40,000 (H-1379)	First regional bathymetric survey in study area, Leadbetter Point, WA, to Clatsop Plains, OR (south of the Columbia River entrance), including Mouth of Columbia River east to Astoria, OR; 1868 - Columbia River entrance east to Astoria, OR (H-1018 and H-1019); 1877 - Offshore Long Beach Peninsula and Columbia River mouth (H-1379)
1926/27	USC&GS Hydrographic Sheets 1:20,000 (H-4618 and H-4619) 1:40,000 (H-4634)	Offshore bathymetric survey from just south of the Columbia River entrance north to Leadbetter Point, WA; 1926 - nearshore surveys (H-4618 and H-4619); Offshore survey (H-4634)
1935	USACE Entrance Survey 1:10,000 (MC-1-203)	USACE bathymetric survey MC-1-203 conducted June 11, 1935 by Portland District survey personnel for the Columbia River entrance east to Warrenton, OR.
1958	USC&GS Hydrographic Sheets 1:10,000 (H-8421 and H-8423) 1:20,000 (H-8416 and H-8417)	Bathymetric survey of Columbia River entrance and adjacent shores; Offshore and entrance surveys (H-8416, H-8417, and H-8423); Interior entrance survey (H-8421)
1988	USACE Bathymetric Survey	Bathymetric survey conducted by the USACE Portland District in fall 1988 seaward of the Columbia River entrance and along the adjacent shores of Washington and Oregon.
1994	USACE Bathymetric Survey	Bathymetric survey conducted by the USACE Portland District in fall 1994 seaward of Columbia River entrance and along the adjacent shores of Washington and Oregon.

As with shoreline data, measurements of seafloor elevation contain inherent errors associated with data acquisition and compilation. Potential error sources for horizontal location of points are identical to those for shoreline surveys (see Table 2). These shifts in horizontal position translate to vertical adjustments of about ±0.3-0.5 m (±1.0-1.6 ft) based on information presented in USC&GS and USACE hydrographic manuals (e.g., Adams 1942). Corrections to soundings for tides and sea level change introduce additional errors in vertical position of ±0.1 to 0.3 m (±0.3 to 1.0 ft). Finally, the accuracy of the depth measurement adds error that is variable depending on the measurement method. Table 6 presents estimates of combined rms error for bathymetry surface comparisons. These estimates were used to denote areas of no significant change on surface comparison maps.

Table 6
Maximum Root-Mean-Square (rms) Potential Error for Bathymetry Change Data (m) for Area Between Tillamook Head, OR, and Long Beach Peninsula, WA

Date	1926/35	1958	1988/94
1868/77	±1.2	±1.1	±1.0
1926/35		±0.6	±0.5
1958			±0.4

Because seafloor elevations are temporally and spatially inconsistent for the entire data set, adjustments to depth measurements were made to bring all data to a common point of reference. These corrections include changes in relative sea level (zero for the study area) through time and differences in reference vertical datums. Vertical adjustments were made to each data set based on the time of data collection. All depths were adjusted to National Geodetic Vertical Datum (NGVD) and projected average sea level for 1994. The unit of measure for all surfaces was meters, and final values were rounded to one decimal place before cut and fill computations were made.

Shoreline Change

Shorelines for three time periods were compiled to document trends of advance and retreat between 1868/74 and 1950/57 between Leadbetter Point, WA, and Tillamook Head, OR. Regional changes in high-water shoreline position are illustrated in Figures 13 and 14. Overall, this shoreline reach has exhibited net advance for the period of record (2.2 m per year (7.2 ft per year) north of the Columbia River entrance and 5.5 m per year (18.0 ft per year) south of the entrance; Table 7). However, a couple of significant areas of erosion impact regional trends. The greatest amount of change along the coast occurred between 1868/74 and 1926 in response to jetty construction at the MCR. After construction of the south jetty, the previously subaqueous Clatsop Shoal became subaerial and translated the shoreline about 400 m seaward of its original position and approximately 4 km to the north. When the north jetty was completed in 1917, a large beach deposit formed north of the jetty to Cape Disappointment (about 3 km (1.9 miles) long, averaging 700 m (2,300 ft) wide; known as Peacock Beach). Along the northern portion of the study area, adjacent to the Willapa Bay entrance, shoreline retreat has been persistent since 1871 at about 2.3 m per year (7.5 ft per year). In fact, the length of coast impacted by retreat has increased by about 10 km (6.2 miles) over the period of record. The only

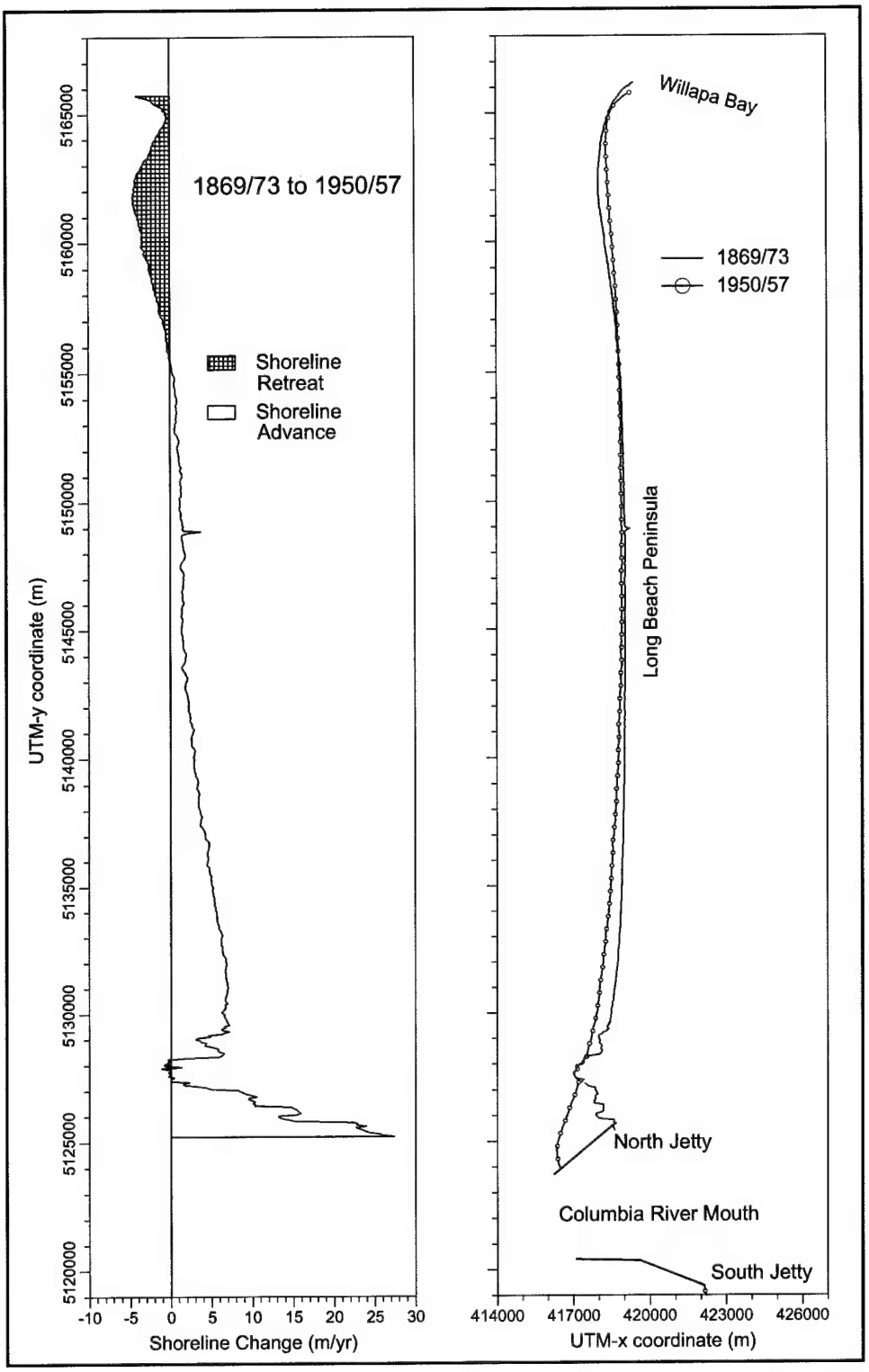

Figure 13. Shoreline change north of Columbia River to Leadbetter Point, WA, 1869/1873 to 1950/57 (after Byrnes and Li 2001)

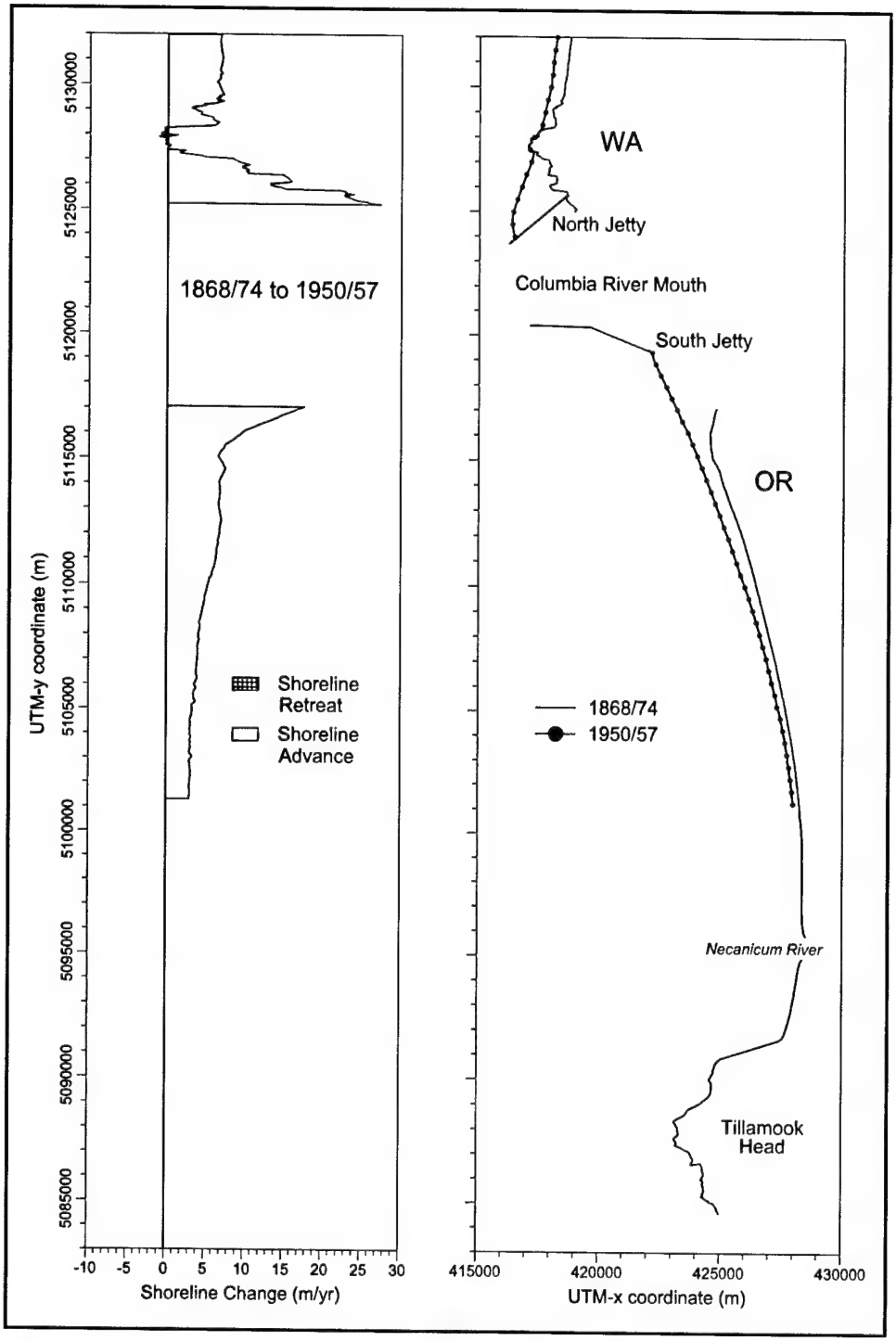

Figure 14. Shoreline change south of Columbia River to Tillamook Head, OR, 1868/74 to 1950/57 (after Byrnes and Li 2001)

Table 7
Shoreline Change Statistics for Study Area

Cell	1868/74 to 1926			1868/74 to 1950/57			1926 to1950/57		
	Alongshore Distance (km)	Mean (m/year)	Range (m/year)	Alongshore Distance (km)	Mean (m/year)	Range (m/year)	Alongshore Distance (km)	Mean (m/year)	Range (m/year)
1	1.6	1.8	0 to 4.0	--	--	--	--	--	--
2	6.0	-2.0	0 to -4.3	10.2	-2.3	0 to -4.5	17.3	-3.6	0 to -16.6
3	30.4	1.9	0 to 5.5	27.3	3.1	0 to 6.5	20.3	7.3	0 to 16.4
4	1.0	-0.5	0 to -1.0	0.7	-0.2	0 to -1.0	0.2	-1.0	0 to -2.0
5	1.7	12.9	0 to 28.0	2.3	13.0	0 to 27.4	3.6	11.7	0 to 19.1
5a	--	--	--	--	--	--	0.4	-2.9	0 to -3.9
Total	*40.7*	***1.7***		*40.5*	***2.2***		*41.8*	***2.9***	
6	17.4	5.5	0 to 30.5	15.8	5.5	3.0 to 17.6	5.1	-5.6	0 to -10.7
7	6.6	-0.5	0 to -1.9	--	--	--	13.2	5.9	0 to 10.5
8	8.4	0.2	-1.5 to 2.5	--	--	--	--	--	--
Total	*32.4*	***3.2***		*15.8*	***5.5***		*18.3*	***2.6***	

other area to exhibit significant erosion is just south of the Columbia River south jetty between 1926 and 1957. The 5-km (3.1-mile) length of coast south of the jetty exhibited a retreat rate of 5.6 m per year (18.4 ft per year) up to 1957. Komar and Li (1991) state that recent surveys indicate a slowing of the retreat rate to near stability by the mid 1980s. Shoreline change away from entrances (north and south) illustrates the same trend; net advance associated with sediment derived from the Columbia River.

Although general shoreline change trends provide a regional overview of coastal response, evaluating spatial changes for each time interval establishes a method to analyze change for segments of coast with similar patterns of shoreline movement. The benefit of this analysis is that it defines natural breaks in shoreline response to incident processes, providing important data for quantifying historical depositional processes. Figures 15-18 document spatial variability in shoreline change for the period of record. Figure 15 illustrates shoreline change north of the Columbia River entrance to Leadbetter Point for the period 1869/73 to 1926. Fine sand transported to the north from the Columbia River resulted in shoreline accretion along much of this 42-km (26.1-mile) segment of coast. However, shoreline retreat downdrift of the entrance to Willapa Bay departs noticeably from the overall trend of shore advance. This 6-km (3.7-mile) stretch of coast has an average retreat rate of 2.0 m per year (6.6 ft per year) (maximum retreat of 4.3 m per year (14 ft per year); Table 7), likely related to wave energy focusing around the entrance shoal to Willapa Bay. It appears that sediment is transported away from the erosion nodal point, north and south to adjacent beaches (near normal distribution of the erosion zone) during the time of erosion. The process is contrary to the trend of net accretion, but consistent with littoral sediment transport processes during summer months when winds and waves are from the north. The only other zone of erosion is associated with the shoreline outlining Cape Disappointment. Although net erosion is documented (0.5 m per year (1.6 ft per year); Table 7), the magnitude of change is close to potential error estimates, and the coast in this area would be most difficult to map.

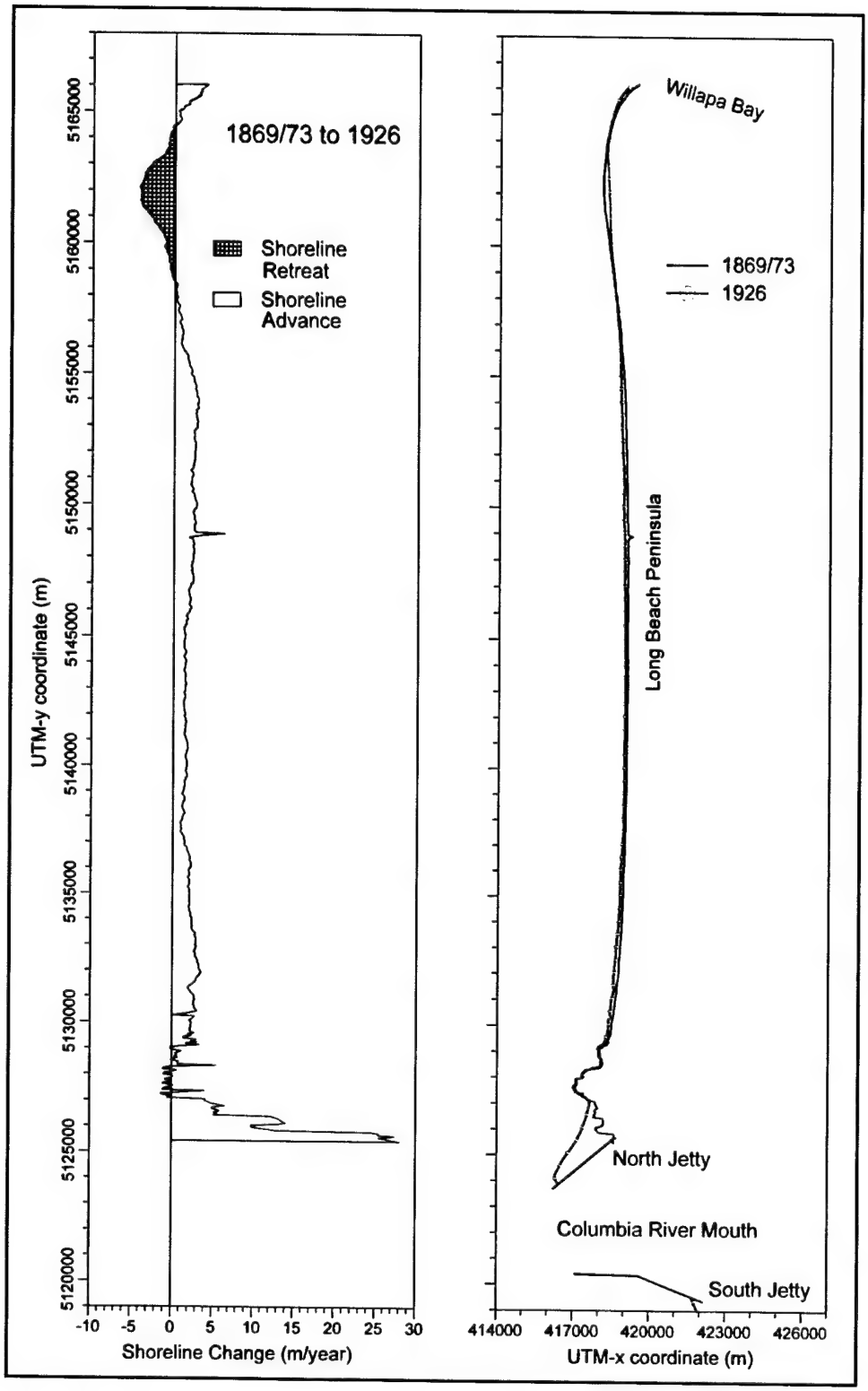

Figure 15. Shoreline change north of Columbia River to Leadbetter Point, WA, 1869/73 to 1926 (after Byrnes and Li 2001)

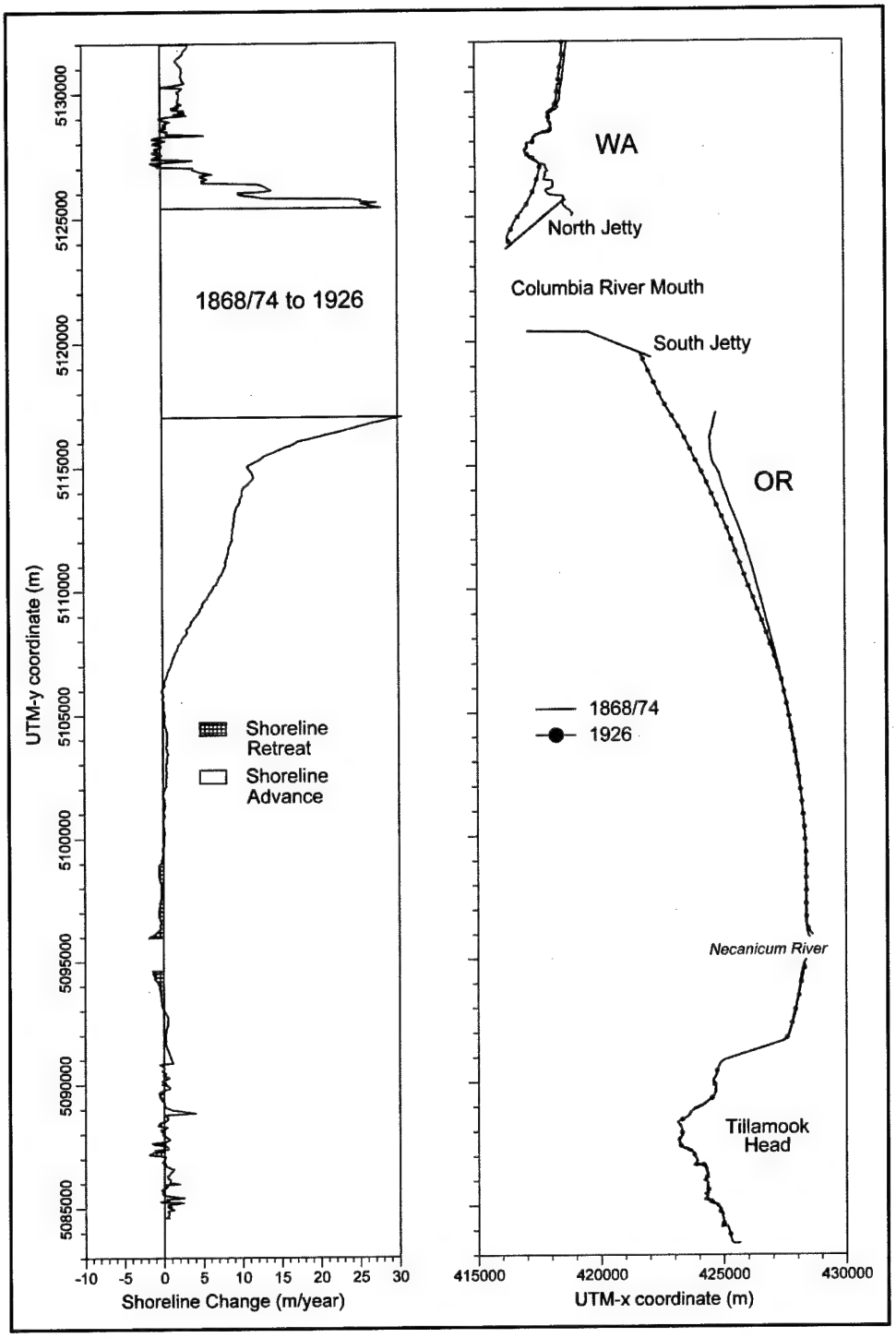

Figure 16. Shoreline change south of Columbia River to Tillamook Head, OR, 1868/74 to 1926 (after Byrnes and Li 2001)

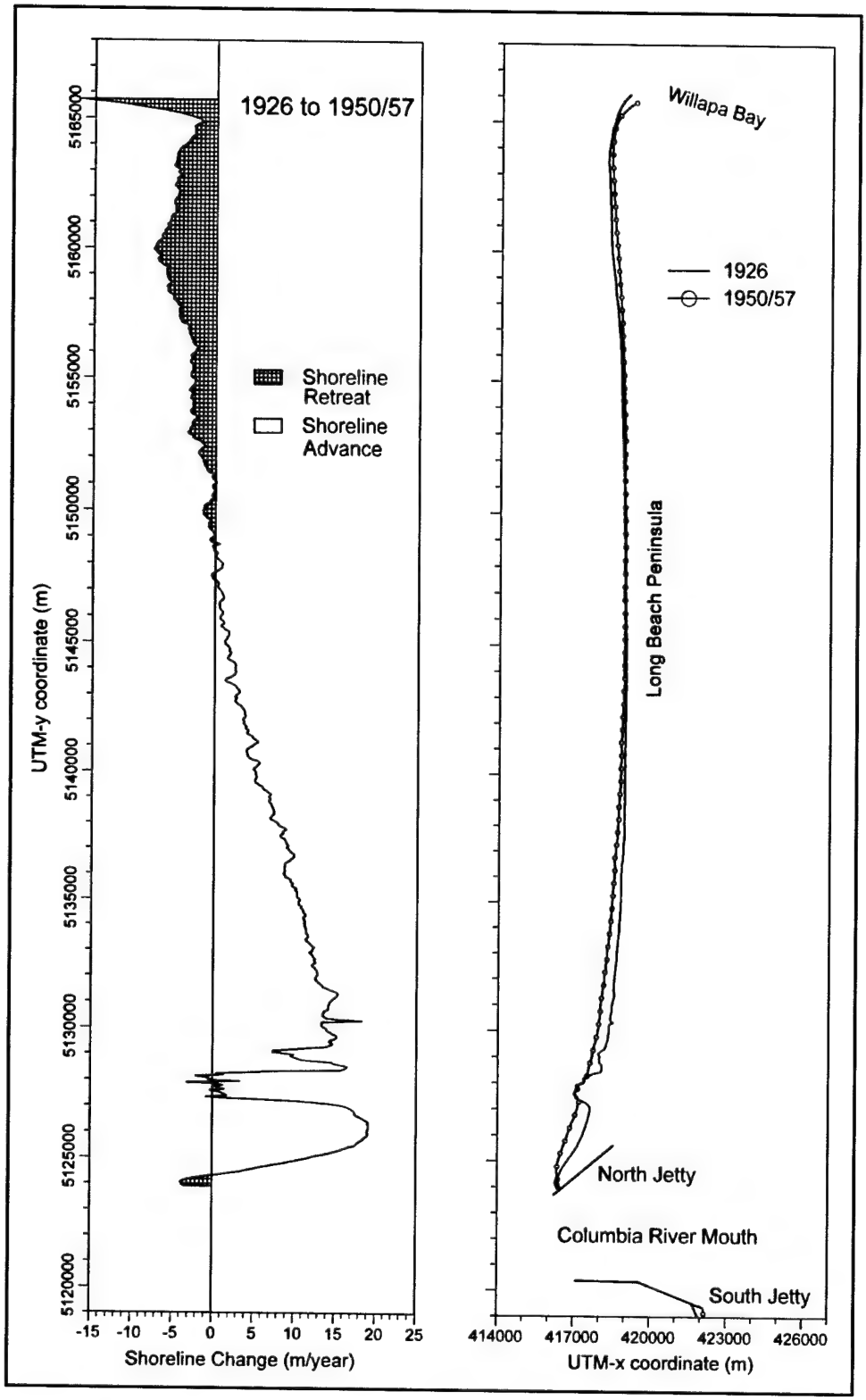

Figure 17. Shoreline change north of Columbia River to Leadbetter Point, WA, 1926 to 1950/57 (after Byrnes and Li 2001)

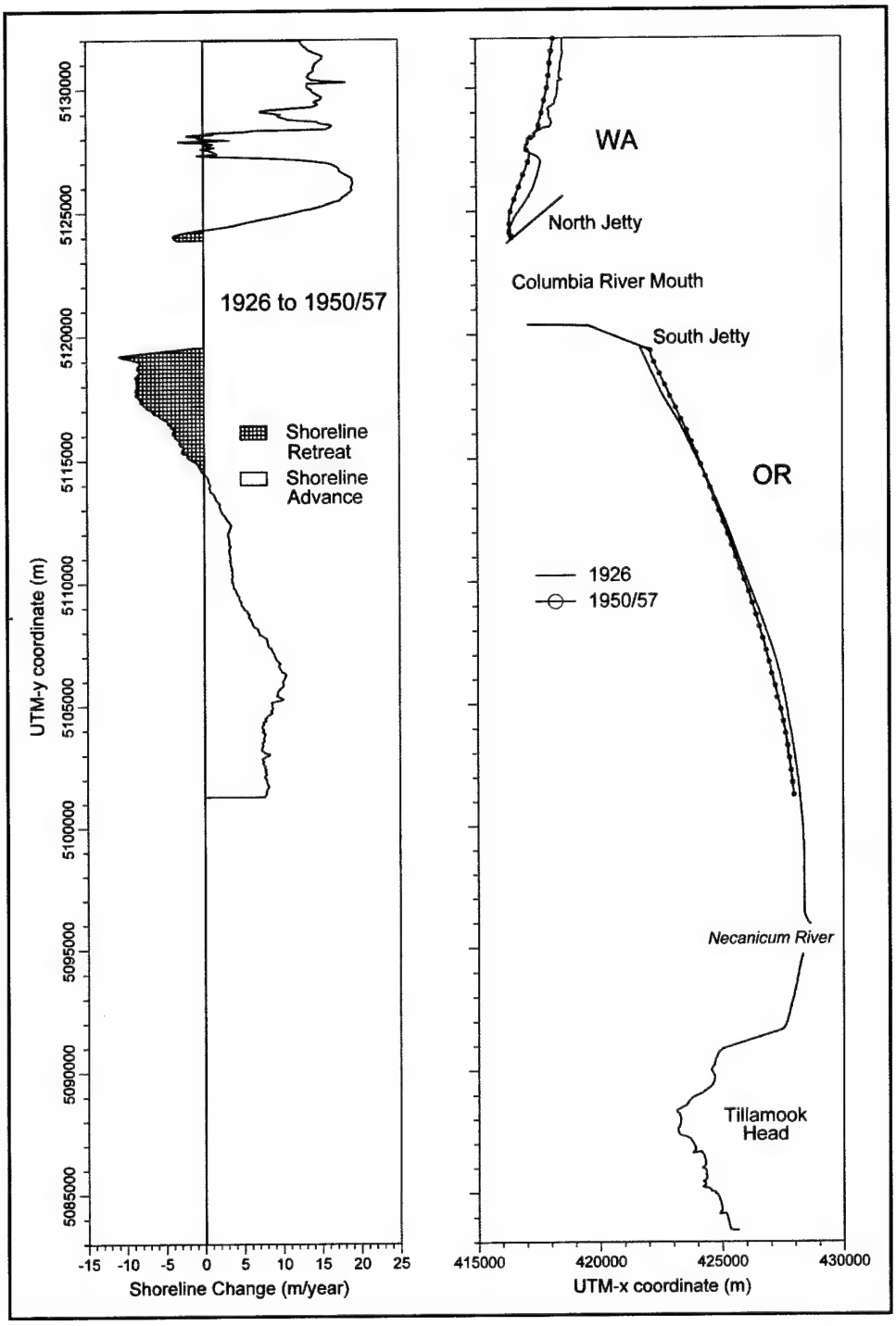

Figure 18. Shoreline change south of Columbia River to Tillamook Head, OR, 1926 to 1950/57 (after Byrnes and Li 2001).

The massive area of sand deposition between the south side of Cape Disappointment and the seaward tip of the north entrance jetty (Peacock Beach) is the result of jetty construction and blockage of sand transport back into the entrance. Prior to jetty construction, a shallow subaqueous shoal existed in this area, providing the platform upon which the 1926 shoreline was formed. The rate of shoreline advance was 12.9 m per year (42.3 ft per year) with a maximum advance was 28.0 m per year (91.8 ft per year), and the area encompassed 245 ha (605 acres).

Figure 16 shows shoreline response south of the Columbia River entrance for the period 1868/74 to 1926. There is a marked zone of accretion south of the south jetty for about 17 km (9.3 miles). This region of accretion does not include the 3-km-long (1.9-mile-long) fillet that formed south of the jetty when Clatsop Shoal became subaerial because an 1868/74 reference shoreline was south of this point at the time. Consequently, the zone of sediment accretion extended 20 km (12.4 miles) south of the jetty in 1926. South of this point, very little deposition or erosion occurred for the next 15 km (9.3 miles) down to Tillamook Head (Figure 16; Table 7). Net shoreline change from the south jetty to Tillamook Head (32 km (19.9 miles)) for the period of analysis is 3.2 m per year (10.5 ft per year).

Between 1926 and 1950/57, some dramatic changes in shoreline response occurred north and south of the Columbia River entrance. The zone of erosion along the northern shoreline of Long Beach Peninsula expanded to 17 km (10.6 miles) of coast from Leadbetter Point to the south. The rate of retreat also increased to 3.6 m per year (11.8 ft per year), resulting in a chronic coastal erosion problem. The zone of shoreline advance south of the erosion area decreased in length, but the average rate of accretion increased more than threefold from 1.9 to 7.3 m per year (6.2 to 23.9 ft per year), creating a wide beach just north of Cape Disappointment. The beach south of Cape Disappointment to the north jetty continued accreting at an average rate of about 12 m per year (39.4 ft per year) (Table 7); however, a small segment of beach adjacent to the north jetty tip exhibits net erosion of 2.9 m per year (9.5 ft per year). Shoreline change recorded along the seaward margin of Cape Disappointment was erratic but consistent with earlier trends.

South of the Columbia River entrance, shoreline retreat dominated for the first 5 km (3.1 miles) of beach at a rate of 5.6 m per year (18.4 ft per year) (Figure 16; Table 7). This is in stark contrast to the 5.5 m per year (18.0 ft per year) of shoreline advance for the previous time period. However, south of this point to the limit of data coverage, the shoreline exhibits net advance at a rate of 5.9 m per year (19.3 ft per year). Overall, the shoreline south of the south jetty shows net advance of 2.6 m per year (8.5 ft per year). It is likely that a portion of the sediment eroded from the beach just south of the south jetty contributes to deposition along Clatsop Plains, the area of shoreline advance.

In summary, the signature of shoreline advance is dominant throughout the period 1868/74 to 1950/57. However, two hot spots of erosion were identified, both associated with entrances. One is along the northern end of Long Beach Peninsula; this appears to be an area of chronic erosion because the magnitude and extent of shoreline retreat have increased with time. The second erosion area

exists just south of the south jetty, likely associated with a decrease in sediment supplied to the local area due to blockage by the jetty and wave energy reflection off the jetty from southwest waves, creating large oblique angles (opening to the south) with the shoreline and beach retreat (Komar and Li 1986). The rest of the study area exhibits increasing shoreline advance with time in a sediment-rich system supplied by the Columbia River.

Regional Bathymetry and Change

Hydrographic surveys of regional nearshore morphology provide a direct source of information for quantifying changes in seabed elevation. This type of analysis is used to document trends in regional-scale coastal evolution, and to evaluate the impact of natural processes and human influences on coastal sediment dynamics. Seafloor elevations to 70-m (230-ft) water depth were compiled and analyzed to identify patterns of erosion and deposition associated with the Columbia River entrance and adjacent nearshore environments. This depth was chosen as the offshore boundary of shelf sediment transport based on threshold of sediment motion calculations under waves and currents (Sternberg 1986) within the study area. The inner shelf littoral zone was defined by the 15-m (49.2-ft) NGVD depth contour as the seaward boundary for significant annual sand transport due to wave action. This means that when evaluating the Hallermeier (1981) equation for determining significant sand transport under steady wave action (d_l) for an extreme wave height exceeded 12 hr per year in the study area, the limit depth for appreciable yearly bottom erosion is about 15 m (49.2 ft). Before using this depth contour for defining the littoral zone boundary, we compared its position with bathymetry change results. In all cases, a clear boundary between change and no change areas for long-term, regional data sets was observed near the position of the 15-m (49.2-ft) depth contour. Besides onshore and offshore zones, specific polygons were established for Columbia River deposits and the entrance channel to differentiate changes north and south of the Columbia River from tidally driven sedimentation processes at the entrance. Specific polygon boundaries will be presented prior to discussing surface change results. Procedures used to quantify changes in seabed elevation are detailed in Byrnes and Hiland (1994a).

Bathymetry surfaces

The primary feature affecting coastal sediment erosion and accretion throughout the study area is the Columbia River entrance. Prior to jetty construction, the entrance and system of shoals appeared typical of fluvial-dominated estuarine entrances (Hayes and Kana 1976; Reinson 1992). Regional characteristics of nearshore morphology for the entrance to the Columbia River estuary and adjacent shelf environs (1868/77) is illustrated in Figure 19. All significant bathymetric features are associated with the lower estuary and entrance shoal/channel deposits. First, the braided channel features of the lower estuary give way to a single primary channel exiting the coast in a south-southwest direction. Substantial shoal deposits exist in the lower estuary and entrance area as a result of sediment input from the river and nearshore marine environments (Lockett 1967; Barnes, Duxbury, and Morse 1972; McManus

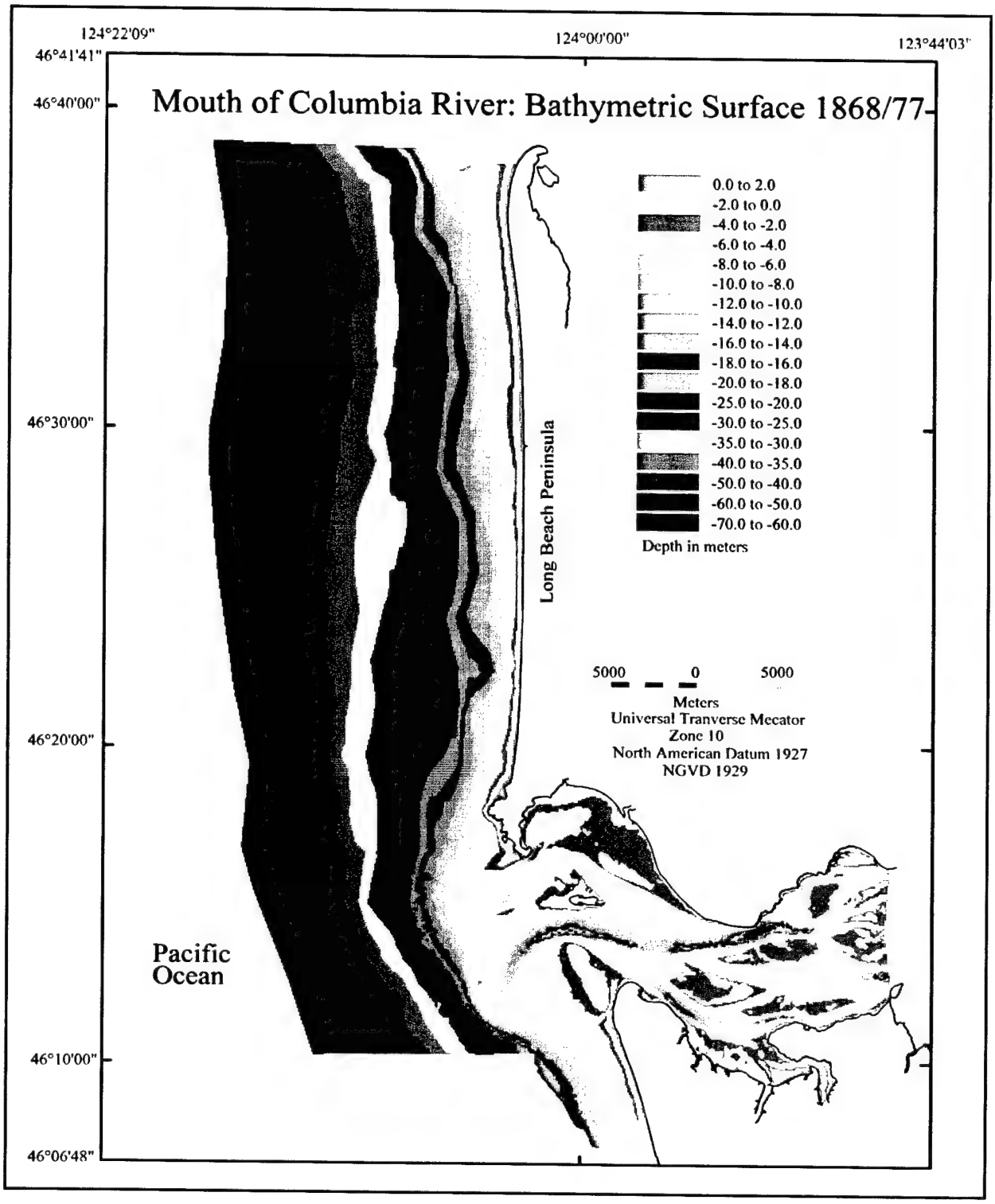

Figure 19. Nearshore bathymetry 1868/77 at and adjacent to MCR, WA/OR (after Byrnes and Li 2001)

1972). A large sand shoal is present along the south margin of the entrance (Clatsop Shoal), extending in a northwest direction off Point Adams. It is about 4 km long and controls channel position and orientation in the entrance area. To the north, seaward of Cape Disappointment, a smaller shoal extends southwestward from the rocky headland along the north margin of the entrance. In between, Sand Island and adjacent shoals and deposits associated with the ebb-tidal delta seaward of the entrance made navigation during peak flows and high-energy events challenging. The shield of the Columbia River ebb shoal is defined by the 20-m (65.6-ft) NGVD depth contour. The continual shifting of these shoals and channels prompted the USACE to propose jetties to control sedimentation processes in the entrance area (Lockett 1967).

From the sedimentation patterns and channel configuration documented in the entrance area, the net direction of transport supplying this system from the marine environment is to the north. Although the channel is skewed to the south-southwest, very little ebb-shoal sediment exists south of the channel as it exits the coast. All of the sediment is deposited north and west of the main channel as a series of shoals. In addition, Clatsop Shoal, along the southern margin of the entrance, was formed by northward-directed transport of sand along the northern Oregon coast and by hydraulic trapping of sediment derived from the river mouth, where the net northward longshore current meets water and sediment exporting the coast at the entrance.

Figure 20 depicts shoal and channel configuration at the Columbia River mouth in 1926/35, after construction of the jetties. Jetty placement has trained the river flow to exit the coast in a southwesterly direction, and sediment has been jetted farther offshore forming a well-defined ebb-tidal delta. The outer edge of the ebb-delta is now defined by the 30-m (98.4-ft) depth contour, and the shoal is approximately 2 km (1.2 mile) seaward of its position in 1868/77. The location of the main channel has shifted to the north where Sand Island used to exist, and the channel is about 5 to 8 m (16.4 to 26.2 ft) deeper. As such, sand deposition from the river mouth when it opened to the south has ceased, resulting in net erosion and contour retreat south of the south jetty.

Adjacent to the entrance, substantial beach deposits have formed in response to jetty construction. To the south, Clatsop Shoal provided the platform for Clatsop Spit, a 5-km- (3.1-mile-) long sand deposit extending seaward and north of the 1868 shoreline past the jetty and into the southern reaches of the entrance channel. This deposit clearly is the result of net northward directed littoral sand transport. North of the north jetty, beach accretion southwest of Cape Disappointment has created a 4-km (2.5-mile) length of shore known as Peacock Beach. Again, this deposit has formed on top of a pre-existing subaqueous shoal resulting from northward sediment transport from the river outlet. In addition to seaward growth of the ebb-shoal, the centroid of deposition has shifted north, and a pronounced subaqueous attachment point exists seaward of the Peacock Beach shoreline, indicating sand bypassing from the river mouth north towards Long Beach Peninsula. Finally, portions of the estuary entrance have filled rapidly (bay east of Cape Disappointment; north side of the south jetty) in response to training structures keeping flow channeled. Although most of the sediment is derived from fluvial deposition, Lockett (1967) suggests that a significant

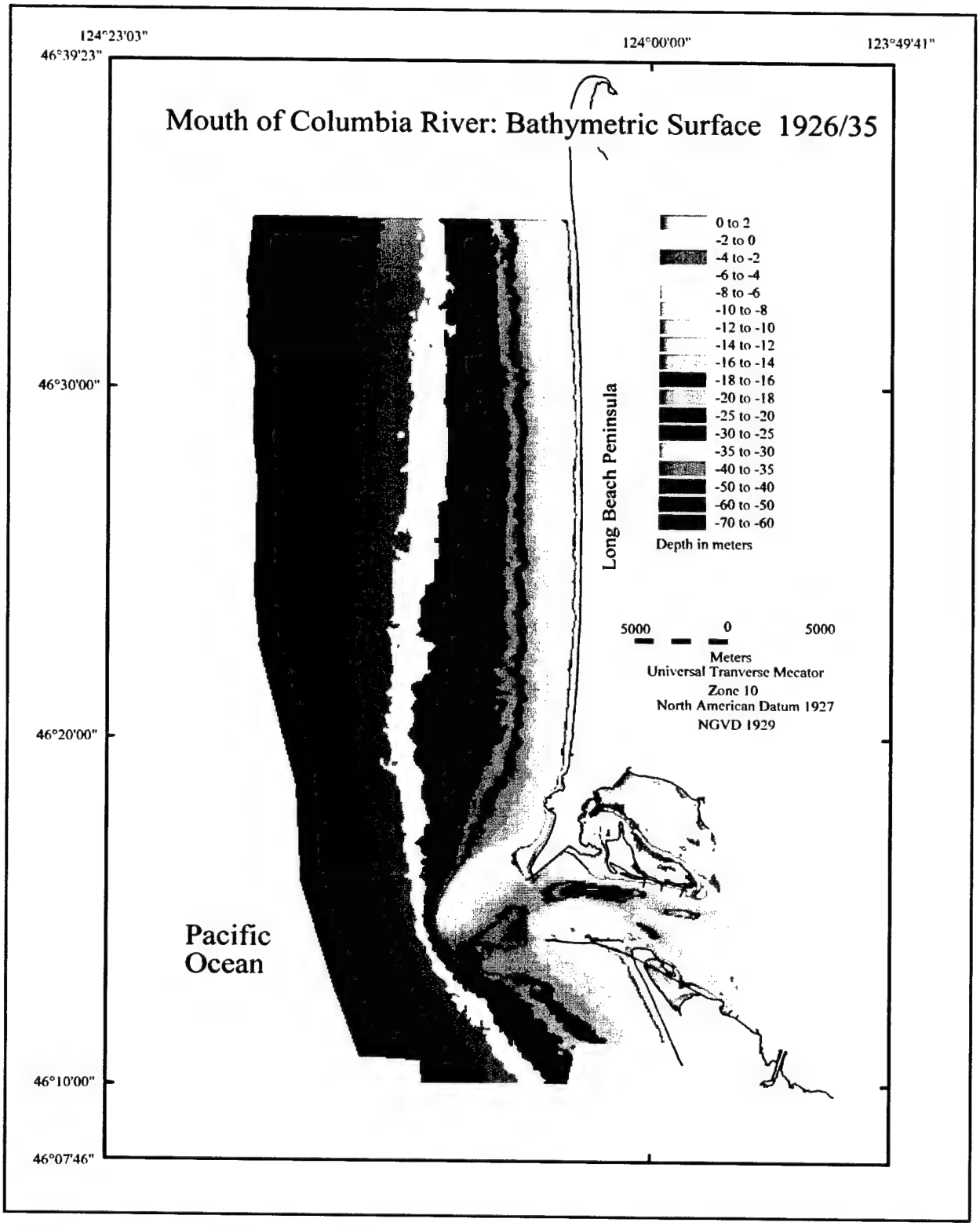

Figure 20. Nearshore bathymetry 1926/35 at and adjacent to MCR, WA/OR (after Byrnes and Li 2001)

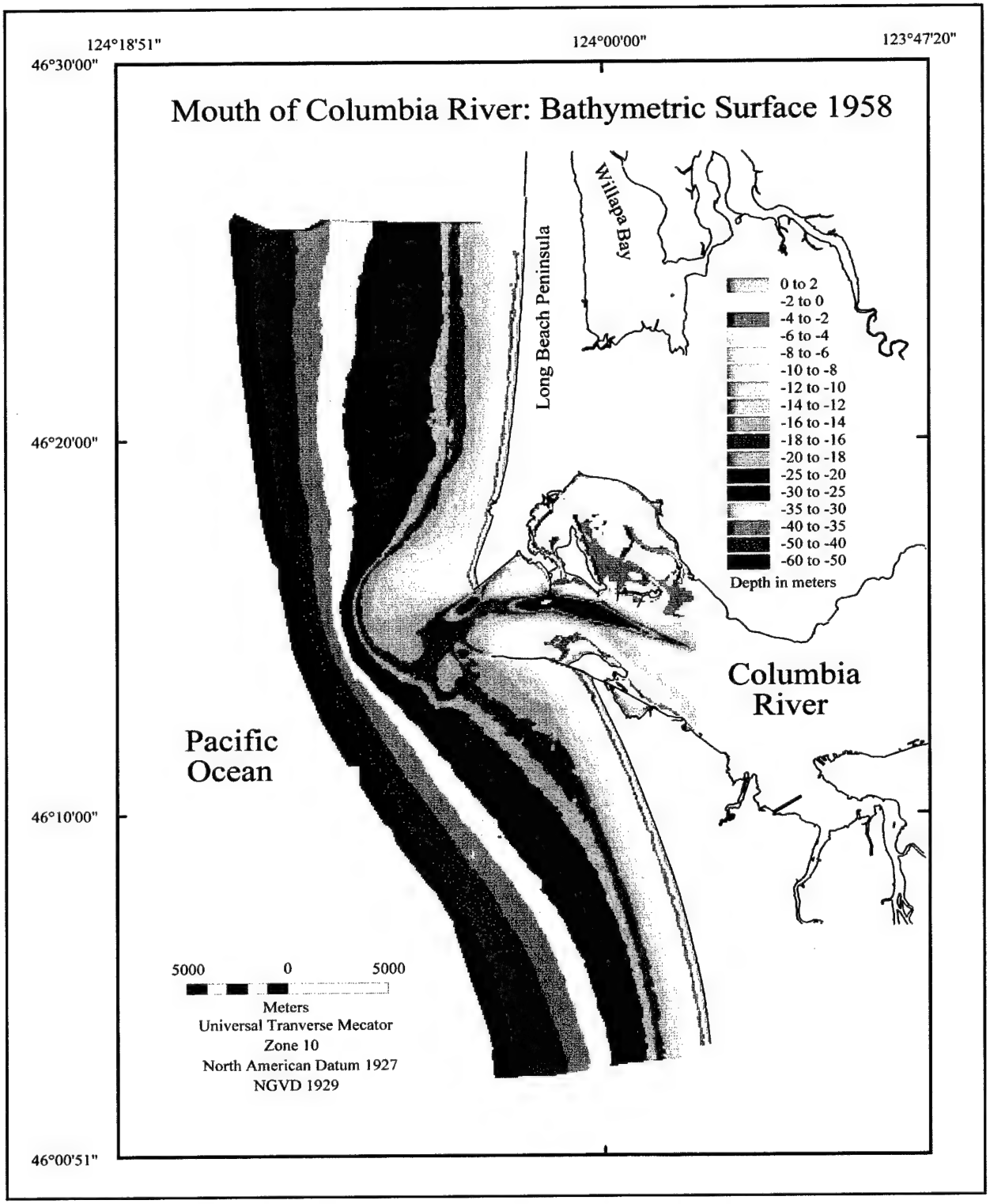

Figure 21. Nearshore bathymetry 1958 at and adjacent to MCR, WA/OR (after Byrnes and Li 2001)

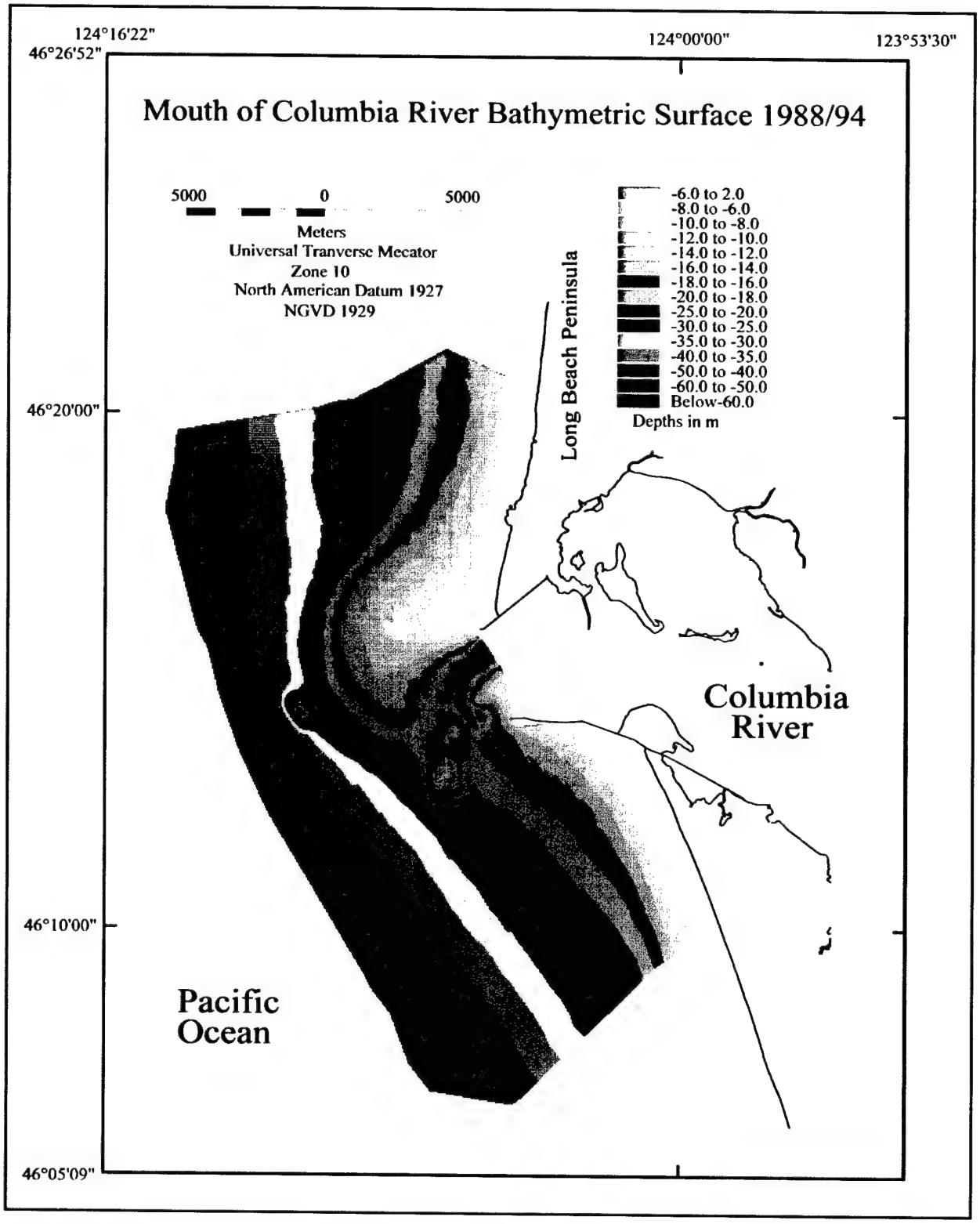

Figure 22. Nearshore bathymetry 1988/94 at and adjacent to MCR, WA/OR (after Byrnes and Li 2001)

amount of sediment filling the lower estuary is of marine origin (based on physical model results and seabed drifter data).

The 1958 bathymetry survey is the most recent regional data set for documenting change at the entrance and along the adjacent coast (Figure 21). A number of important changes have been recorded since 1926. First, the seaward edge of the ebb-tidal delta (30-m (98.4-ft) depth contour) extends just slightly seaward of the 1926 shoal of 0.3 km (0.2 miles), but the centroid of deposition has again shifted to the north, creating an extensive subaqueous shoal seaward of Peacock Beach. Significant beach accretion is indicated along southern Long Beach Peninsula, where Cape Disappointment is almost nonexistent due to beach accretion and shoreline advance. Northward directed sediment from the Columbia River has created seaward contour growth and beach accretion since the jetties were constructed. Conversely, the shoreline south of the south jetty that initially advanced due to northward sand transport and deposition along the south jetty, experienced substantial retreat between 1926 and 1958. Within the entrance, north of the south jetty, sand deposition and shoal growth continued, but shoreline retreat was dominant for a zone 5 km (3.1 miles) south of the jetty (see Figures 18 and 21). Channel orientation exiting the coast shifted slightly to the north, creating a west-southwest alignment. Channel depths along the thalweg increased slightly as the project depth increased with time.

The most recent bathymetric surface is a composite of the 1988 and 1994 USACE bathymetric surveys (Figure 22). It is a smaller survey than the previous surfaces, but it provides a recent snapshot of shoal growth and dredged material placement impacts since 1958. It is difficult to draw conclusions regarding shoreline response relative to 1958 (a recent shoreline survey was not available), but a few important changes are illustrated. First, the main channel is wider and deeper than in 1958, although its orientation has not changed significantly. Flow from two exit channels off the main channel encompasses ODMDS A and the existing sediment mound (14- to 20-m (45.9- to 65.6-ft) water depth). The last significant morphological change since 1958 exists seaward of the ebb-shield in 30-m water depth. This area is designated as ODMDS B and contains a 12-m-(39.3-ft-) thick sediment mound. ODMDS B likely has little influence on navigation (as long as mounding does not exceed the height of the ebb shoal) or local beach sediment transport, but ODMDS A appears to have direct impact on channel hydraulics, sedimentation, and navigation at the entrance. Lockett (1967) refers to ODMDS A as a problem area for dredging management.

Surface changes

To quantify changes in morphology, overlapping portions of bathymetric surfaces were compared for each time interval. Differences in elevation across a common surface area were calculated to assess sediment volume adjustments to natural processes and engineering activities. Bathymetric change polygons were established for each change model surface to quantify sediment cut and fill associated with significant geomorphic features throughout the study area. Between 1868/77 and 1926/35, massive adjustments in sediment volume occurred at the entrance where the ebb-tidal delta moved seaward about 3 km (1.9 miles), depositing approximately 189 million cu m (247 million cu yd) of

sediment in 30-m (98-ft) water depth (Figures 23 and 24; Table 8). The ebb shoal that formed is strongly skewed to the north, even though the channel exits the coast to the south-southwest. Deposition of northward directed sand from the ebb shoal created Peacock Beach, just north of the north jetty and south of Cape Disappointment. Clatsop Spit evolved in association with construction of the south jetty, creating a 5-km- (3.1-mile-) long beach and filling the 1868 entrance channel (136 million cu m (178 million cu yd) of sand) as the new channel shifted north and displaced Sand Island (Figure 24; Table 8). Sediment deposition north of the channel and in Bakers Bay of 117 million cu m (153 million cu yd), east of Cape Disappointment, appears to be the result of decreased flow in the area resulting from jetty placement and channel realignment. Conversely, seafloor erosion south of the south jetty is the result of decreased sediment supply to the area when the entrance channel shifted to the north, jetting much of its sediment load seaward to the ebb shoal (Figure 24). Sediment erosion associated with channel realignment and erosion south of the south jetty of 448 million cu m (586 million cu yd) controlled the sediment budget in the entrance area, resulting in an overall net deficit of about 11 million cu m

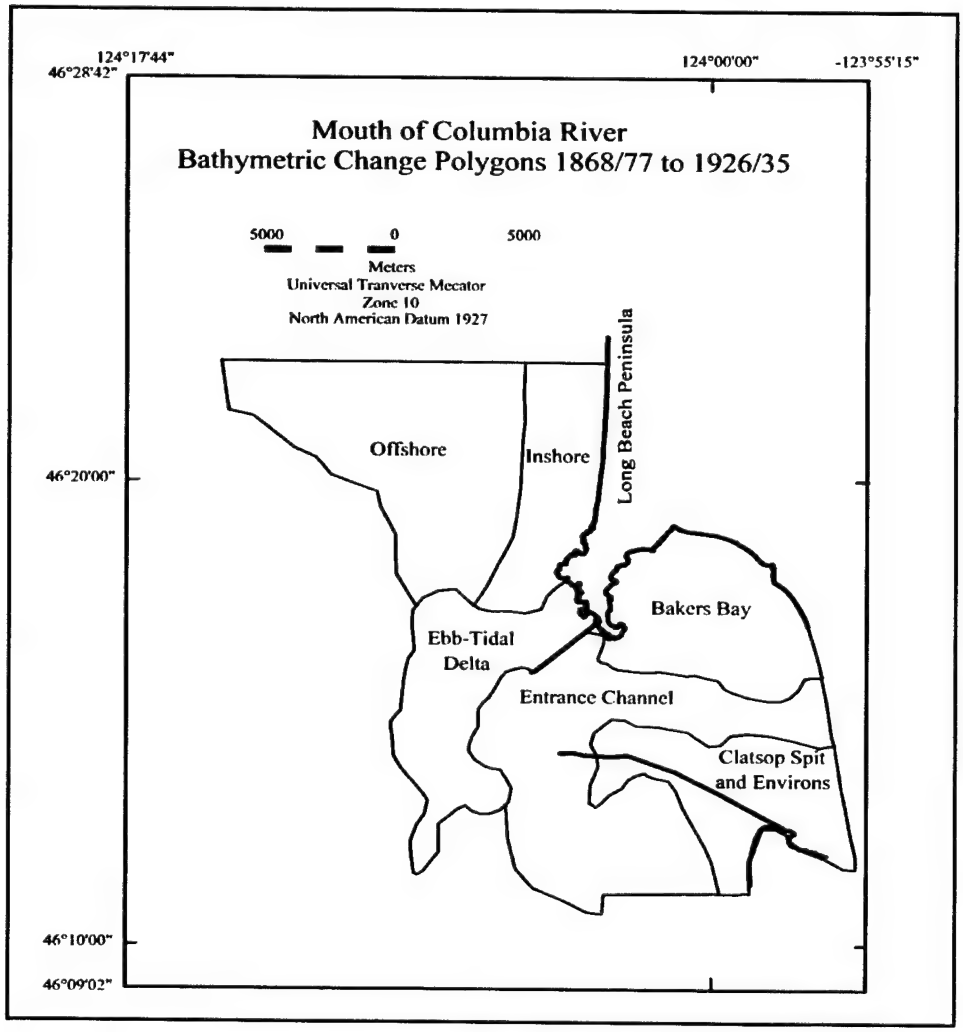

Figure 23. Polygon boundaries for sediment volume calculations across change surface, 1868 (after Byrnes and Li 2001)

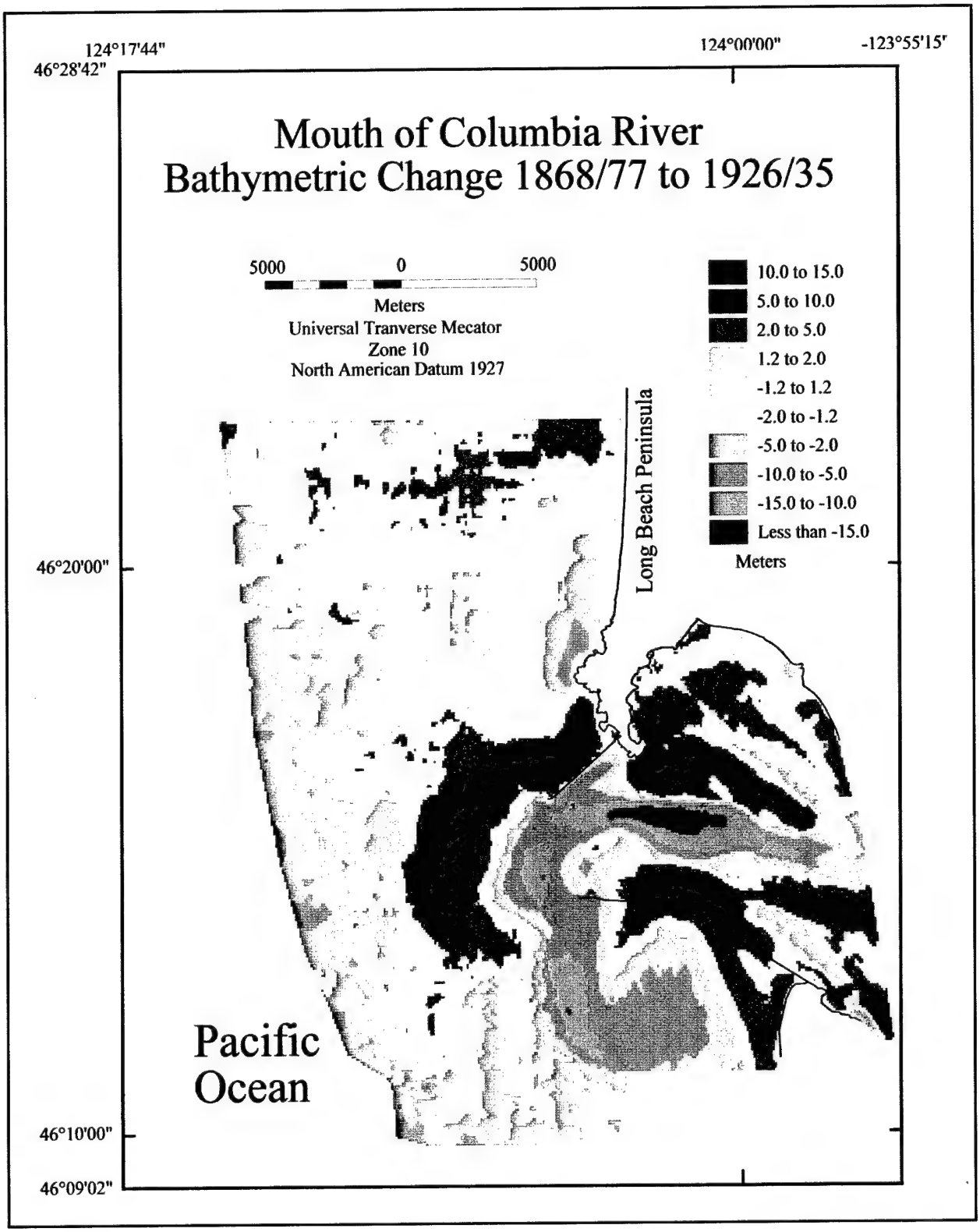

Figure 24. Bathymetric change 1868/77 to 1926/35 at and adjacent to MCR, WA/OR (after Byrnes and Li 2001)

Table 8
Bathymetric Change Statistics for Overall Study Area

	Deposition, cu m	Erosion, cu m	Net Change, cu m
1868/77 to 1926/35			
Ebb-Tidal Delta	188,950,000	470,000	188,480,000
Entrance Channel	1,590,000	449,170,000	-447,580,000
Clatsop Spit and Environs	136,250,000	9,770,000	126,480,000
Bakers Bay	117,390,000	8,370,000	109,020,000
Long Beach Peninsula - Inshore	13,830,000	35,060,000	-21,230,000
Offshore	48,960,000	21,340,000	27,620,000
Net Change	506,970,000	524,180,000	-17,210,000
1926/35 to 1958			
Ebb-Tidal Delta	128,530,000	200,000	128,330,000
Old Ebb-Shoal and Entrance Channel	11,170,000	62,940,000	-51,770,000
Clatsop Spit and Environs – Offshore	750,000	30,460,000	-29,710,000
Clatsop Spit and Environs – Inshore	2,320,000	9,880,000	-7,560,000
Interior Entrance Area	77,510,000	91,400,000	-13,890,000
Long Beach Peninsula - Inshore	59,420,000	710,000	58,710,000
Offshore	183,640,000	14,400,000	169,240,000
Net Change	463,340,000	209,990,000	253,350,000
1868/77 to 1958			
Ebb-Tidal Delta	276,240,000	170,000	276,070,000
Entrance Channel	1,880,000	546,720,000	-544,840,000
Clatsop Spit and Environs	143,360,000	7,090,000	136,270,000
Bakers Bay	108,170,000	6,470,000	101,700,000
Long Beach Peninsula - Inshore	40,040,000	10,120,000	29,920,000
Offshore	84,520,000	13,060,000	71,460,000
Net Change	654,210,000	583,630,000	70,580,000

(14.4 million cu yd). Inshore -21 million cu m (-27.5 million cu yd) and offshore 28 million cu m (36.6 million cu yd) surface elevation changes north of the entrance appear to be minimally influenced by northward-directed sand transport at this time (Figure 24; Table 8).

Although many studies have made reference to sediment deposition from the Columbia River sediment along the coast and across the continental shelf off Washington and Oregon, the offshore portion of the 1868/77 to 1926/35 change surface (approximately 30 m (98 ft) and deeper) indicates substantial erosion. These changes are controlled by data from the 1877 offshore survey. It is likely that the depth measurements recorded for this area during that time were incorrect; the farther older survey ships were from land-based control stations (horizontal positioning and vertical adjustments due to tides and currents), the greater that chance for measurement error. Consequently, these changes were

not included in volume change calculations. Net change for the analysis area encompassing all defined polygons (see Figure 23) documented a net loss of sediment of 17.2 million cu m (22.5 million cu yd). This result is difficult to accept given the amount of sediment supplied to the coast annually by the Columbia River.

Bathymetric changes recorded for the period 1926/35 to 1958 illustrate similar depositional trends as the previous surface comparison, but many differences are documented as well. Figure 25 illustrates the polygon boundaries used for calculating volume changes across the surface. Zones of accretion and erosion are clearly defined in Figure 26, as natural processes and engineering activities redistribute sediment throughout the system. A number of trends emerge from the data set. First, net northward transport of sediment is illustrated by the north-oriented ebb shoal. The shoal depocenter again moved seaward in response to flow from the increasingly deeper channel of -12.2 to -14.6 m (-40 to -48 ft)

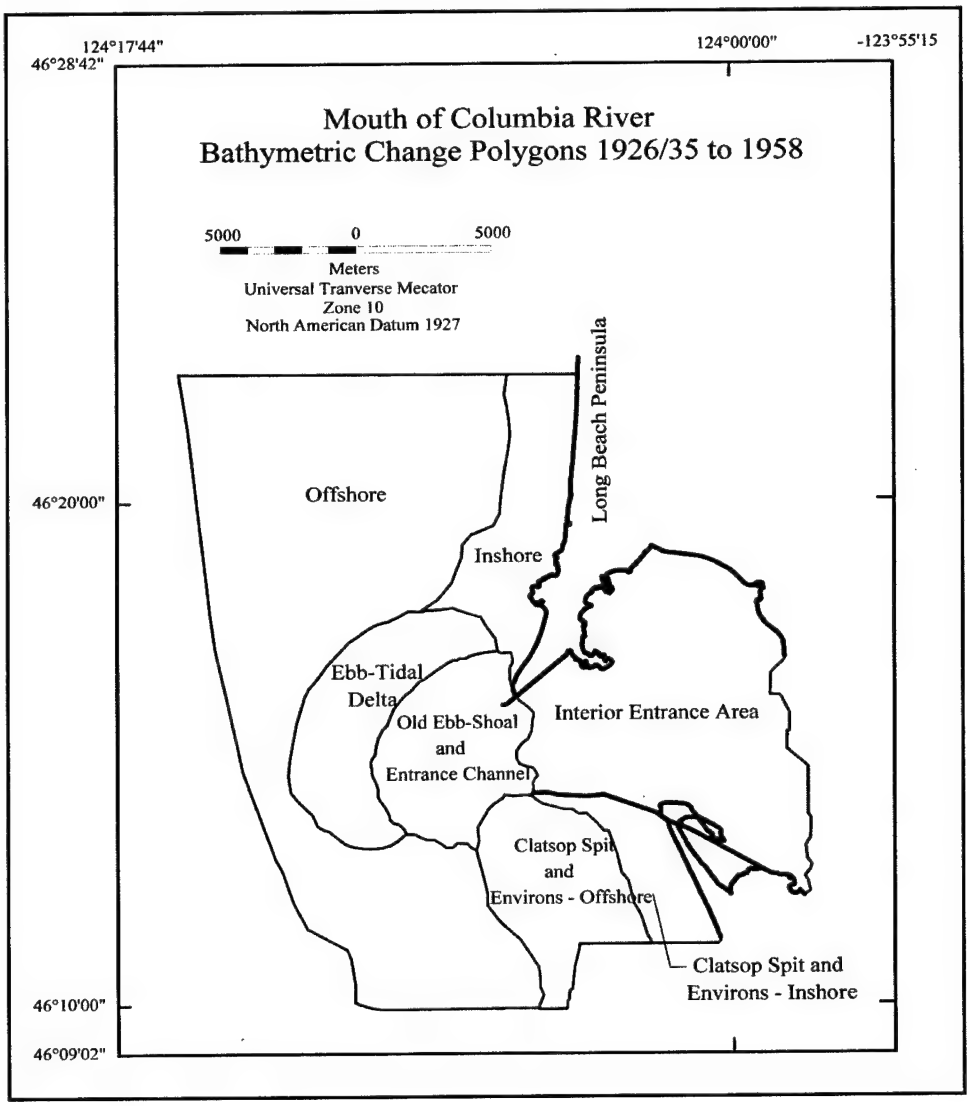

Figure 25. Polygon boundaries for sediment volume calculations across change surface, 1926/35 to 1958 (after Byrnes and Li 2001)

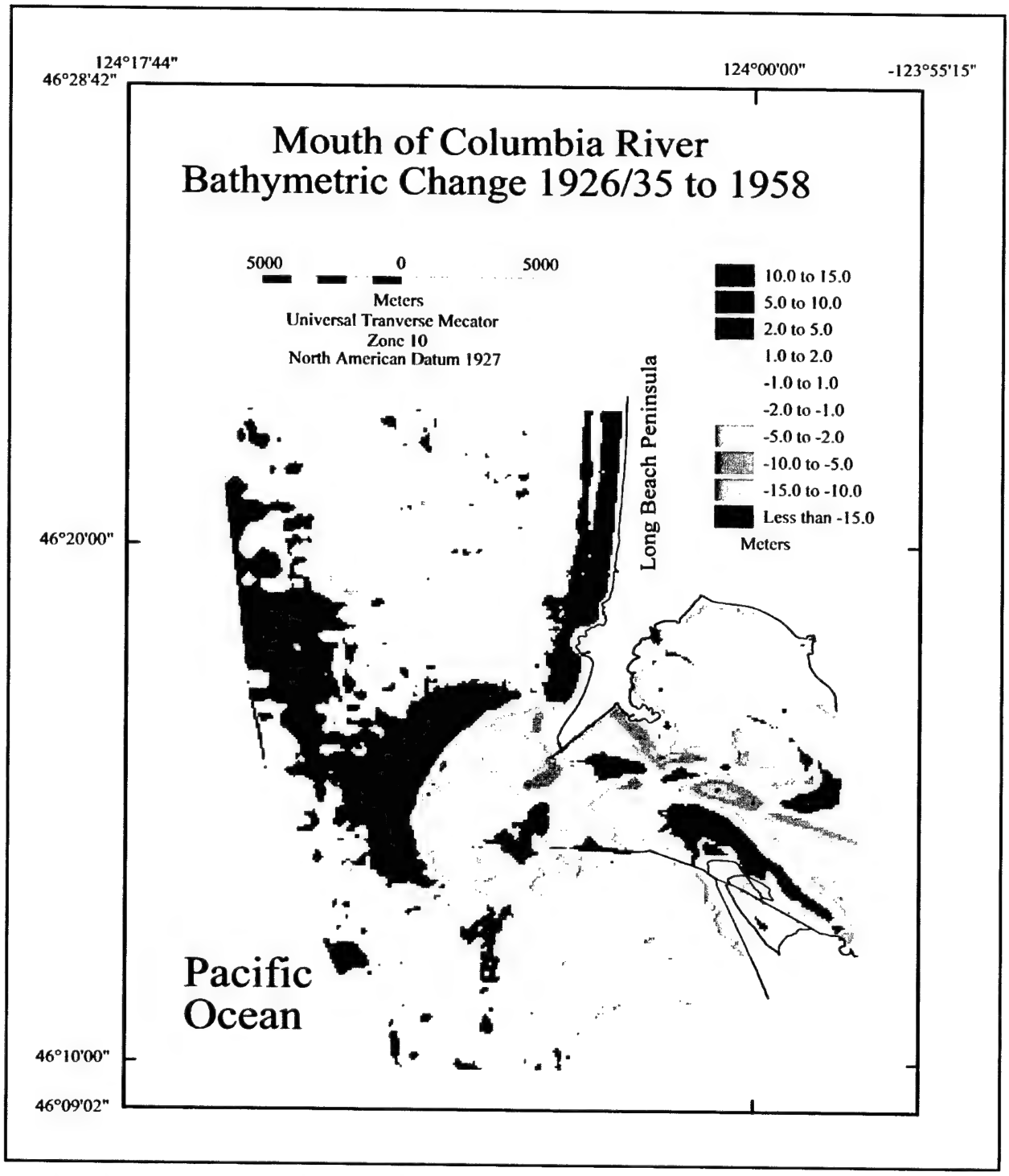

Figure 26. Bathymetric change 1926/35 to 1958 at and adjacent to MCR, WA/OR (after Byrnes and Li 2001)

during this time period); sediment deposition on the ebb shoal during this time was 128.5 million cu m (167 million cu yd) (Table 8). A substantial zone of erosion exists just landward of the ebb shoal, marking the position of the 1926 ebb-tidal delta. The magnitude of erosion for this feature of 62.9 million cu m

(82.2 million cu yd) is about half of the deposition recorded for the ebb shoal. Second, another indication of northward sand transport is the apparent streaming of sand north from the ebb-tidal delta to the beaches along the coast of Long Beach Peninsula (Figure 26). As indicated in the shoreline change analysis, beaches are accreting along this entire stretch of coast. Approximately 59.4 million cu m (77.6 million cu yd) of sand deposited along the coast during this time period (Table 8).

Third, a final piece of evidence illustrating net northward drift of sediment from the Columbia River mouth is the zone of deposition trending northwest off the ebb-tidal delta. This represents the silt and clay fraction of sediment exiting the entrance as suspended load, gradually settling to the shelf surface as water and sediment are transported to the northwest by shelf currents. This phenomenon has been documented by using seabed drifters, by using Mount St. Helens detrital ash carried to the coast by the Columbia River as a tracer, by using ^{210}Pb geochronology to document accumulation rates on the shelf, and by using sediment dispersal patterns and input estimates for documenting the accumulated sediment budget on the Washington Shelf. However, this is the first time direct evidence from sequential bathymetry data sets have been used to corroborate earlier findings.

The interior entrance area illustrates zones of erosion and deposition associated with channel migration, dredging, and deposition at the north end of Clatsop Spit. Overall, erosion of 91.4 million cu m (119.4 million cu yd) is greater than deposition of 77.5 million cu m (101.3 million cu yd) in the entrance area, creating a net sediment loss of 13.9 million cu m (18.2 million cu yd). To the south of the south jetty, sediment erosion is occurring along the beach of 7.6 million cu m (9.9 million cu yd) and on the shelf of 29.7 million cu m (38.8 million cu yd); Figure 26; Table 8). The sediment deficit is related to jetty placement and blocking of sand from the entrance that used to supply sediment to the northern Oregon coast. Shoreline change data suggest that this is a local phenomenon (with 5 km (3.1 miles) of the jetty), with net shoreline advance indicated south of this point. Komar and Li (1991) discuss this spatial variability in shoreline response and state that in recent years, shoreline retreat south of the jetty has diminished and stabilized.

Finally, the offshore portion of the change surface illustrates substantial sediment deposition, a result consistent with the quantity of sediment exporting the river mouth on an annual basis (about 8 million cu m per year (10.5 million cu yd per year); Whetten, Kelly, and Hanson 1969). Between 1926/35 and 1958, the offshore received about 169 million cu m (221 million cu yd) of sediment, resulting in a net change across the entire change surface of about 253 million cu m (331 million cu yd). When the Whetten et al. (1969) estimate of 8 million cu m (10.5 million cu yd) is multiplied by the time encompassed between surveys (32 years), the predicted amount of sediment supplying this area is 256 million cu m (335 million cu yd) remarkably consistent with net change recorded from bathymetric surveys.

Net change in sediment volume throughout the study area between 1868/77 and 1958 illustrates (Figures 27 and 28; Table 8) (a) translation of the ebb shoal offshore in response to jetty construction, and substantial deposition near the

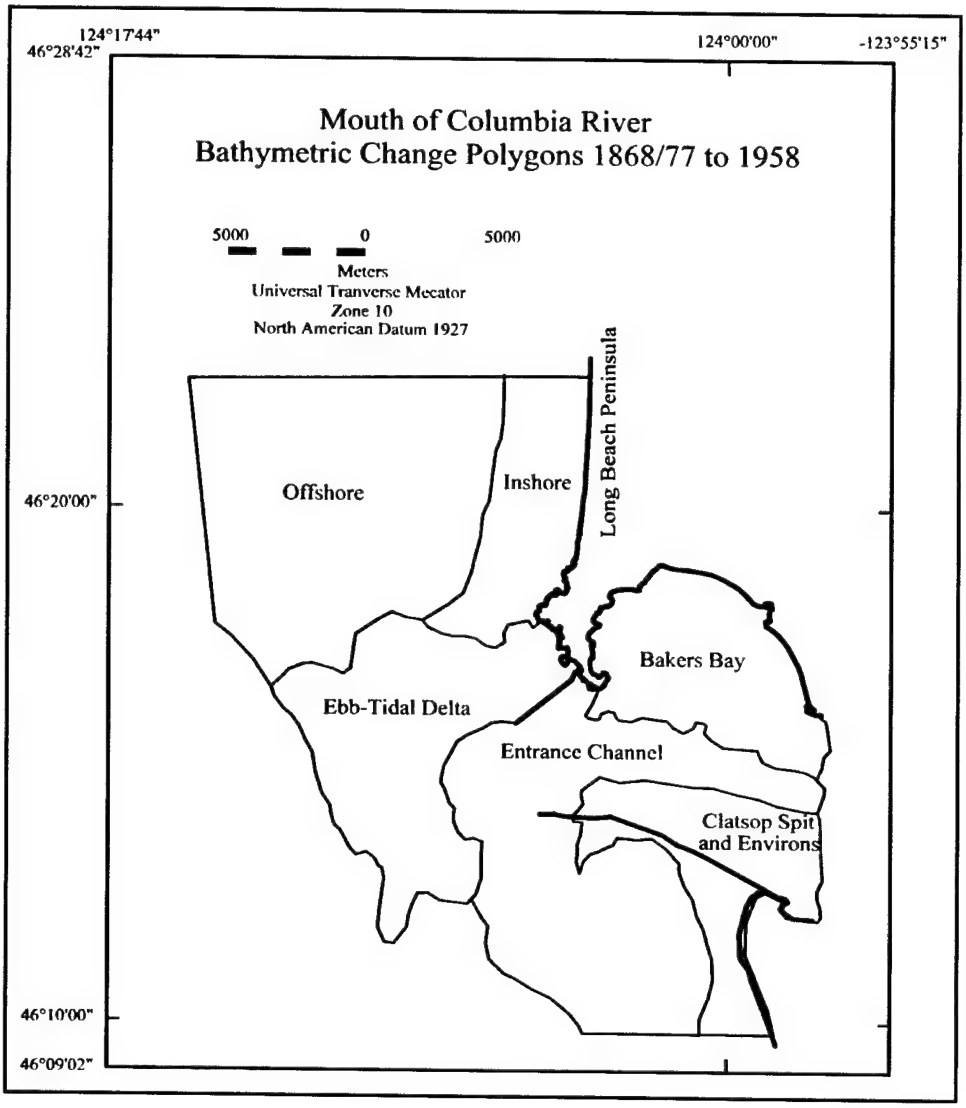

Figure 27. Polygon boundaries for sediment volume calculations across change surface, 1868/77 to 1958 (after Byrnes and Li 2001)

30-m (98-ft) depth contour to the shoreline south of Cape Disappointment of 276 million cu m (361 million cu yd), (b) massive erosion of the entrance channel and nearshore zone south of the south jetty of 545 million cu m (712 million cu yd), (c) infilling of the entrance area north (Bakers Bay) of 102 million cu m (133 million cu yd) and south (Clatsop Spit) of 136 million cu m (178 million cu yd) of the channel, (d) net deposition in the littoral zone along the Long Beach Peninsula of 30 million cu m (39.2 million cu yd), and (e) net deposition in the offshore northwest quadrant of the study area of 71 million cu m (92.8 million cu yd). Overall, net sediment deposition was recorded for the period of record of 71 million cu m (92.8 million cu yd); however, the magnitude of change is not consistent with the 1926/35 to 1958 data set nor existing sediment transport studies for the area. Sediment accumulation forming the ebb shoal is consistent for all time periods; the primary difference in overall trends is controlled by the inordinate amount of erosion recorded for the entrance channel and nearshore

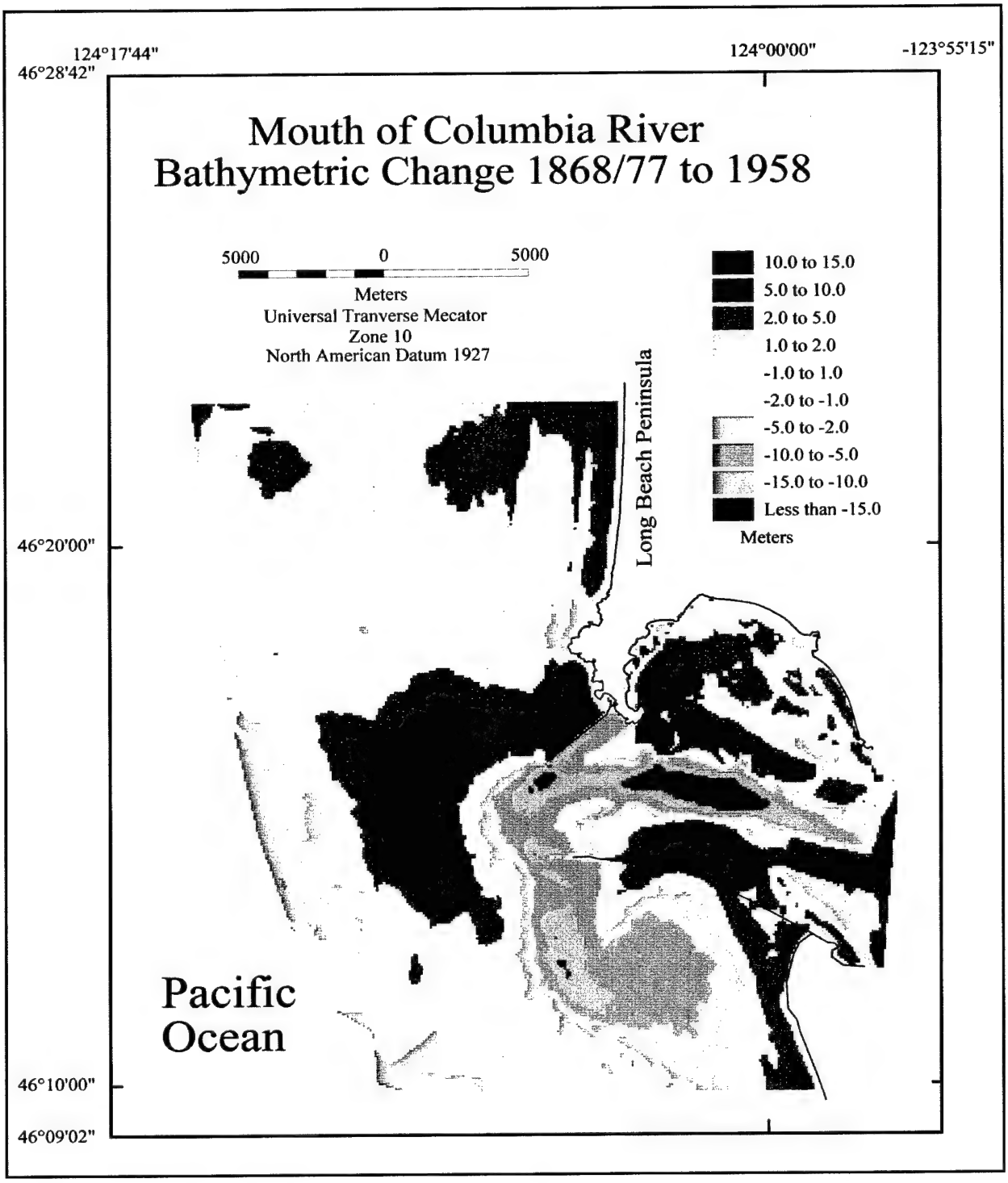

Figure 28. Bathymetric change 1869/77 to 1958 at and adjacent to MCR, WA/OR (after Byrnes and Li 2001)

area south of the south jetty. Again, due to potential survey problems discussed earlier, seafloor erosion offshore and south of the ebb shoal is not considered reliable and is not included in net volume change.

Two recent bathymetric surveys conducted by the Portland District. were employed to evaluate geomorphic changes at the Columbia River mouth up to 1994. Surface comparisons were made for three time periods: 1926 to 1988/94; 1958 to 1988/94; and 1988 to 1994. Change calculations were not completed relative to the 1868/77 data set due to uncertainties with measurement accuracy (discussed earlier). The 1926 to 1988/94 seafloor change map illustrates the same general trends as those presented for the 1926/35 to 1958 comparison, except the magnitude of accretion and erosion has increased. The centroid of deposition on the ebb shoal (minus the impact of dredged material placement at ODMDS B) has shifted to the north, and deposition on the shelf northwest of the ebb shoal has increased (Figure 29). Sediment accretion north of the entrance along Long Beach Peninsula continues to occur as the shoreline moves seaward. In addition, erosion associated with the 1926 ebb-tidal delta has increased, and the magnitude of sediment deficit south of the south jetty has been enhanced. One major difference relative to the 1958 surface comparison is the presence of two well-developed mound areas representing ODMDS A and B. These areas have been accumulating dredged material since 1956, the dynamics of which will be discussed later in the report.

Four volume-change polygons were defined to quantify geomorphic changes across the area of coverage (Figure 30). The ebb-tidal delta area includes the modern shoal and the area of the shoal in 1926. The area of deposition contains about 222 million cu m (290 million cu yd) of sand, whereas the eroded ebb delta indicates a loss of about 86 million cu m (112 million cu yd) (Table 9). The nearshore zone south of the south jetty illustrates the impact of blocking sediment supply from the entrance to this area by the south jetty. This erosion zone represents a net loss of about 56 million cu m (73 million cu yd). North of the ebb-tidal delta, sand continues to accrete along Long Beach Peninsula as a result of steady sand transport to the north from the entrance area. Sediment deposition in this area of 18 million cu m (23.5 million cu yd) and offshore on the continental shelf of 126 million cu m (165 million cu yd) represent a substantial component of net accretion recorded across the entire surface of 224 million cu m (293 million cu yd).

Between 1958 and 1988/94, a net sediment deficit was computed for the entire surface. This was primarily influenced by the amount of erosion occurring offshore and south of the south entrance jetty (Figure 31). Seaward and north of the entrance, sand deposition was dominant in response to northward directed transport. Furthermore, the centroid of deposition on the ebb shoal is strongly skewed to the north, supporting the same trend noted for every time interval. The polygons defined for this time interval are similar to those for the 1926 to 1988/94 comparison, except a greater proportion of the erosion area south of the entrance is available due to wider data coverage. Figure 32 illustrates the five polygons used to characterize elevation change across the surface. Once again, the ebb-tidal delta polygon includes erosion of the initial shoal deposit (1958) of 47.5 million cu m (62.1 million cu yd) and accretion associated with the 1994

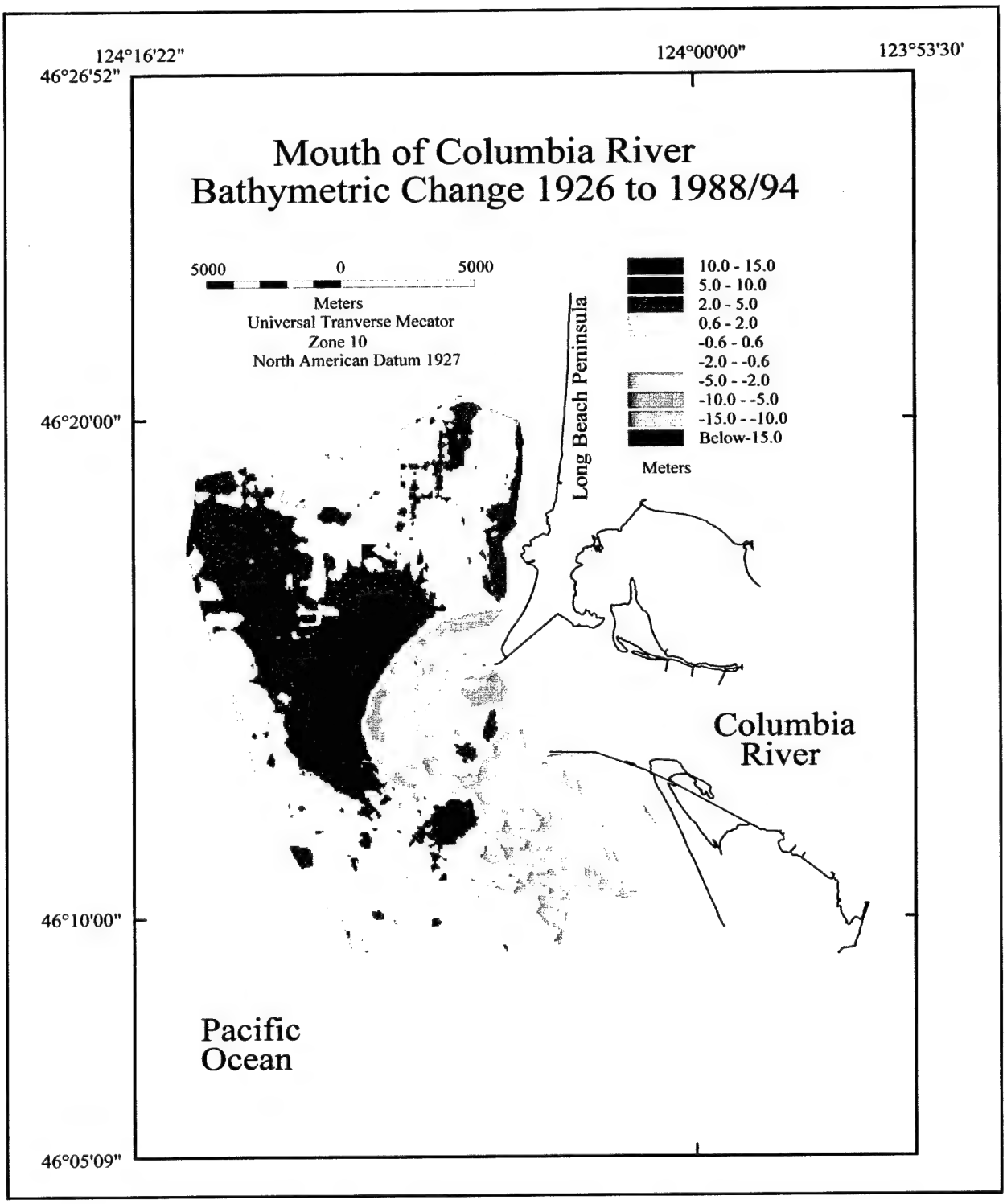

Figure 29. Bathymetric change 1926 to 1988/94 at and adjacent to MCR, WA/OR (after Byrnes and Li 2001)

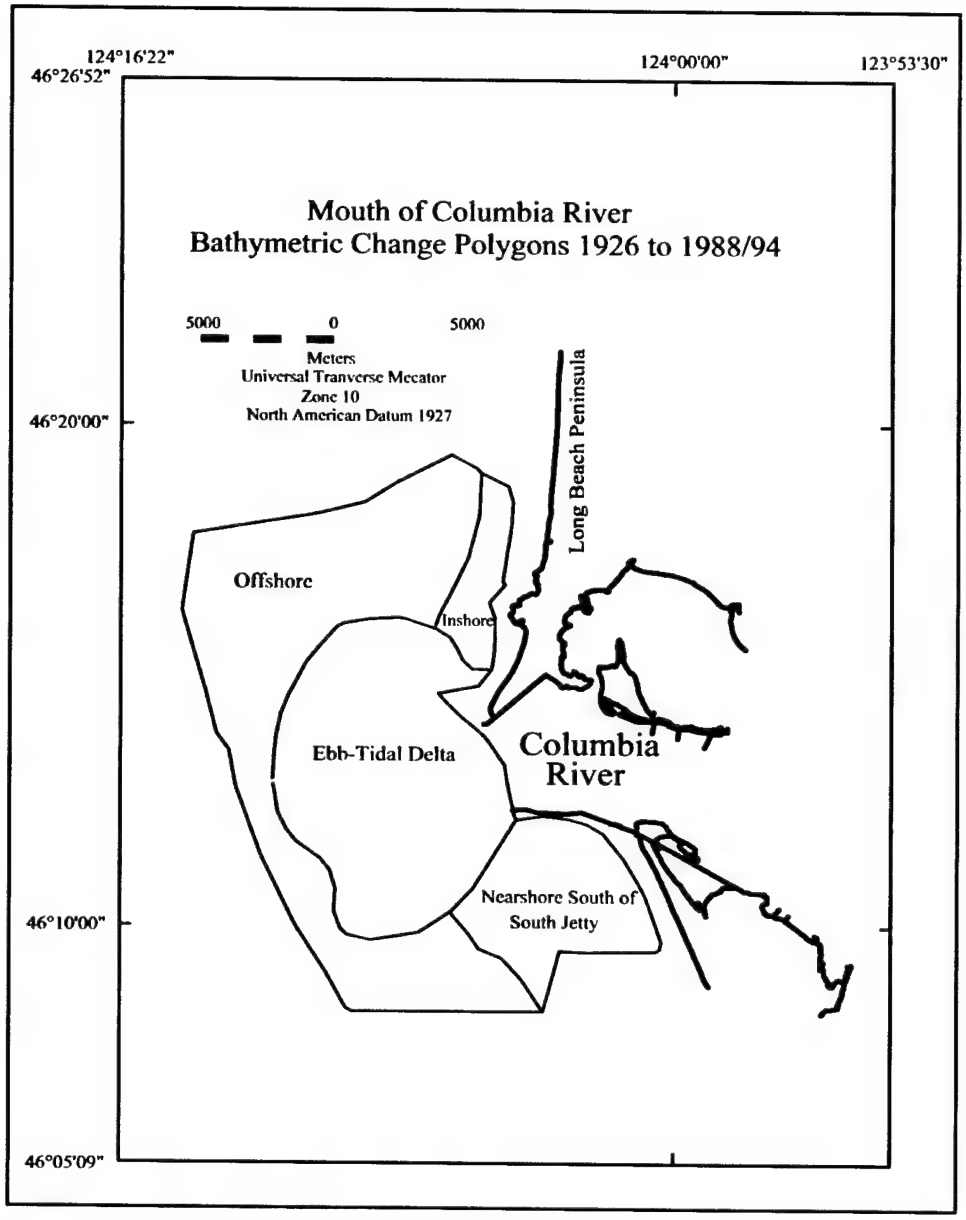

Figure 30. Polygon boundaries for sediment volume calculations across change surface, 1868/77 to 1958 (after Byrnes and Li 2001)

feature of 88.5 million cu m (115.7 million cu yd) (includes dredged material placed at ODMDS A, B, and F). North of the entrance, net sand deposition for inshore and offshore polygons totals about 31 million cu m (40.5 million cu yd), whereas seafloor erosion for inshore and offshore polygons south of the entrance totals about 97 million cu m (127 million cu yd) (Table 9). Overall, elevation change for the entire surface results in a net sediment deficit of 24.5 million cu m (32 million cu yd).

The final surface comparison is for the 1988 and 1994 survey dates. Largest changes are associated with offshore dredged material placement. Figure 33 shows the location of ODMDS A and B relative to calculated sediment volume

Table 9
Bathymetric Change Statistics Relative to 1988/94 Survey Area

	Deposition, cu m	Erosion, cu m	Net Change, cu m
1926 to 1988/94			
Ebb-Tidal Delta	221,860,000	85,930,000	135,930,000
Nearshore South of South Jetty	90,000	56,110,000	-56,020,000
Long Beach Peninsula - Inshore	18,180,000	70,000	18,110,000
Offshore	136,910,000	11,140,000	125,770,000
Net Change	377,040,000	153,250,000	223,790,000
1958 to 1988/94			
Ebb-Tidal Delta	88,510,000	47,520,000	40,990,000
Clatsop Spit – Nearshore	50,000	11,750,000	-11,700,000
Clatsop Spit – Offshore	510,000	85,400,000	-84,890,000
Long Beach Peninsula - Inshore	4,450,000	300,000	4,150,000
Offshore	33,420,000	6,460,000	26,960,000
Net Change	126,940,000	151,430,000	-24,490,000
1988 to 1994			
Ebb-Tidal Delta	29,480,000	14,710,000	14,770,000
Clatsop Spit – Nearshore	130,000	7,610,000	-7,480,000
Clatsop Spit – Offshore	1,570,000	28,210,000	-26,640,000
Long Beach Peninsula - Inshore	650,000	80,000	570,000
Offshore	2,460,000	16,790,000	-14,430,000
Net Change	34,290,000	67,400,000	-33,210,000

changes. USAED, Portland (1995a) states that 6.8 million cu m (8.9 million cu yd) of fine sand was placed at ODMDS A between the survey dates, and 3.3 million cu m (4.3 million cu yd) of accretion was calculated, implying that less than 50 percent of the material is retained at the disposal site. For ODMDS B, 12.4 million cu m (16.2 million cu yd) of material was placed during this time, and measured volume change was 7 million cu m (9.2 million cu yd) or 57 percent retention. The deeper offshore location for ODMDS B prevents dispersion of sediment resulting from natural wave and current processes. Although these sites are hot spots for accretion, most change is associated with erosion across the shelf surface. In fact, the amount of erosion recorded offshore Clatsop Spit of 28 million cu m (36.6 million cu yd) nearly equals the amount of deposition on the ebb-tidal delta of 29.5 million cu m (38.6 million cu yd); Figure 34; Table 9). The general trend of deposition at the shoal and north is still evident, but the magnitude of change is small (compared with potential error estimates) due to the short period of time between surveys. A net deficit of 33 million cu m (43.1 million cu yd) of sediment is calculated for the entire surface.

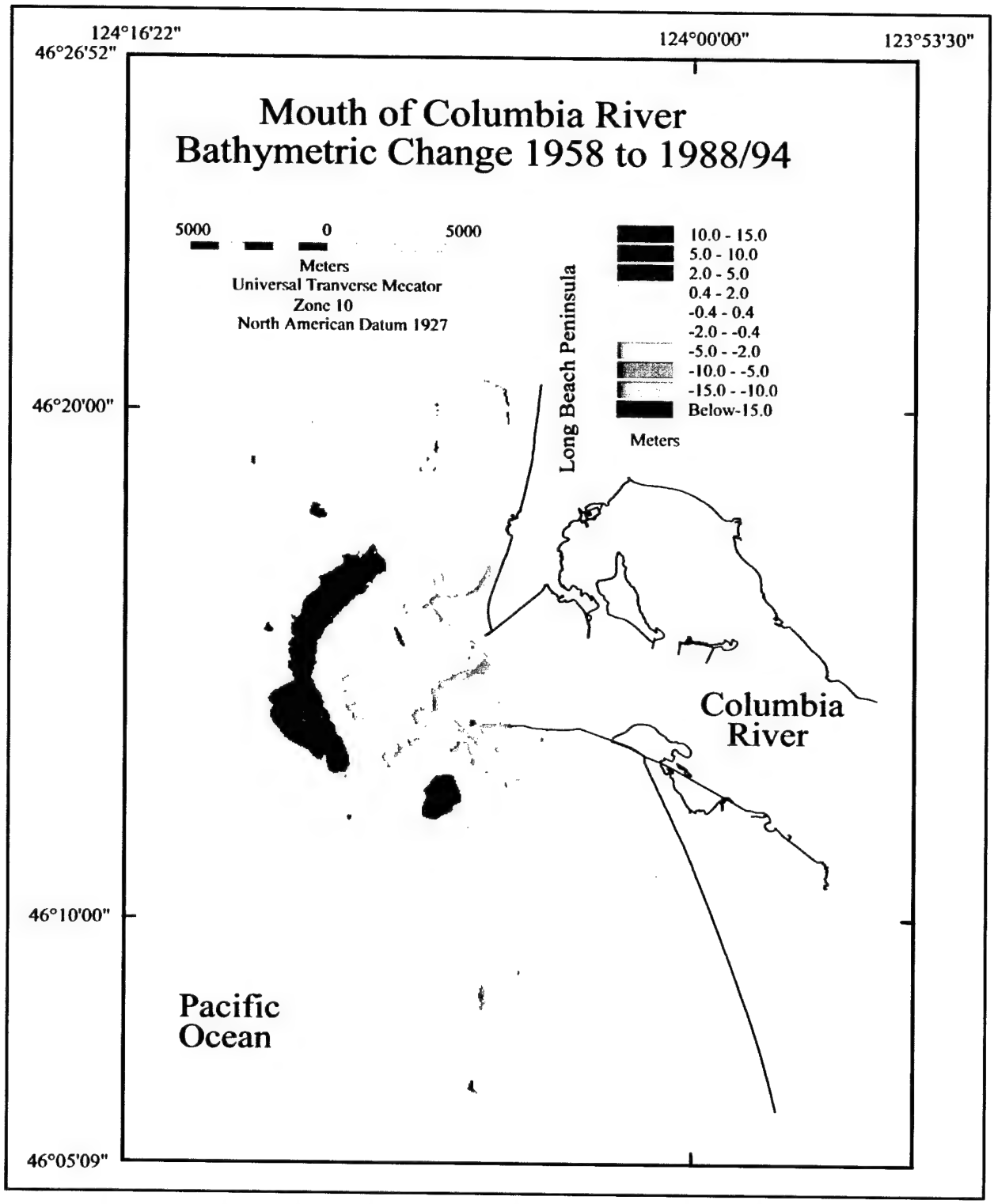

Figure 31. Bathymetric change 1958 to 1988/94 at and adjacent to MCR, WA/OR (after Byrnes and Li 2001)

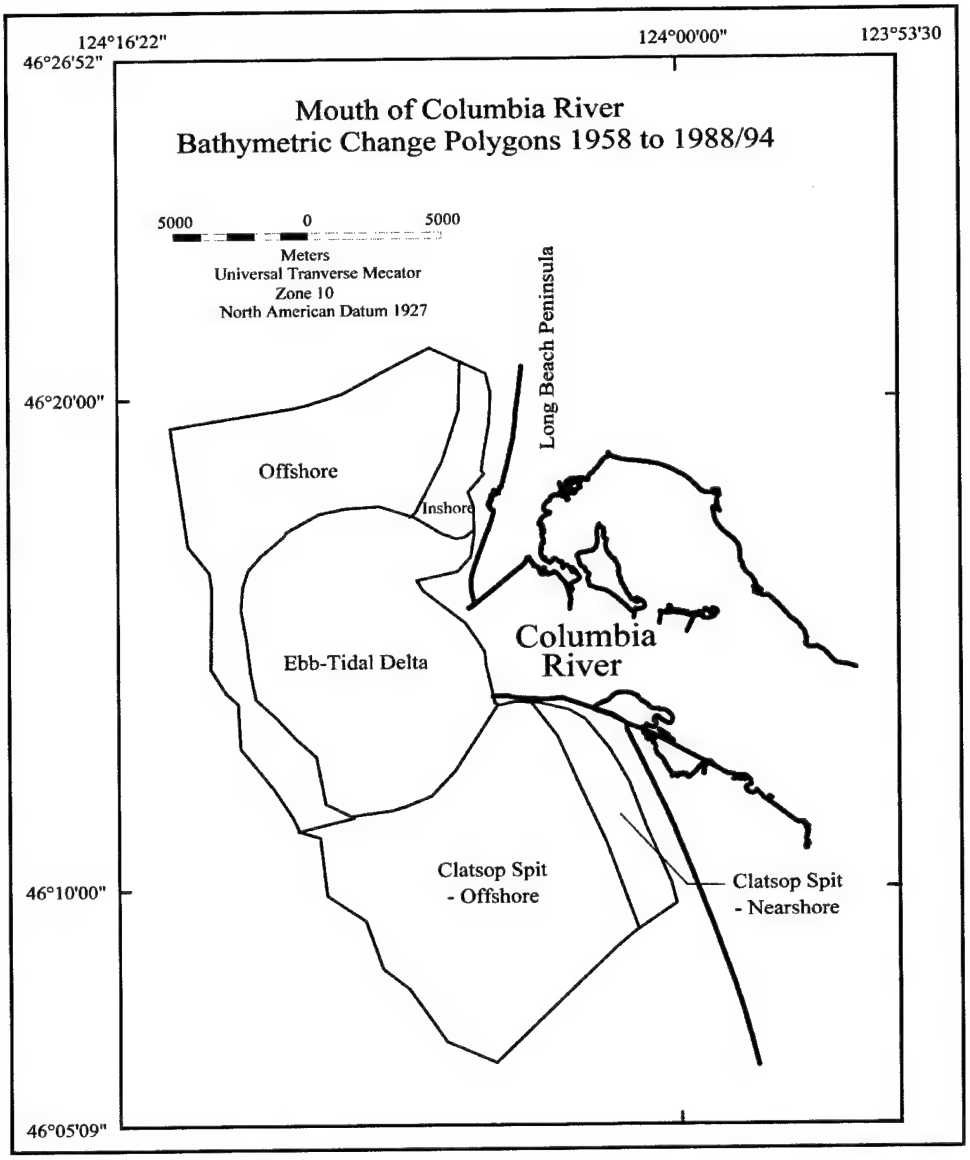

Figure 32. Polygon boundaries for sediment volume calculations across change surface, 1958 to 1988/94 (after Byrnes and Li 2001)

In summary, all bathymetric change maps and computations indicate that net northward drift is dominant for all time periods. After the jetties were constructed, the ebb-tidal shoal moved offshore in response to channeled flow through a narrower entrance. By 1958, the ebb shoal was displaced seaward about 3 km (1.9 miles) into 30-m (98-ft) water depth. Approximately 276 million cu m (361 million cu yd) of sediment has deposited offshore of the entrance to form this feature since 1868/77. Between 1926 and 1958, fine sand transport to the north along Long Beach Peninsula and offshore resulted in beach accretion, shoreline advance, and shallowing across the continental shelf. The inshore area received about 59.4 million cu m (77.6 million cu yd) from the Columbia River entrance and ebb-tidal shoal, and net offshore change results indicated about 183.6 million cu m (240 million cu yd) of deposition. South of the south jetty, seaward of Clatsop Spit, the zone of littoral transport indicates

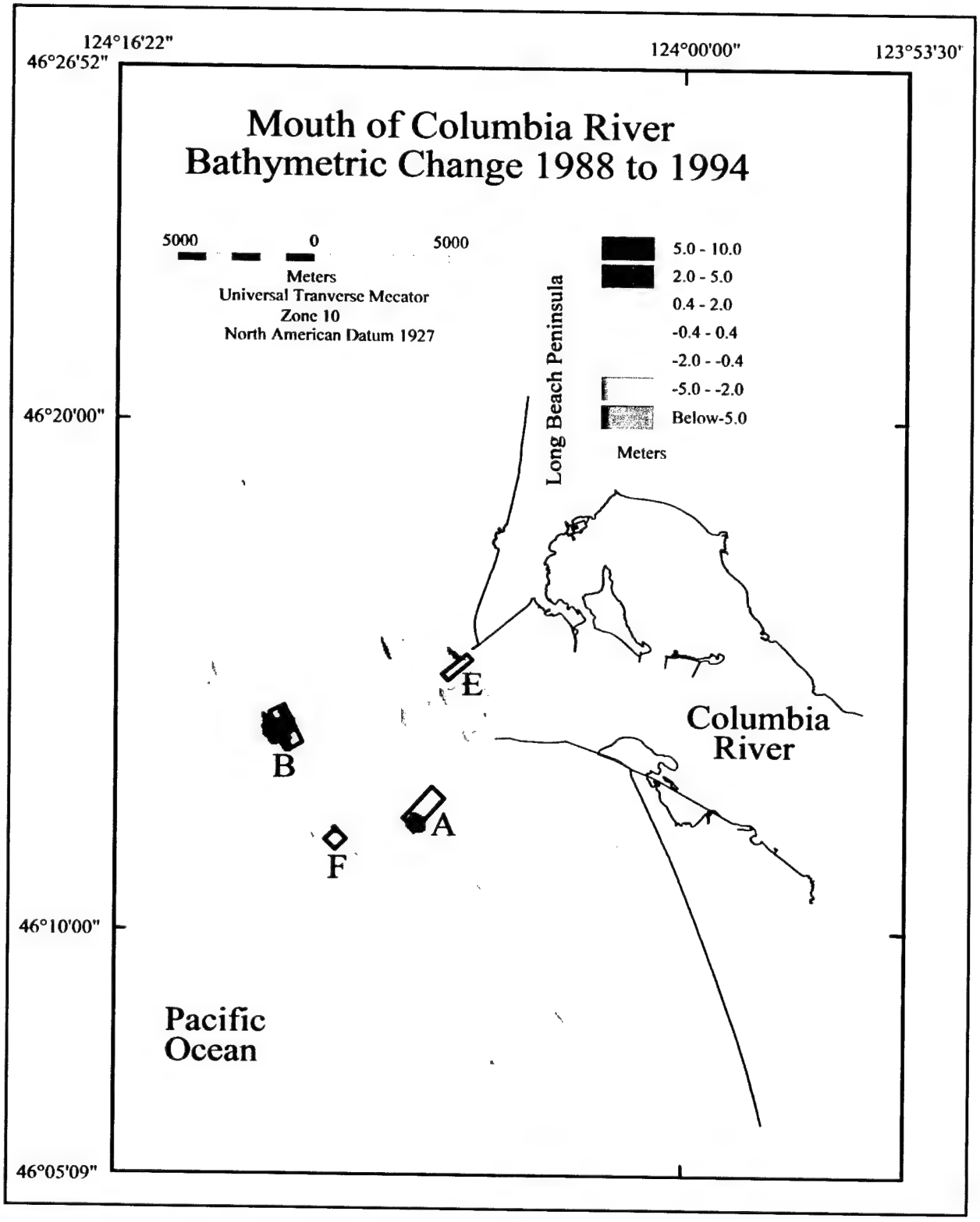

Figure 33. Bathymetric change 1988 to 1994 at and adjacent to MCR, WA/OR (Letters and polygons represent ODMDS; A and B are the primary sites) (after Byrnes and Li 2001)

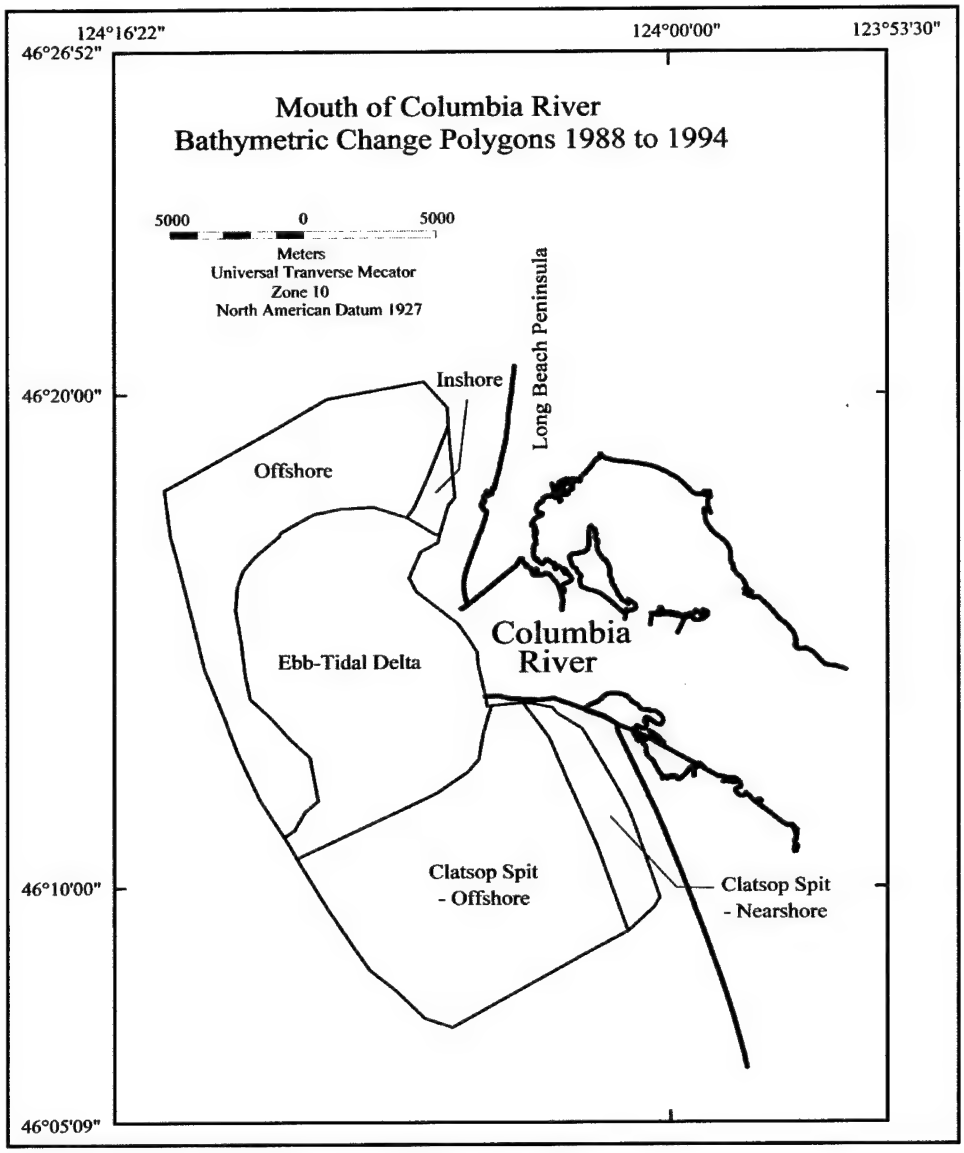

Figure 34. Polygon boundaries for sediment volume calculations across change surface, 1988 to 1994 (after Byrnes and Li 2001)

net sediment erosion of 7.5 million cu m (9.8 million cu yd) between 1926 and 1958, and the offshore showed even greater loss of 29.7 million cu m (38.8 million cu yd). Substantially greater erosion in these areas was documented for the period 1868/77 to 1958; however, the order of magnitude difference in erosion volumes is not considered realistic for an entrance with an average annual sediment supply of about 8 million cu m (10.5 million cu yd). Therefore, even though a net loss is recorded south of the entrance between 1926 and 1958, it is consistent with the observations of Komar and Li (1991) and comparisons with the more recent bathymetry data sets.

Surface change comparisons for a smaller area seaward of the entrance (defined by the 1988/94 USACE composite bathymetric surveys) between 1926 and 1988/94 illustrate the same depositional and erosional trends as identified for

the larger data coverage area. Large quantities of sediment have been deposited on the ebb-tidal delta, and redistribution of sediment from earlier ebb-shoal locations (1926 and 1958) is well documented (see Figures 29 and 31). The magnitude of sand transport and accretion north of the entrance supports previous study findings regarding net northward sediment transport from the Columbia River mouth. Two well-defined sediment accumulation zones exist as inshore fine sand deposits seaward of Long Beach Peninsula and an offshore silt deposit trending northwest from the ebb shoal. Bathymetric comparisons with the 1988/94 surface document accumulation trends at ODMDS A and B. Since 1958 ODMDS A has retained approximately 48 percent of the deposited sediment, whereas at ODMDS B about 74 percent of sediment disposal has remained onsite.

Sediment Dynamics and Dredged Material Placement Considerations

A primary objective of the regional geomorphic change analysis was to quantify sediment dynamics within the context of dredged material disposal operations. Since about 1945, a series of ocean dredged material disposal sites (ODMDS) have been designated for dredged material originating from the Columbia River entrance channel (USAED, Portland, 1995a). Although seven different sites have been used since 1956, the most active sites have been ODMDS A, B, and E. The total of about 155 million cu m (203 million cu yd) of sediment was placed at these ODMDS between 1956 and 1995.

Regional sediment transport patterns for the Columbia River entrance and adjacent environs is consistent for all analysis time intervals. Although coastal process measurements identify two distinct seasonal circulation trends, net sediment deposition and erosion in the study area is relatively steady and predictable. Prior to jetty placement, the entrance area was much wider and shoals would shift regularly in response to sediment and water input from the river and their interaction with marine processes. After jetty placement, the ebb-tidal shoal was displaced seaward by about 3 km (1.9 miles) as sediment jetted offshore from the entrance was deposited in 30- to 40-m (98- to 130-ft) water depth. The centroid of deposition for the ebb-shoal shifted north since 1926 in response to the dominance of northward directed transport. Furthermore, nearshore deposition along the beaches of Long Beach Peninsula have created net shoreline advance for a distance of about 24 km (15 miles) north of the north jetty. Sediment deposition to the northwest off the ebb shoal is documented since 1926, and this result supports the findings of previous studies (e.g., Sternberg 1986). All regional geomorphic response data suggest that high-energy, northward directed flow, characteristic of the winter season, controls net transport direction in the study area.

Sediment dynamics associated with regional change analyses can be used to help site and manage dredged material disposal sites. Assuming that disposal strategies include keeping dredged sediment permanently away from the area from which it was dredged and providing sand-sized sediment dredged from channels to adjacent beaches, the following suggestions are presented for future

operations. Although disposal ODMDS A exists south of the designated channel, bathymetry and change data indicates that the site is too shallow and may be affecting flow from the entrance channel. Figure 35 illustrates the position of disposal sites relative to the 1988/94 bathymetric surface. The main channel appears to diverge when it encounters the mounds associated with ODMDS A, and sediment retention at the site is only 48 percent of the original disposal quantities. It is likely that on flooding tide, a substantial amount of sediment dumped at the site is mobilized and transported back into the lower estuary, potentially resulting in channel shoaling problems. This concern was discussed by Lockett (1967) as a reason for potentially abandoning the site. Conversely, ODMDS B is in deeper water along the outer margin of the ebb shoal. Between 1958 and 1994, approximately 74 percent of disposal material stayed at the site, the remainder of which dispersed in a wider area around the site (see Figure 33) and/or is transported to the north to supply the Continental Shelf and beaches with sediment. ODMDS F has been used primarily in the 1990s and poses minimal direct impact on the entrance because it exists at about 40-m (130-ft) water depth. ODMDS E has been used since 1973 as a disposal site for supplying beaches to the north of the north jetty with channel sand. Although most material was placed in this site prior to the 1990s, it continues to be used.

Given the dynamics of the area, it is suggested that ODMDS E be utilized whenever possible to add sand to the littoral system. Although beaches to the north of the entrance have been experiencing accretion throughout the period of record, a 17-km (10.6-mile) length of coast north of this accretion zone has been expanding to the south with time. The problem is chronic and would be best mitigated with sediment added to the system. Assuming ODMDS E is not overfilled, it would seem cost-effective to dispose of sandy sediment at this site to nourish beaches to the north. Furthermore, because erosion along beaches of Clatsop Spit can be associated with blocking of sediment from the river by the south entrance jetty, it would be reasonable to establish a disposal site in this area to fortify beaches. Assuming the operation to be cost-effective relative to other sites, this disposal practice could reduce the need for ODMDS A.

Conclusions

A regional analysis of shoreline and bathymetry change was completed to evaluate sediment transport dynamics associated with natural processes at the Columbia River entrance and engineering activities since 1868. Historical data sets include shoreline position from USC&GS maps and bathymetry data from the USACE and the USC&GS. The analysis time period is from 1868 to 1994. The following is a summary of key results and recommendations relative to dredged material management and selection of disposal sites.

a. Shoreline change data for the periods 1868/74 to 1926 and 1926 to 1950/57 illustrate net shoreline advance throughout the study area. However, significant shoreline retreat zones occur along the northern 5 km of Clatsop Spit of 5.6 m per year (18.4 ft per year) and the northern 17 km (10.6 miles) of Long Beach Peninsula of 3.6 m per year (11.8 ft per year) (1926 to 1950/57). From 1868/74 to 1950/57, average shoreline

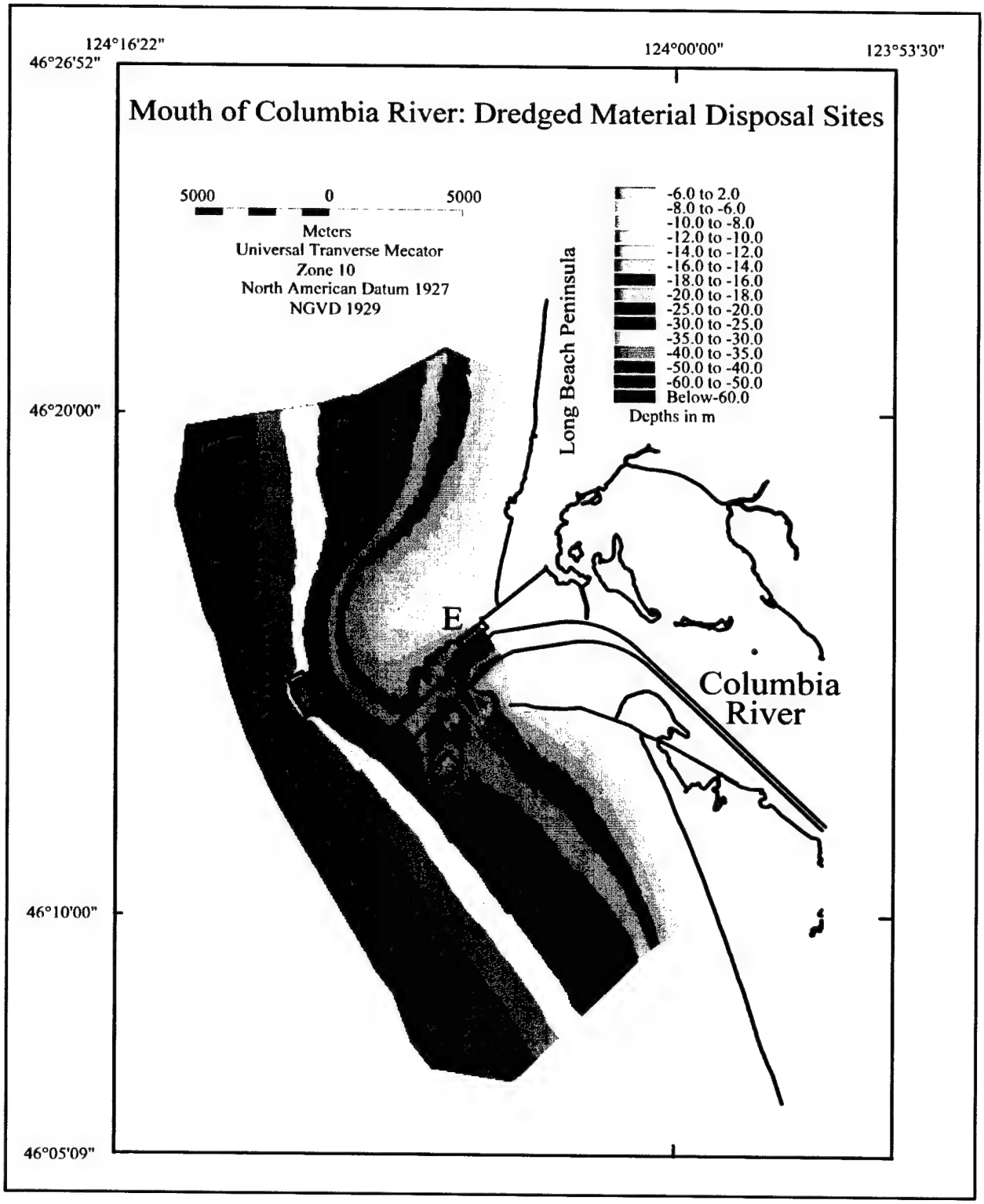

Figure 35. Location of ODMDS A, B, E, and F, relative to 1988/94 bathymetry surface (after Byrnes and Li 2001)

change north of the Columbia River entrance was 2.2 m per year (7.2 ft per year). South of the entrance jetty, net shoreline advance is documented at 5.5 m per year (18.0 ft per year).

b. Three bathymetry surfaces were compiled for quantifying nearshore geomorphic change. Volume change estimates were established for specific polygons to relate grouped cut and fill relationships with natural and human processes. For the overall area, four distinct depositional trends were identified. (a) The modern ebb-tidal delta developed as a result of jetty construction. Currently, it resides about 3 km (1.9 miles) seaward of the original feature in about 30- to 40-m (98- to 130-ft) water depth. The deposit contains about 276 million cu m (361 million cu yd) of sediment, approximately half of which comes from the old ebb shoal. (b) The depocenter for sedimentation on the ebb shoal is to the north of center, and it migrates to the north with time. (c) Northward directed sediment transport from the entrance has resulted in net accretion along the shoreline and on the continental shelf seaward of Long Beach Peninsula. (d) Erosion south of the south jetty is the result of sediment blocking by the jetty and subsequent transport towards the ebb shoal and onto the continental shelf (see Figure 26).

c. Surface change comparisons for a smaller area seaward of the entrance (defined by the 1988/94 USACE composite bathymetric surveys) between 1926 and 1988/94 illustrate the same depositional and erosional trends as identified for the larger data coverage area. Large quantities of sediment have been deposited on the ebb-tidal delta, and redistribution of sediment from earlier ebb-shoal locations (1926 and 1958) is well documented (see Figures 29 and 31). The magnitude of sand transport and accretion north of the entrance supports previous study findings regarding net northward sediment transport from the Columbia River mouth. Two well-defined sediment accumulation zones exist as inshore fine sand deposits seaward of Long Beach Peninsula and an offshore silt deposit trending northwest from the ebb shoal.

d. Bathymetric comparisons with the 1988/94 surface document accumulation trends at ODMDS A and B. Although ODMDS A exists south of the designated channel, bathymetry and change data indicate that the site is too shallow and may be affecting flow from the entrance channel. The main channel appears to diverge when it encounters the mounds associated with ODMDS A. It is likely that on flooding tide, a substantial amount of sediment dumped at the site is mobilized and transported back into the lower estuary, potentially resulting in channel shoaling problems. Conversely, ODMDS B is in deeper water along the outer margin of the ebb shoal. Between 1958 and 1994, approximately 74 percent of disposal material stayed at the site, the remainder of which dispersed in a wider area around the site and/or is transported to the north to supply the continental shelf and beaches with sediment. ODMDS E has been used since 1973 as a disposal site for supplying beaches to the north of the north jetty with channel sand. Although most material was placed in this site prior to the 1990s, it continues to be used.

e. Given the dynamics of the area, it is suggested ODMDS E be utilized whenever possible to add sand to the littoral system. Although beaches to the north of the entrance have been experiencing accretion throughout the period of record, a 17-km (10.6-mile) length of coast north of this accretion zone has been expanding to the south with time. The problem is chronic and would be best mitigated with sediment added to the system. Assuming ODMDS E is not overfilled, it would seem cost-effective to dispose of sandy sediment at this site to nourish beaches to the north. Furthermore, because erosion along beaches of Clatsop Spit can be associated with blocking of sediment from the river by the south entrance jetty, it would be reasonable to establish a disposal site in this area to fortify beaches. Assuming the operation to be cost effective relative to other sites, this disposal practice could reduce the need for ODMDS A.

4 Field Data Collection and Analysis

Introduction

To fulfill its mission of designing, building, and maintaining coastal projects, the USACE relies on accurate data about the dynamic ocean. Measurements of waves, currents, and other parameters are essential elements of informed decisions and efficient designs. Sophisticated sensors may be lowered into the water for one minute or left in place for years, and deployment techniques must be adapted to a variety of environments. The traditional platform for this work is a research vessel or barge, an approach that is appropriate if sea conditions are mild. However, there are times and places where conditions can render this form of deployment unsafe, logistically difficult, or economically unfeasible.

Installing instruments in the surf zone and in large inlets is particularly challenging, even under the calmest of conditions. Amphibious vessels have proven useful in many situations, but for some locations such as the MCR along the Northern Pacific coast of the United States, dangerously energetic surf is normal. Here the USACE contracted with the O. H. Hinsdale Wave Research Laboratory, Oregon State University, to design, construct, deploy, and retrieve four data collection open-frame tripod platforms for the acquisition of necessary environmental data pertaining to conditions at the MCR.

Each of the four tripod platforms was outfitted with Doppler wave and current sensors, temperature, pressure, and salinity sensors, and OBS that measure suspended sediment concentrations. The tripod platforms and instrumentations were capable of being remotely deployed for extended periods of time. The three deployment periods were (a) Deployment 1: 19 August – 09 October 1997, (b) Deployment 2: 15 April – 24 August 1998, and (c) Deployment 3: 27 November 1998 – 01 March 1999). Upon retrieval after each of these three deployments, the platforms were returned to OSU for data analyses. The tripods were deployed and retrieved by oceanographic research vessels.

USACE also developed techniques for using helicopters to accomplish the data-collection mission. This methodology will be exceedingly useful for long-term management of ODMDS nationwide.

Instrumentation[1]

To obtain a complete description of the environment at the MCR, data on currents, waves, temperature, pressure, salinity, and concentrations of suspended solids were collected. The highly energetic sea state of the region required utilization of a stable and robust platform mounted with specialized equipment which could remotely collect and store data until retrieval of the instrument package.

Data collection criteria

To select an appropriate instrumentation package and platform design, the USACE provided criteria for the data to be collected at the MCR, as follows:

a. Basic data consisting of current velocity and direction, temperature, pressure, and salinity must be obtained.

b. The format of the data files must allow for extracting wave information including height, period, and direction.

c. Current velocity and direction must be determined at a distance as close to the bottom as reasonably possible, given the potential for partial burial of the platforms due to sedimentation or settlement.

d. Data must provide the current profile throughout the length of the water column at periodic heights from the bottom to the surface.

e. Suspended sediment concentrations must be collected in conjunction with the other data.

Given these criteria, OSU proceeded with instrumentation procurement, and tripod platform design and construction.

Instrumentation selection

Selection of an appropriate instrumentation package was dependent upon identifying equipment that met the preceding general criteria and the following additional stipulations:

a. Must be capable of withstanding the extreme waves and currents encountered at the Columbia River Mouth and Bar.

b. Must be capable of autonomous remote deployment for extended periods.

c. Procurement and life cycle costs must be within budget constraints.

d. Must have low maintenance requirements with resistance to fouling and corrosion.

[1] This section is extracted essentially verbatim from Lund et al. (1999).

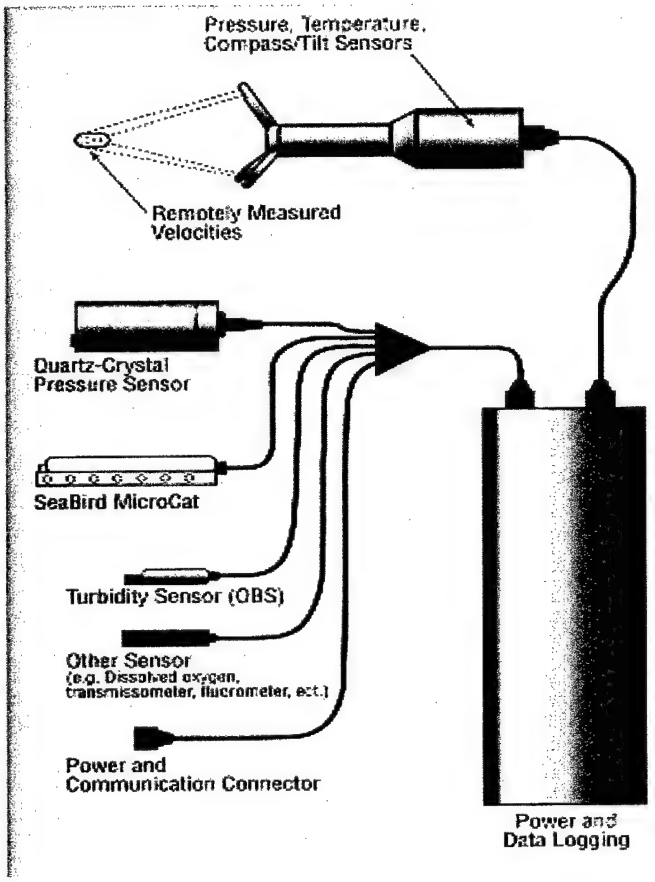

Figure 36. SonTek Hydra oceanographic data collection system (single point velocity meter, Acoustic Doppler Velocimeter (ADV), Optical Backscatter Sensors (OBS), Paroscientific pressure sensor, and Conductivity-Temperature (CT) sensor) (after Moritz et al. 1999)

Instrumentation meeting the preceding requirements was available off-the-shelf in a compact, versatile package from SonTek, Inc., a San Diego, CA, company specializing in the development and manufacture of water velocity meters for the freshwater and marine environments. The SonTek system selected consists of two instruments. The first, the Hydra (Figure 36), contains a single point velocity meter, the Acoustic Doppler Velocimeter (ADV), optical backscatter sensors (OBS) for suspended solids, a Paroscientific pressure sensor, and a Conductivity-Temperature (CT) sensor. Sensor data are collected and power supplied via the power and data logging unit. The second instrument is a profiling velocity meter, the Acoustic Doppler Profiler (ADP) (Figure 37). The ADP is capable of measuring velocity at several different locations, or cells, perpendicular to the sensor head and providing a profile through depth or distance, depending upon sensor orientation. Sensor data for the ADP is collected and power supplied via its own power and data-logging unit. In addition to the data collecting instrumentation, each tripod was equipped with an acoustic transponder for use in locating the platform if the retrieval and marker system was missing at the time of retrieval.

Acoustic Doppler Profiler (ADP)

The SonTek ADP measures water velocity through measurements of the Doppler shift between a transmitted and reflected sound signal. According to the Doppler shift principle, the velocity of a particle in the suspending medium may be determined by reflecting a sound signal off the object and observing the shift between the original transmitted frequency and the receiving frequency (SonTek 1997a).

The SonTek ADP chosen for this application consists of three monostatic transducers oriented 25 deg from vertical with 120-deg horizontal separation between each transducer. Each monostatic transducer acts both as a sound

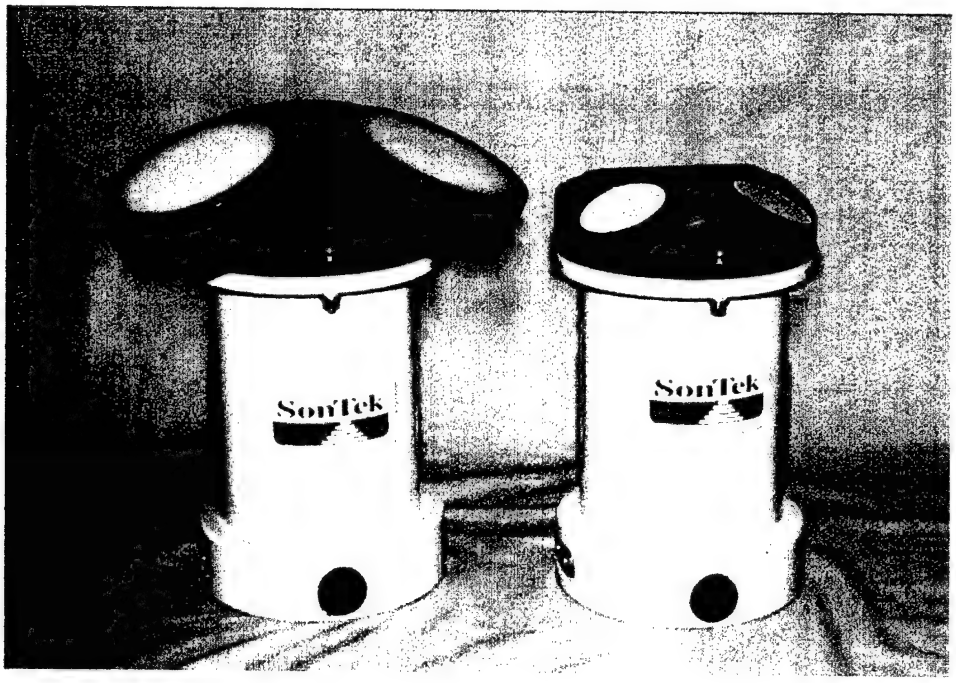

Figure 37. SonTek profiling velocity meter Acoustic Doppler Profiler (ADP) (after Moritz et al. 1999)

transmitter and receiver, generating a pulse along its axis during the transmission phase and receiving the return pulse only moments later. The ADP is able to provide a complete profile of the water column by generating a sound signal and then sampling the return signals at various time intervals. By increasing the interval between transmission and sampling, the reflected sound that is received, penetrated further into the water column prior to its reflection. By sampling at multiple intervals, a complete profile of the water currents is obtained. The ADP has an internal magnetic compass and tilt sensor that enables the instrument to be deployed without knowing its actual orientation. With the compass enabled, the ADP will output data in terms of East/North/Up (ENU) velocity components.

When used in remote applications, the ADP is normally set to sample data in interval or burst mode. When in burst mode, the ADP is programmed to sample for a discrete period of time at a specified interval. For example, during the April 1998 deployments, the 1,500 kHz ADP was set to sample for a 10-min burst every 1-hr interval. During the sampling burst, the ADP collected velocity data for each cell, averaged the data, and provided one output velocity set per cell per burst.

Two versions of the SonTek ADP were procured for this project, the 500 kHz and the 1,500kHz models, due to variations in water depth. The shallower water Sites B1 and E were equipped with higher frequency 1,500 kHz ADPs while the deeper Sites B2 and M were equipped with the lower frequency systems. This variation was required to account for the attenuation of higher frequency components by the deeper water column.

Acoustic Doppler Velocimeter (ADV)

The SonTek ADV, like the ADP, operates using the Doppler shift principle and measuring the frequency shift caused by reflection of sound waves off a moving particle in the suspending medium. Unlike the monostatic ADP, the ADV is a bistatic current meter that utilizes a separate acoustic transmitter and receiver. As with the ADP, the ADV requires three different transducers oriented in three planes to resolve XYZ velocity components. For the 3-D meters, as used in the MCR, the three probes are slanted 30 deg off the transmitters and rotated at 120-deg relative azimuth angles. The ADV also comes equipped with a magnetic compass and tilt sensor and may be configured to output information in ENU coordinates.

The ADV is a single sample volume instrument, unlike the ADP which provides a profile through depth. The ADVs chosen for the MCR applications were oriented facing down and sampled a cylindrical volume of water approximately 1-cm- (0.39-in.-) diam. and 2 cm (0.78 in.) long at a distance of 18 cm (7.1 in.) from the transmitter. The velocity measured is the bistatic velocity, which is the velocity projection onto the receiver's three bistatic axes (SonTek 1997b)

The ADV may be configured for burst sampling or continuous sampling. Unlike the ADP burst-sampling program, the ADV samples during a burst at a user specified sampling rate (i.e.; 1 Hz). The ADV pings transmit a sound pulse, 150-250 times per sec dependent upon programmed settings based upon expected velocities. Given the sampling rate, the ADV will average the data received from all pings during a sample. The data is then reduced and stored in XYZ or ENU coordinates, if compass equipped. Thus for a 10 min (600 sec) burst sampled at 1 Hz, a total of 600 data points will be collected and stored versus the single data point per cell of the ADP collected for a burst of similar duration. The software enables the user to program in three different burst sampling programs, a useful option if the user wants to look at currents caused by different sources (e.g., sampling mean tidal currents and wave induced velocities. Obviously, the sampling rates for the wave-induced velocities would need to be much higher than the sampling rates of the tidal current velocities.

Optical Backscatter Sensor (OBS)

Each instrumentation platform was outfitted with two D & A Instrument Company's optical backscatter sensors (OBS). The OBS measures suspended solids by emitting pulses of infrared radiation and measuring with photo diodes the amount of infrared light reflected and returned to the sensor. The returned light signal generates a voltage across the optical sensor, that is conditioned and output to a data storage device. The intensity of the output voltage may be translated into suspended concentrations through calibration equations.

Conductivity sensors

Two different conductivity sensors were utilized during data collection for determining salinity. On the original three instrumentation platforms deployed at Sites B1, B2, and E, the Hydra instrumentation package purchased in 1997 came equipped with a Falmouth Scientific Conductivity-Temperature (C-T) sensor. Prior to completion of the fourth platform, SonTek modified the Hydra system to include the Sea-Bird Electronics MicroCAT SBE 37 SI Conductivity and Temperature Recorder (Sea-Bird), a significantly more accurate and durable conductivity sensor.

The Falmouth Scientific C-T sensor is a low-cost, low-power sensor built for collecting data in the harsh marine environment. A ceramic sensor head houses the temperature sensor and the inductively coupled conductivity sensor. Collected data is processed through a self-calibrating, internal electronics board and may be recorded directly or serve as input to compatible instrumentation.

The Sea-Bird is a high accuracy, low-power conductivity and temperature sensor designed for marine deployment in depths to 7,000 m (22,970 ft). It is equipped with a titanium housing that provides strength and resists corrosion and biofouling. Internal fouling of the sensor may be prevented through the use of sacrificial antifouling devices. Calibration of the sensors is conducted at the factory prior to shipment, and the results are provided in the operating manual. The Sea-Bird comes equipped with versatile software that enables the user to program a desired sampling scheme. The collected data may be output in several different manners, either in Binary or a converted ASCII file format, as raw data, or corrected data using the internal calibration coefficients. Alternatively, the sensor can convert data directly to salinity instead of outputting only conductivity.

Paroscientific pressure gage

The Paroscientific pressure gauge is a fully submersible and extremely durable system designed for precision water-level measurements. The sensor has a typical accuracy of 0.01 percent with a resolution of $1x10^{-8}$, full scale. The system has excellent long-term stability, low power consumption, and high reliability. The internal electronics package enables the sensor to be easily connected to other instrumentation and data storage devices, which makes it an ideal sensor for the MCR environment (Paroscientific 1998).

Location transponder

In the event the surface mooring system was lost during a deployment, each platform was equipped with a Datasonics, Inc., Underwater Acoustic Transponder. This device is activated remotely and emits a signal detectable by a submersible hand-held locator operated by a diver.

Instrumentation calibration

Laboratory calibrations of each ADV, ADP, Paroscientific pressure sensor, and OBS were conducted at OSU prior to deployment. The calibration tests included steady speed tows of the ADV and ADP sensors in a large 2-D wave channel, random and monochromatic waves for the ADV and pressure sensors also in the wave channel, and suspended sediment concentrations for the OBS sensors. Upon retrieval of the tripods, the OBS sensors were returned to the factory for calibration using the local MCR sediment material. The factory calibration method for the OBS sensors was a cost-effective option which provided accurate calibration curves for future data analysis.

Tripod Platform Design and Construction[1]

Upon procurement of the SonTek instrumentation package and determination of mounting requirements, selection of platform design and construction material was completed. The instrumentation characteristics, the data collection requirements, and the local MCR environment imposed several additional design criteria for the platform system. First and foremost, the platform design needed to be durable, rigid, deployable, and capable of protecting instrumentation in the extreme environment expected at the MCR. The platform design should minimize interference with data collection and local environmental conditions. Also the ADVs must be able to sample current velocities as close to the bottom as possible while avoiding data corruption due to proximity of a boundary and the potential for the platforms to settle into the bottom or to be partially buried by accumulating sediment. Finally, the platforms must be heavy enough to avoid being moved by the environmental conditions, yet light enough and small enough to be easily deployed and retrieved by the few personnel on a small vessel.

Using previous experience with remote deployments in harsh environments, the OSU staff designed an open frame tripod. Variations of the tripod design have proven effective at protecting equipment without impairing data collection at several sites along the Oregon and Washington coasts. The three points of the tripod enable the platform to remain stable on an uneven or gently undulating or sloping bottom. The multilevel open frame design enables the instrumentation to be fully restrained and protected, while minimizing interference with local velocities.

Design plans were completed for both the tripods and the associated mounting hardware. The three tripod feet were each ballasted with 222 kg (490 lb) of lead obtained from military surplus. The initial three tripod frames and mounting brackets were constructed from aluminum plate and extrusions (alloy 6061-T6). Fabrication of the tripods was completed by L & M Welding, a Corvallis, Oregon company at an approximate cost of $4,300 each. The aluminum brackets for attaching the instruments were fabricated at OSU. In an attempt to reduce the effects of fouling and corrosion, the initial three tripods were epoxy powder coated. The powder coating was found to not be durable to abrasion and marine exposure. The fourth tripod was fabricated from marine grade aluminum

[1] This section is extracted essentially verbatim from Lund et al. (1999).

(alloy 5086), and was not powder coated. The remaining hardware, nuts, bolts, etc. are stainless steel and were procured locally. Instrumentation installation, calibration, and programming were completed by the OSU staff. The complete, fully instrumented tripods are depicted in Figures 38 and 39.

Deployment of Instrumented Tripod Platforms by OSU Research Vessels[1]

Deployment and retrieval of the tripods in the MCR proved to be a challenge to both vessel and crew. Although similar instrumentation platforms and mooring systems had been deployed and retrieved in other locations, the 908-kg (1-ton) platform weight combined with the MCR environment provided some unique challenges. The crew continuously found itself adapting and revising the operations as tides changed, seas rose and fell, and deck equipment was discovered to be marginally adequate for the job.

Tripod deployment

The deployment and retrieval of the tripods is a straightforward operation capable of being undertaken by a small crew on a small vessel with suitable hydraulic and deck gear. Although continuously changing environmental conditions and site characteristics precluded the use of a single deployment method and a single retrieval method, a standardized procedure was developed for the operations. The crew, in response to environmental conditions and vessel modified this procedure on a case-by-case basis.

Step one. The wire ropes for the bottom line and the surface line are shackled together and spooled onto a hydraulic winch, bottom line first. The free end of the surface line is attached to one end of a 3.05-m (10-ft) bridle of 1.27-cm- (1/2-in.-) diam. chain. The other end of the chain is attached to the steel surface float via a swivel that allows the float to rotate without kinking the mooring cable.

Step two. The vessel approaches the assigned deployment position to determine set and drift. The set and drift dictates the distance and direction from which to commence the deployment. In particular, once the anchor has been deployed, the vessel's movements may become moderately constrained. Responding to the local environmental conditions, one allows the vessel to drift over the assigned tripod position, and when timed properly, deploy the tripod in the correct location.

Step three. The steel float is deployed overboard and spooled off to its connection with the bottom line. While spooling the wire rope off the winch, forward way is placed on the vessel to tension the cable, move the cable and float away from the stem and propeller and thereby avoid a backlash and subsequent bird's nest on the winch.

---

[1] This section is extracted essentially verbatim from Lund et al. (1999).

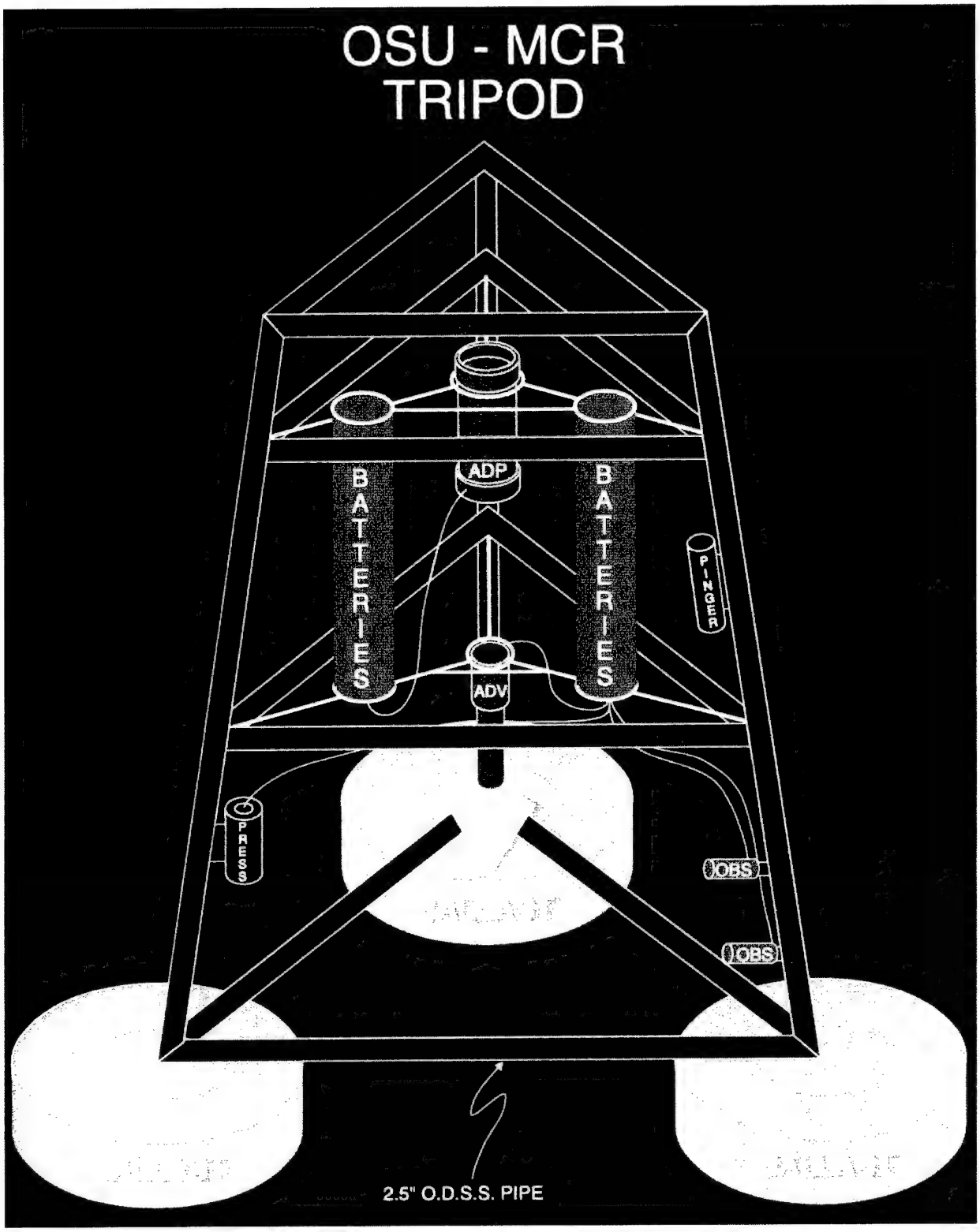

Figure 38. Oregon State University instrumented tripod platform for obtaining oceanographic data at MCR (elevation view) (after Lund et al. 1999)

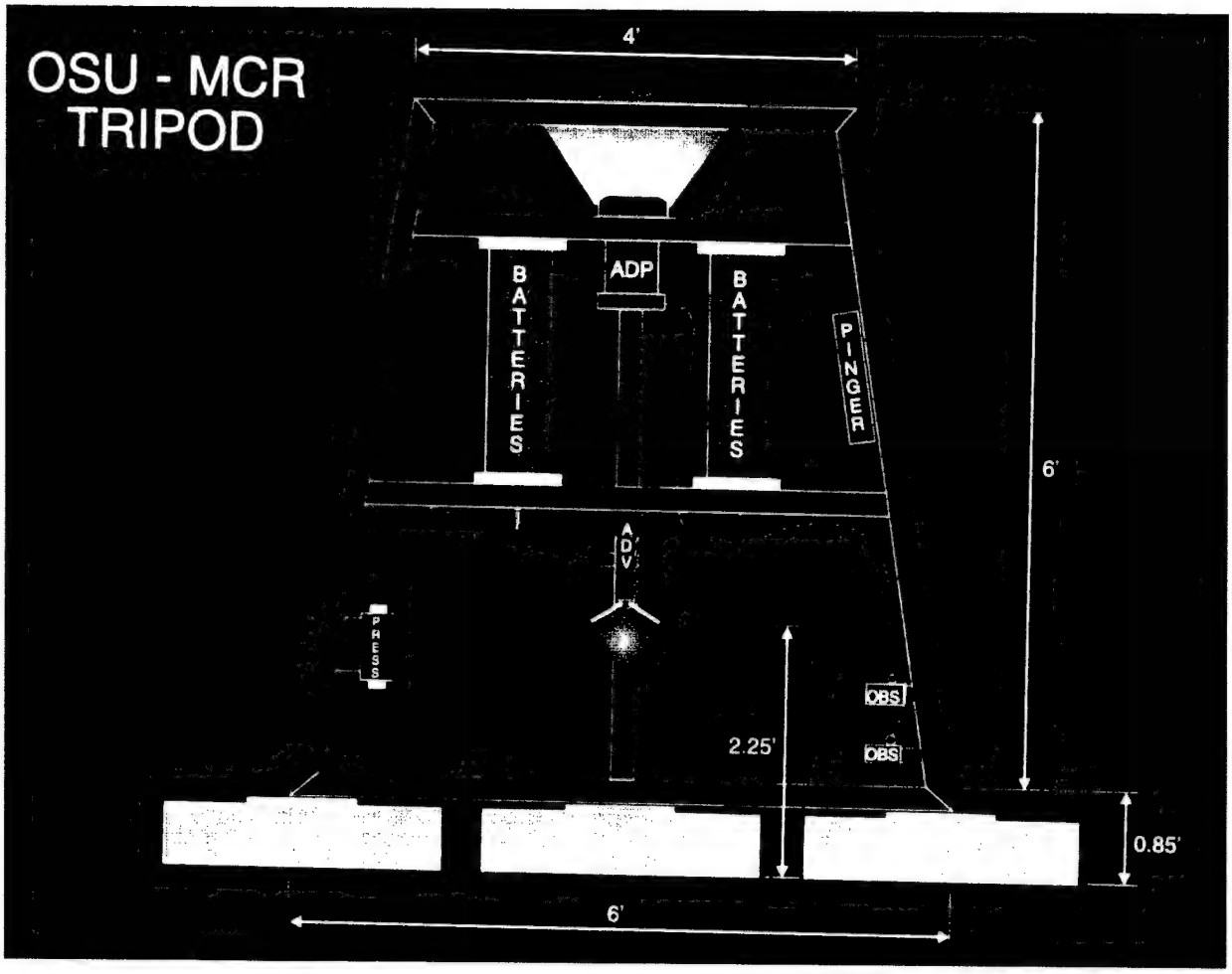

Figure 39. Oregon State University instrumented tripod platform for obtaining oceanographic data at MCR (front view) (after Lund et al. 1999)

Step four. Once the bottom and surface line connection is reached at the winch, the vessel engines are disengaged to put slack into the lines. A 3.05-m (10-ft) length of 1.27-cm- (1/2-in.-) diam. chain is shackled to the connection joining the surface and bottom line. The opposite end of the chain is then shackled to the Danforth anchor.

Step five. The vessel is maneuvered as needed into position to deploy the anchor. The anchor is deployed, and spooling off of the bottom line commences. Light forward way is put on the vessel to again assist with deploying the wire rope.

Step six. Once the bottom line is spooled off, the free end is shackled to a 3.05- m (10-ft) length of 1.27-cm- (1/2-in.-) diam. chain. The other end of the chain is attached to a short chain bridle on the center foot of the tripod via a swivel.

Step seven. The lowering cable, a 91.5-m- (300-ft-) long, 0.635-cm- (1/4-in.-) diam. wire rope, spooled onto the hydraulic winch prior to leaving the

pier, is inserted through the vessel's running rigging through two tripod sheaves at diagonal corners of the top rectangular frame and then made fast to a fixed point on the vessel. Tension is applied to the cable to lift the tripods, which are then maneuvered overboard and slowly lowered to the bottom by the hydraulic winch. As the tripod is being lowered, the secondary retrieval line is manually let out to avoid entanglements.

Step eight. Once the tripod reaches the bottom, the lowering cable is cut at the fixed point and the secondary retrieval floats and remaining line are cast overboard. The winch is engaged, and the lowering cable is retrieved by pulling it back through the running rigging and the sheaves in the tripod. Once the lowering cable is pulled clear of the tripods, the deployment is complete, and the deck and equipment may be prepared for the next deployment.

Tripod retrieval

Step one. Once located, the steel float is approached, and a 1.27-cm (1/2-in.) nylon line is hooked in the eye on the top of the float. The line is then wrapped around a hydraulic crab block, and the steel float lifted out of the water to deck level.

Step two. A 0.953-cm- (3/8-in.-) diam. wire rope is inserted from the hydraulic winch through a block on a stanchion on the starboard side of the vessel, and connected to the surface line wire rope at its connection with the steel float chain. Once this attachment is made the chain is disconnected from the surface wire rope, and the float and chain are brought aboard and stowed.

Step three. The surface line is spooled onto the winch until moderate tension develops. Spooling ceases while the vessel motion is used to dynamically load the anchor and slowly break it free. Once the anchor is broken free, the remaining surface line is retrieved and the anchor is raised to the stanchion block. The anchor and chain are disconnected from the mooring and stowed aboard.

Step four. The winch is re-engaged and the bottom line is slowly retrieved. Tension is visually monitored, and if heavy tension is encountered, spooling ceases to allow dynamic loading to break the cable free. Once the wire rope is brought to short stay, the line is taught at the tripod and retrieval ceases to allow vessel motion to dynamically load and break free the tripod. Once the tripod is broken free from the bottom it is lifted off the bottom several feet and then returned to ensure it is entirely free.

Step five. With the free tripod resting on the bottom, the retrieval line is made slack and passed from the stanchion block to a block on a swing boom reaching out over the water. The elevated boom allows the tripod to be lifted out of the water clear of the gunwales and then brought aboard. Retrieval then continues until the tripod is safely aboard.

Step six. Since the tripod is brought on board the vessel by the center foot, its center of gravity causes it to come aboard and lie on its side on the deck. If additional retrievals are planned, the tripod must be rotated to its upright position

and relocated on the deck. This action is accomplished by disconnecting the retrieval line from the foot, attaching it to the top level of the tripod, and applying tension to rotate the tripod. If the tripod must be moved to a different location on deck, the retrieval line can be inserted through a combination of deck blocks, connected to the tripod, and the tripod dragged to an appropriate position.

Lessons learned

The four tripod platform deployments and retrievals proved to be valuable learning experiences for the OSU staff. Working with new equipment and platform designs and employing old methods in new situations required a continuous evaluation of the tools and procedures used to accomplish the job. As a result of the operations, several lessons were learned and adaptations made to assist in future deployments and retrieval of these and other tripod designs. The most important of these lessons learned and adaptations relate to the vessel utilized, the tripod mooring system, and general operational planning.

The OSU research vessel *Honcho*, although a sound and seaworthy craft, was marginally adequate for deployment and retrieval of the tripods. The deck space proved too small for efficient operations and limited the amount of equipment that could be accommodated. The deployment conducted from the larger vessel *Karelia* on demonstrated that four tripods could be deployed in a single day with good weather conditions. The elimination of the need to conduct two trips to deploy all four tripods was not only a cost saving measure, but demonstrated that the tripods could be deployed even if the available weather window was only 1 day.

The available deck gear on both vessels was adequate for the job, but not the optimal choice and quantity of gear. The *Honcho* trolley system failed to provide enough overhead or stern clearance. The *Karelia* overhead boom did not have adequate stays, and once suspended, the tripod and boom were free to move longitudinally with the rolling of the vessel. This rolling motion proved potentially dangerous on several occasions. Ideally, the vessel utilized for deployment and retrieval should have adequate overhead and deck clearance, a hydraulic boom with stays to control vertical and longitudinal motion, and at least two winches to provide a minimum of two points of control on the suspended tripods.

At the request of local mariners, the steel mooring floats were replaced with vinyl floats. Several individuals had expressed concern about potential vessel damage resulting from a collision with the unlighted buoys. There was some conjecture that the missing steel float may have been struck by a vessel, or perhaps vandalized. The vinyl floats, although more susceptible to damage by vandals, are likely more survivable if struck by a vessel providing they are not struck by the screw. The most beneficial mooring change was the replacement of the small nylon line with the 1.9-cm- (3/4-in.-) diam. braided line. This modification provides redundancy of retrieval methods and provides a means of dynamically loading the tripods to break them free from bottom suction.

Minor planning and operational changes were made to ensure future operations are conducted smoothly. First, completion of an entire deployment or

retrieval is considered an exceptional day, and should not be counted as routine, especially in the MCR environment. When planning for future operations, a minimum of 3 days should be allowed: 2 days for operations, and the third day for travel. By scheduling for 3 days, both the crew and vessel will be available and dedicated to the operation. Sea state, tides, and currents must be considered when choosing times to get under way and work at each tripod site. An opposing current can double the time it may take a vessel to transit from the Astoria pier to the MCR sites. The shallower sites also were more easily worked during slack water or a slightly flooding tide. The ebb current, notorious at the MCR, intensified sea conditions and rendered shallow operations impossible. Finally, crew size must be adequate for the operation to proceed smoothly. In addition to the vessel skipper, one deck hand and an OSU crew of four was found to be ideal for deployment and retrieval purposes.

Deployment of Instrumented Platforms by Helicopter[1]

Background

A technique for using helicopters to deploy and retrieve oceanographic instrumentation platforms was developed at the MCR. This technique, developed for helicopter data acquisition at this location, will be applicable to other similar situations. Previous uses of helicopters for ocean measurements include surveying (Graig and Team 1985), deploying permanent floating and bottom-mounted gages, laying cables through the surf zone (McGehee and Welp 1994), and taking spot measurements of the current (Pollock 1995). In each case, the over-water hover time was short, on the order of a few minutes. Although many measurements can be obtained with a short-duration insertion, a wave measurement requires a sample length of about 20 to 40 min during which the instrument must remain stationary on the sea floor. The two options for the helicopter are (a) remain attached to the instrument in a prolonged, near-stationary hover, or (b) drop and recapture the instrument after the measurement period. A manually controlled, 20-min hover is severely taxing on the pilot, even over land where there are visual references to the helicopter's position. It is nearly impossible offshore, where visual references are limited or distant.

The procedure developed at the MCR permitted repeated release and recovery of the instrument package. The Chinook helicopter (CH-47) was selected for this mission because of its dual, releasable cargo hooks, lift capability, multihour flight duration, and high maneuverability. Lessons learned may be applied to other helicopter platforms regarding how to equip and operate a helicopter to deploy an instrument frame through the water column to the seafloor in shallow water. Depending on the length of the desired measurement, the frame can be immediately withdrawn and repositioned, or released and subsequently recovered with the helicopter. The advantages of the technique relative to traditional sampling from a vessel are significantly higher operational

[1] This section is extracted essentially verbatim from McGehee and Mayers (2000).

thresholds for waves and currents and much shorter transit times between stations.

The technique was demonstrated during two trials conducted in the summer of 1996 and the winter of 1997 offshore of the MCR. The widest river entrance on the western side of North America, a large semidiurnal tidal range, and an unrestricted fetch across the North Pacific, makes the MCR one of the roughest coastal regions in the world. Breaking waves occur at the study site under even moderate wave conditions. Dependable occurrence of breakers in the inlet prompted the U.S. Coast Guard to locate its school for motor lifeboat operators here. The winter trial successfully collected data from 10 sites, in water depths ranging from 10 to 50 m (33 to 165 ft), when surface currents exceeded 6 knots (7 mph) and breaking waves exceeded 6 m (20 ft) in height. Safe navigation of a vessel and over-side research vessel operations such as deploying instruments would not have been possible under these conditions.

Deployment and retrieval techniques

Figure 40 illustrates the instrument package in flight, suspended from the helicopter. The principal components of the system are (a) the instrument frame, (b) a mooring line, (c) a surface buoy, (d) a buoyant recovery line, (e) a stopper buoy, (f) a triple-hook grapnel, and (g) a lift line. To deploy the instruments, the assembly is lowered until the surface buoy is floating and the recovery line is slack. For a short (on the order of minutes) measurement, the pilot maintains a hover, without tensioning the recovery line. For a longer measurement, the frame is released by continuing downward until the stopper buoy is floating and the grappling hook disengages. Recovery (Figure 41) is accomplished by approaching the streaming recovery line perpendicularly, with the grappling hook just below the surface. Continuing forward and upward slides the recovery line through the hook until the stopper ball is reached. At that point the recovery line is secure, and the load can be picked up for repositioning or return to shore.

Components

Instrument frame. The instrument frame has a 1.5-m (4.9-ft) square base, constructed of 7.5-cm (3-in.) aluminum H-beam and bolted connections. A 0.6-m- (2.0-ft-) high Aroll cage© is made from 5-cm- (2-in.-) square aluminum tubing to protect the instruments. The frame is also the anchor for the surface buoy, so it must be sufficiently heavy to maintain position under the expected conditions. To hold the surface buoy in high-current, surf-zone regimes, eight trapezoidal sections of 2.5-cm- (1-in.-) thick lead plates are bolted to the frame, bringing its total weight to about 1,350 kg (3,000 lb). Brackets for individual instruments are bolted to the base of the frame. Typically, several instruments (for example, wave gauge, and current meter) may comprise on one package, and their combined weight can exceed 100 kg (220 lb). In addition, a transponder acoustic beacon is usually included to provide a means of locating the frame in the event it becomes separated from the surface float.

A 4-part lift bridle, made from 2.5-cm- (1-in.-) diam. double-braided Dacron line is secured at each corner with 5-cm (2-in.) shackles. The four lift lines

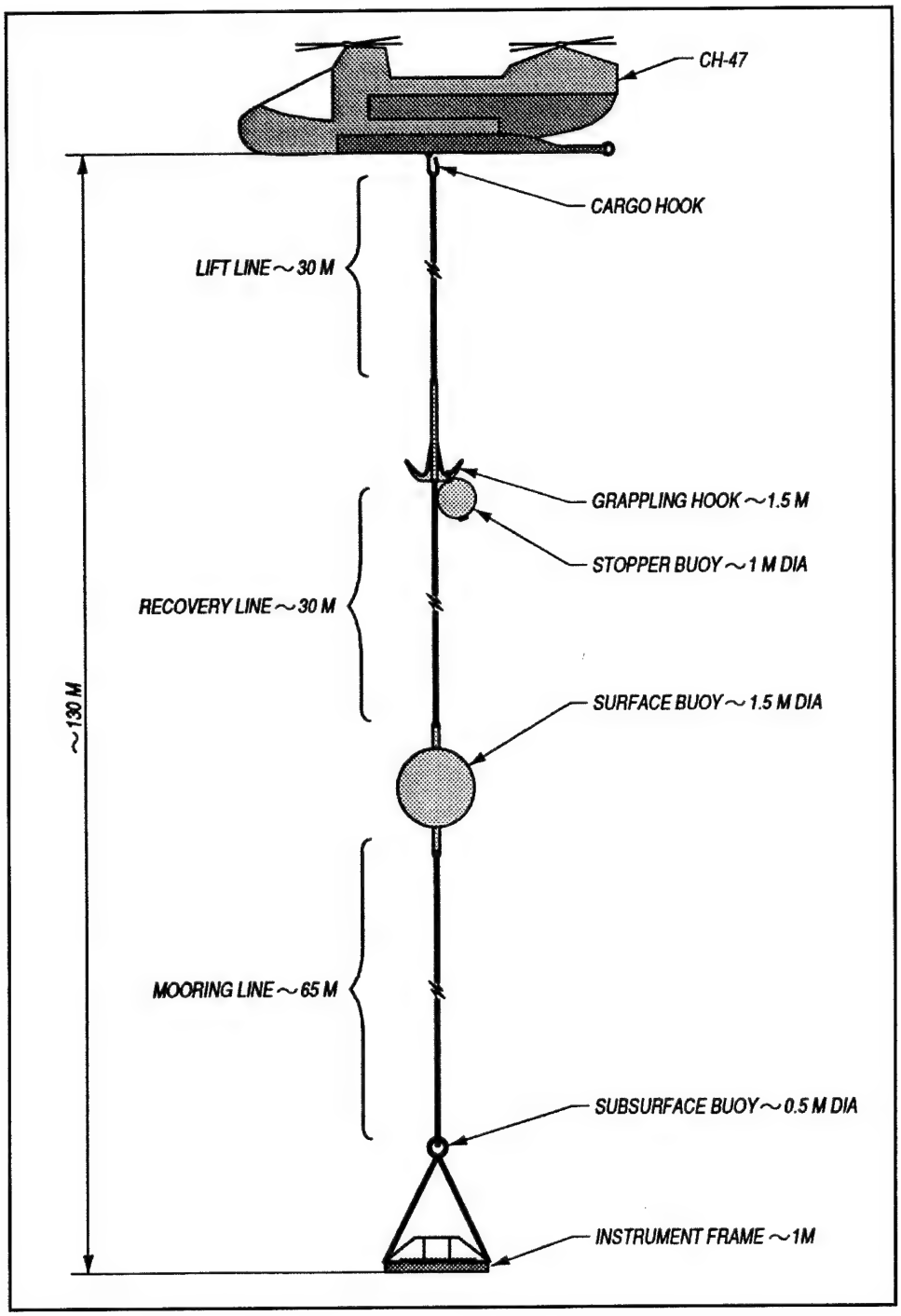

Figure 40. Helicopter instrumentation system suspended while in flight (after McGehee and Mayers 2000)

converge to a 2.5 cm (1 in.) section steel D-ring, approximately 1 m (3.3 ft) above the base of the frame. A float secured to the D-ring prevents the slack bridle from becoming entangled in the frame or instruments during a measurement. The float should have about 15 kg (40 lb) of positive buoyancy and be rigid, so that it will maintain buoyancy at depth.

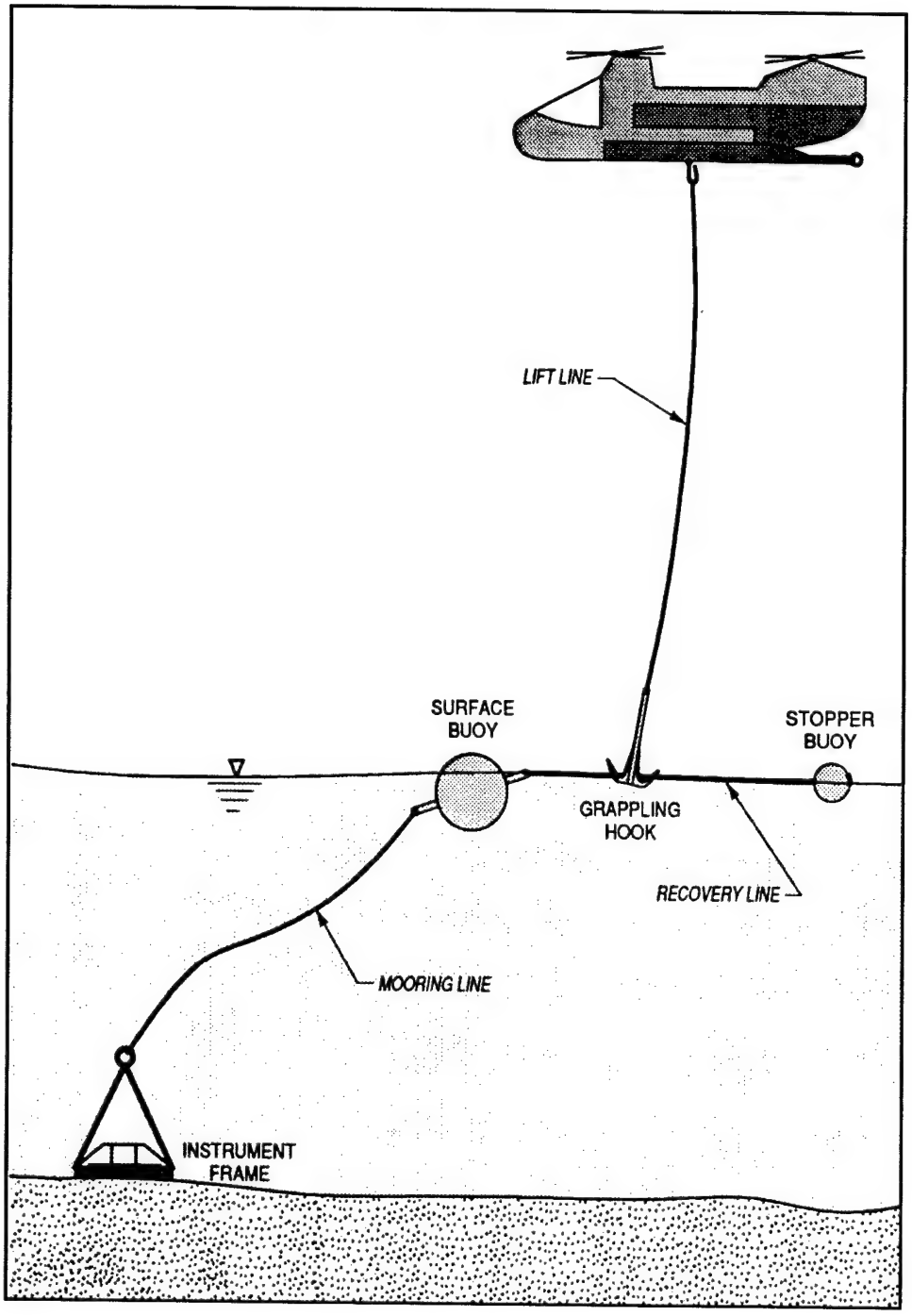

Figure 41. Helicopter system recovery (after McGehee and Mayers 2000)

Mooring line. The mooring line is a 2.5-cm- (1-in.-) diam. synthetic line with an aramid braided core and a double braided polyester jacket for abrasion protection. This is a torque-balanced construction that combines high strength (25,900 kg (6,000 lb) breaking) with extremely low stretch (less than 1 percent at 30 percent of rated strength). The length is adjusted to be about twice the maximum water depth expected or about 65 m (213 ft) for the MCR experiment. Soft

eyes (i.e., without thimbles) are back-spliced in each end for connecting to 5-cm (2-in.) shackles.

Surface buoy. The surface buoy is a 1.2-m- (4-ft-) diam spherical buoy made from rolled 6-mm (1/4-in) steel plate (Figure 42). A 1.8-m- (5.9-ft-) long, 10-cm- (4-in.-) diam schedule-80 steel pipe forms a strain member through the central, vertical axis. An internal pad eye on the bottom of the pipe accepts a 5-cm (2-in.) shackle. The weight of the buoy is about 275 kg (606 lb). To improve pitch/roll stability of the buoy, an additional 360 kg (880 lb) of 5-cm- (2-in.-) diam anchor chain was attached to the bottom of the pipe as external ballast, providing a metacentric height of approximately 15 cm (5.9 in.). The attachment point for the recovery line is a welded bail of 2.5-cm- (1-in.-) diam steel bar at the top of the central pipe. A battery-powered light can be placed under the bail if the system is to be left at sea overnight.

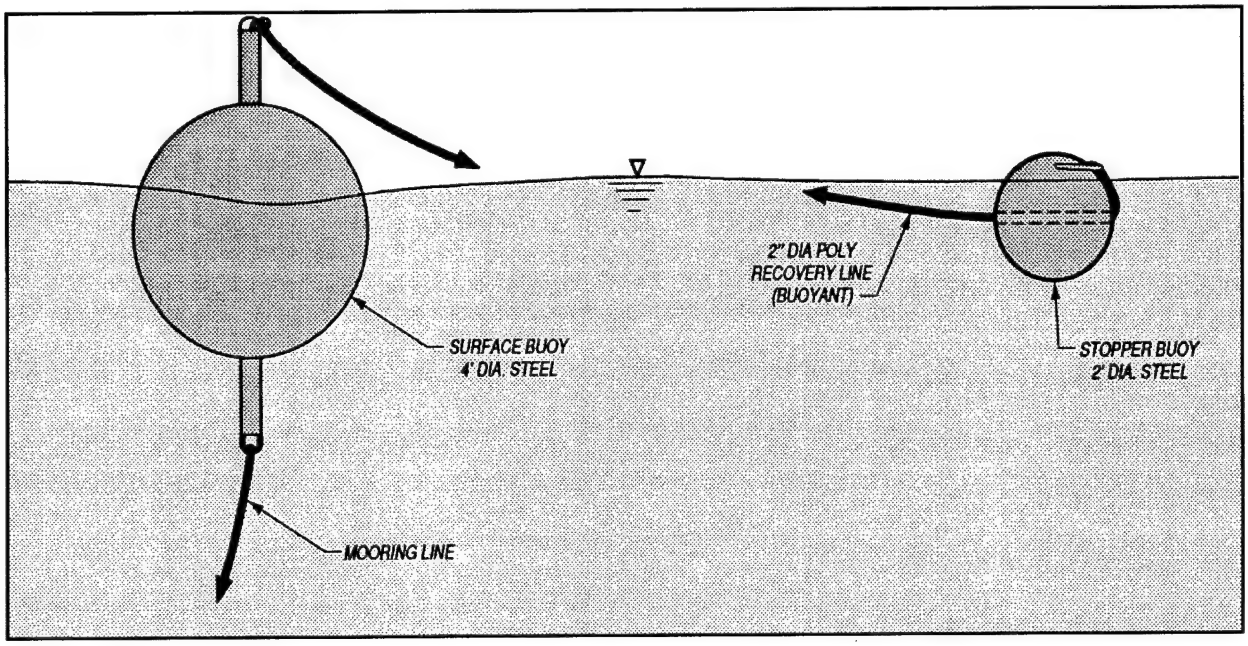

Figure 42. Surface buoy and stopper buoy (after McGehee and Mayers 2000)

Recovery line. The buoyant recovery line is a 30-m (98-ft) length of 5-cm- (2-in.-) diam, 3-strand, braided polypropylene line. The line is attached to the bail on the surface buoy with a 5-cm (2-in.) shackle and a 45,000-kg (50-ton) rated crane swivel.

Stopper buoy. A 61-cm- (2-ft-) diam spherical buoy of 6-mm (1/4-in.) steel serves as the stopper to capture the grappling hook as it slides down the recovery line (Figure 42). A 7.5-cm- (3-in.-) schedule-40 steel pipe is welded flush through the center, as a guide for the recovery line, and as compressive reinforcement for the impact loads from the grappling hook. At the opposite side, a 2.5-cm- (1-in.-) round steel bar is bent into a V-shape and welded to the buoy. The bitter end of the recovery line is pushed through the guide pipe, and a soft eye was backspliced around the V-shaped bar. This arrangement ensured that the stopper buoy could not disengage or slide freely down the recovery line.

Because chafing of the line against the guide pipe is a concern, the exit hole is carefully radiused and smoothed, and the line wrapped with tape at that point.

Grappling hook. The shaft of the hook is a 1.5-m- (4.9-ft-) long, 8.9-cm- (3.5-in.-) diam, double-X steel pipe (Figure 43). Three hooks are cut from 1.9-cm (0.75-in.) steel plate and welded to the shaft. Sections of 2.5-cm (1-in.) pipe are slotted to fit over the inside surface of the hooks as fair-lead, to prevent abrasion of the recovery line. A 6-cm- (2.4-in.-) diam hole in the upper end accepts the 5-cm (2-in.) shackle; next is another 45,000-kg (50-ton) rated crane swivel, to prevent torque transferring up the lift line to the cargo hook.

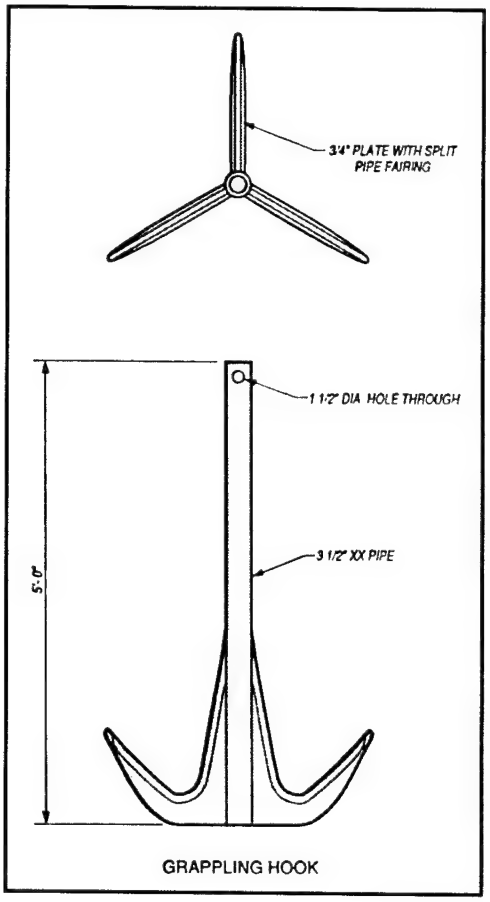

Figure 43. Grappling hook (after McGehee and Mayers 2000)

Lift line. The lift line is a 30-m (98-ft) length of the same Spectra line used for the mooring line with soft eyes. At the upper end, a special high-tensile steel shackle, a piece of standard hardware for the CH-47, makes the connection to the helicopter's cargo hook.

Discussion

Several points should be considered in planning this type of operation. The ability to measure coastal waves and currents in situ at multiple sites, under extreme wave and current conditions, has been demonstrated at the MCR. However, weather restrictions prevent this from being an all-weather option. Deployment by helicopter is a VFR (visual flight rules) operation; a ceiling of at least 500 m (1,640 ft) is required. Although it can fly in strong winds, the CH-47 cannot start its engines in winds exceeding 30 knots (35 mph). If the winds exceed 60 knots (69 mph), the aircraft cannot remain outdoors, but must be secured in a hanger.

With practice, each wave measurement should take 30 to 45 min. If a landing area is available in the vicinity, four to five sites per fueling are possible. Refueling takes about as long as one wave measurement. The process is logistically challenging.

Functioning aircraft and instrumentation have to coincide with personnel schedules and operational flying conditions for a successful day of measurements. Adequate time must be allowed for crew training and aircraft maintenance on top of the expected field delays. A full week should be allowed for most data collection experiments. The expertise of the aircrew is central to the success of the mission. Refinements in the hardware and procedures can reduce the reliance on crew skill, but precise hovering and positioning over rough water will always exercise piloting skills. More so than most field operations,

advanced planning and design of every component are essential success. Every nut and bolt must be examined in light of its marine, aeronautical, safety, and measurement function.

Analysis of Collected Data

Frequency distribution of wind and wave parameters[1]

Frequency distributions of wave and wind conditions were computed to compare the environmental climate of the periods of data collection at the MCR to longer-term averages. Instrument deployments correspond to the following time periods:

a. Deployment 1: 19 August – 22 September 1997.

b. Deployment 2: 17 April – 28 June 1998.

c. Deployment 3: 30 October 1998 – 08 March 1999.

All data included in the frequency histograms come from a merged database of conditions from three NDBC buoys located off the Pacific Northwest coast during the 12-year period from January 1987 through April 1999. Distributions for the period of tripod deployment are determined from the buoy data for the specific time of instrument deployment and distributions for the 12-year data are compiled from data with calendar dates corresponding to the deployment of interest.

Figures 44 through 46 present frequency distributions for wave conditions for Deployments 1-3. Figures 47 through 49 present frequency distributions of wind speed and wind direction and directional distribution of wind energy for Deployments 1-3.

Current data analysis[2]

Overview. Reduction of the current data was a multistep process that culminated in the creation of several analysis programs suitable for any deployment with similar data collection characteristics. The four tripods were programmed and deployed with a predetermined data-sampling scheme designed to maximize the quantity of collected data. The tripods remained on station for approximately 2 months, were retrieved, and the raw ADV and ADP data files were downloaded from each tripod. Using SonTek extraction and conversion programs included with the instrumentation software, the required current data fields from the raw files were extracted from their binary files to easily manipulated ASCII files. File extraction was completed both for the complete record and in 1-day segments. MATLAB, a computation and visualization program, was used to

[1] This section was taken from Gailani, J. Z., and Smith, S. J. (2000). "Analysis of sediment transport processes, mouth of the Columbia River (MCR), Washington/Oregon," Unpublished manuscript, U.S. Army Engineer Research and Development Center, Vicksburg, MS.

[2] This section is extracted essentially verbatim from Lund et al. (1999).

develop three programs to analyze the ASCII files, and determine and plot several different current characteristics. The first program analyzed an entire site record, saved significant results in a file accessible to other applications, and created two plots of the record. The first plot depicted current velocity and standard deviation versus time, and current direction and standard deviation versus time. The second plot depicted a polar scatter plot representation of the current velocity. The second program plotted depth-averaged current velocity and average current direction versus time for a user- specified 8-day period of data from one site. The final plotting algorithm analyzed a user-specified single day's information and provided a 3-D profile over depth of current and standard deviation for each of the burst samples collected during the day. Two versions of each program were written. One version enabled the user to analyze and merge ADP and ADV current information on dates when both data types are available. The second version allowed the user to analyze the ADP data only.

Sampling scheme. The data sampling scheme was developed by OSU staff and USACE to obtain the maximum amount of data, given the power and data storage capacity of the ADP and ADV. To obtain both current and wave information, each ADV was programmed with two data sampling programs. The first program, designed for current analysis, collected samples for the first 10 min of every one-half hour at a specified sampling rate of 1.0 Hz for Site B1, and 0.1 Hz for Sites B2 and E. The second sampling program, designed for wave analysis, collected samples for the first 17 min of every one-third hour at a sampling rate of 4.0 Hz. Each ADP was programmed to sample 12 cells during the first 10 min of every one-half hour and provide a single profile for the sampling period

Since the ADV was programmed with two sampling schemes and collected data more frequently and in greater quantity, each ADV utilized 60-75 percent of its available 85 megabytes of memory and exhausted its batteries prior to retrieval. In contrast, during the deployment each ADP utilized less than 10 percent of its available 10 megabytes of memory and had adequate power to remain onsite for several more months.

Raw data files. When collecting data, both the ADP and ADV saved the data in a compressed binary format to minimize the amount of storage space. Although the binary data files may be accessed directly, most analysis programs are designed to operate on data in ASCII format. To meet the needs of these analysis programs, the SonTek software was programmed with several different MS-DOS data extraction and conversion algorithms that enabled the extraction of various pieces of data for all or for a finite number of profiles.

Data from the four retrieved ADP sensors were downloaded from the sensors to a laptop computer and then transferred to a desktop computer running the Windows 95 operating system. The file name can be pre-set by the user as desired; however, the extensions ".ADP" and ".ADV" are automatically annotated once data collection commences and are required for the extraction programs to recognize the file.

ADP data extraction. To complete the ADP data analyses, four SonTek conversion programs were utilized. This was a time consuming process;

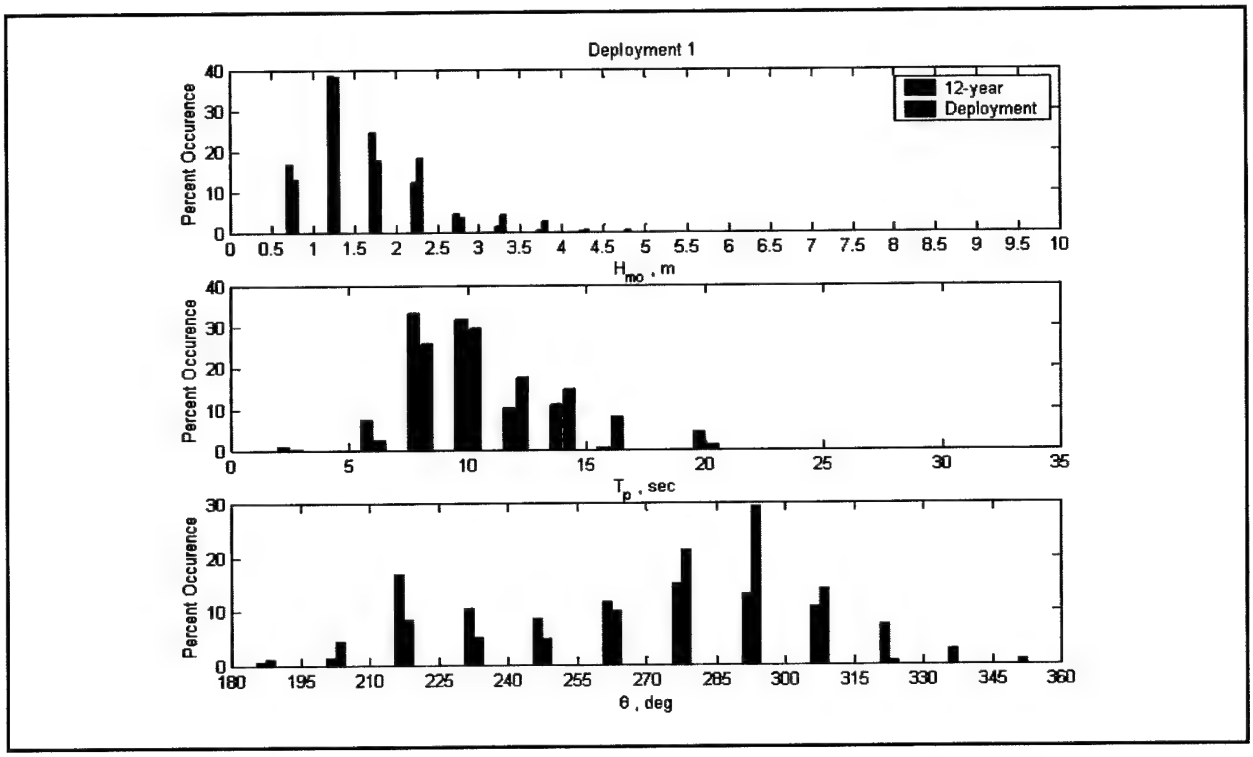

Figure 44. Frequency distribution of wave conditions for Deployment 1 (after Gailani and Smith, op. cit., p. 101)

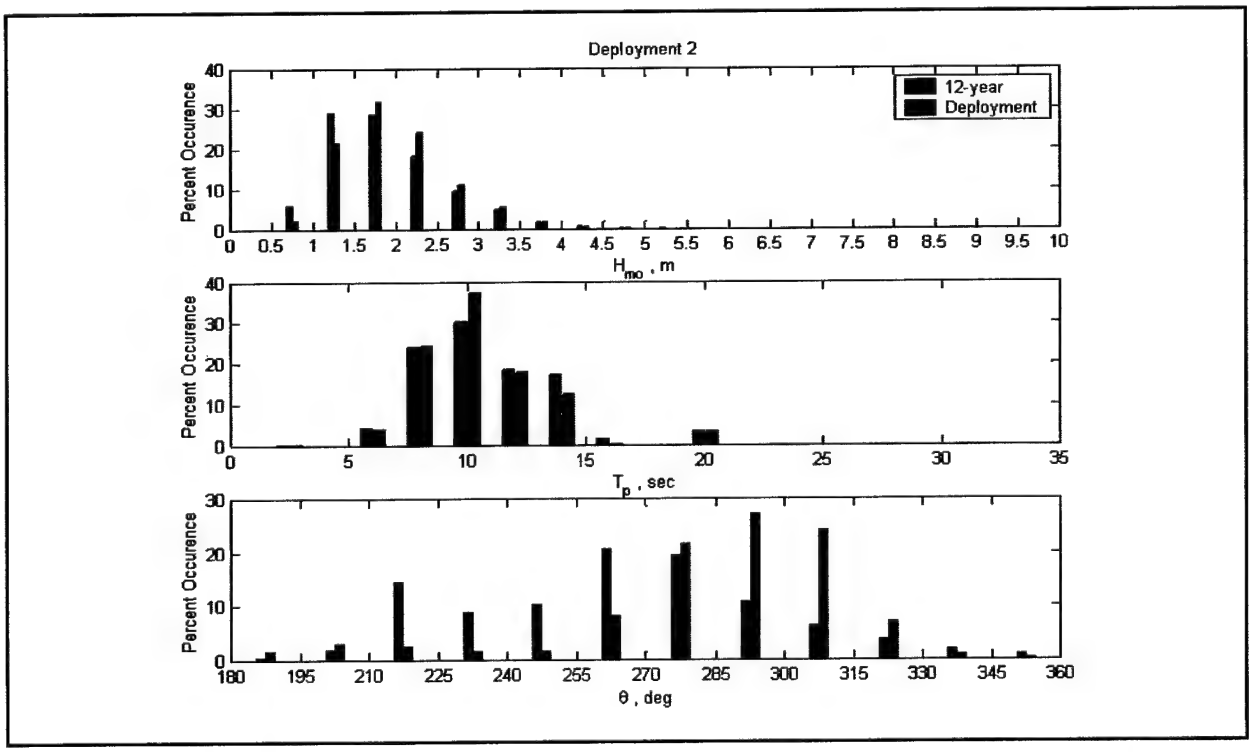

Figure 45. Frequency distribution of wave conditions for Deployment 2 (after Gailani and Smith, op. cit., p. 101)

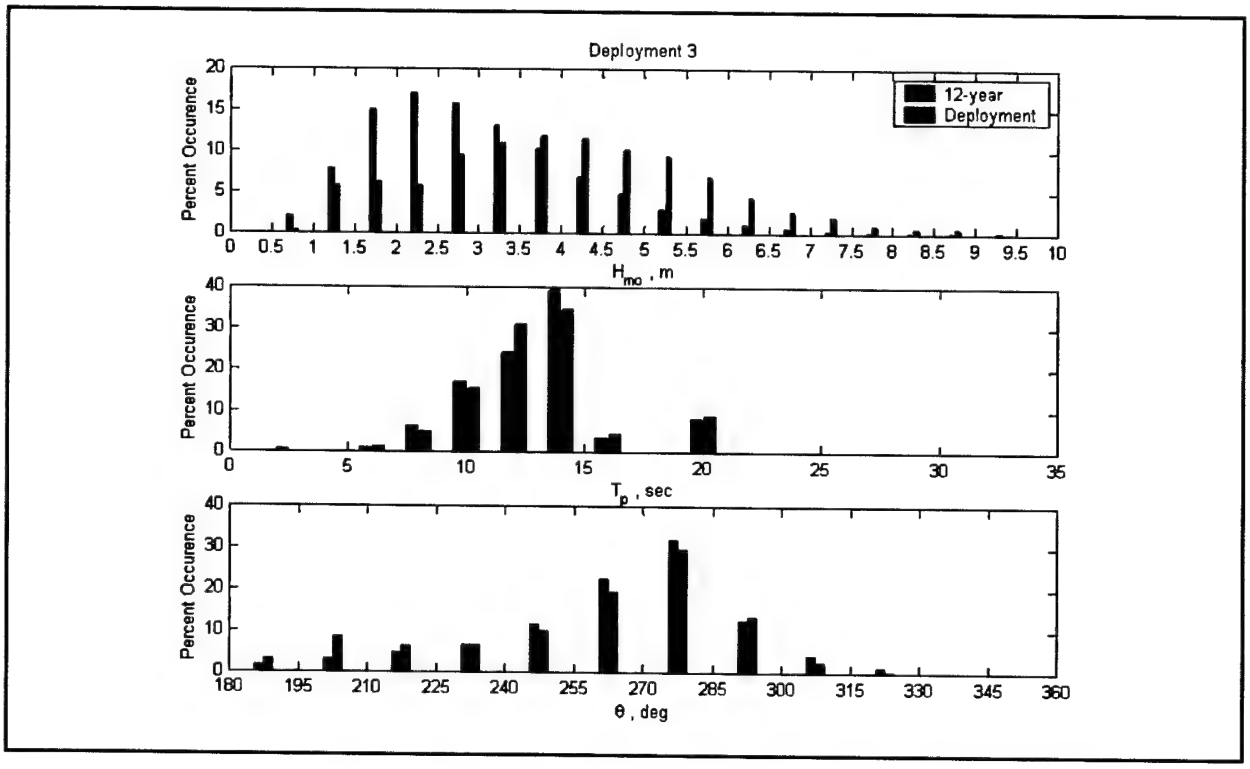

Figure 46. Frequency distribution of wave conditions for Deployment 3 (after Gailani and Smith, op. cit., p. 101)

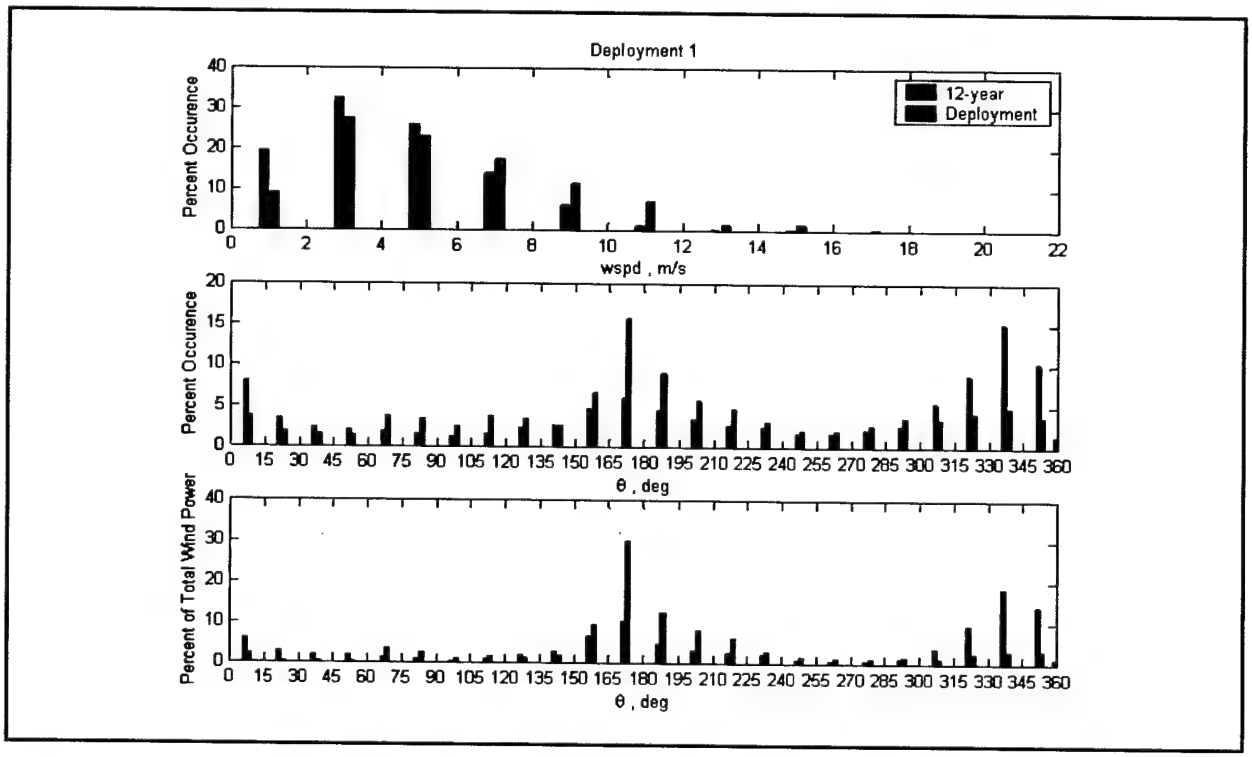

Figure 47. Frequency distribution of wind conditions for Deployment 1 (after Gailani and Smith, op. cit., p. 101)

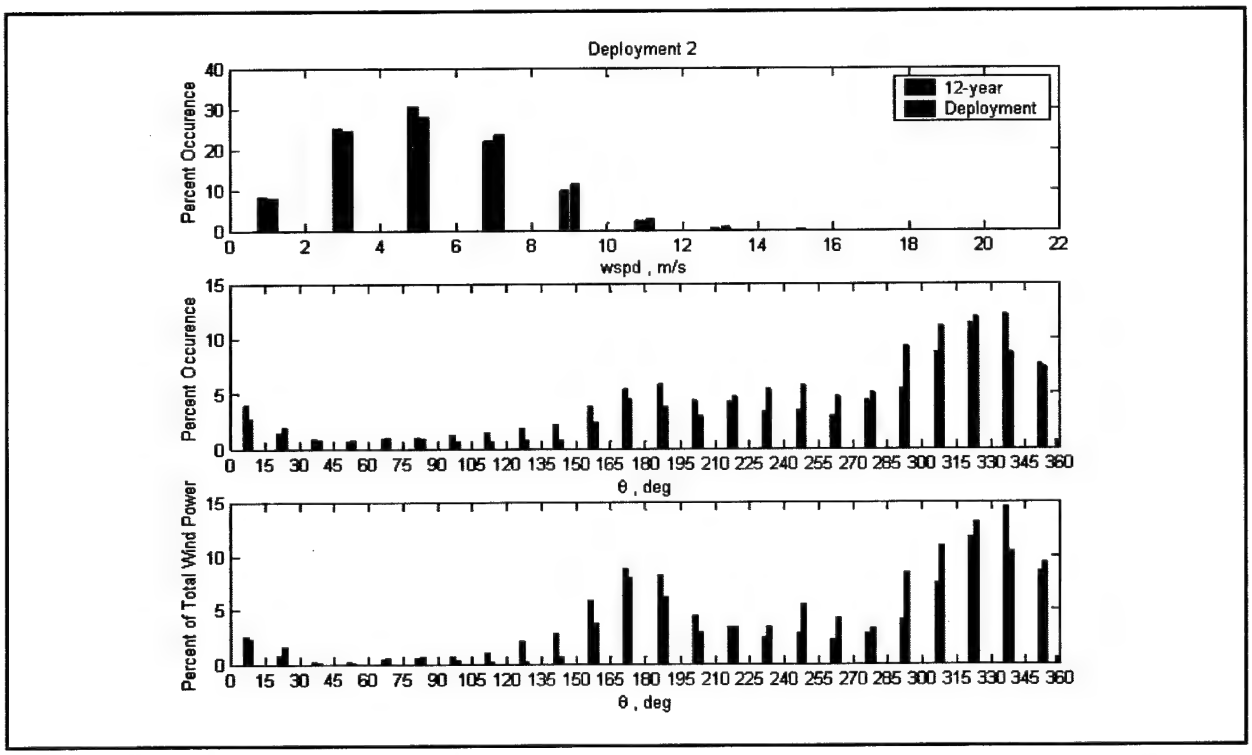

Figure 48. Frequency distribution of wind conditions for Deployment 2 (after Gailani and Smith, op. cit., p. 101)

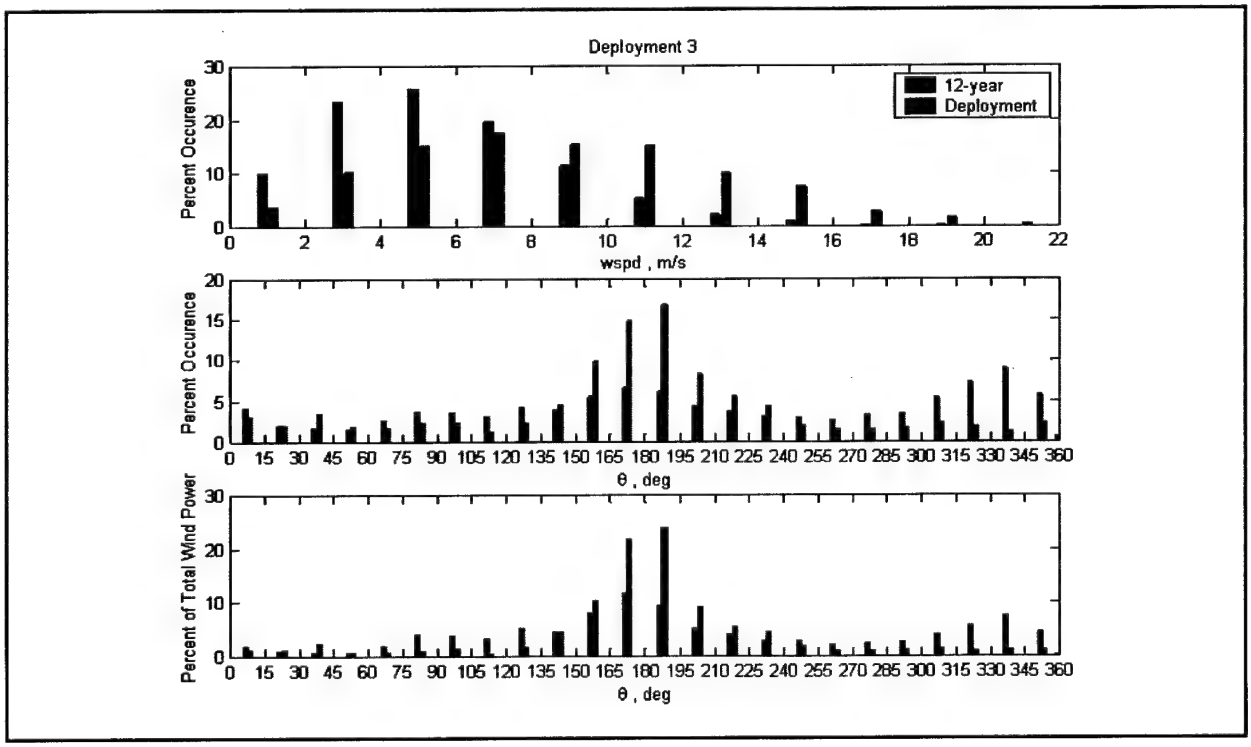

Figure 49. Frequency distribution of wind conditions for Deployment 3 (after Gailani and Smith, op. cit., p. 101)

however, each program extracted a certain segment of the profile and there was no redundancy of data between extracted fields. In the case of the ADP data analysis, the required data consisted of the east and north velocity components, the east and north velocity component standard deviation values, the profile header which contains information on time and date of sampling for each profile, and the control data (a 2-page listing of both the data collection settings programmed into the sensor prior to deployment and information on number of profiles taken).

For these analyses, data were extracted both for the entire record and in 1-day increments for each site. Since the deployment and activation times were preset and the ADP sensors were programmed to collect current data once every one-half hour, determination of the profile numbers to extract for a given day was simply a manner of breaking each complete day into its respective 48 profiles. To accomplish this, the control file was first extracted. At the very beginning of the control file, the time and date of the first and last bursts are recorded. All times are referenced to Greenwich Mean Time (GMT). Knowledge of the profile numbers and dates is a prerequisite to utilizing the MATLAB algorithms discussed later. Although, it is possible to extract all profile information quickly and simultaneously for a given data field, the extra time used reducing the data to discrete single-day information was found to be invaluable when developing the analysis algorithms and examining the analysis results. Additionally, the fully extracted files were extremely large, especially the ADV files, which exceed 100 megabytes when extracted.

Once the profile numbers were determined, a file naming convention was selected to simplify the process and avoid confusion regarding which data file corresponded to which site or date. The naming convention consisted of the site location, using "B1", "B2", "E", or "M" as the site indicators, and the 4-digit date, expressed as 2-digit month and 2-digit day. Extracted files containing the complete record were given the name "All", site designator, year, and the extracted component; i.e., file AllB1H is the entire header record for Site B1.

Using the ADP extraction software resulted in the generation of five different files per day; (a) the header file, (b) north velocity component, (c) east velocity component, (d) north standard deviation, and (e) east standard deviation. Since data were originally collected in 3-D coordinates, the software also automatically extracted the Up components for both velocity and standard deviation. However, since the analysis was concerned with the 2-D profile, the Up components were manually deleted. Further, file renaming was conducted to help distinguish more clearly between file types. This step was not required since each extracted file has a unique extension that the analysis program can be modified to recognize. However, the velocity extraction protocol and the standard deviation protocol, when utilized, extract both the east and north components into files of the same name with extension ".VI" and ".SDl" for east components and ".V2" and ".SD2" for north components. Since this originally resulted in four files with the same name but only different extensions, there was some initial confusion during programming. As a remedy, the file names were altered to include additional distinguishing information about the file. Therefore, the north velocity component was amended to read the site indicator, the 4-digit date, "N" and its extension; i.e., BI0819N.v2 for Site Bl, August 19, north velocity file. Similar

changes were made to the other files with an "E" used with the east velocity component, and "SDE" and "SDN" for the east and north standard deviation components, respectively. Header files, extension ".hdr" required no renaming, but were amended during extraction to include an "H" after the date. All files and site folders for 1997 (for example) were placed within a folder named "ExtractedData1997" to avoid conflicts regarding the year the data were collected.

ADV data extraction. Extraction of ADV data varied little from the extraction of ADP data. As with the ADP files, the ADV control file was consulted to determine the times and dates of the first and last sample burst. That information was used to determine dates and their corresponding burst numbers. Since analysis of wave conditions was not being considered here, only the current data (program No.1) was extracted and utilized. The ADV velocity data were extracted both for each site's entire record and for daily samples. Unlike the ADP, the required ADV information could be found in one file versus having to extract several different files. The naming convention utilized for the ADV file name consisted of an "X" followed by the site designator (B1, B2, E, or M), the 4-digit date and the automatically appended ".ts" extension. Thus, file "XEO824.ts" corresponds to ADV samples at Site E on August 24. The complete record at each site was also extracted and named "XAliE.ts", "XAliB1.ts", and "XAliB2.ts", respectively.

Extracted file formats. The ASCII files created by the SonTek extraction process are in matrix format and are easily manipulated by a number of analysis programs. The basic extracted file consists of rows and columns of data. For the ADP, each row corresponds to one profile. The ADP velocity and standard deviation files are of similar format. The first column lists the profile number, and the remaining columns correspond to the number of cells being sampled, with the closest cell being first. Thus for the 1997 deployment, the ADP velocity and standard deviation files had 13 columns with rows equal to the number of profiles. The ADP header file contained an equivalent number of rows, but had 20 columns of data including profile time and date, speed of sound used to calculate velocity, temperature, and pressure. For purposes of this analysis, the only information needed from the header was the date and time information, columns two through seven.

The ADV velocity file was also in matrix format with 19 columns. The first column corresponded to the burst number and the second column corresponded to the sample number within a given burst. Columns 3 through 5 provided the east, north, and up velocity components, respectively. Other information stored within this ADV file included the temperature, the pressure recorded from the Paroscientific pressure gauge, and the OBS data. For this analysis, only the east and north velocity components were utilized.

MATLAB overview. In compliance with USACE analysis methods, OSU personnel completed the MCR current data analysis utilizing MATLAB. MATLAB, is a computing language that combines computation, visualization, and programming into an environment where the problems and solutions are posed in mathematical notation. The basic MATLAB data element is an array, which allows the user to solve problems with data in vectors, strings of numbers,

or matrices. A powerful set of graphical tools enables the user to plot data in one of several standard formats, or to program custom formats. In addition, MATLAB is compatible with Microsoft and other software packages, and can be programmed to import and export data of various file types provided the data is in vector or matrix format. MATLAB version 5.2 was utilized for this analysis.

Current data results and conclusions[1]

An evaluation of the current data collected at Sites B1, B2, and E during the 19 August – 09 October 1997 deployment was performed by OSU. Although a 60-day record may be insufficient for a complete annual interpretation of the MCR, one may immediately perceive several trends. Site E was located closest to the terminus of the Columbia River and the north jetty, and was in the shallowest location. Conversely, Site B1 was farther offshore and deeper, and Site B2 was several miles from the jetties and located in water nearly twice as deep as the other two sites.

Site E demonstrates the greatest variability in both velocity magnitude and current direction during this time period, and also the greatest velocity magnitude, being approximately 225 cm per sec (7.38 ft per sec), or 4.3 knots (5 mph). It appears that the normal mean velocity for the record is approximately 50 cm per sec (1.64 ft per sec), or 1 knot (1.2 mph) during this time period, and the corresponding direction is towards the west-southwest, approximately 245 deg from true north which corresponds closely to the river channel orientation in that region. The standard deviation values for both current and direction are about the same magnitude as Sites B1 and B2.

The natural features and the jetties provide a narrow conduit through which the tide floods and ebbs in the Columbia River. Although the Columbia River is a pooled river throughout much of its length, the USACE provides sufficient flow to generate hydroelectric power and maintain channel depth. This flow has an exacerbating effect on ebb tides by adding to the volume of water and a mitigating effect on flood tides by impeding the inland migration of the tide. Therefore, one should expect to see weak flood tides and strong ebb tides, as is evident at Site E. Additionally, at such close proximity to the river channel and terminus, one should expect the tidal flow to be aligned with the natural channel, a trend that is also readily observed.

As one progresses offshore to Site B1, one observes both a decrease in the variability of current velocity and direction, and a decrease in the occurrence of extreme velocity events. In this instance, the median velocity once again appears to correspond to approximately 50 cm per sec (1.64 ft per sec). In regards to current direction, there appears to be a strong westerly current and a strong northerly component. The response at Site B1 follows inferred behavior. The further progression offshore accounts for decreasing velocities due to flow expansion. The current direction, rotating from west-southwest at Site E to west at Site B1 also demonstrates a consistent pattern that could be the result of tidal

[1] This section is extracted essentially verbatim from Lund et al. (1999).

current interactions with local longshore currents, the latter directed south to north for fall storm conditions.

Site B2 shows a continuing decrease in extreme current velocities and an apparent decrease in the median current at the site, approximately 40 cm per sec (1.31 ft per sec), or 0.75 knots (0.86 mph). This again can be attributed to flow expansion due to increasing distance and depth. One will observe the directional profile is nearly a mirror image of Site B1, again indicating potential offshore and longshore effects.

Two significant trends may be observed when comparing the results of these three sites. At each location one may perceive at least three unusual events and potentially a fourth event. The weakest of these four events appears to be evident over days 5-10, or approximately August 24- 30. The second and apparently longest event occurred during days 25-31, or approximately September 12-19. The third and fourth events occurred during days 42-52, or approximately September 30-October 10. These dates correspond well with the unseasonably high wave events encountered during that year's El Nino.

The second trend may be discerned from the mean current direction plots from Sites B1 and B2. If one were to remove the outlying data points and the extreme events and smooth the plots, one would observe the current direction varying in a consistent periodic wave with an approximate period of 30 days. Given the lunar cycle is 29-½ days, there appears to be a correlation between the current direction and lunar cycle, although the record length is too short to confirm this. A similar trend in current magnitude may also be observed; however, it is not as readily apparent.

Polar plots provide an additional overall picture of each site, and help clarify trends identified on time dependent plots. One can again identify the strong west-southwest ebb dependency and the very consistent and relatively weak flood at Site E. The results at Site B1 vary somewhat, with the results indicated by time dependency plot. One may observe the westward directed components as was evident from the time dependent plot, but in addition, one obtains a true impression of the impact and strength of the northward directed current. Finally, at Site B2, one also obtains a better impression from polar plot of the strength and impact of the northward directed currents. Overall, polar plots also demonstrate the impact of flow diffusion with increasing depth and offshore distance. As one progresses from Site E to Site B1 to Site B2, one sees the data transition from a loose pattern of data points to a concentrated pattern grouped more closely around the origin. Therefore, with decreasing depth and offshore distance the current velocity does decrease.

Suspended solids from Optical Backscatter Sensor (OBS) Data[1]

Optical Backscatter Sensors (OBS) measure the reflection of emitted radiation off of solids suspended in the water column, regardless of the source of

[1] This section was written by Joseph Z. Gailani and S. Jarrell Smith, U.S. Army Engineer Research and Development Center, Vicksburg, Mississippi (Gailani and Smith, op. cit., p. 101).

reflection (sand, fine particles, organic material, biological fouling, aquatic organisms, etc.). Assuming that fine particles that result in turbidity are well mixed and do not settle rapidly and that sand particles are suspended and settle out intermittently, a defined level of background turbidity can be established and subtracted from the indicated OBS signal (Beach and Sternberg 1988). The method for estimating the background turbidity involves the application of a moving window for which a 10^{th} percentile value of OBS signal is determined. This 10^{th} percentile value represents the concentration for which 10 percent of the concentration values within the window limits are less than. The 10^{th} percentile concentration, or the background turbidity, is then subtracted from the signal to result in a concentration that is assumed to represent the concentration of sand in the water column.

During the periods of data collection for Deployments 1 and 2, the OBS signal often contained spurious signals that were not representative of the suspension and settling of sand with signal magnitudes inconsistent with the forcing conditions measured. Small plumes of fine sediments discharged from the river, aquatic life, suspended debris were presented as conjectural explanations for the anomalous signals, but identification of the sources of signal contamination was not possible. The OBS signals were further analyzed to eliminate signals inconsistent with the suspension of sandy material.

A method was developed to identify OBS signals consistent with the suspension of sand from the orbital velocities of passing waves. The initial step in this method required visual inspection of the OBS signals for each site and deployment to identify a representative set of data bursts for which little signal contamination was evident. The selected bursts were further analyzed, and tables were developed indicating maximum plausible concentration as a function of wave height and OBS position above the bed. (No correlation was found between magnitude of the mean current and measured concentration.) The remainder of the data set was then filtered as guided by the statistics from the visually inspected "clean" data bursts. Data bursts with severely contaminated signals were eliminated from the analysis.

Inspection of the clean data sets at ODMDS B and E indicated that concentration signals at the two locations were quite different. ODMDS E included numerous high concentration bursts that were less frequent at ODMDS B. This is consistent with bathymetry data described earlier which indicate that ODMDS E is more dispersive. However, there may be other reasons for these high concentrations. The elevation of the dredged material configuration at ODMDS E is only 1-2 m (3.3-6.6 ft) above the finer native sediments. OBS measurements at ODMDS E may therefore include suspension of the finer native sediments. In addition, bathymetry data indicate that dredged material placed at ODMDS E generally disperse within 1 year of placement, so only small quantities of the 0.22 mm dredged sediment may have remained at ODMDS E during portions of the two deployments. At ODMDS B, the OBS is atop a 21.4-m (70-ft) mound created exclusively of the coarser MCR-dredged material, which isolates the measurements from suspension of the finer native material.

5 Numerical Modeling

Modeling Objectives and Study Objectives[1]

Modeling objectives

Under the USACE Dredging Research Program (DRP), several sediment fate numerical simulation models (STFATE, LTFATE, MDFATE, HPDPRE, HPDSIM, and ADCIRC) were developed or enhanced to improve the reliability of long-term site management of ODMDS. The numerical simulation modeling objectives of this MCNP monitoring at the MCR include:

a. Verifying the applicability of the DRP numerical models for the evaluation of ODMDS.

b. Assessing the data collection needs for site evaluation by the DRP models.

c. Identifying the capabilities and limitations of the DRP models.

d. Developing a systematic methodology for the application of the DRP models at other Corps districts.

The primary restriction of the DRP sediment fate models is that reliable environmental input (oceanographic) data is required to accurately simulate dredged material behavior at a specific ODMDS. Such required prototype environmental data did not previously exist at the MCR, and had to be acquired by the deployment of four tripod instrumentation platforms discussed in Chapter 4, "Field Data Collection and Analysis." These precise data were used to correlate oceanographic processes with seabed change at the MCR, and to simulate the fate of dredged material placed in the MCR ODMDS.

A wave transformation numerical simulation model (RCPWAVE) was also applied at the MCR to ascertain the extent of wave height amplification and resulting hazards to navigation by the MCR ODMDS. This analysis found wave height amplification factors as high as 1.8 for a 16-sec wave in the lee of the ODMDS. Although these results may be conservative, they confirm reports of hazardous conditions from vessels transiting the project area.

Since 1957, dredged-material disposal activities have placed approximately 123 million cu m (161 million cu yd) of material in the area of the ebb-tidal shoal at the MCR. Prior to 1977 there were no restrictions on dredged material

[1] This section was written by Heidi P. Moritz and Hans R. Moritz, USAED, Portland.

placement. In 1977, interim disposal site boundaries were established primarily to address environmental concerns related to mounding of the dredged material. In 1997, the Portland District was again looking at expanding the site boundaries to eliminate the chances of mounding and to increase the site capacity. In addition to disposal site size, disposal locations are also limited by the 4-mile radius about the MCR that is referred to as the zone of feasibility for maintenance dredging. This radius delineates the cost-effective haul distance for dredge disposal vessels at the MCR.

Study objectives

The study objectives of this MCNP monitoring at the MCR pertain to the following:

a. Managing large volumes of dredged material in small disposal sites.

b. Minimizing the haul distance for disposal activities.

c. Avoiding the creation of adverse navigation conditions.

d. Reducing the need for expensive prototype data collection efforts.

The focus region of the MCNP effort for attaining the study objectives includes ODMDS B located on the ebb-tidal shoal, and ODMDS E located near the north jetty and adjacent to the navigation channel.

The annual volume of dredged material placed at the MCR ODMDS is approximately 3.8 million cu m (5 million cu yd), and is dredged from water depths that range from 18 to 43 m (60 to 140 ft). ODMDS B and E represent two distinctly different sites. ODMDS B is believed to be wave-dominated and appears to be nondispersive. ODMDS E is believed to be current-dominated and appears to be very dispersive.

ODMDS B site management problem is apparent anomalous mounding of placed material. One instrumentation tripod platform (Site B2) was placed seaward of the high mound in water about 36 m (118 ft) deep (Figure 4). Dredged material was placed in this area, and a dump-free corridor was established within 150 m (500 ft) of this tripod. The tripod measured waves incident to the ODMDS complex, and provided hydrodynamic information on the material placed in deeper water. A second tripod (Site B1) was placed directly on top of the mound in water about 18 m (60 ft) deep (Figure 4). Reasons for this placement were (a) the mound is a long-standing problem, and data are required to understand and quantify sediment movement here, (b) the data will support DRP numerical simulation model evaluations, and (c) combined with information from the offshore tripod at Site B2, wave transformation can be examined to address navigation-safety issues.

ODMDS E provided an opportunity for increased beneficial use of dredged material because beaches to the north in the State of Washington will benefit directly by northward moving sands placed at the ODMDS. The question was whether the material placed at ODMDS E returns to the channel in any particular seas or class of hydrodynamic events. A third tripod (Site E) was placed at

ODMDS E in water about 15 m (50 ft) deep (Figure 4). Reasons for this placement were to (a) understand and quantify sediment movement under quasi-steady discharges from the Columbia River as well as from the tidal current, (b) test the DRP models under tidal and discharge conditions, (c) provide direct information to the Portland District for management of ODMDS E, and (d) characterize seasonality in the hydrodynamics at the site, including river discharge.

Attaining the numerical simulation modeling objectives of verification and accuracy determination of the DRP-developed fate models will significantly contribute to attaining the MCNP study objectives of development of a standardized method for data collection and ODMDS management that can be used by other Corps District offices.

Numerical Simulation Models[1]

The numerical simulation sediment FATE models (STFATE, LTFATE, and MDFATE) and HPDPRE, HPDSIM, and ADCIRC were either developed or enhanced by the DRP. The numerical simulation wave model RCPWAVE was developed by another funding source. All of these models were applied at the MCR ODMDS.

Regional Coastal Processes WAVE (RCPWAVE)

The RCPWAVE (Ebersole 1984; Ebersole et al. 1986) model is a 2-D model that predicts the transformation of monochromatic waves over complex bathymetry and includes refractive, diffractive, and shoaling effects. Finite difference approximations are used to solve the governing equations and the solution is obtained for a finite number of rectilinear grid cells that comprise the domain of interest. RCPWAVE computes the wave field resulting from the transformation of an incident, linear, monochromatic wave over a region of arbitrary extent and bathymetry. Both refraction and diffraction are included in the model since the latter effect becomes increasingly important in region with complex bathymetry. Shoaling effects are inherently included in the model. The solution technique employed is a finite difference approach. Thus, the wave climate in terms of wave height (H), wave period (T), and wave direction-of-approach (ϕ) is available at a large number of computational points throughout the domain of interest, and not just along wave rays. Computationally, the model is very efficient for modeling large areas of coastline subjected to widely varying wave conditions and, therefore, is an extremely useful tool in the solution of many types of coastal engineering problems. RCPWAVE is ideally suited for estimating the amount of wave height amplification in the lee of an underwater mound as oncoming incident waves refract and diffract around the mound, and then interact in an exceedingly complex manner resulting in potential hazards to navigation.

[1] This section was written by Heidi P. Moritz and Hans R. Moritz, USAED, Portland.

Height Period Direction PREliminary (HPDPRE)

The HPDPRE (Borgman and Scheffner 1991) wave model was developed to simulate a time series representation for wave height, wave period, and direction-of-approach for any location where a USACE Wave Information Study (WIS) database has been produced. HPDPRE uses an empirical simulation technique to calculate statistical parameters describing the intercorrelation among the wave field variables for the existing data. Existing data is obtained from the entire WIS database for a specific oceanic region. Once the intercorrelation matrix has been computed, the original WIS data is no longer required in the synthetic wave data generation procedure.

Height Period Direction SIMulation (HPDSIM)

Using the intercorrelation matrix generated by HPDPRE, the wave model HPDSIM (Borgman and Scheffner 1991) generates arbitrarily long generic time sequences of wave height, wave period, and direction-of-approach that are statistically similar to those of an existing finite length time series. Seasonality and wave sequencing are preserved in these synthetic time-series data. Since WIS data are used as the "training" data sets for generation of the synthetic wave time series, the synthetic data have the same statistics as the WIS data. The HPDPRE and HPDSIM methodology for short waves is analogous to the calculation of harmonic constituents for a tidal time series that can be used to generate accurate long-term tidal reproductions. The LTFATE and MDFATE sediment fate models have been configured to accept the HPDSIM generated wave time series as input for wave data in terms of a 3-hr time-step.

The wave environment in the Pacific Northwest is characterized by a bimodal spectrum. There is typically a dominant wave period associated with locally generated seas (T_{sea}) that is different from the dominant period associated with swell (T_{swell}). Swell wave period typically exceed 18 sec whereas locally generated waves rarely exceed 15 sec. In the case of a synthetic data set for WIS, the peak spectral period assigned to the WIS database is based upon the locally generated sea. Wave period is truncated above 14.5 sec due to the method of resolving peak spectral wave period. The reported wave height is based on the RMS value of H_{sea} and H_{swell}. Hence, measured wave data had to be collected and processed to allow specification of characteristic wave height and period in term of sea, swell, and combination of sea and swell. This was necessary to fully compare measured wave data to synthetic wave data, and resolve the appropriateness of characterizing the synthetic wave environment based on T_{sea} and $H_{rms(sea+swell)}$.

ADvanced CIRCulation (ADCIRC)

A finite-element numerical 3-D hydrodynamic circulation model (ADCIRC) was developed for the specific purpose of generating long time periods of hydrodynamic circulation along shelves and coasts, and within estuaries. ADCIRC predicts tidal elevations and shelf tidal currents. (The current generated by flood and ebb flow from the Columbia River estuary is not included in the

ADCIRC-predicted tidal current.) The intent of the model is to produce long numerical simulations (on the order of a year) for very large computational domains (e.g., the entire east coast of the United States). Therefore, the model was designed for high computational efficiency, and was tested extensively for both hydrodynamic accuracy and numerical stability. The theory, methodology, and verification of ADCIRC are presented by Luettich et al. (1992) and Hench et al. (1995).

ADCIRC was developed to (a) provide a means of generating a database of harmonic constituents for tidal elevation and current at discrete locations along the east, west, and Gulf of Mexico coasts of the United States, as well as the west coast of the United States and eastern north Pacific Ocean, and (b) utilize tropical and extratropical global boundary conditions to compute storm-surge hydrographs along U.S. coasts. The database of storm and tidal surface elevation and current data was developed to provide site-specific hydrodynamic boundary conditions for use in analyzing the long-term stability of existing or proposed dredged material disposal sites. The overall intent of that research was to provide a unified and systematic methodology for investigating the dispersive or non-dispersive characteristics of an ODMDS. These goals can be realized through the use of hydrodynamic, sediment transport, and bathymetry change models. ADCIRC provides the tidal- and storm-related hydrodynamic forcings necessary for site-specific ODMDS site designation.

ADCIRC was developed and implemented as a multilevel hierarchy of models. A 2DDI (two-dimensional depth-integrated) option solves only the depth integrated, external model equations using parametric relationships for bottom friction and momentum dispersion. A 3DL (three-dimensional, local) option uses horizontally decoupled internal mode equations to solve the vertical profile of horizontal velocity and to evaluate bottom friction and momentum dispersion terms for the depth-integrated external mode solution. A 3DLB (three-dimensional, local, baroclinic) option includes baroclinic terms as a diagnostic feature. Finally, the 3DL and 3DLB options solve the complete internal mode equations for nonstratified and stratified flows, respectively.

ADCIRC achieves a high level of simultaneous regional/local modeling, accuracy, and efficiency. This performance is a consequence of the extreme grid flexibility, the optimized governing equation formulations, and the numerical algorithms used in ADCIRC. Together, these allow ADCIRC to run with order-of-magnitude reductions in the number of degrees of freedom and the computational costs of many presently existing circulation models. A user's manual for ADCIRC-2DDI has been prepared by Westerink et al. (1994).

Short-Term FATE (STFATE)

The physical processes acting on dredged material placed in open water are mainly gravity, waves, and currents. Field evaluations by Bokuniewicz et al. (1978) and laboratory tests by Johnson and Fong (1995) have shown that open water disposal of dredged material conforms to a three-step process. These three steps are (a) convective descent during which the material falls through the water column under the influence of gravity, followed by, (b) dynamic collapse during

which the descending plume impacts the bottom or arrives at a level of neutral buoyancy, and finally (c) passive transport-dispersion commencing when material transport is governed more by ambient processes than by the dynamics of the disposal operation. Apart from gravity, the current in the water column is the dominating factor, in terms of the environmental forces that act on dredged material when placed in open water. This scenario characterizes the short-term fate of dredged material placed in open water. The dredged material can be dispersed through the water column and ultimately spread out on the seabed to varying degrees, depending upon the speed of the disposal vessel, water depth, water column current, ambient bathymetry, dredged material type, and other variables.

An existing numerical model for computing DIsposal From Instantaneous Dumps (DIFID) developed by Koh and Chang (1973) was extensively modified by Johnson (1992) and Johnson and Fong (1995) to yield a more versatile, accurate, and robust disposal model called STFATE. To allow for disposal from hoppers or moving barges, and for a more accurate representation of the disposal material, the concept of multiple convecting clouds was developed that allows for stripping of material during descent. Computation of the bottom surge was based upon energy concepts. The resulting model was subsequently verified using laboratory data collected by Johnson et al. (1993).

STFATE was used to predict the bathymetric distribution of dredged material after it passed through the water column and impacted the seabed, on an individual "dump" (disposal vessel load) basis. Grid results described the areal configuration and thickness of dredged material on the seabed. Grid cell dimensions could have been as small as 30.5 m × 30.5 m (100 ft × 100 ft). Maximum number of grid cells in each orthogonal direction could have been 64. The processes modeled by STFATE have time scales from 1 min to 3 hr. At the MCR ODMDS, STFATE was used in a 2-D capacity.

Long-Term FATE (LTFATE)

Dredged material dispersion can also occur after the placed material has come to rest on the receiving bathymetry. After dredged material comes to rest on the seabed, waves and/or currents can transport it from the site. If many loads of dredged material are placed one on top of another such that a steep aggregate mound develops on ambient bathymetry, the mound will avalanche and material will be transported downslope. The combination of these processes defines the long-term fate of dredged material placed in open water. Water depth, wave activity, and current regime are the primary factors that contribute to the long-term dispersion of dredged material placed at a given ODMDS. For locations predominated by strong wave and current regimes, sediment transport calculations based on averaged wave and current data may easily show the site to be dispersive. If the local environmental conditions are not severe, it may take months or years before significant amounts of sediment are transported from the disposal site. In that case, long-term simulations are required, probably longer than available actual input data is available. Thus, long-term simulated data from HPDSIM and ADCIRC are necessary. The ability to identify long-term dispersive sites is especially important because eroded material could be transported

into environmentally sensitive areas. The primary restriction of the DRP sediment FATE models is that reliable environmental input data is required to properly simulate dredged material behavior at a given location.

LTFATE is a numerical modeling system for systematically estimating the long-term response of a dredged material disposal site to local environmental forcings. The methodology is based on the development of databases of wave and current time series, and the application of these boundary conditions to coupled hydrodynamic, sediment transport, and bathymetry change models. The approach was developed to provide an estimate of long-term material fate for use in determining whether an existing or proposed disposal site would be dispersive or nondispersive over periods of months to years. Grid results describe the post-simulated morphology of the modeled bathymetric features of interest. Grid cell dimensions are typically 30.5 m × 30.5 m (100 ft × 100 ft). Maximum number of grid cell in each orthogonal direction can be 200. The processes modeled by LTFATE have time scales from 3 hr to 1 year. LTFATE is a 2-D model.

LTFATE simulations are based on the use of local wave and current condition input. Local site-specific hydrodynamic input information is developed from numerical model-generated databases; however, if real data are available, they can be substituted for the database-generated files. LTFATE has the capability of simulating both noncohesive and cohesive sediment transport. In addition, avalanching of noncohesive sediments and consolidation of cohesive sediments are accounted for to accurately predict physical processes that occur at a site.

Noncohesive mound movement. LTFATE uses the equations reported by Ackers and White (1973) as the bases for the noncohesive sediment transport model. The equations are applicable to uniformly graded noncohesive sediment with a grain diameter in the range of 0.04 to 4.0 mm. Because many disposal sites are located in shallow water, a modification of the Ackers-White equations was incorporated to reflect an increase in the transport rate when ambient currents are accompanied by surface waves (Scheffner et al. 1995).

Cohesive mound movement. An algorithm developed by Teeter and Pankow (1989) was incorporated into LTFATE to account for transport of fine-grained materials such as silt (0.004 to 0.072 mm) and clay (0.00045 to 0.004 mm). They reasoned that because of the differences in cohesive and settling characteristics, fine-grained sediments are sometimes characterized as the algebraic sum of expressions for settling velocity, deposition, and resuspension. Consolidation calculations are based on finite strain theory, which is well-suited in cases of thick deposits of fine-grained material. It provides for the effect of self-weight, permeability varying with void ratio, a nonlinear void ratio/effective stress relationship, and large strains.

Multiple Dump FATE (MDFATE)

A dredging project that includes open water disposal of dredged sediment typically consists of numerous dredged material placements ranging from a few to a few thousand. The operational duration of such projects can range from days

to several months. The life cycle of an offshore ODMDS may be many tens of years.

A multiple-dump fate (MDFATE) dredged material placement model was developed by Moritz (1994) to predict postdisposal bathymetry for ocean dredged material disposal sites. This PC-driven numerical simulation model for determining the fate of multiple dumps incorporates existing numerical models to simulate the overall (short- and long-term) behavior of dredged material placed within an ODMDS. MDFATE spatially accounts for bathymetric change within an offshore disposal area, and can be used to assist with selection of the most efficient layout for a proposed disposal site or provide guidance for optimizing dredged material placement options.

MDFATE defines an ODMDS in terms of a numerical grid and incorporates modified versions of STFATE and LTFATE models to predict or hindcast ODMDS bathymetry resulting from a series of disposal cycles or dumps. In this regard, STFATE (Johnson 1992) and LTFATE (Scheffner et al. 1995) models were coupled by Moritz (1994) within the MDFATE simulation. Execution of MDFATE is controlled by an easy-to-follow menu and prompt-input interface. The processes modeled by MDFATE have time scales from 1 min to 1 year. MDFATE was operated in the 2-D mode at the MCR ODMDS, and uses the same parameters used in STFATE and LTFATE.

Discretizing an ODMDS. As a first step in simulating a disposal operation, MDFATE is used to produce a discretized representation (rectangular digital elevation model) of the ODMDS that is of interest. It is assumed that the ODMDS is rectangular. All that is required from the user are the ODMDS corner coordinates and the desired grid interval in which to discretize the ODMDS. Horizontal control (x,y) is manifested in terms of the coordinate system used to describe the site in the prototype scale. State plane and geographic (latitude-longitude) coordinate systems are supported. Up to 40,000 grid points can be used to represent a given ODMDS in terms of an MDFATE grid. This is sufficient to represent a 3,050-m × 3,050-m (10,000-ft × 10,000-ft) disposal site in terms of a 15-m (50-ft) grid interval. Bathymetric (z) data are represented in terms of a given elevation reference datum. Subsequent modification of an ODMDS grid's bathymetry is performed with respect to the vertical datum established during the creation of the disposal area grid. MDFATE can either automatically generate the ODMDS grid bathymetry (flat or sloping), or adapt survey data (ASCII format) consistent with the sites' coordinate system. Survey data are fitted to the MDFATE digital elevation model (DEM) by a multipoint polynomial interpolation scheme.

MDFATE is able to produce 2-D contour and 3-D surface renderings of an ODMDS grid of interest. At the conclusion of every MDFATE activity, two data files are produced for post-processing and informational purposes. An ASCII (x,y,z) DEM data file is produced for additional post-processing purposes of the ODMDS bathymetry. This file is generic and can be used by a variety of 2-D or 3-D software packages. The second file serves as a schematic representation of the ODMDS grid and contains parameters describing the site.

Simulating a dredged material disposal operation. Once a particular ODMDS grid has been created, MDFATE can be used to simulate a given disposal operation which may extend over 1 year and consist of hundreds of disposal cycles or dumps. A dump consists of one load of dredged material being released into open water from either a barge, scow, or a hopper dredge.

For modeling purposes, the dredging and disposal season is considered to be divided into two discrete time periods. At the MCR ODMDSs, dredging disposal normally begins during the April-May time frame and continues through the summer until September- October. After October, the ODMDSs are not used and are affected by the energetic MCR environment until the following April-May time frame when dredged disposal again commences.

The following describes how the MDFATE model could be applied to simulate dredged material disposal at a candidate MCR ODMDS. During periods of active dredged material disposal, short-term and long-term fate processes are simulated at the disposal sites for a 5-month period (April- September). The disposal operation is divided into separate week-long episodes over which long-term fate processes governing dredged material behavior on the seafloor are simulated using a modified version of the LTFATE model. Results are modeled in a cumulative manner. Long-term processes include self-weight consolidation, sediment transport by waves-currents, and mound avalanching.

Within each disposal episode, a modified version of STFATE simulates short-term fate processes which govern individual dumps occurring within the ODMDS of interest. Short-term processes are those which influence placed dredged material up to the point at which all momentum imparted to the material from the dump activity is expended through convection, diffusion, and bottom friction. Utilizing HPDSIM and ADCIRC simulations (or by inputting actual field data), wave and tidal information is defined for every 3-hr interval during the disposal operation. This information is utilized by the modified STFATE model within MDFATE to simulate wave-current effects acting upon each dump as dredged material passes through the water column and comes to rest on the seafloor. The modified STFATE model uses the actual ODMDS bathymetry to simulate cumulative mound distribution arising from each dump.

After simulating the active disposal period, long-term fate processes are then simulated for a 7-month period, until the following year when the annual cycle begins again. Semiannual ODMDS bathymetric surveys are typically taken during April-May and September-October, which makes the preceding disposal cycle discretization desirable in terms of comparing before and after surveys to simulated results.

FATE Model data requirements. In terms of the MDFATE simulation, specification of the disposal operation is performed through a menu-driven format, in which the user specifies basic data defining the following:

a. Dredging disposal vessel parameterization.

(1) Vessel type (split-hull or hopper), dimensions, and volumetric capacity.

(2) Placement duration per load (time to place each load).

(3) Vessel speed and heading during placement.

(4) Definition of dredging disposal volume placed during period of interest.

b. Method of disposal vessel control during the disposal operation, using four dump placement options.

(1) Within a specified radial distance of a predetermined geographic location (i.e., coordinates defining a disposal buoy location). Dumps are placed in a random manner and are weighted in the direction of disposal vessel approach.

(2) Along a predetermined transect line based on beginning and ending coordinates.

(3) Each dump location defined by the user entering coordinates.

(4) Dump locations are based upon prerecorded coordinates for each load. Coordinates (x,y) are contained in an ASCII data file queued by MDFATE.

c. Dredged material parameters (density, grain size, solids concentration, void ratio, and shear angle).

d. Data collected during the MCNP study at the MCR ODMDS.

(1) Bathymetry for the ODMDS of interest (predisposal conditions).

(2) Time series data for tidal elevation and depth-averaged (or vertical profile) current.

(3) Definition of ambient density profile using single observation (or time series data).

(4) Time series data for wind-driven surface waves.

(5) Residual depth-averaged current (or vertical profile data).

Sediment Suspension at MCR[1]

Moritz et al. (2000) investigated seabed sediment suspension due to the presence of waves and currents at the MCR. Relevant data were measured at ODMDS B, instrumentation tripod platform Site B1 (Figure 3), 6 km (3.7 miles) offshore of the MCR in a water depth of 18 m (60 ft) with seabed sediment composed of fine to medium sand. The analyses by Moritz et al. (2000) addressed the effect on bottom sediment (sand) when waves and currents interact along the seabed of an ebb-tidal shoal. Special considerations included (a) assessing the modification of waves by current, (b) describing the spectral relationship between bottom current and peak sediment suspension, and (c) investigating wave group effects.

[1] This section is extracted essentially verbatim from Moritz et al. (2000).

Wave, current, and suspended sediment data had been acquired synchronously at Site B1 during Deployment 1, 19 August – 22 September 1997. Site B1 is located at the ocean/estuarine margin and is perched on top of a 20-m- (65-ft-) high mound of sandy dredged material (dredged material was fine-medium sand and placement was discontinued in 1997). According to Moritz et al. (1999), Site B1 exhibits the following characteristics. The current through the upper two-thirds of the water column is dominated by estuarine flow from the MCR. The current in the lower one-third of the water column is controlled by inner shelf processes. During storms, the current through the entire water column is intensified almost uniformly due to wind stress. Waves as small as H_{mo} = 2 m (6.6 ft) high and T_p = 8 sec can influence bottom flow and bottom sediment suspension.

For the suspended sediment data acquired by OBS which was nominally located 55 cm (21.7 in.) off the seabed), digital filtering of the data was performed to account for the presence of silt-clay material. The digital filtering of the OBS signal essentially removed the turbidity effect (associated with silt-clay) from the signal of the OBS to produce a quantitative parameter describing the time-varying suspension of sand. Based on the characteristics of Site B1, this filtering process produced an OBS data stream describing the response of sandy bottom sediment (D_{50} = 0.13-0.28 mm) due to waves and currents.

Columbia River flow

Annual mean Columbia River discharge is a 7,500 cu m per sec (265,000 cu ft per sec) and the tidal prism is about 1,100,00 cu m (1,438,000 cu ft). At the MCR, the mean spring tidal range is 2.6 m (8.5 ft). The average water depth through the throat of the MCR entrance is about 15 m (50 ft), with local excursions to 33 m (110 ft). During the peak of ebb tide, the combination of riverine and estuarine flow through the jettied 3.7-km- (2.3-mile-) wide entrance of the MCR can produce currents greater than 2.5 m per sec (8.2 ft per sec) and flow rates that exceed 42,000 cu m per sec (1,484,000 cu ft per sec). At the MCR and adjacent coastal waters, tidal currents account for more than half of the water motion over periods of several days (Stevenson, Gravine, and Wyatt 1974). The Columbia River entrance is characterized by exceptionally strong wave-current interactions. The sea state at the river entrance during storm conditions is produced by high swell incident from the northwest to southwest combined with locally generated wind waves from the south to west. During intense winter storms, $H_{1/3}$ can exceed 9 m. In this regard, the MCR furnishes all the dynamics needed to evaluate in situ sediment movement due to a range of environmental forcings.

Bottom sediment at Site B1

Between 80-90 percent of the lower Columbia River's sediment load is composed of suspended sediment, yet little suspended sediment is retained in the main stem of the estuary or at the entrance to the MCR (Hubbell and Glenn 1973; Roy et al. 1982). Hence, the MCR plume (ebb flow discharge of

estuarine/riverine water) transports a considerable amount of suspended sediment (including silt and clay) into the ocean.

On the ocean side of the MCR, fine-medium sand (0.13-0.28 mm) is present near the Columbia River entrance during all oceanographic seasons. Although very fine sand (0.063-0.12 mm) and silt (0.0125-0.063 mm) is often observed at the MCR, these sediments are transitory and more common during the summer than winter (Roy et al. 1982).

Figure 4 shows the location of Site B1 within context of an east-west profile running across the ebb-tidal shoal of the MCR. Due to the perched location of Site B1, the bottom sediment at Site B1 is composed exclusively of fine-medium sand, and the site is not subject to ephemeral deposition of silt-clay material by the MCR plume. This scenario makes Site B1 ideal for measuring waves and free-stream current on top of an ebb-tidal shoal, while controlling the effect of fine-grained sediment. Although the presence or deposition of fine-grain bottom sediment at Site B1 was considered unlikely, the presence of suspended fine-grain material moving past the site (i.e., a background turbidity effect due to the plume) was considered likely. To suppress the turbidity component within the observed time-varying suspended sediment data stream, the OBS data were processed to remove the background signal associated with suspended fine-grain material. Thus, all results relate the OBS data to sand-based sediment.

Instrumentation and data collection

The instrumentation development and data collection program was conducted by Oregon State University (Lund et al. 1999), and is described in Chapter 4, "Field Data Collection and Analysis." Figure 50 summarizes the burst-averaged data from approximately 350 bursts acquired at Site B1 during deployment 1 (19 August – 26 September 1997). While not apparent in the top caption of Figure 50 (due to scaling), there is significant coherence between waves and bottom sediment suspension. During nonstorm periods (periods of little wave action), the magnitude of depth-averaged ADP current is heavily modulated by estuary tidal flow, while bottom ADV current is irregular. During certain conditions, surface current is much different (speed and direction) than current at middepth. During storm events, the water column exhibited sheet flow characteristics. The magnitude of depth-averaged current increased and tidal modulation was diminished. The magnitude of the bottom current increased significantly and appeared to be driven by flow in the upper water column. Until day 29, the instrument platform remained stationary on the seabed. On day 29, scour/sediment liquifaction due to an intense storm event with H_{mo} = 4.9 m (16 ft) caused the instrument platform to settle 30 cm (1 ft). During Deployment 1, the Columbia River flow rate was constant at 5,000 cu m per sec (176,700 cu ft per sec).

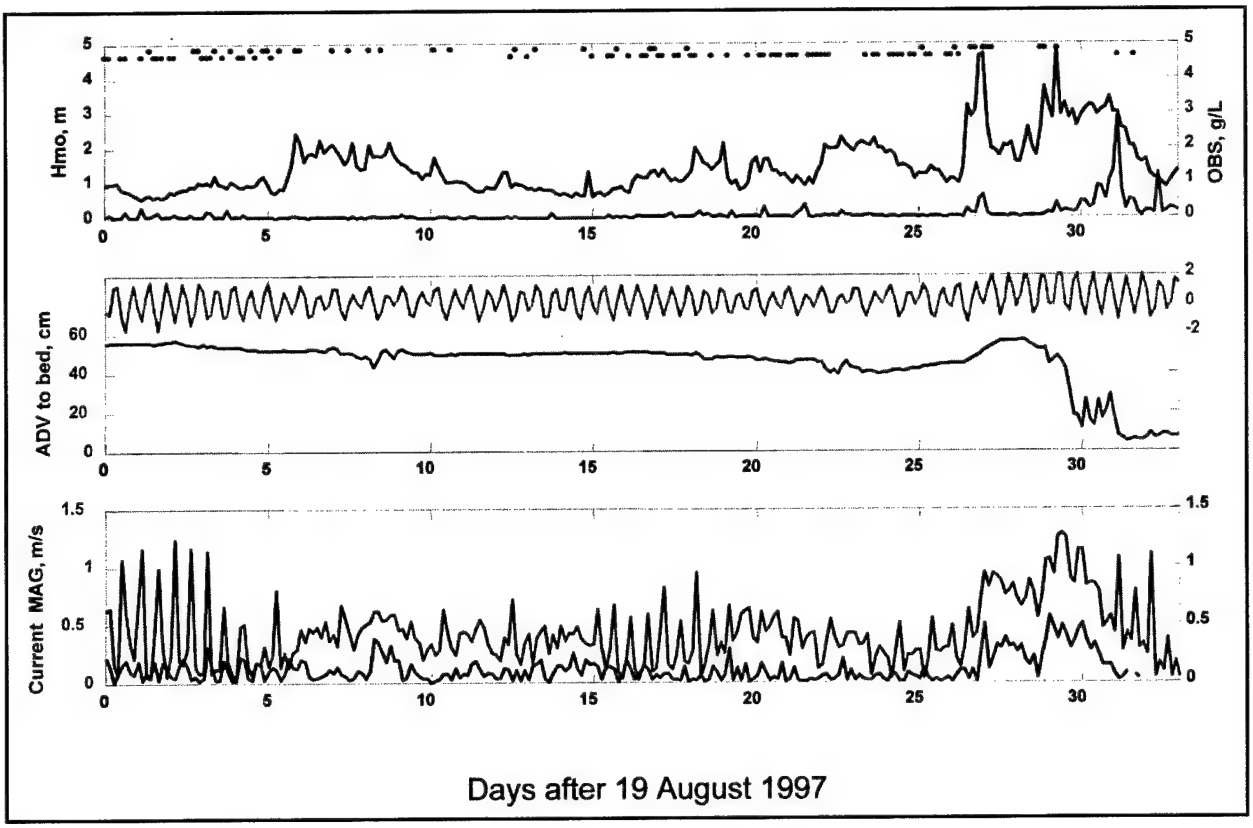

Figure 50. Summary of data record for Site B1 during Deployment 1, 19 August – 26 September 1997 (after Moritz et al. 2000)

Current at Site B1 and effect on PUV data

The current throughout the water column was observed via ADP concurrently with the PUV (pressure, and x- and y-components of velocity) data, providing information to assess potential current effects on PUV data analysis. Figure 50 highlights several events when strong current was observed throughout the entire water column at Site B1. Strong currents occurred during periods of large waves. Both were driven by the same process of intense wind stress on the sea surface. During storms, waves and currents progressed in the same direction (following condition). During spring tide, the current through the upper half of the water column at Site B1 exceeded 1 m per sec due to strong ebb flow from MCR. During periods when tidal flow was dominant, the directionality between waves and currents was highly variable (opposing, following, and oblique). Based on cursory viewing of Figure 50, it appears likely that currents would have some effect on the observed dynamic pressure as previously discussed. To properly account for the amount of current actually affecting the wave, a representative current had to be estimated. Lee (1990) introduced the concept of equivalent current in wave-current computations. The estimate for equivalent current is a function of water depth and wavelength, and is based on the fact that the part of the current closest to the water surface has the greatest influence on waves. Moritz et al. (2000) used the Lee method to estimate the net equivalent current (following or opposing component) affecting waves.

The directional alignment of current through the water column (measured by the ADP) at Site B1, was highly variable due to the sporadic influence of the Columbia River estuary and open coastal flow. The synopsis of current profile alignment vs. wave direction is: (a) *Opposing* conditions (current for all ADP bins was within 135-225 deg of wave direction θw) = 14 percent of all observations; (b) *Following* conditions (current for all ADP bins was within ±45 deg of wave direction θw) = 7 percent; (c) *Crossing* (current for all ADP bins was within 45-135 deg or 225-315 deg of wave direction θw) = 40 percent; and (d) *Others* (current for the ADP profile was complex, being sheared and not aligned) = 39 percent. The dots within top caption of Figure 50 shows the occurrence of following vs. opposing current. The uppermost dots define following current conditions, while the lower dots define opposing conditions.

Figure 51 illustrates the effect of current on spectral estimates based on PUV data. If a 1 m per sec (3.3 ft per sec) *following* current is ignored when processing PUV data applicable to Site B1, the spectral energy density is overestimated. Note the pronounced effect near the high frequency part of the spectrum. This is an important consideration for assessing wave transformation. For the burst shown in Figure 51, the difference in H_{mo} between including vs. ignoring the current is about 15 percent (i.e., H_{mo} for ignoring a following current is 15 percent larger than for correctly including current in spectra calculations). On a deploymentwide basis for Site B1, the difference for H_{mo} between including vs. ignoring current was 2-20 percent, depending on current magnitude, direction, and wave properties. In Figure 51, the "Intrinsic" spectral energy density is the equivalent spectrum for no current. "Current Included" properly accounts for the presence of current when processing PUV data. "Ignore Current" ignores the presence of a 1 m per sec (3.3 ft per sec) following current when processing the PUV data, and overestimates the spectra.

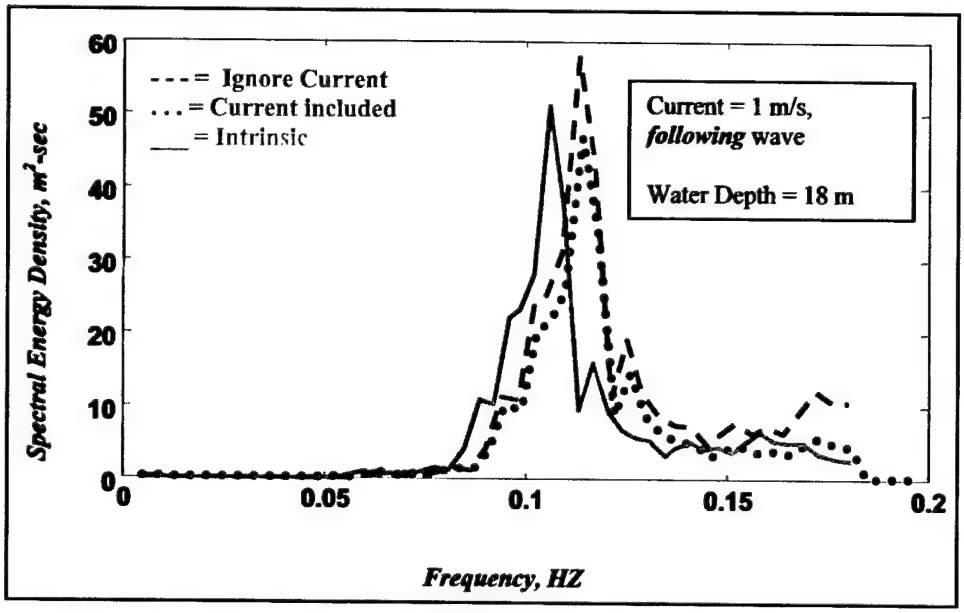

Figure 51. Sea surface spectral energy density (SED) estimates for a single PUV burst, illustrating the effect of current on PUV-based spectral density estimates (after Moritz et al. 2000)

Relationship between waves and suspended sediment

Water-surface variation, bottom current, and suspended sediment data were acquired concurrently for 1,024 sec every 3 hr using a 4-Hz sampling rate. These data were used to describe the high frequency variability of short waves, associated bottom water movement, and suspension of sandy bottom sediment at Site B1. These data facilitated direct spectral comparison of ambient bottom current, wave-induced water motion, and associated response of bottom sediment at the seabed (via bed material suspension). Bottom sediment suspension is constrained to sand via filtering of the OBS signal. The objective of the frequency domain analysis was to investigate the relationship between forcing due to waves and the response of bottom water due to waves, and the response of bottom sediment (suspension) due to wave-induced bottom water motion.

An energy burst obtained during the peak of a storm is shown in Figure 52a, and exemplifies conditions that qualitatively apply to bursts with H_{mo} as small as 2 m (6.6 ft). During this burst, PUV and OBS measurements were made 50 cm above the bed. Note the effect of wave grouping and the associated response on sediment suspension (OBS) and bottom water motion (ADV). The ADV velocity components have been orthoganalized in terms of wave direction ("with-wave" vs. "cross-wave" component), and the mean bottom current has been removed. The less pronounced the "with-wave" component, the more directionally confused the sea state. For the burst shown in Figure 52a, there is a dominant series of waves approaching from the SSW. When individual waves exceeded 4 m (13 ft) in height, the wave-induced water motion 40-50 cm (16-20 in.) off the bed exceeded 100 cm per sec (3.3 ft per sec) and OBS concentration exceeded 1 g per L (0.133 oz per gal).

Figure 52b shows a 132-sec subsample of the burst in Figure 52a. The response of sediment suspension is directly related to the forcing of waves, although there is a 4-8 sec lag between the two signals. The interaction of mean bottom current with the "with-wave" and "cross-wave" components produces a complex overall current, as reported by the RMS value for bottom current (bottom graph). Near the nodal point between two wave groups, wave-induced bottom current and suspended sediment diminish. The middle graph in Figure 52b shows some wave-wave interaction in the form of truncated "with-wave"current at t = 240 sec, and increased "cross-wave" current (at the expense of the "with-wave" component) during t = 310-346 sec. The wave-wave interaction influenced the degree of suspended sediment. Greater wave-wave interaction attenuates wave-induced bottom water motion (at the meso-scale level of temporal detail) and produces less sediment suspension.

Conclusions

Laboratory-quality wave, current, and suspended sediment data were acquired at a highly energetic prototype setting on top of an ebb-tidal shoal in 18-m (60-ft) water depth at the MCR. Moritz et al. (2000) utilized data collected during August-September 1997 to investigate how current can affect the quality of wave statistics derived from PUV data, and the frequency domain (spectral) response of a sandy seabed to the processes of waves and currents.

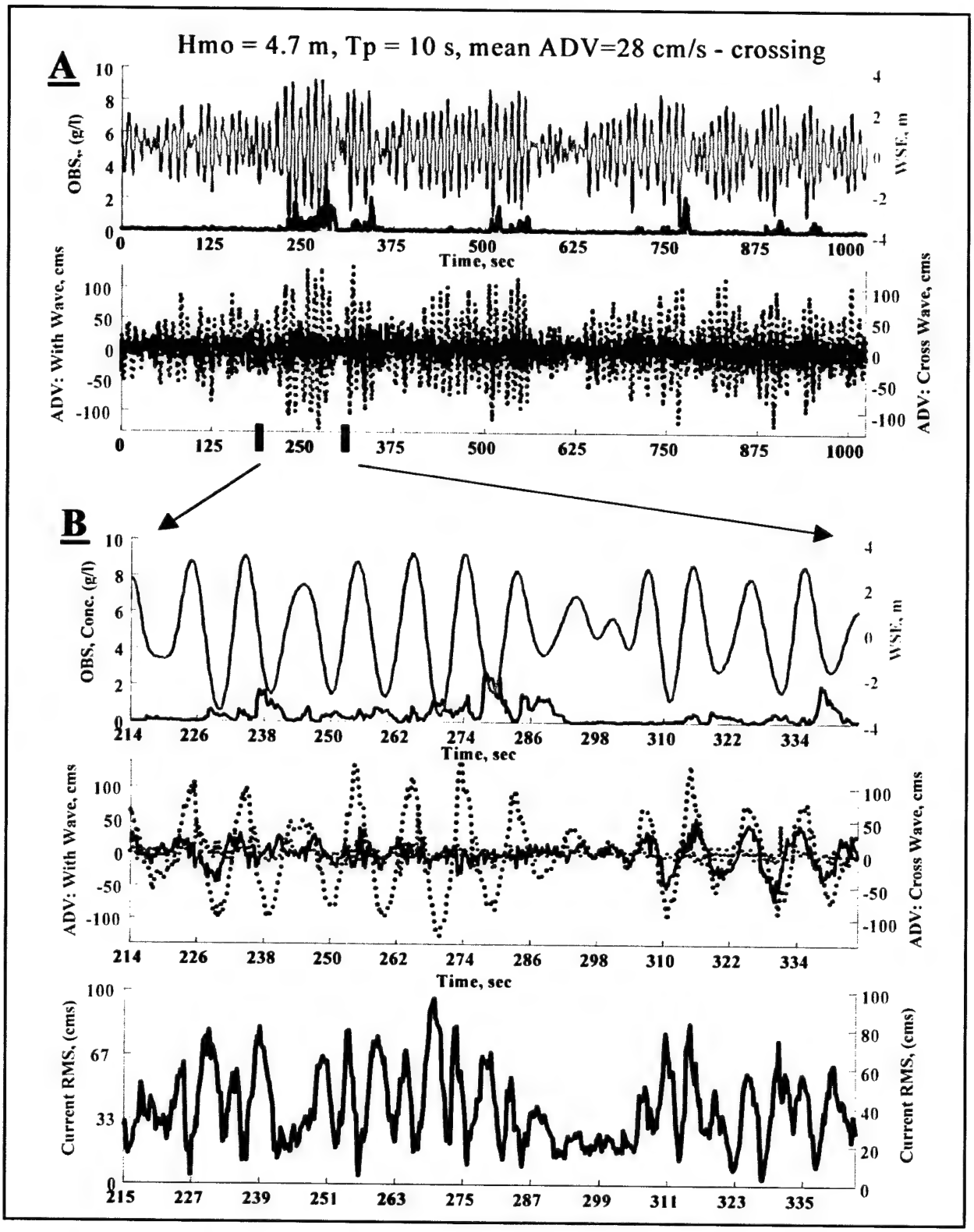

Figure 52. (A) Site B1 PUV and OBS burst during moderate storm (top graph is water-surface elevation and OBS; bottom graph is ADV bottom-current components along- (dots) and cross- (solid) wave direction); (B) Subsample of burst showing along-, cross-, and vertical-components of ADV current; bottom graph shows RMS of ADV (after Moritz et al. 2000)

The presence of a strong current greater than 50 cm per sec (1.6 ft per sec) through the water column can affect PUV measurements used to describe short-wave statistics. The effect can be up to 25 percent for H_{mo}. Whenever PUV measurements are proposed for observing waves within the inner shelf where depth = 3-40 m (10-130 ft), concurrent measurement of water column current (via ADP) should be seriously considered. The technological advancement and affordability of ADPs makes their use highly effective.

During August-September 1997, the suspension of seabed sediment at Site B1 was dominated by wave processes and secondarily by processes governed by mean bottom current. Spectral decomposition of measured bottom current and suspended sediment (OBS) indicated a range of suspended sediment response to wave action: Grouping only (47 percent); Grouping + Wave (34 percent); Grouping + Wave + 2nd harmonic (12 percent). At Site B1, the coherence between either ADV-RMS or ADV-"with wave" vs. OBS exceeded 0.5 for about 60 percent of all wave bursts. This indicated that transport of sand suspended by wave action occurred 60 percent of the time during data collection.

Oceanographic Processes and Seabed Change at MCR[1]

Moritz et al. (1999) correlated oceanographic processes at the MCR with seabed changes that occurred at ODMDS Sites B1, B2, and E during Deployment 1 (19 August – 22 September 1997) by the Oregon State University data acquisition phase of the MCNP study. The locations of ODMDS Sites B1, B2, and E are shown in Figures 3 and 4. Based on the textural variation of bottom sediment at the MCR, both suspended and bed-load aspects of sediment transport were measured to fully describe sediment response vs. environmental forcing.

Bottom sediment at MCR

Between 80-90 percent of the lower Columbia River's sediment through flow is composed of suspended sediment, yet relatively little suspended sediment is retained in the main stem of the estuary or at the MCR. The dominant sediment in the main channels of the estuary is sand that is transported as bed load, with silts and clays prevalent only in the upper estuary and peripheral bays (Roy et al. 1982). In terms of the overall estuary, average bottom sediments have been characterized as having 1 percent gravel, 84 percent sand, 13 percent silt, and 2 percent clay (Hubbell and Glenn 1973; Roy et al.1982).

On the ocean side of the MCR, marine sand is transported to the MCR by the north and southbound littoral currents. The net direction of littoral transport is believed to be toward the north (Ballard 1964), with significant excursions toward the south (Lockett 1967). The seasonal variation in bottom sediment texture at MCR and adjacent offshore areas has been described in numerous reports (Sternberg et al. 1979; Roy et al. 1982). Fine-medium sand

[1] This section is extracted essentially verbatim from Moritz et al. (1999).

(0.13-0.28 mm) is present at the Columbia River entrance during all oceanographic seasons. Although very fine (0.063-0.12 mm) sand is often observed at the MCR, these sediments are transitory and more common during the summer than winter (Roy et al. 1982). The grain size associated with very fine sand is characteristic of native sediment observed along the inner shelf at the MCR (excluding the coarser ebb-tidal shoal sediments associated with the Columbia River).

It has been observed that winter storms winnow the silt fraction (>0.0625 mm), from sediments between the MCR entrance and the outer edge of the ebb-tidal shoal in 37-m (120-ft) depth. The seaward advance, or uncovering, of medium-fine sand has been observed to occur with onset of the spring freshet (high river discharge) (Roy et al. 1982). The silt size fraction returns to the MCR sediment regime in the spring and increases markedly through the summer in the form of intermittent patches. The area offshore of the MCR ebb-tidal shoal deeper than 37 m (120 ft) is believed to receive sediments from adjacent inner-shelf areas during the summer. Previous studies indicate that some of the sand-sized sediments within the Columbia River estuary may have been transported through the MCR and into the estuary from adjacent nearshore and shelf regions of the Washington and Oregon coasts (Lockett 1967; Roy et al 1982).

Measured process and response data

An excerpt of measured process data acquired at Site B2 in water depth = 36 m (120 ft) during the Deployment 1 is shown in Figure 53. The Columbia River flow rate, which was constant during Deployment 1 at 5,000 cu m per sec (176,700 cu ft per sec), was observed at a location inland from the MCR. Wind speed was observed 30 km (18.6 mile) offshore from the MCR. Note the increase in average surface-water elevation SWE, +0.5 m (+1.6 ft) and bottom water temperature (+5° C) after day 25. This is believed to represent the onset of the 1997 El Nino along the Northwest U.S. Pacific Coast.

Recorded response data include bottom sediment concentration (turbidity reported by the OBS every 30 min) and vertical displacement of the seabed (bed form activity relative to the ADV reported every 30 min). OBS-reported data were converted to suspended sediment concentration using OSU-derived calibration criteria. Figures 54-56 show relevant data records at each MCR monitoring site during Deployment 1. Note the dates of data collection for each location. Although all instruments began acquiring data on 20 August 1997, the instruments at Site B1 stopped recording after day 35. Likewise, instruments at Site E stopped recording data after day 45. At Site B2, the ADV did not acquire a coherent bottom velocity signal until day 10.

During 20 August-10 October 1997, measured significant wave height varied between 0.6-6.2 m (2-20 ft), wave period varied between 5-21 sec, bottom current magnitude varied between 0-85 cm per sec (0-2.8 ft per sec), and seabed displacement exceeded 10 cm (3.9 in) over several hours, as reported by the ADV. Several trends are easily observed from Figures 54-56. The variation of cumulative seabed change measured at Sites B1, B2, and E appears to be coincident in time, both with respect to each location and with respect to episodes of

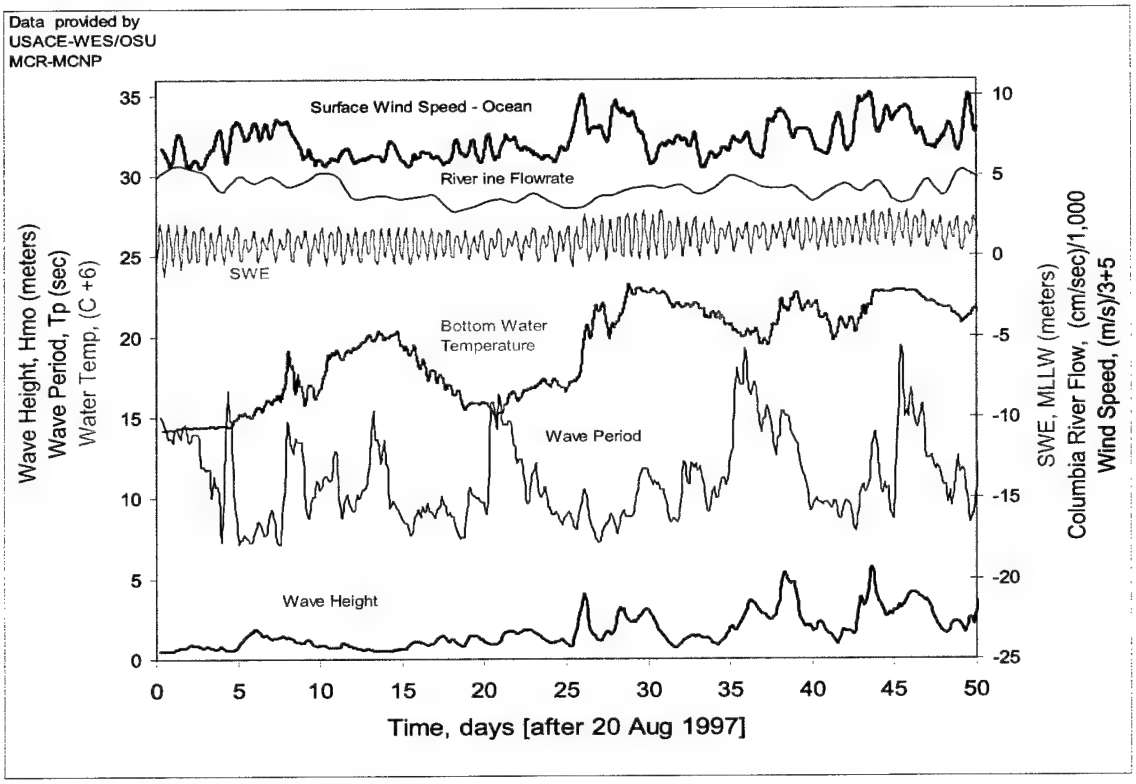

Figure 53. Measured process data at MCR Site B2 during August-October 1997 (after Moritz et al. 1999)

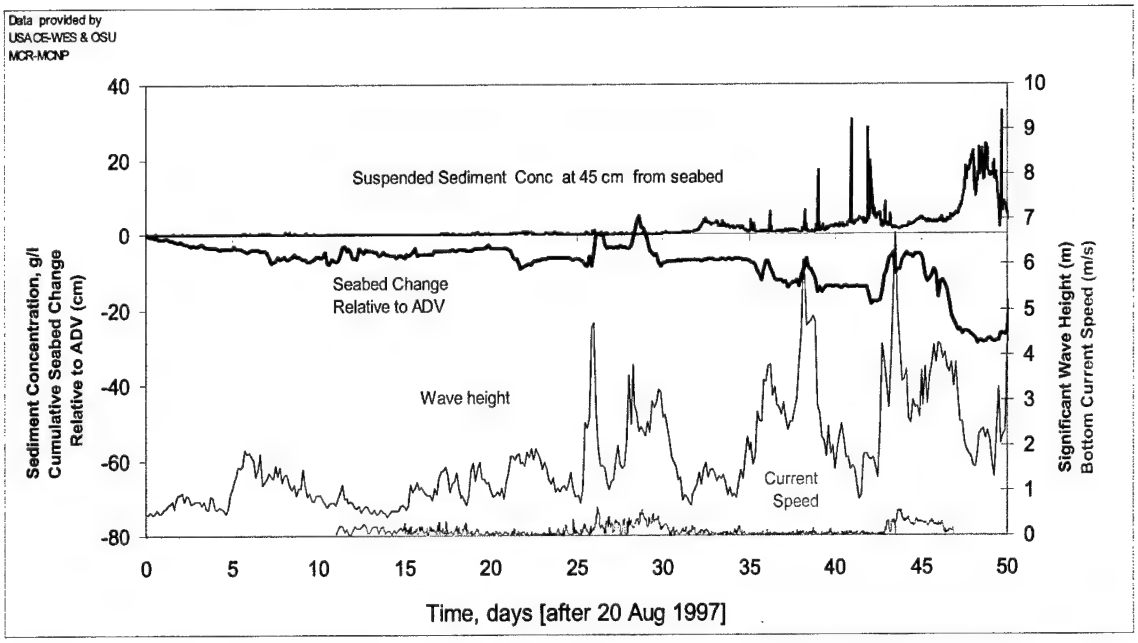

Figure 54. Measured process and response data at MCR Site B2 during August-October 1997 (after Moritz et al. 1999)

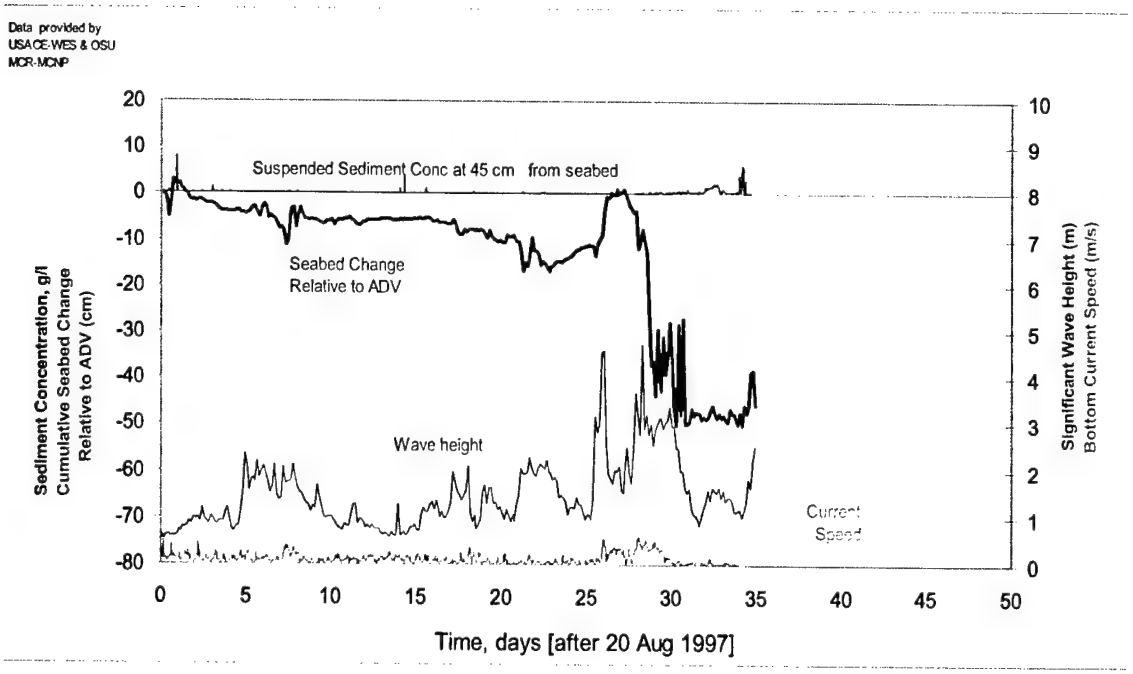

Figure 55. Measured process and response data at MCR Site B1 during August-October 1997 (after Moritz et al. 1999)

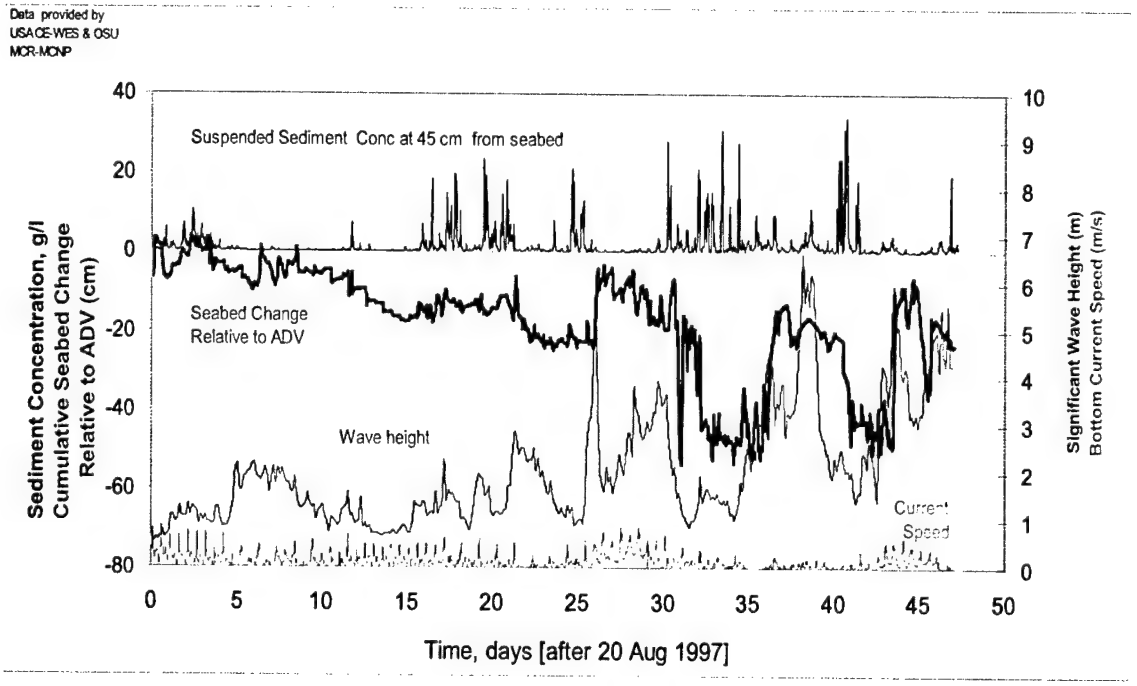

Figure 56. Measured process and response data at MCR Site E during August-October 1997 (after Moritz et al. 1999)

prominent wave (height) activity. Water depth appeared to have an attenuating effect on seabed change. The shallower Sites E and B1 have more short-term variation and larger magnitude change than does the deeper Site B2. Measured suspended sediment concentration at Site E was consistently higher than Sites B1 and B2, and suspended sediment at Site B2 was higher than Site B1. Even though Site B2 is located at a water depth of 36 m (120 ft), waves 2-m- (6.6-ft-) high appeared to influence bed form activity with 5-10 cm (2-4 in.) amplitude. Periods of increased bottom current amplitude (during days 25-30 and 42-45) corresponded with large wave events. Although not shown, the current through the entire water column (ADP-measured) also exhibited increased activity during large wave events. The concurrence of large (locally generated) waves with increased current is due to wind-induced forcing which affects local sea state and flow throughout the water column along the inner shelf.

Data analyses

Three measured parameters were selected for the purpose of relating observed environmental forcing (processes) to observed vertical variation of the seabed (response). Mean ADV bottom current and ADV-wave standard deviation (SD) were used to describe time-varying environmental processes (bottom current and wave action, respectively) potentially affecting seabed change. ADV-measured seabed altimetry was used to describe the time varying response of seabed vertical position, with respect to the ADV sensor. To meaningfully relate process measurements to response measurements, data was transformed using methods of normalizing and differencing. Finally, serial correlation between transformed process and response data was obtained.

Parameter differencing and normalizing

To facilitate direct comparison of cumulative seabed change (30-min data) to the process (3-hr) data, the 30-min ADV-altimetry data were resampled based on a 3-hr time increment corresponding to the measured ADV-SD and ADV-mean bottom current data. Next, the 3-hr ADV-altimetry data were differenced to obtain a relative seabed change from one time increment to the next. The previous ADV-SD data transformations resulted in the relative seabed change parameter being reported in a 3-hr time increment.

To compare process data with differenced response data on a similar magnitude scale, all three data types (waves, currents, and seabed change) were normalized. The result of the normalizing process for relevant data at Site B2 is shown in Figure 57. Data at Sites B1 and E were treated similarly.

Upon inspection of normalized data for all three sites (B1, B2, and E), it was evident that there was little consistency between positive/negative seabed change vs. the variation in wave or current magnitude. Numerous attempts were made to determine some relationship of positive or negative seabed change with wave direction, current direction, or tide, but to no avail. It was reasoned that the only consistent method of relating seabed change to the forcing environment was by examining the absolute value of seabed change with respect to the magnitude of

the forcing environment (waves and currents). Thus, parameters shown in Figure 57 were subjected to an absolute value function.

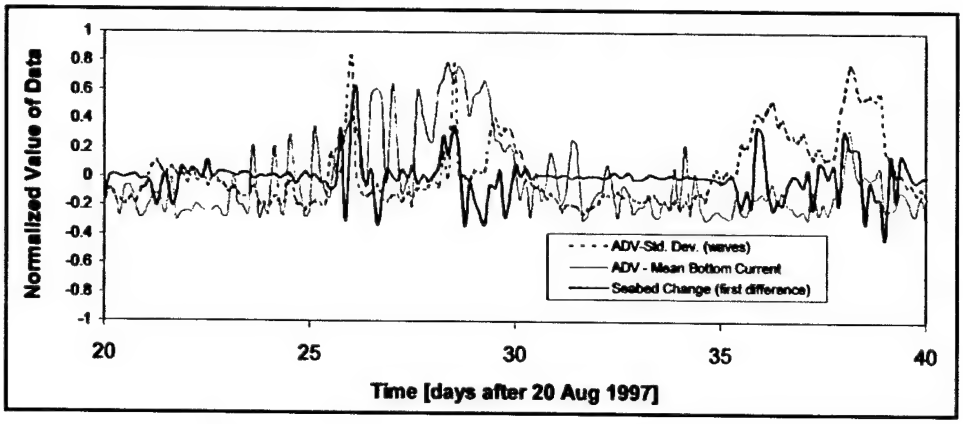

Figure 57. Normalized process and response data at Site B2 (after Moritz et al. 1999)

The result of applying the absolute value process to relevant data at Site B2 is shown in Figure 58. Data at Sites B1 and E were treated similarly. Figure 58 documents seabed change with respect to the magnitude of wave and current activity. At Site B2, there was noticeable dependence between ADV-SD (waves) and seabed change. When the normalized value for ADV-SD fell below 0.2 or about 2 m (6.6 ft), very little seabed change occurred irrespective of mean bottom current. When the normalized magnitude of ADV-SD exceeded 0.3 or about 3 m (9.8 ft), seabed change became significant. Similar trends were observed for Sites B1 and E.

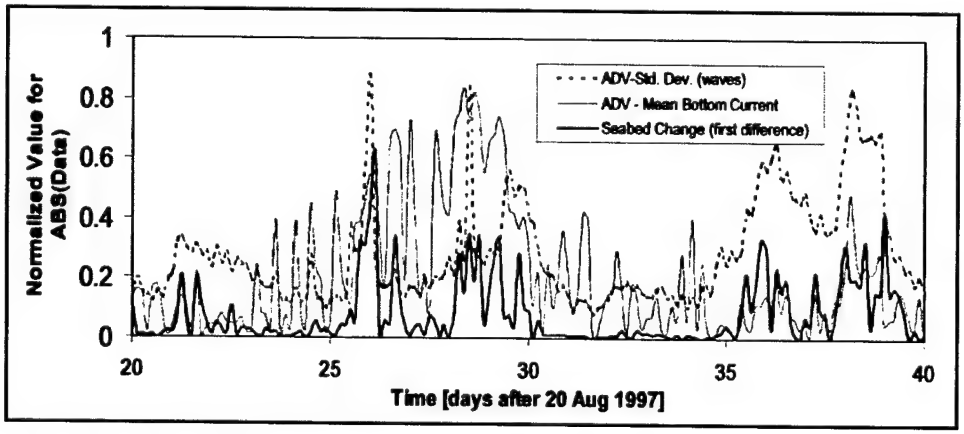

Figure 58. Normalized absolute magnitude for process and response data at Site B2 (after Moritz et al. 1999)

To further assess the causal relationship of seabed change with waves and currents, the correlation between differenced data sets was determined. The change in seabed (every 3 hr) was compared to the corresponding change in wave (ADV-SD) and mean current (ADV) conditions. Figure 59 shows the result of differencing the observed ADV-SD and ADV data, and comparing with

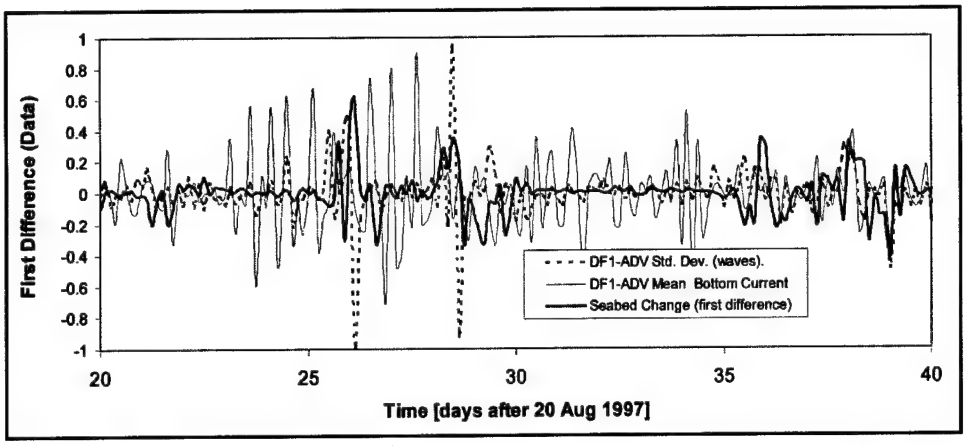

Figure 59. Normalized first difference for process and response data at Site B2 (after Moritz et al. 1999)

seabed change for Site B2. Note the inconsistency between positive and negative change for seabed response with respect to wave and current processes. To obtain a sign independent comparison between difference data, the parameters shown in Figure 59 were subjected to an absolute value function. Figure 60 shows the normalized differenced data for Site B2. When differenced mean current exhibited large variability, the seabed did not follow suit. However, when wave action became highly variable, the seabed responded in a similar manner. Similar trends were observed at Sites B1 and E.

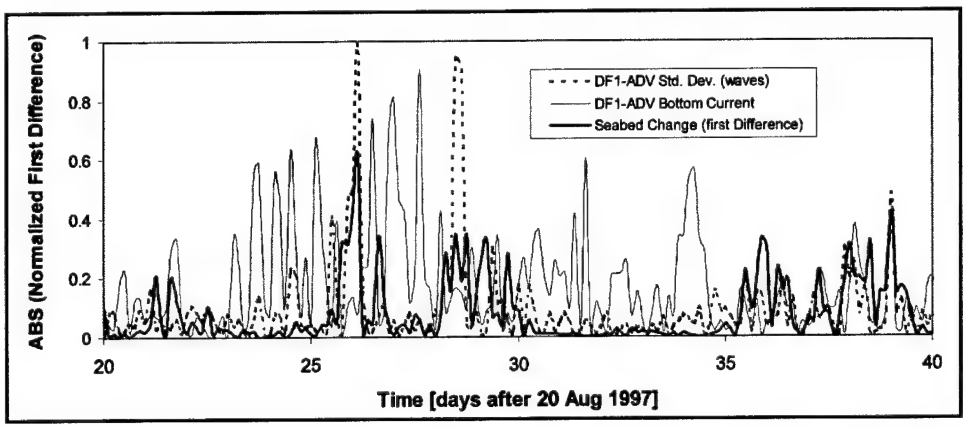

Figure 60. Normalized magnitude of differenced process and response data at Site B2 (after Moritz et al. 1999)

Discussion and conclusions

Moritz et al. (1999) compared, via computed correlation, the magnitude of seabed change to the forcing environment at three MCR monitoring sites during 20 August-10 October 1997. Whether or not observed seabed change was positive (accretion) or negative (erosion) was taken as not relevant; only that there was an observed change was important. The time period of correlation analysis for each site was with respect to 20 August 1998: Site B1 = days 3-27; Site B2 = days 11-50; and Site E = days 3-32.

The cross-correlation of lag 0 for the magnitude of wave action vs. seabed response (Figure 58, typical) was large (0.46-0.66) indicating that these two parameters were correlated simultaneously in time. Cross-correlations of lags 1 and 2 (for wave magnitude vs. seabed change) were moderate, but the trend decreased rapidly with increasing lag. This means that on the average, there is some effect for the delayed response of seabed change due to wave magnitude. Cross-correlation for the difference in wave action vs. seabed change (Figure 60, typical) was moderate, with lag 1 being slightly higher than lags 0 or 2 at Sites E and B1. This indicates that a sudden change in wave height (either increase or decrease) may have affected the seabed, and in the case of Sites B1 and E, the seabed response lagged behind the change in wave height. The cross-correlation of lag 0 for the magnitude of bottom current vs. seabed response was low (0.13-0.31), indicating that these two parameters were weakly correlated in time. Correlation of lags greater than 1 quickly decayed toward 0 indicating, that once bottom currents subside, seabed change diminishes. The difference in mean bottom current vs. seabed change did not cross-correlate well, indicating that a sudden change in bottom current speed does not dictate a seabed response.

Although correlation does not prove causation, serial correlation results obtained for Sites B1, B2, and E strongly indicate that during 20 August-10 October 1997, the response of the seabed at these sites was affected primarily by wave processes and secondarily by bottom current processes.

Effect of ODMDS A and B on Wave Climate (1994 Bathymetry)[1]

As waves (swell or locally generated seas) travel from offshore locations (deep water) to inshore areas (shallow water), the waves shoal (wave height is increased) and steepen as they encounter progressively shallower water. Eventually, the waves will reach a critical steepness and break. In the case of a long stretch of uniform sloping shoreline, the area where waves break (breaker line) is fairly consistent (predictable) for a given set of offshore wave conditions. That is not the case with an irregular shoreline or with complex underwater bathymetry. Under such conditions, incoming waves not only shoal but also refract and diffract as they pass over and around the underwater mounds. The complex interactions of shoaling, refraction, and diffraction can cause the waves to break unexpectedly, and add significant risk to navigation. Such is the case with the approaches to the MCR, where the ebb-tidal shoal is neither uniform in areal configuration nor bottom slope. The presence of large underwater mounds at the existing MCR ODMDS exacerbates wave amplification to the point of breaking, and adversely impacts marine safety with resulting hazards to navigation.

The numerical simulation wave model RCPWAVE (Ebersole, Cialone, and Prater 1986) was used to predict behavior of waves as they are shoaled, refracted, and diffracted by the bathymetry that the waves pass over. RCPWAVE was used to compare the MCR wave climate due to the present (1994) ODMDS

[1] This section is extracted essentially verbatim from USAED, Portland/USEPA (1997).

bathymetry (Figure 61), with the wave climate due to past (1985) bathymetry before prominent mounds had formed.

The issue of dredged material mounds at existing ODMDS creating potential hazardous wave conditions for navigation MCR is illustrated in Figures 62-64. The figures describe the estimated change (amplification) in wave height due to the changed bathymetry at the MCR between 1985 and 1994 (Figure 62 for 6-sec period waves, Figure 63 for 10-sec period waves, and Figure 64 for 16-sec period waves, respectively). Effects due to currents are not included. (The outline border for Figures 62-64 corresponds to the boxed RCPWAVE analysis area shown in Figure 61.)

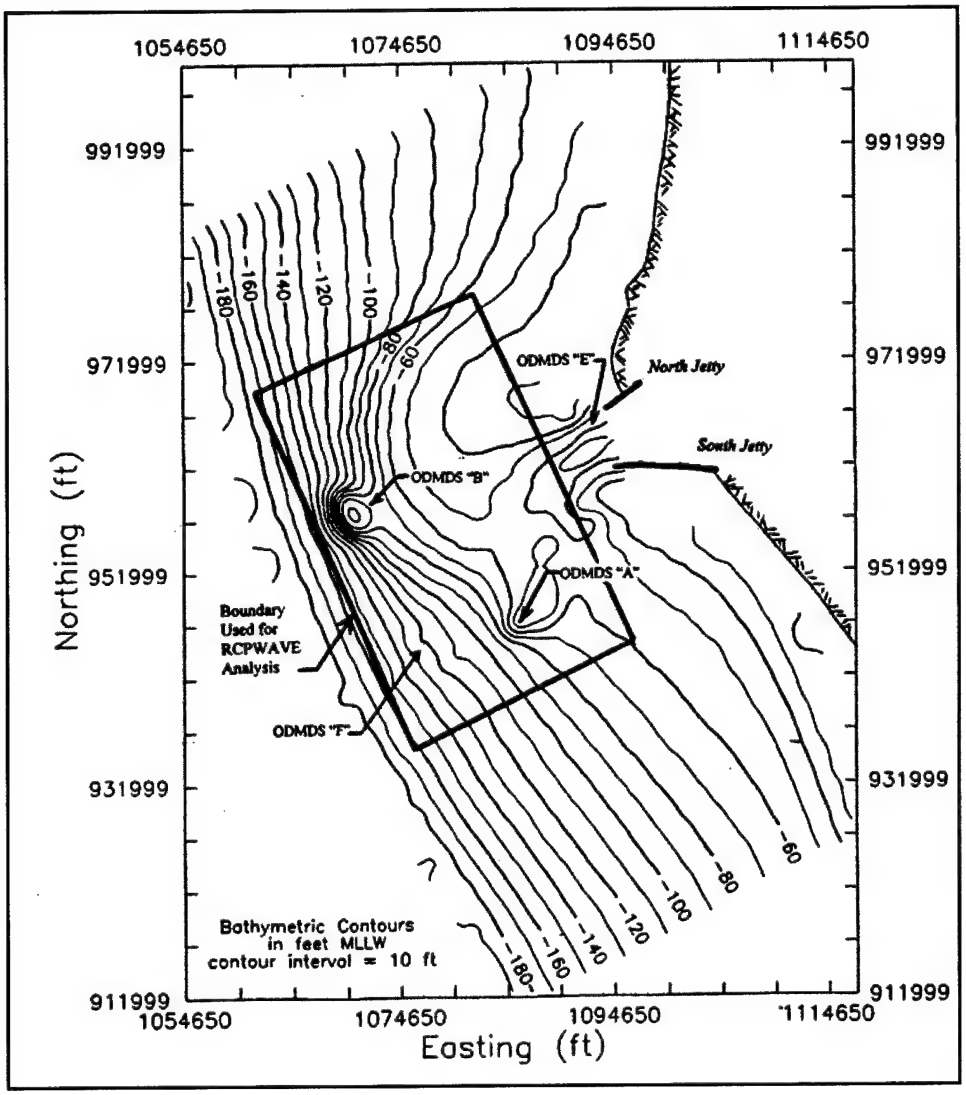

Figure 61. Regional bathymetry used by numerical model RCPWAVE to determine wave amplification caused by ODMDS mounds, 1994 bathymetry (after USAED, Portland/USEPA 1997)

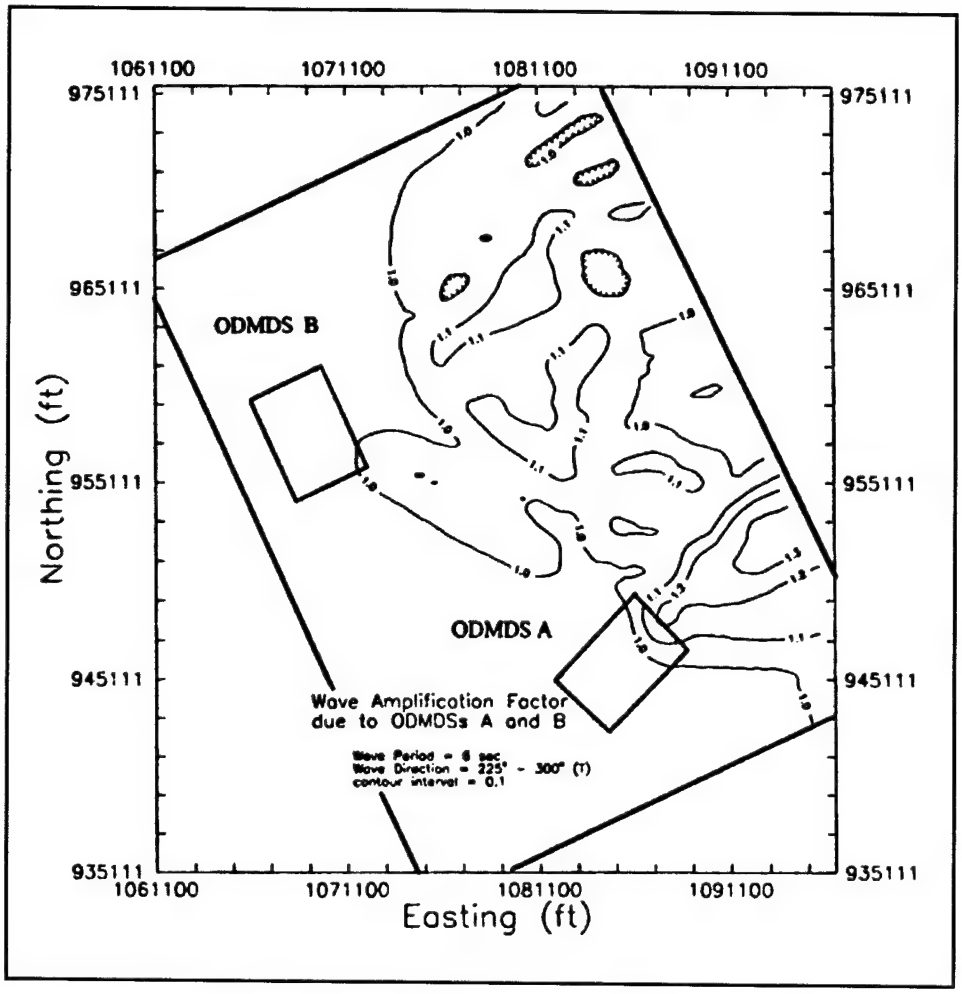

Figure 62. Wave amplification predictions by RCPWAVE caused by ODMDS A and B at MCR resulting from 6-sec period waves (after USAED, Portland/USEPA 1997)

Based on the results displayed in Figures 62-64, the existing dredged material mounds at ODMDS A and B may have increased the height of incident waves within or in proximity to the ODMDS by 30 percent for 6-sec waves, 60 percent for 10-sec waves, and 80 percent for 16-sec waves, compared to 1985. A 10 percent increase in wave height due to shoaling could cause a wave to break. The areas most affected by dredged material mounds at ODMDS A and B are located immediately north and south of the MCR entrance.

Presently, the safest ocean approach to the MCR entrance channel is directly in-line with ODMDS F. The present wave condition at the MCR requires that strict site management measures be implemented to (a) prevent additional mounding at ODMDS A and B, and (b) prevent the formation of new mounds at ODMDS F which could adversely affect incoming waves to the MCR.

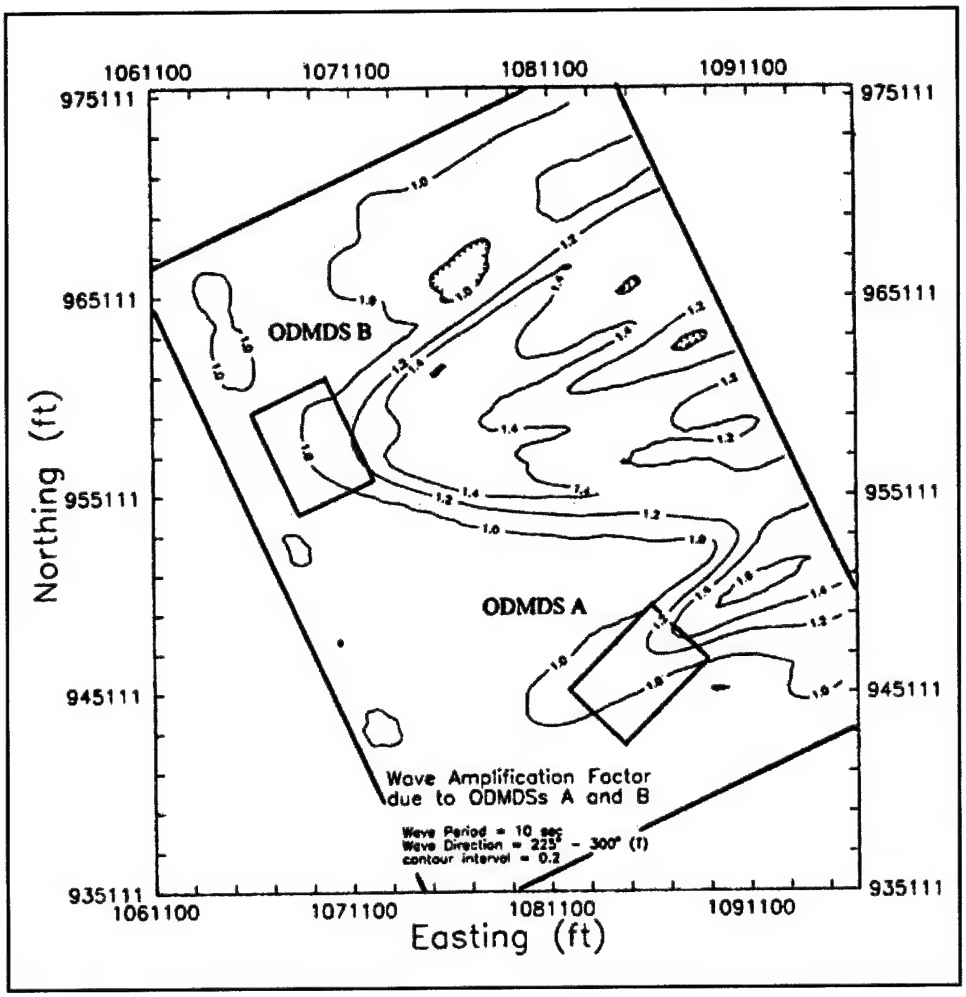

Figure 63. Wave amplification predictions by RCPWAVE caused by ODMDS A and B at MCR resulting from 10-sec period waves (after USAED, Portland/USEPA 1997)

FATE Model Simulations at ODMDS B (1994 Bathymetry)[1]

Early in 1995, the Portland District was considering limiting most of ocean dredged material disposal operations at the MCR to ODMDS B for the 1995 dredging season. This was due to potentially adverse navigation impacts associated with placing dredged material at ODMDS A and F. The MCR bar pilots and other navigational interests were concerned with contractor dredges crossing the entrance channel and interfering with the shipping lane traffic when dumping at ODMDS A and F. Operation of ODMDS E was expected to continue as in past practices. To avoid placement of dredged material at ODMDS A and F, approximately 4.3 million cu yd of sandy dredged material were assumed to be placed at ODMDS B during 1995.

[1] This section is extracted essentially verbatim from USAED, Portland (1995a).

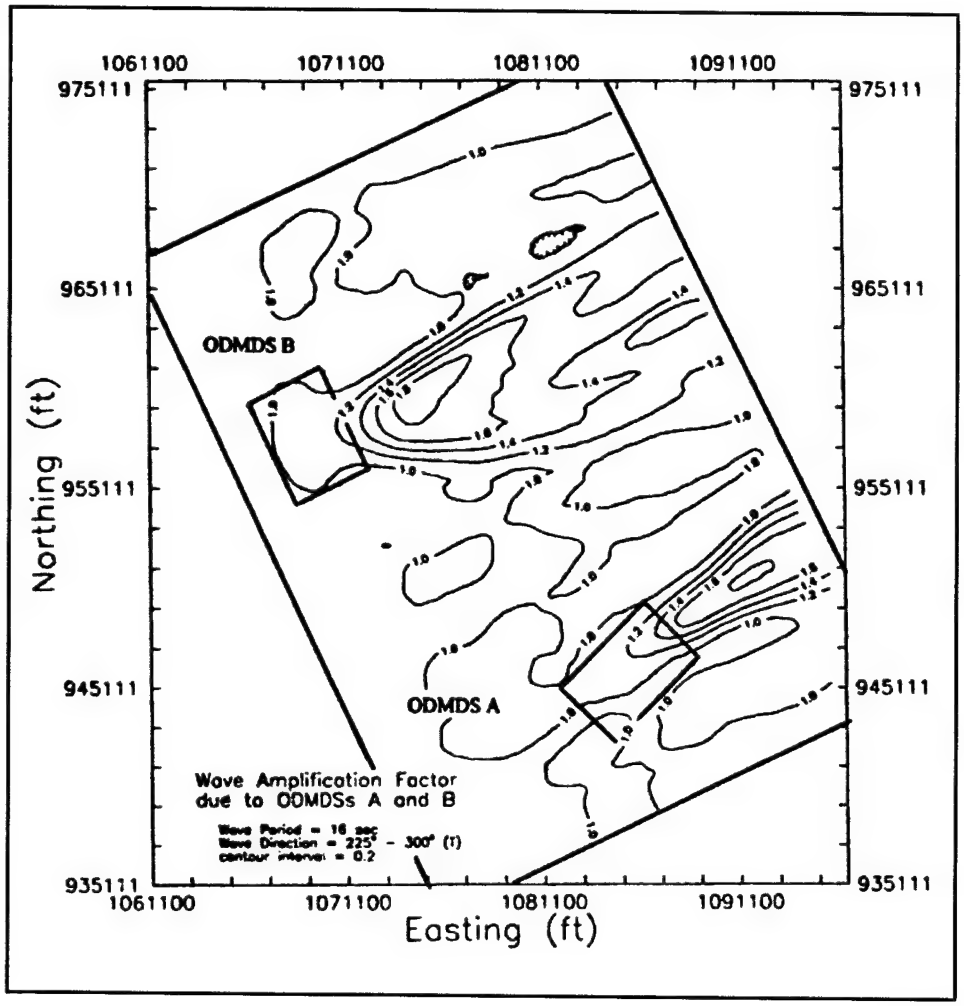

Figure 64. Wave amplification predictions by RCPWAVE caused by ODMDS A and B at MCR resulting from 16-sec period waves (after USAED, Portland/USEPA 1997)

STFATE simulations

STFATE (Johnson 1992; Johnson and Fong 1995) was used to predict the bathymetric distribution (footprint) of dredged material after it has passed through the water column, on an individual dump (disposal vessel load) basis. The model accounts for various disposal vessel, water column, and dredged material parameters.

The disposal mound footprint was estimated for the four hopper dredges most often used at the MCR. The *Essayons* is a government-owned vessel. *The Manhattan Island, Padre Island,* and *Newport* are privately-owned contractor dredges. Two vessel speeds were examined in order to assess this effect upon footprint geometry. The *Essayons* was modeled as moving at and 3 knots (3.5 mph) while placing dredged material. The *Newport, Manhattan Island*, and *Padre Island* were modeled at 0 and 2 knots (0 and 2.3 mph). Disposal cycle duration (time to empty disposal vessel) was modeled as 10 min for the *Essayons*

and 5 min for the *Newport, Manhattan Island*, and *Padre Island*. The dredges were assumed to progress in a straight line while dumping.

Results of footprint geometry for individual dumps were obtained for two disposal vessel speeds: (a) stationary disposal, and (b) vessel moving at 2-3 knots (2.3-3.5 mph). STFATE was used to predict the mound developed for disposal water depths ranging from 9 to 46 m (30 to150 ft). Currents and waves were neglected for this phase of the MCNP study. This minimized dispersion of dredged material within the water column and predicted individual mound shape immediately after disposal (i.e., predicted a conservative dump footprint in terms of height). The dumps were modeled over a flat horizontal bottom.

The depositional void ratio (ed) assumed for these initial STFATE simulations was 0.71. This was the best available estimate at the time of the model runs. A more reliable estimate for ed at the MCR was later determined to be 1.064. It was estimated that the new value of ed would have increased the predicted height of the dump footprint by approximately 33 percent. Therefore, the results for STAFTE-predicted dump footprint geometry here are considered to represent the lowest reasonable estimate for dump footprint height.

Three parameters were used to describe the mound footprint created by disposal of individual loads of dredged material in open water; (a) mound length, (b) mound width, and (c) mound height. Results are based upon a grid interval of 30 m (100 ft). The finer the STFATE grid, the more accurate the predicted mound geometry. The dredges *Padre Island* and *Manhattan Island* are equivalent in terms of physical characteristics and operating parameters; hence, STFATE results for both dredged were reported based on the *Padre Island.*

Results of STFATE simulations

For similar operating conditions (vessel speed, water depth, and still water), the larger the disposal vessel capacity, the higher the resultant mound footprint. For average operating conditions in 15 m (50 ft) of water depth, the dredge *Essayons* will produce a deposition mound 0.2 m (0.5 ft) high. The *Padre Island* and *Newport* will produce a mound 0.09 and 0.11 m (0.30 and 0.35) ft high, respectively.

The most significant parameter affecting mound geometry (length and height) is disposal vessel speed, assuming that the time required to empty a given disposal vessel remains constant. Reducing vessel speed during material release from 3 knots (3.5 mph) to 0 knot (0 mph) increases mound height by a factor of 4 for all the dredges (*Essayons, Newport*, and *Padre Island*).

For dredges that are moving while dumping, increasing the water depth by a factor of 3 from 15 to 45 m (50 to 150 ft) decreases disposal mound height for a single dump by a factor of 0.5 for the dredge *Essayons,* and by a factor of 0.7 for the dredges *Padre Island* and *Newport.*

Mound length is directly related to disposal vessel speed and dump duration. For normal operating conditions, the *Essayons* produces a dump footprint about

854 m (2,800 ft) long, while the *Newport* and *Padre Island* produce a dump footprint about 366 m (1,200 ft) long. For stationary dumps, footprint length is the same as the width, and is directly related to water depth. For a stationary dump in 15-m (50-ft) water depth, the average footprint width and length are about 75 m (250 ft) each. For a 45-m (150-ft) water depth, the footprint width and length are about 150 m (500 ft) each.

For vessels moving while dumping, mound width also is directly related to water depth, but at a decreasing proportionality. Increasing water depth by a factor of 3 from 15 to 45 m (50 to 150 ft) increases footprint width by a factor of 2 from 75 to 150 m (250 to 500 ft). Mound width for the split-hull hopper dredges is typically 60-120 m (200-400 ft) wider than for the multiple-bin door hopper dredges. This is primarily due to the larger hull opening for the split-hull dredges and the slower vessel speeds at which the split-hull dredges were modeled at 2 knots (2.3 mph) vs. the multiple bin door hopper dredges of 3 knots (3.5 mph).

Within STFATE, the volume of dredged material placed into the water column is treated as a sequence of convecting clouds (Johnson and Fong 1995). The use of multiple convecting clouds within the simulation allows for a more realistic representation of disposal from a moving vessel where the disposal operation typically requires up to 10 min for completion.

The assumption of disposal vessels dumping while along a constant heading may not be completely valid for operations at the MCR. Usually, the dredges are turning while dumping. The vessels enter the ODMDS heading away from the dredging site and by the time the dredge has completed the dump, it is heading back toward the dredging site. The U-turn course of dredges while dumping at the MCR ODMDS should be incorporated into the MDFATE simulation model to accurately account for a shortened disposal lane.

LTFATE and MDFATE simulations

LTFATE (Scheffner et al. 1995) and MDFATE (Moritz 1994; Moritz and Randall 1995) were used to predict the bathymetry at the MCR ODMDS B resulting from a series of dumps and simulate long-term change (sediment transport) of the resultant bathymetry. MDFATE can be used to simulate a disposal operation that could extend over 1 year and consist of hundreds of dumps. The model accounts for the overall disposal operation and environmental parameters such as waves, tides, and currents. Waves and currents are incorporated to account for the sediment transport processes affecting the short- and long-term fate of the dredged material placed in open water. The reason for using MDFATE is to provide realistic estimates of aggregate mound formation at ODMDS B.

A prime assumption for the MDFATE model is that, other than the placed dredged material, no sedimentary material enters the ODMDS. This assumption may be invalid at times of high estuary discharge when sediment enters the MCR ODMDS from estuarine transport.

For modeling purposes, the annual dredging and disposal season at the MCR was broken into two discrete time periods. Dredging disposal at the MCR ODMDS normally begins during the April-May time from and continues through the summer until September-October. After October, the ODMDS are not used and are affected by the energetic MCR environment until the following April-May time frame when dredged disposal again commences.

Short-term fate processes (dredged material disposal) was simulated at the disposal sites for a 5-month period (April -September). Long-term fate processes were then simulated for a 7-month period, until the following year when the annual cycle begins again. Semiannual ODMDS bathymetric surveys are typically taken during April-May and September-October, which made the disposal cycle discretization desirable in terms of comparing before and after surveys with simulated results.

Placement of dredged material at ODMDS B was to be restricted to the western half of the site, an area 610 m x 1,830 m (2,000 ft x 6,000 ft) due to excessive mounding in the eastern half. The feasibility of operating ODMDS B to accommodate disposal of 3.3 million cu m per year (4.3 million cu yd per year) in the site's western half for a 3-year period was investigated through these simulations with MDFATE.

An annualized wave environment was simulated for ODMDS B at the MCR using HDPRE and HDPSIM (Borgman and Scheffner 1991). The tidal environment at ODMDS B was simulated using the five primary tidal constituents generated from the ADCIRC-derived database for the eastern North Pacific coast (Hench et al. 1994).

The residual (mean, time averaged) current at the MCR was estimated based upon several data sources (Sternberg et al. 1977). The residual current was estimated to be 0.2 m per sec (0.5 ft per sec) at 280° F. To properly characterize the total effective current at the MCR, the simulated tidal current data were combined with the estimated residual current to simulate the effective water column current at ODMDS B.

Two disposal scenarios were assessed using LTFATE and MDFATE:

a. The western half of ODMDS B was divided into three cells, each 610 m × 610 m (2,000 ft × 2,000 ft). Dredged material was placed randomly about the centroid of each cell based upon a 425-m (1,400-ft-) radius. Random placement was weighted towards the vessel's approach direction.

b. The western half of ODMDS B was divided into 12 cells, each 305 m × 305 m (1,000 ft × 1,000 ft). Dredged material was placed randomly about the centroid of each cell based upon an 245-m- (800-ft-) radius. Random placement was weighted towards the vessel's approach direction.

For both disposal scenarios, the *Essayons* was assumed to be the operating dredge dumping at:

a. 3,440 cu m per dump (4,500 cu yd per dump) capacity (total of 957 dumps per year).

b. Approaching the disposal site from the southeast.

c. Dumping while underway at 1.1 m per sec (3.5 ft per sec), equal to 2.1 m per sec (7 ft per sec) and U-turning while dumping.

d. Duration of active disposal per dump estimated at 4 min.

e. Dredged material parameters were:

(1) Dredged material type = fine sand (SP).

(2) D_{50} = 0.20 mm.

(3) S.G. = 2.71.

(4) C_s (disposal) = concentration of solids by volume in the disposal vessel = 0.50.

(5) ed = depositional void ratio = 0.71 (best estimate at time of simulation).

(6) φ_s = subaqueous shearing angle = 1.8°.

(7) φ_{ps} = subaqueous post-shearing angle = 1.5°.

f. Predisposal bathymetry at ODMDS B = Fall 1994.

Results of LTFATE and MDFATE simulations

For both disposal scenarios (3-cell and 12-cell), overall bathymetric impacts to ODMDS B should not be significant due to the proposed disposal operation. The largest increase in bathymetric relief for scenario a is 7 m (23 ft), near the northwest end of ODMDS B. The largest bathymetric increase for scenario b is 5 m (16 ft), near the west center of ODMDS B.

Based on the MDFATE results, it was not advisable to continue the proposed disposal operation at ODMDS B for additional years past 1995. Mounding would be rapid and might worsen wave conditions at the site. The problem area (high point) associated with the existing mound at ODMDS B would not be made worse by the proposed disposal operation as long as disposal was limited to the western half of ODMDS B and material was evenly distributed. According to the MDFATE results, the existing mound at ODMDS would experience additional increase along the western and northwestern areas due to the 1995 disposal operation. While difficult to predict, if the 1995 disposal operation were to have any additional negative affect upon the wave environment, it would be at the northern end of ODMDS B.

Dump scenario b would minimize potential wave effects due to the lower resultant mounding than scenario a. Overall, disposal scenario b provides for better, more uniform, dispersal of dredged material along the western half of ODMDS B than does scenario a. Both dump scenarios result in 5-10 percent of

placed dredged material leaving the formal boundaries of ODMDS B upon disposal from the hopper dredge.

It is believed that disposal direction plays an important role in confining dredged material disposal within the formal site boundaries. The southeast approach direction assumed for this investigation produces the best case for keeping material within ODMDS B. Temporary acquisition of a placement buffer extending 230 m (750 ft) beyond the existing site boundaries would prevent dredged material from being placed outside of ODMDS B.

Dredged material placed in the western half of ODMDS B for 1995 would not experience any significant long-term movement except during severe storm events. What is placed there will essentially stay there. This is due to the significant water depths along the western part of ODMDS B of 43 m (140 ft), compared to the depth at the top of the existing mound of 15-18 m (50-60 ft).

MDFATE simulations versus actual disposal operations

At the time of this analysis, the 1995 predisposal and postdisposal surveys at ODMDS B were not available. However, the 1994 dredging disposal cycle at ODMDS B was similar to the anticipated event in 1995 in terms of positioning control during disposal. The volume placed at the western portion of ODMDS B during 1994 was 1,567,000 cu m (2,048,000 cu yd) (767,000 cu m (1,003,000 cu yd) placed by the *Newport* and 800,000 cu m (1,045,000 cu yd) placed by the *Essayons*), or about 52 percent of the volume proposed for 1995. The two dredges have approximately the same dump footprint, if vessel speed is the same. Approximately 460,000 cu m (600,000 cu yd) placed by the *Essayons* was dredged from the disposal mound located in the eastern part of ODMDS B. This was necessary in order to reduce the height of the mound for safety purposes. Thus, the 1994 disposal operation was similar to the proposed 1995 disposal operation.

The MDFATE predicted post-disposal bathymetry was compared to the bathymetry resulting from the actual disposal operation conducted in 1994. The maximum mound height for the actual disposal operation (1994) was approximately 3.1-3.7 m (10-12 ft). The maximum mound height for the simulated MDFATE (1995) run was 7 m (23 ft), which is about twice as high as that of the 1994 postdisposal bathymetry. This would be expected since the 1995 operation was intended to place about twice the volume in ODMDS B than had taken place in 1994. The most significant difference between the predicted and actual cases was the steepness of the postdisposal bathymetry. The maximum gradient for predicted bathymetry was fixed at $\Delta z/\Delta x = 0.0314$. The bathymetric gradient for the actual postdisposal bathymetry was approximately one-half that of the predicted case. A better estimate was needed for the avalanching angles (φ_s and φ_{ps}) of dredged material.

FATE Model and RCPWAVE Model Simulations at ODMDS F (1995 Bathymetry)[1]

In 1996, the MCR ODMDS A, B, and E could accept only limited amounts of dredged material. Placement of dredged material at ODMDS A has not occurred since 1995 and was currently restricted. Disposal at ODMDS B was limited to 1.53 million cu m per year (2 million cu yd per year) for 1996 (Siipola and Braun 1995). In 1997, disposal at ODMDS B was revised down to 460,000 cu m per year (600,000 cu yd per year), and could be further restricted beyond 1997. Dredged material disposal at ODMDS E was at that time limited to less than 0.76 million cu m per year (1 million cu yd per year). Excluding ODMDS F, the total capacity of the MCR ODMDS was 2.3 million cu m (3 million cu yd) per year for 1996, and could decrease to 0.76 million cu m per year (1 million cu yd per year) after 1997. The annual volume of sediment dredged from the MCR project and placed in ODMDS varied from 3.1-3.8 million cu m per year (4-5 million cu yd per year).

Given the capacity limitations on the MCR ODMDS, ODMDS F would be expected to receive as much as 3.1 million cu m per year (4 million cu yd per year) after 1996. To confidently rely on ODMDS F to handle present and future MCR dredging disposal requirements, the capacity of ODMDS F (for 1996 and beyond) was assessed in June 1996 with respect to impacts on navigation. Figure 65 defines the region of interest. The dashed line refers to ODMDS F boundaries as expanded in 1992.

Adverse impacts to navigation are related to increased wave activity due to bathymetric changes (mounding). The threshold criteria for adverse navigation impacts was that wave conditions at a given ODMDS should not be increased greater than 10 percent over the baseline condition wave environment (prior to ODMDS use) due to dredged material mounding. The solid line in Figure 65 refers to the bathymetric area surrounding ODMDS F used for the RCPWAVE analysis of waves with respect to various predicted dredged material mound geometries. For this wave analysis, the 1995 survey was considered to represent the baseline condition at ODMDS F. The 1995 bathymetric condition of ODMDS F was the result of limited disposal operations conducted at this site since 1989.

Bathymetric difference between the 1992 and 1995 condition survey of ODMDS F showed multiple mounds 1.2-2.4 m (4-8 ft) high distributed throughout the southeastern half of ODMDS F. The formation of these mounds has prompted the Portland District to examine how to maximize the use of ODMDS F capacity, and to determine the end-point at which ODMDS F should no longer be used for dredged material disposal. There was a 305-m (1,000-ft) buffer zone surrounding ODMDS F. To reduce the risk of dredged material being placed outside of the designated site boundaries, no dredged material disposal was permitted within the site's buffer zone although it was formally part of ODMDS F.

[1] This section is extracted essentially verbatim from USAED, Portland/USEPA (1997).

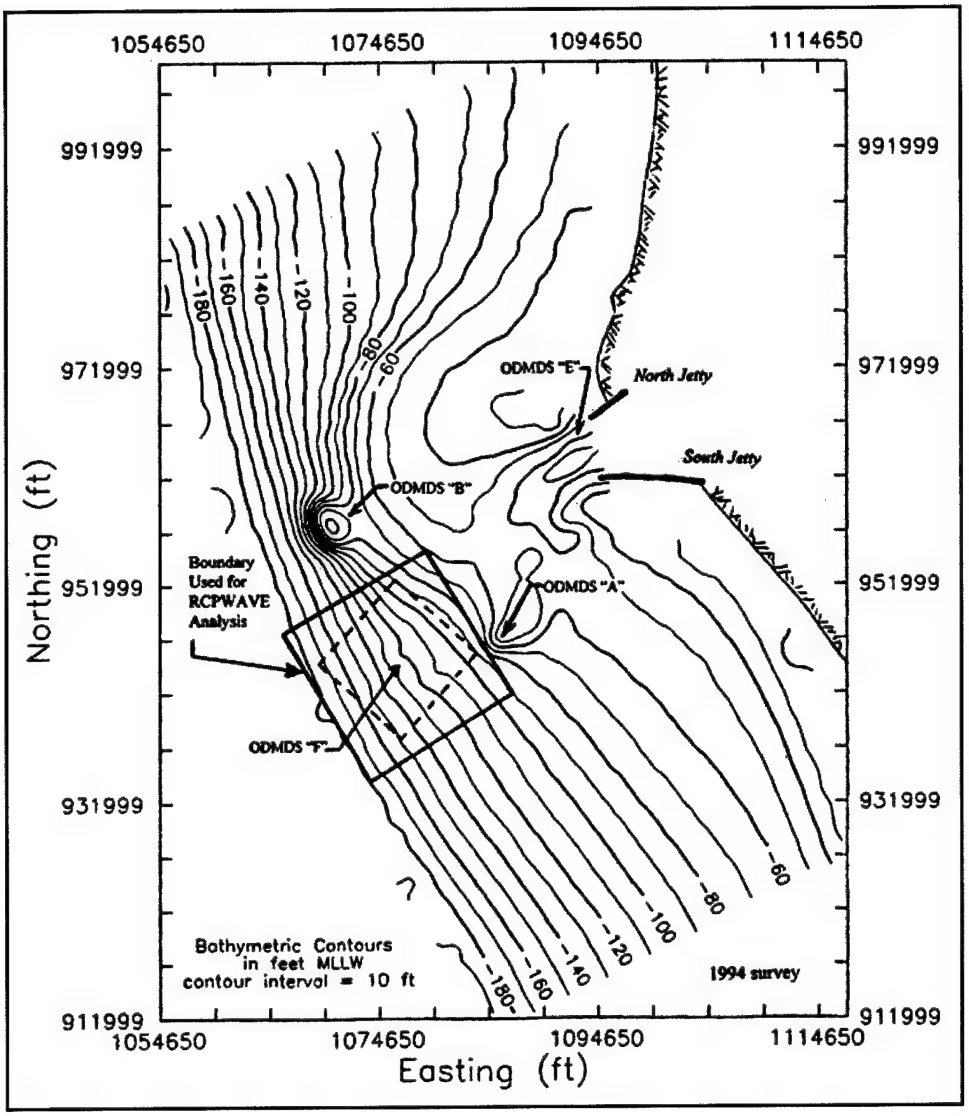

Figure 65. MCR regional bathymetry used for RCPWAVE and MDFATE simulations at ODMDS F (after USAED, Portland/USEPA 1997)

Disposal scenarios at ODMDS F

Two scenarios were examined to assess the remaining capacity of ODMDS F. In both disposal scenarios, it was anticipated that ODMDS F would handle all MCR dredged material disposal in excess of what was expected to be placed in ODMDS E of 0.76 million cu m per year (1 million cu yd per year). Scenario 1 represented a lower bound for ODMDS F use based on 1-year disposal of 2.3 million cu m (3 million cu yd) (3.1 million cu m (4 million cu yd) total MCR dredging disposal). Scenario 2 represented an upper bound based on 2 years disposal of 3.1 million cu m (4 million cu yd) (3.8 million cu m (5 million cu yd) total MCR dredging disposal per year). Future dredged

material disposal at ODMDS F would not be permitted to degrade (increase) the wave environment by more than 10 percent over the 1995 condition.

Disposal Scenario 1. This was the lower bound for 1 year of disposal. The feasibility of placing 2.3 million cu m (3 million cu yd) of dredged material in the southeastern half of ODMDS F for 1 year was assessed in terms of predicted bathymetric change at the ODMDS, and related impacts upon the wave environment. The disposal operation conforming to Scenario 1 was defined as:

a. The southeastern half of ODMDS F, cells 9-16, with overall dimensions of 1,220 m × 2,440 m (4,000 ft × 8,000 ft) was divided into eight disposal lanes. Each disposal lane was 150 m (500 ft) wide × 2,440 m (8,000 ft) long, and was oriented NE-SW. Dredged material was placed randomly within each lane based upon a 120-m (400-ft) radius. To accurately account for operational reality, each randomly selected dump location was weighted toward the direction from which the dredge was approaching the disposal site.

b. Dredged material disposal at ODMDS F was expected to occur during July to October, during which 2.3 million cu m (3 million cu yd) of material would be equally distributed along the eight disposal lanes. LTFATE and MDFATE predictions were made for sediment transport at ODMDS F during November 1996-June 1997.

c. The impact of the predicted dredged material mound at ODMDS F upon the wave environment was assessed by RCPWAVE for wave periods of 10 sec and 16 sec. Wave approach direction included all angles for which offshore waves are incident to the northern Oregon coast, and ranged from 225 deg (SW) to 300 deg (NW).

Disposal Scenario 2. This was the upper bound for 2 years of disposal. The feasibility of placing 3.1 million cu m per year (4 million cu yd per year of dredged material in the southeastern half of ODMDS F, for two consecutive years was assessed in terms of predicted bathymetric change at the ODMDS, and related impacts upon the wave environment. The disposal operation conforming to Scenario 2 was defined as:

a. The southeastern half of ODMDS F was divided into eight cells, 9-16, each 610 m × 610 m (2,000 ft × 2,000 ft). Dredged material was placed randomly about the centroid of each cell based upon a 275-m (900-ft) radius. Dump location was weighted toward the direction from which the dredge was approaching the disposal site.

b. Dredged material disposal at ODMDS F was expected to occur during July to October, during which 3.1 million cu m (4 million cu yd of material was equally distributed in the eight dump cells. LTFATE and MDFATE predictions were made for sediment transport at ODMDS F during November-June. Dredged material disposal was simulated for 1996 and 1997.

c. The impact of the predicted dredged material mound at ODMDS F upon the wave environment was assessed for wave periods of 10 sec and 16 sec. Wave approach direction ranged from 225 deg (SW) to 300 deg (NW).

Results of FATE model simulations at ODMDS F

The LTFATE and MDFATE sediment transport models, and the RCPWAVE wave transformation model, were used for the ODMDS F assessment. The method used to apply the models is summarized as follows:

a. For both scenarios, the *Essayons* was assumed to be the operating dredge dumping at:

(1) 3,440 cu m per dump (4,500 cu yd per dump) capacity.

(a) Total of 666 dumps for 1 year for Scenario 1.

(b) Total of 888 dumps per year for 2 years for Scenario 2.

(2) Approaching the disposal site from the northeast (aligned with the MCR navigation channel).

(3) Dumping while underway at 1.1 m per sec (3.5 ft per sec).

(4) Duration of active disposal per dump estimated at 10 min.

b. Dredged material parameters were (Paxton 1990):[1]

(1) Dredged material type = fine sand (SP).

(2) D_{50} material dredged from the MCR = 0.20 mm.

(3) Fines content (D<O.0625 mm) = 4 percent (silt).

(4) S.G. of dredged material solids = 2.71.

(5) C_s (disposal) = concentration of solids by volume in the disposal vessel = 0.485.

(6) ed = depositional void ratio = 1.062.

(7) φ_s = subaqueous shearing angle = 1.8 deg.

(8) φ_{ps} = subaqueous postshearing angle = 1.5 deg.

(9) Baseline predisposal bathymetry at ODMDS F for this analysis = summer 1995.

c. Waves and currents used:

(1) Time series for waves = WIS-III sta 22 (Jensen and Hubertz 1989).

(2) Time series for tidal currents = ADCIRC constituents (Hench et al. 1994).

(3) Residual currents for ODMDS F (and ODMDS B) (Sternberg et al. 1977).

(4) Spring (April-June) = 0.03 m per sec (0.09 ft per sec) at 320 deg, maximum 0.64 m per sec (2.1 ft per sec) at 315 deg.

(5) Summer (July-October) = 0.18 m per sec (0.60 ft per sec) at 213 deg, maximum 0.88 m per sec (2.9 ft per sec) at 251 deg.

---

[1] Paxton, J. A. (1990). U.S. Army Corps of Engineers, Portland District, Memorandum for the Commander, Results from W. O. #90-Sh-1734, report of sediment test samples at the MCR.

(6) Winter (November -March) = 0.29 m per sec (0.96 ft per sec) at 294 deg, maximum 0.73 m per sec (2.4 ft per sec) at 284 deg.

(7) Total effective current at ODMDS F = tidal current + residual current.

Results of disposal Scenario 1. The predicted mound formation after 1 year of disposal at the southeastern half of ODMDS F of 2.3 million cu m (3 million cu yd) for 1 year was:

a. A fairly uniform mound covering the southeastern half of ODMDS F was predicted to be added onto the existing bathymetry (1995), after 1 year of dredged material disposal (1996).

b. Total bathymetric change within the southeastern half of ODMDS F from 1992 to 1996 (including predicted accumulation for 1996) was expected to be +3.7 m (+12 ft).

Disposal of 2.3 million cu m (3 million cu yd) (for 1 year) in the southeastern half of ODMDS F was expected to add a fairly uniform 0.9- to 1.8-m- (3- to 6-ft-) high mound in that area of ODMDS F, on top of the existing 1995 bathymetry.

Predicted changes in wave height at ODMDS F due to mound formation during 1996 using 1995 as the baseline condition are as follows:

a. For average wave conditions (10-sec period waves, all applicable directions of wave approach), the predicted mound was not expected to affect wave height in the southeastern half of ODMDS F.

b. For large swell wave conditions (16-sec period waves, all applicable directions of wave approach), the predicted mounds were expected to increase wave height by no more than 10 percent in the southeastern half of ODMDS F.

It was predicted that the wave environment at ODMDS F would be minimally impacted by a 3.7-m- (12-ft-) high mound (total height relative to the 1992 bathymetry). Following disposal Scenario 1, waves at the affected part of ODMDS F were expected to increase by no more than 10 percent of the 1995 baseline condition.

Scenario 1 would result in a mound that is at or below the threshold limit in terms of affecting the wave environment at the southeastern half of ODMDS F. Additional future disposal at the southeastern half of Site F would result in increased wave heights at the ODMDS F, and would probably result in exceedance of the 10 percent threshold criteria.

Results of disposal Scenario 2. The predicted mound formation after 2 years of disposal at the southeastern half of ODMDS F of 3.1 million cu m per year (4 million cu yd per year) for 2 years was:

a. Two elongated mounds (berms) covering the southeastern half of ODMDS F were predicted to be added onto the existing bathymetry (1995), after 2 years of dredged material disposal (1997).

b. Total bathymetric change (accumulation) since 1992 was expected to be +6.7 m (+22 ft) within the southeastern half of ODMDS F.

Disposal of 3.1 million cu m per year (4 million cu yd per year) for 2 consecutive years in the southeastern half of ODMDS F was expected to create 3.7- to 5.5-m- (12- to 18-ft-) high mound(s) in that area of ODMDS F, on top of the existing 1995 bathymetry. The regularity of the predicted mound features was due to the small radius used to control the placement of dredged material within each dump cell.

The Scenario 2 result is not trivial. Dump Scenario 2 reproduced a similar bathymetric trend as was observed at ODMDS A and B during 1986-94 when dredged material disposal was confined within small placement areas. The random radius that was used in Scenario 2 to place dredged material in cells 9-16 varied between 0-275 m (0-900 ft). Random placement was achieved using a uniform distribution. The mean value for the random dump radius was about 135 m (450 ft). Since each dump cell was 610 m (2,000 ft) on each side (or about 305-m (1,000-ft) radius), most of Scenario 2 placement was confined to areas 135 m (450 ft) from the center of each dump cell. The alignment of cells 9-16, combined with the dredging vessel approach heading (NE to SW) during disposal, resulted in a narrow two-lane disposal control plan. Given this result, disposal Scenario 1 (eight lanes) is much more effective at dispersing placed dredged material than Scenario 2 (two lanes).

Predicted changes in wave height at ODMDS F in 1996 due to mound formation resulting from disposal Scenario 2 since the 1995 baseline condition were:

a. For average wave conditions (10-sec period waves, all applicable directions of wave approach), the predicted mounds are expected to increase the wave height by 10-20 percent in the southeastern half of ODMDS F. Results for the predicted wave increase between 1995 (baseline condition) and 1997 are shown in Figure 66.

b. For large swell wave conditions (16-sec period waves, all applicable directions of wave approach), the predicted mounds were expected to increase the wave height by 10-30 percent in the southeastern half of ODMDS F.

Following disposal Scenario 2, the wave environment at ODMDS F was predicted to be significantly impacted by a 5.5- to 6.1-m- (18- to 20-ft-) high mound. Waves could be 10-30 percent higher than at present. Scenario 2 would result in a mound that exceeds the threshold limit in terms of affecting the wave environment at the southeastern half of ODMDS F. A disposal sequence conforming to Scenario 2 would be unacceptable from the standpoint of navigation impacts.

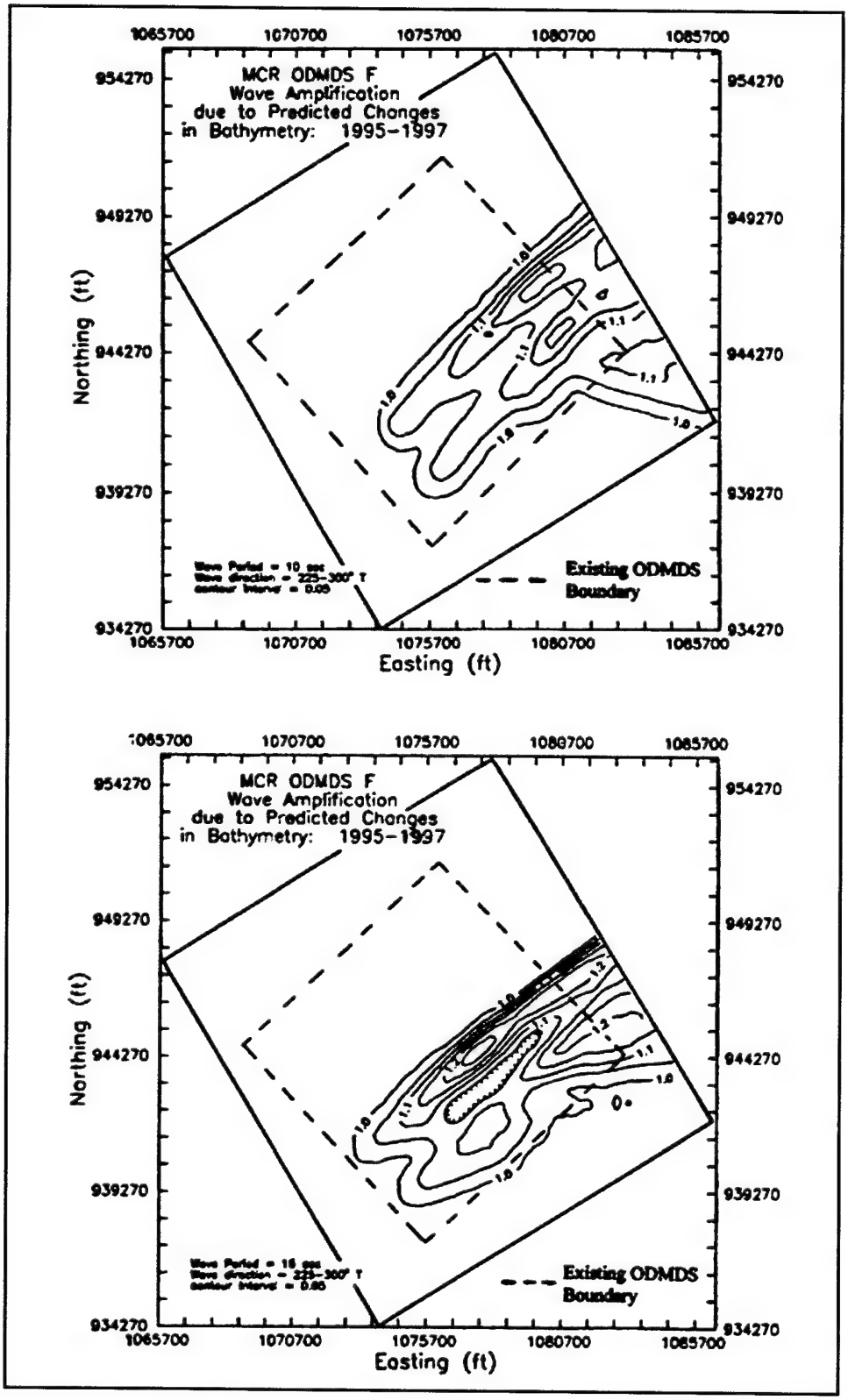

Figure 66. RCPWAVE predictions of wave amplification at ODMDS F for disposal Scenario 2 (top, 10-sec period waves; bottom, 16-sec period waves) (after USAED, Portland/USEPA 1997)

Conclusions from FATE simulations at ODMDS F

At the beginning of the 1996 dredging season, the remaining capacity for the southeastern half of ODMDS F was approximately 2.3 million cu m (3 million cu yd). A disposal sequence conforming to Scenario 1 would fill the southeastern half of ODMDS F. After 1996, the total volume of dredged material placed in the southeastern half of ODMDS F was expected to be 6.8 million cu m (8.9 million cu yd) from 1989-1996, assuming 2.3 million cu m (3 million cu yd) was added in 1996. Conducting dredged material disposal in the southeastern half of ODMDS F in excess of 2.3 million cu m (3 million cu yd) total, beginning with 1996 disposal, would likely result in increased wave conditions (above the 10 percent criteria).

Dredged material placed in ambient water depths at ODMDS F of -30 to -55 m (-100 to -180 ft) mllw would not significantly disperse in the long-term time frame. Material placed within ODMDS F stay there. This was concluded from LTFATE calculations for dredged material behavior at ODMDS F. USACE could not risk negatively impacting navigation at or near ODMDS F. The water depths at that location would preclude any dredge from reworking placed dredged material to mitigate for inadvertent mounding problems caused by dredging disposal.

ODMDS F is in the direct line of approach to the MCR entrance channel. Bar pilots use the area as a staging location for transferring pilots to vessels of commerce. ODMDS A and B have been used to an extent such that safe navigation is presently impaired at or near those ODMDS, due to significant mounding and related wave conditions. If similar conditions were created at ODMDS F, overall navigation at MCR would be impaired.

FATE Model and RCPWAVE Model Simulations at Expanded ODMDS B and E (1996 Bathymetry)[1]

During site assessment studies in 1966 by the Portland District, the only feasible option for providing an additional 2.3-3.1 million cu m per year (3-4 million cu yd per year) disposal capacity for the MCR navigation project was to temporarily expand existing ODMDS. The expanded ODMDS would be used for dredged material placement until which time new ODMDS were formally designated. As a conservative estimate, the expanded sites were expected to be utilized for 5 years, beginning in 1997.

ODMDS A and F were not considered for site expansion for reasons of impeding navigation. That decision left ODMDS B and E as the only remaining sites available for temporary expansion. Both ODMDS B and E together were considered for temporary expansion to allow for greater operational flexibility and to minimize the potential impacts associated with using a single ODMDS for all the MCR disposal needs.

---

[1] This section is extracted essentially verbatim from USAED, Portland/USEPA (1997).

During a 5-year utilization period, expanded ODMDS B and E would need to accept 19.1 million cu m (25 million cu yd) of dredged material (assuming a disposal requirement of 3.8 million cu m per year (5 million cu yd per year). At the MCR ODMDS, approximately 96 percent of placed dredged material is composed of sand and 4 percent is composed of fines (silt), on a per load basis. The proposed boundaries for expanded ODMDS B and E were configured as shown in Figure 67. Expanded ODMDS B would be approximately 3,660 m × 3,660 m (12,000 ft × 12,000 ft). Expanded ODMDS E would be approximately 610 m × 3,050 m (2,000 ft × 10,000 ft).

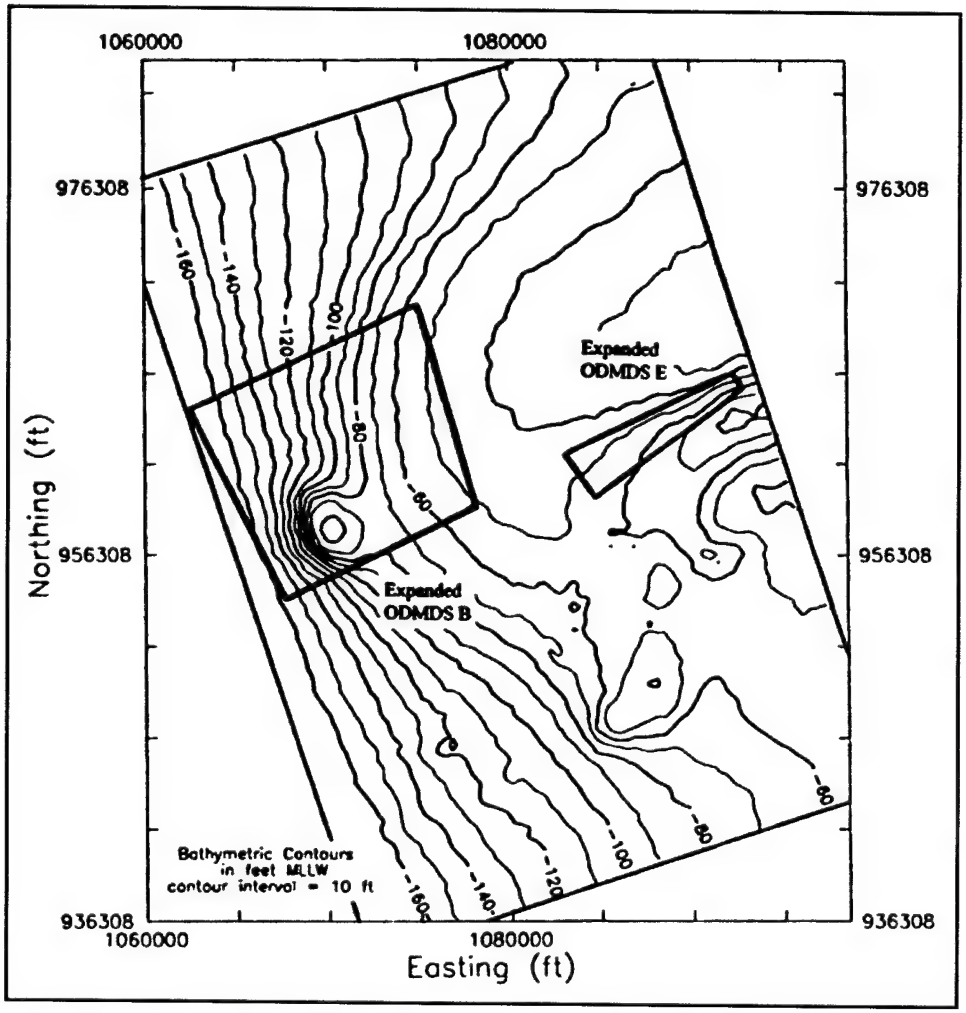

Figure 67. Proposed expanded ODMDS B and E (after USAED, Portland/ USEPA 1997)

It was assumed that expanded ODMDS B would receive 3.1 million cu m per year (4 million cu yd per year) of dredged material, and that expanded ODMDS E would receive no more than 1 million cu yd per year, due to the proximity of ODMDS E to the MCR navigation channel. There was great concern that disposed dredged material would be transported back into the channel. However, as the analysis of expanded ODMDS B progressed, it became apparent that increased volumes of dredged material could be placed within expanded

ODMDS E. That measure would reduce the volume of material to be placed in ODMDS B.

Expanded ODMDS B

The proposed configuration of expanded ODMDS B was intended to minimize haul distance from the site of dredging in the MCR navigation channel, while maximizing the return of dredged sediments back to the littoral environment. Minimum existing water depth within the expanded ODMDS B boundaries is 15 m (50 ft), as compared to 24 m (80 ft) for the present ODMDS B boundary. A 15-m (50-ft) water depth is considered a minimum safe navigable depth for hopper dredges operating at the western flank of Peacock Spit.

By placing dredged material in a shallower water depth, it was anticipated that more dredged material would be transported by waves and currents back into the littoral system. This would maintain ODMDS capacity and minimize any perceived erosion problem north of the MCR. During the 5-year period of expanded site operation, ODMDS B was assumed to receive at total of 15.3 million cu m (20 million cu yd). It was initially assumed that half of the material to be placed in ODMDS B would be placed in the shallow part of the ODMDS at 7.7 million cu m (10 million cu yd) during a 5-year period. The deeper part of the site would receive the other half of the dredged material volume of 7.7 million cu m (10 million cu yd) during a 5-year period.

Dredged material placement within the shallower area where depth = 15-21 m (50-70 ft) of expanded ODMDS B would be conducted in manner that would avoid increasing wave heights greater than 10 percent over the existing condition. It was initially assumed that formation of a mound feature less than or equal to 2.4 m (8 ft) in height would achieve the 10 percent criterion. Applying 7.7 million cu m (10 million cu yd) into the formation of a mound 2.4 m (8 ft) tall would require dimensions of 1,800 m (5,900 ft) long and 1,035 m (3,400 ft) wide at the base with 0.012 (1V:80H) side slopes.

Within the deeper part at depths of 27-50 m (90-160 ft) of expanded ODMDS B, it was initially assumed that dredged material placement that avoided the formation of any mound feature greater than 4.6 m (15 ft) in height would achieve the 10 percent wave criterion. Applying 7.7 million cu m (10 million cu yd) into the formation of a mound 4.6 m (15 ft) tall would require dimensions of 1,370 m (4,500 ft) long and 1,250 m (4,100 ft) wide at the base with 0.012 side slopes. Both mounds were constructed geometrically similar.

It was anticipated that by limiting dredged material accumulation, the wave environment at the MCR would not be worsened due to mound-induced wave shoaling. Increasing wave height (for seas or swell) greater than 10 percent over the existing (non- mound) bathymetric condition was considered unacceptable.

Expanded ODMDS E

The proposed configuration for expanded ODMDS E was intended to take advantage of the high rate of sediment dispersion that occurs at ODMDS E. ODMDS E is a highly dispersive site. Material that is presently placed within the present boundaries of ODMDS E at about 0.77 million cu m per year (1 million cu yd per year) does not accumulate within the ODMDS. Some of the material is transported northward onto Peacock Spit during fall and winter where it is reintroduced into the littoral system north of the MCR. During summer, the littoral transport at ODMDS E is believed to be southward toward the navigation channel. A volumetric analysis of ODMDS E indicated that from 1990 to 1995, ODMDS E had lost 2.8 million cu m (3.7 million cu yd) despite 2.6 million cu m (3.4 million cu yd) of dredged material being placed within this site during the same time period. Expanded ODMDS E would be in similar water depths as the present configuration. ODMDS E was expanded to facilitate the use of this ODMDS by two dredges placing dredged sediment at the same time, and allow more area to be used for dispersal of dredged material to prevent mounding. Presently, the site is too small for more than one dredge to navigate within while disposing, during a given dredging and disposal operation.

Dredged material placement within expanded ODMDS E would be conducted in manner that would avoid formation of any mound feature greater than 1.2 m (4 ft) in height. If a mound feature did form at expanded ODMDS E, it was anticipated that it would not remain for more than 1 year before being obliterated by the site's wave and current regime. The formation of a mound 1.2 m (4 ft) tall containing 0.77 million cu m (1 million cu yd) of sediment (1 year of disposal) would have dimensions of 1,585 m (5,200 ft) long and 305 m (1,000 ft) wide at the base (0.012 side slope). It is highly unlikely that this type of bathymetric feature would form at an energetic site such as ODMDS E. It was only considered from the standpoint of a conservative site impact assessment.

As an initial site management goal, expanded ODMDS E would receive 1.5 million cu m per year (2 million cu yd per year) of dredged material disposal. As confidence was gained concerning the favorable disposition of placed material (site surveys indicating that material was not accumulating in the expanded site or moving into the navigation channel), the annual volume of dredged material placed into ODMDS E would be increased. The amount of dredged material placed into expanded ODMDS B would be reduced while placement in expanded ODMDS E would increase. This scenario will enhance the transport of dredged sediment into the littoral environment of Peacock Spit while minimizing benthic impacts to biota at ODMDS B.

STFATE modeling at expanded ODMDS B and E

STFATE simulations were conducted for the disposal of dredged material from two types of hopper dredges; (a) a split-hull hopper dredge (*Newport*), and (b) a multiple bottom door hopper dredge (*Essayons*). Since 1990, about half of all dredging disposal at the MCR ODMDS has been performed by the *Essayons*. The *Newport* has performed about 30 percent of the MCR dredging disposal. The vessel speed during disposal was assumed to be 2 knots (2.3 mph) for both

dredges. The duration of placement for an individual load of dredged material was assumed to be 5 min for the *Newport* and 8 min for the *Essayons*. STFATE simulations were conducted for disposal water depths ranging from 12 to 60 m (40 to 200 ft). Three types of current conditions were also tested; (a) no current, (b) a 0.3-m per sec (1-ft per sec) current, and (c) a 1.2-m per sec (4-ft per sec) current. Currents were modeled as being oriented 45 deg into the heading of the disposal vessel. The current regime at the MCR ODMDS ranges from 0.2 to 1.5 m per sec (0.5 to 5 ft per sec). The characteristics of sediment dredged from the MCR project and placed at the ODMDS was described previously in Chapter 5, "FATE Model Simulations at ODMDS F," of this report.

For typical conditions at the expanded ODMDS B, the mound resulting from an individual dump could be expected to have the following configuration:

a. Mound length = 400 to 640 m (1,300 to 2,100 ft).

b. Mound width = 120 to 245 m (400 to 800 ft).

c. Mound thickness = 0.06 to 0.24 m (0.2 to 0.8 ft).

d. Displacement of mound during disposal = 30 to 120 m (100 to 400 ft).

For typical conditions at the expanded ODMDS E, the mound resulting from an individual dump could be expected to have the following configuration:

a. Mound length = 365 to 490 m (1,200 to 1,600 ft).

b. Mound width = 640 to 460 m (800 to 1,500 ft).

c. Mound thickness = 0.06 to 0.18 m 0.2 to 0.6 ft.

d. Displacement of mound during disposal = 120 to 365 m (400 to 1,200 ft).

LTFATE and MDFATE modeling at expanded ODMDS B and E

The long-term fate of dredged material to be placed within the expanded ODMDS B and E was assessed using LTFATE (Scheffner et al. 1995) and MDFATE (Moritz 1994; Moritz and Randall 1995). Transport of sediment off the dredged material mounds was simulated for a period of 1 year.

The dredged material parameters and current regimes used in the LTFATE and MDFATE models were the same as those used for the LTFATE analysis of the previous section. Wave conditions were generated using the WIS correlation coefficient matrix (Borgman and Scheffner 1991; Jenson and Hubertz 1989). Long-term fate simulations were run separately for the expanded ODMDS B and E. Each 1-year-long simulation was divided into oceanographic seasons based on changes in the seasonal residual current.

Results of LTFATE and MDFATE modeling at expanded ODMDS B. Results from the long-term fate simulations for ODMDS B are summarized in terms of applicable residual current seasons:

a. April-June-no net movement of mound dredged material (sediment).

b. July-October-very little movement of 13,000 cu m (17,000 cu yd) of sediment to the southwest, mound height reduction was less than 0.15 m (0.5-ft).

c. November-March--appreciable sediment movement of 0.45 million cu m (1.47 million cu yd or 8 percent of the total mound volume) to the northwest, maximum mound height erosion was 0.6 m (2 ft) for the 4.9-m- (16-ft-) high deepwater mound, and 1.8 m (6 ft) for the 2.4-m- (8-ft-) high shallow-water mound. Net aggregate mound movement was about 75 m (250 ft) to the northwest.

LTFATE simulation results for the expanded ODMDS B indicate that the spring and summer seasons produce little sediment transport or mound movement. The winter storm season produces appreciable sediment transport on dredged material mounds at ODMDS B. The largest changes in mound geometry apply to the shallow-water area of the ODMDS where mound height erosion was 1.8 m (6 ft), where the entire mound was initially 2.4 m (8 ft) in some locations. Based on the simulation results, the shallow-water area of expanded ODMDS B had favorable potential for dispersing placed dredged material and reintroducing dredged sediments into the littoral zone.

Results of LTFATE and MDFATE modeling at expanded ODMDS E. Results from the long-term fate simulations for ODMDS E are summarized in terms of applicable residual current seasons as follows:

a. July-October--movement of 122,400 cu m (160,000 cu yd) of sediment of the 0.77 million cu m (1 million cu yd) simulated was to the southwest, mound height erosion 0.6 m (2 ft) for the 1.2-m- (4-ft-) high mound, net aggregate mound movement of 305 m (1,000 ft) toward the southwest.

b. November-June--significant sediment movement of 0.5 million cu m (0.66 million cu yd) of the (0.77 million cu m (1 million cu yd) simulated) to the north, mound height erosion 1.1 m (3.5 ft), net aggregate mound movement 215 m (700 ft) toward the north.

Long-term fate results for expanded ODMDS E clearly indicate that this site is dispersive in terms of transport of dredged material placed on the seabed. Given the amount of sediment transport predicted for 1 year, it appears that 1 million cu yd of dredged material could be dispersed annually at ODMDS E. The direction of sediment transport during the summer is toward the southwest.

A southwest transport direction would disperse placed dredged material back into the navigation channel. This is an unacceptable circumstance. This simulated trend concurs with field experience at ODMDS E. Dredged material is not placed at ODMDS E during early to later summer, due to migration of the material back into the MCR navigation channel. During the winter and spring season, a 1.2-m- (4-ft-) high dredged material mound at ODMDS E would be dispersed toward the north, away from the navigation channel and onto Peacock Spit. This is a highly desirable circumstance, assuming that dispersed dredged material does not reaccumulate in a manner that becomes a hazard to navigation.

RCPWAVE simulations at expanded ODMDS B and E

Changes in wave height at the MCR due to bathymetric changes at the expanded ODMDS (formation of dredged material mounds) were estimated using the RCPWAVE wave simulation model. RCPWAVE is a 2-D numerical model that simulates behavior of waves as they are shoaled, refracted, and diffracted by the bathymetry that the waves pass over and around.

Two MCR bathymetry data sets were assessed using RCPWAVE. The two bathymetry data sets describe the same geographic area. The baseline condition documented the MCR bathymetry before disposal was simulated in the expanded ODMDS. The mounded configuration accounts for 15.3 million cu m (20 million cu yd) of dredged material placed within the expanded ODMDS B and E. For both bathymetry configurations, waves were transformed from offshore through the area of interest. The RCPWAVE simulation was performed for offshore wave directions between 225 deg and 300 deg, and wave periods of 10 and 16 sec.

The increase in wave height (amplification) from the baseline bathymetric condition to the mounded condition was determined by this wave assessment. Amplification of wave height greater than 10 percent over the baseline bathymetric condition was considered unacceptable. Wave amplification results are shown in Figures 68 and 69 for wave periods of 10 and 16 sec, respectively. The results were calculated in terms of (mounded wave height)/(baseline wave height). For both 10 and 16 sec period waves, the 10 percent criterion will be exceeded within the expanded ODMDS B by the mounded bathymetry. Both the deepwater and shallow-water mounds of 4.9 m (16 ft) and 2.4 m (8 ft) high, respectively, within ODMDS B contribute to exceedence of the wave criterion. The 1.2-m- (4-ft-) high mound within ODMDS E does not significantly affect the wave environment at the MCR.

Based on the preceding wave analysis results, it is recommended that 15.3 million cu m (20 million cu yd) of dredged material not be placed (over a 5-year time span) within the expanded boundaries of ODMDS B as initially proposed.

Initial and recommended revised expansions of ODMDS B and E

Initial expansions of ODMDS B and E. To meet the 10 percent wave amplification criterion at ODMDS B, the total volume of dredged material to be placed within the initial expanded configuration shown in Figure 67 must be reduced to 3.8-5.4 million cu m (5-7 million cu yd, or 0.77-1.15 million cu m per year (1-1.5 million cu yd per year) for 5 years. Additionally, the placement of dredged material must be done in such a way as to avoid forming dredged material mounds higher than 1.2 m (4 ft) in the shallow-water area of 15-21 m (50-70 ft) water depth of expanded ODMDS B. This would require thin-layer disposal of dredged material. Disposal vessels would place material while underway to maximize dispersal rather than releasing material at a slow speed (point-dump). Within the deeper area of 27-50 m (90-160 ft) water depth of

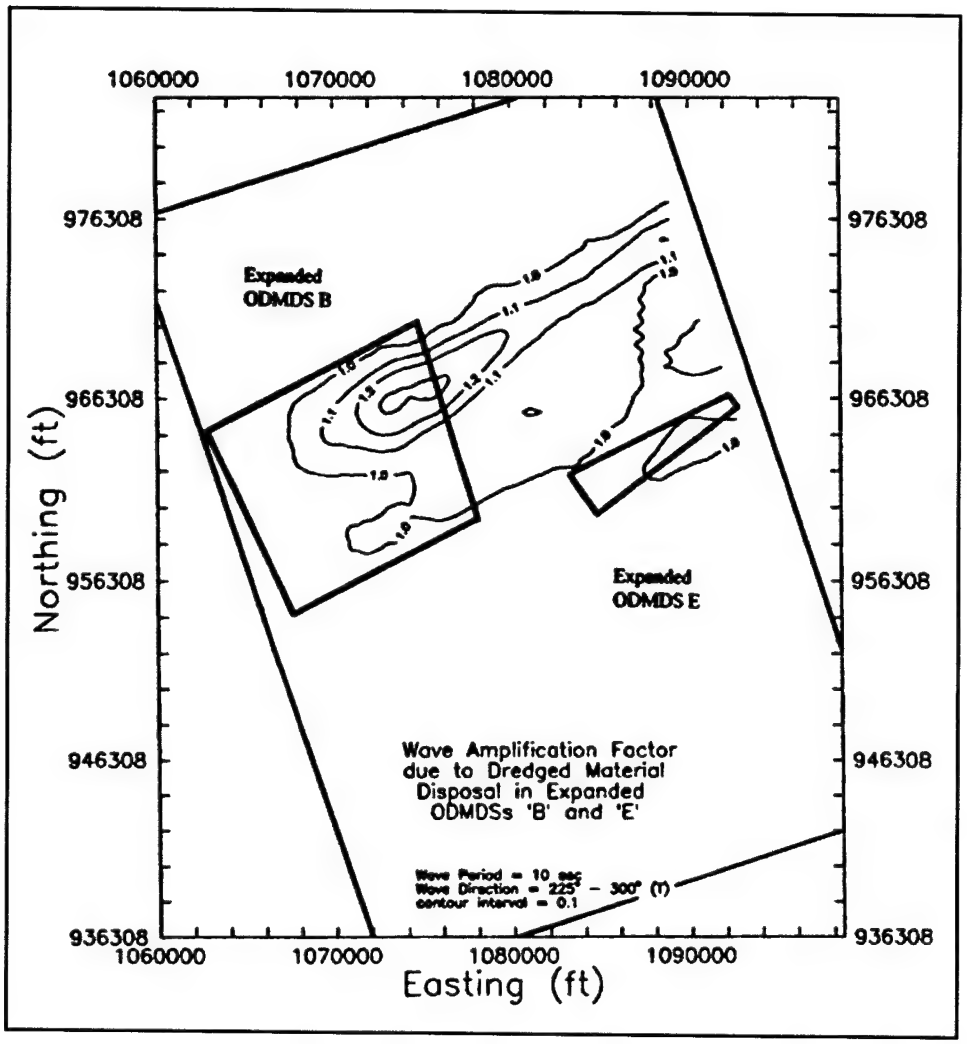

Figure 68. RCPWAVE wave amplification simulations for 10-sec period waves at expanded ODMDS B and E (after USAED, Portland/USEPA 1997)

expanded ODMDS B, formation of dredged material mounds higher than 8 ft should be avoided to prevent exceeding the 10 percent wave criterion.

As initially proposed, utilization of expanded ODMDS E avoids exceedence of the 10 percent wave criterion as long as dredged material mounds are not allowed to exceed 1.2 m (4 ft) in height with respect to the present bathymetry.

The boundaries of expanded ODMS E, as shown in Figure 67, are considered adequate for utilizing ODMDS E in a fully dispersive manner. Dredged material mounds higher than 1.2 m (4 ft) would not be permitted to form within the site. Additionally, expanded ODMDS E would be utilized in a manner that would prevent dredged material volume accumulation greater than 0.77 million cu m (1 million cu yd) from one disposal season to the next (1 year).

Recommended revised expansions of ODMDS B and E. To permit disposal of 15.3 million cu m (20 million cu yd) of dredged material in

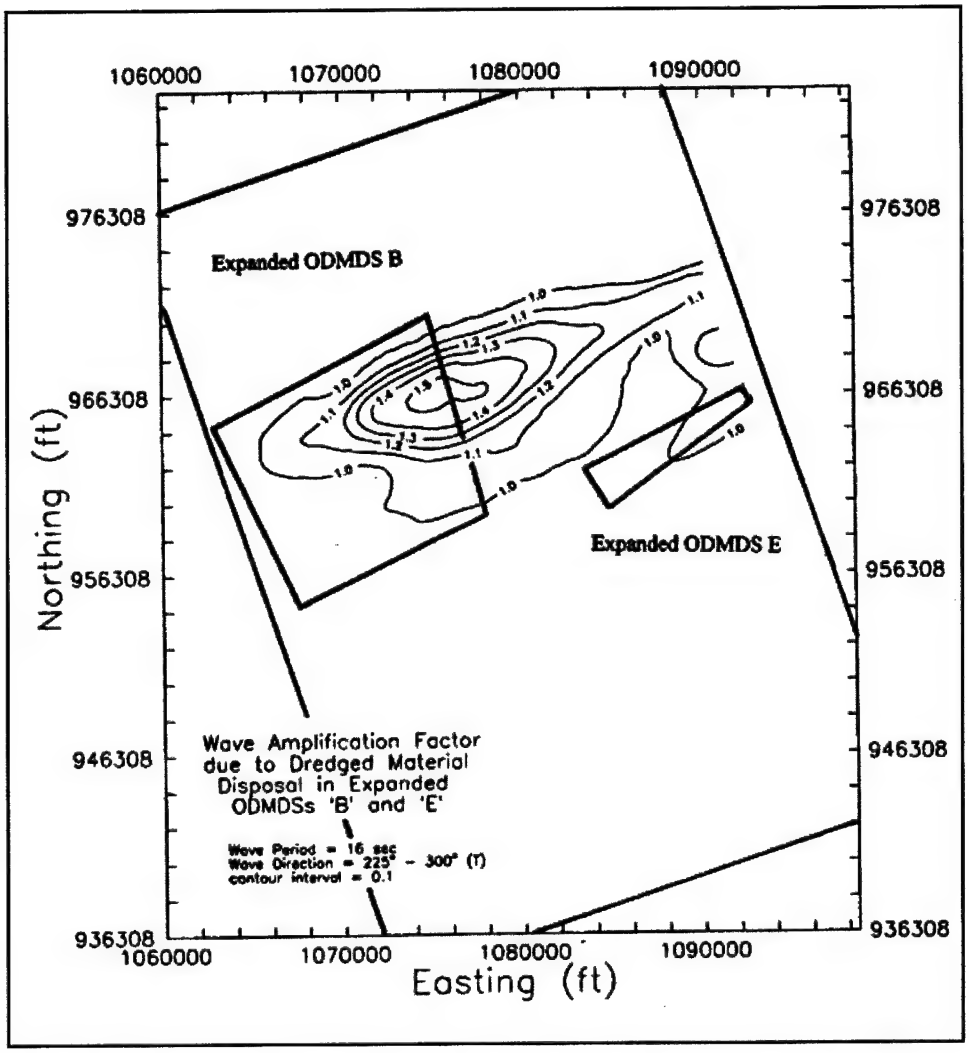

Figure 69. RCPWAVE wave amplification simulations for 16-sec period waves at expanded ODMDS B and E (after USAED, Portland/USEPA 1997)

ODMDS B without negatively affecting the wave environment due to mounding, the site's boundaries must be expanded beyond the initially proposed configuration shown in Figure 67. The optimal configuration for ODMDS B would be to additionally expand the site seaward in the same manner as was initially proposed for the landward expansion. To ease the description of boundary geometry for ODMDS B, the easternmost boundary of this site was straightened. The final revised expanded configuration for both ODMDSs B and E is shown in Figure 70 (revised expanded ODMDS are shown in dashed red lines). The revised expanded ODMDS B would be composed of two distinct zones; (a) an offshore zone situated in water depth 50-67 m (160-220 ft) and (b) a nearshore zone situated in water depth 15-50 m (50-160 ft).

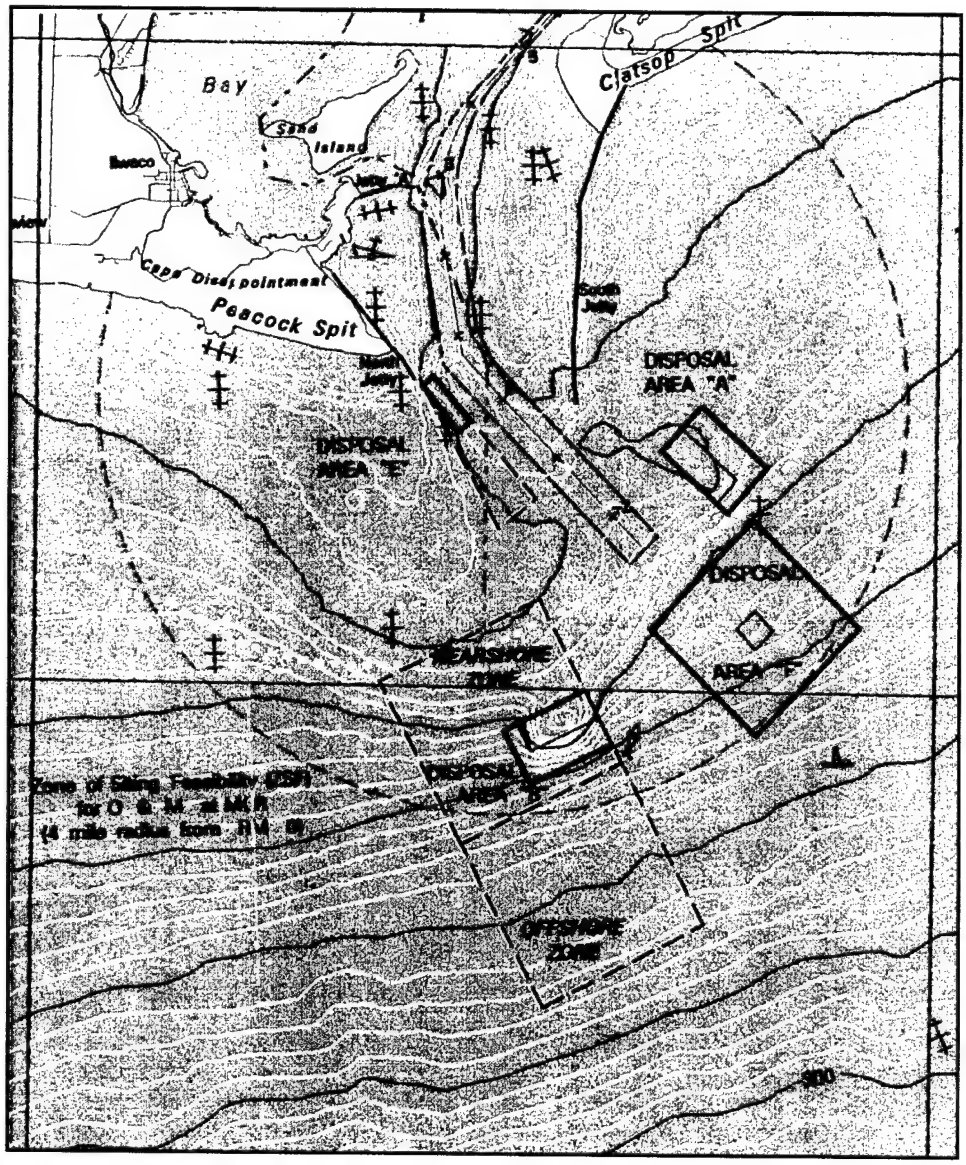

Figure 70. Recommended revised expanded ODMDS B and E (after USAED, Portland/USEPA 1997)

FATE Model Simulations at Expanded ODMDS E (1998 Bathymetry)[1]

Moritz, Kraus, and Siipola (1999) conducted FATE model simulations of dredged material deposited at ODMDS E that is located near the north jetty and adjacent to the navigation channel. They applied the 19 May 1998 bathymetric surveys and the environmental data from Deployment 2 (15 April-24 August 1998) obtained by Oregon State University (Lund et al. 1999). Since one of the governing parameters in an efficient dredging disposal program is minimization of the haul distance for the dredge, disposal sites such as ODMDS E can be very

[1] This section is extracted essentially verbatim from Moritz, Kraus, and Siipola (1999).

advantageous. In contrast to the more oceanward sites, ODMDS E is believed to be current- rather than wave-dominated and has been very dispersive in past disposal operations. The energetic dispersiveness of the site, however, also represented an extreme test of the robustness of the DRP FATE models. This study addressed a predictive 2-month application of the FATE models at ODMDS E using oceanographic data that were collected at the same time as the dredge disposal operation.

Physical environment

ODMDS E is located just oceanward of the jetty entrance, approximately 400 m (1,310 ft) north of the navigation channel. Figure 71 illustrates the pre-disposal bathymetry at ODMDS E as documented by the 19 May 1998 bathymetric survey. Elevations across the site range from -20 m (-65 ft) mllw at the southern boundary to -14 m (-45 ft) mllw at the northern boundary. Portions of the site are steeply sloping with representative gradients of 0.04. The instrumented platform was located at the seaward boundary of Site E.

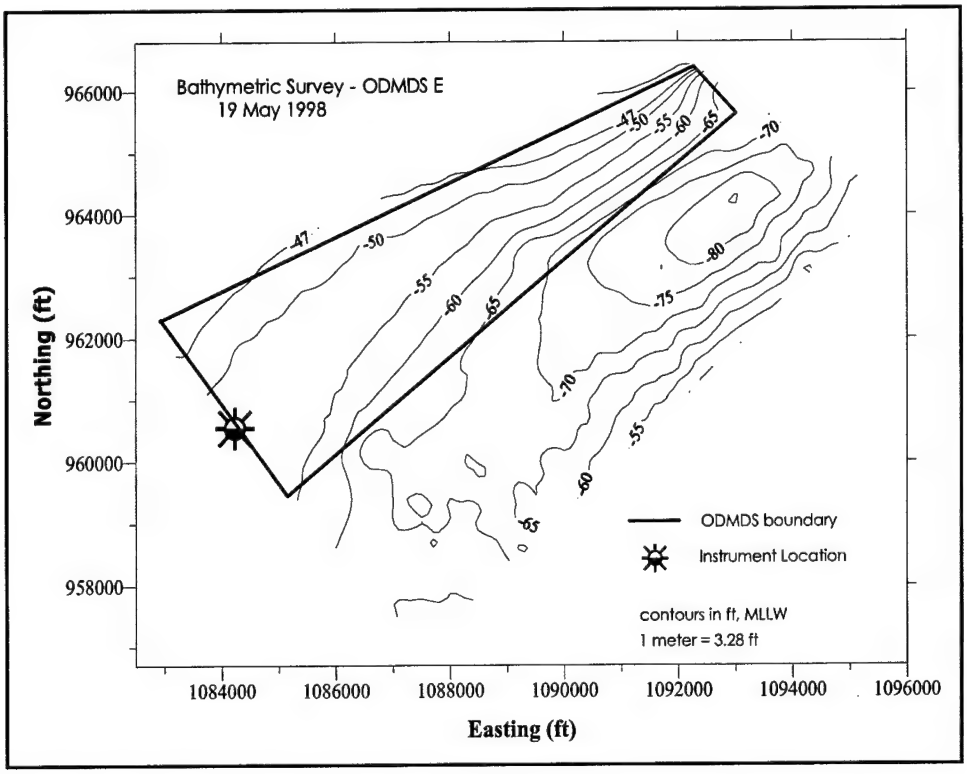

Figure 71. Pre-1998 disposal bathymetry for FATE simulations at ODMDS E (after Moritz, Kraus, and Siipola 1999)

Near the MCR, estuarine circulation exerts its influence, tending to draw near bottom marine waters into the estuary while discharging low salinity waters at the surface. Within the estuary, ebb flow in the northern portion of the river entrance is seaward, both at the surface and seabed. During flood tide, saltwater tends to intrude along the southern side of the river channel. Consequently,

sediments tend to enter the estuary with the marine waters through the southern portion of the mouth during the flood tide. Sediments tend to exit the entrance through the northern part of the channel and are carried offshore during the ebb-tidal flow (Sternberg et al. 1979). ODMDS E is located on the north side of the entrance to the Columbia River estuary in the primary area of seaward transport. This makes this site attractive from a sediment dispersion perspective.

The time-varying environmental data that are used in the FATE models are wave height, wave period, and depth-averaged current velocity. Waves were measured at ODMDS E from 15 April 1998 to 24 August 1998 during the summer instrument deployment at the MCR, and are shown in Figure 72. Wave

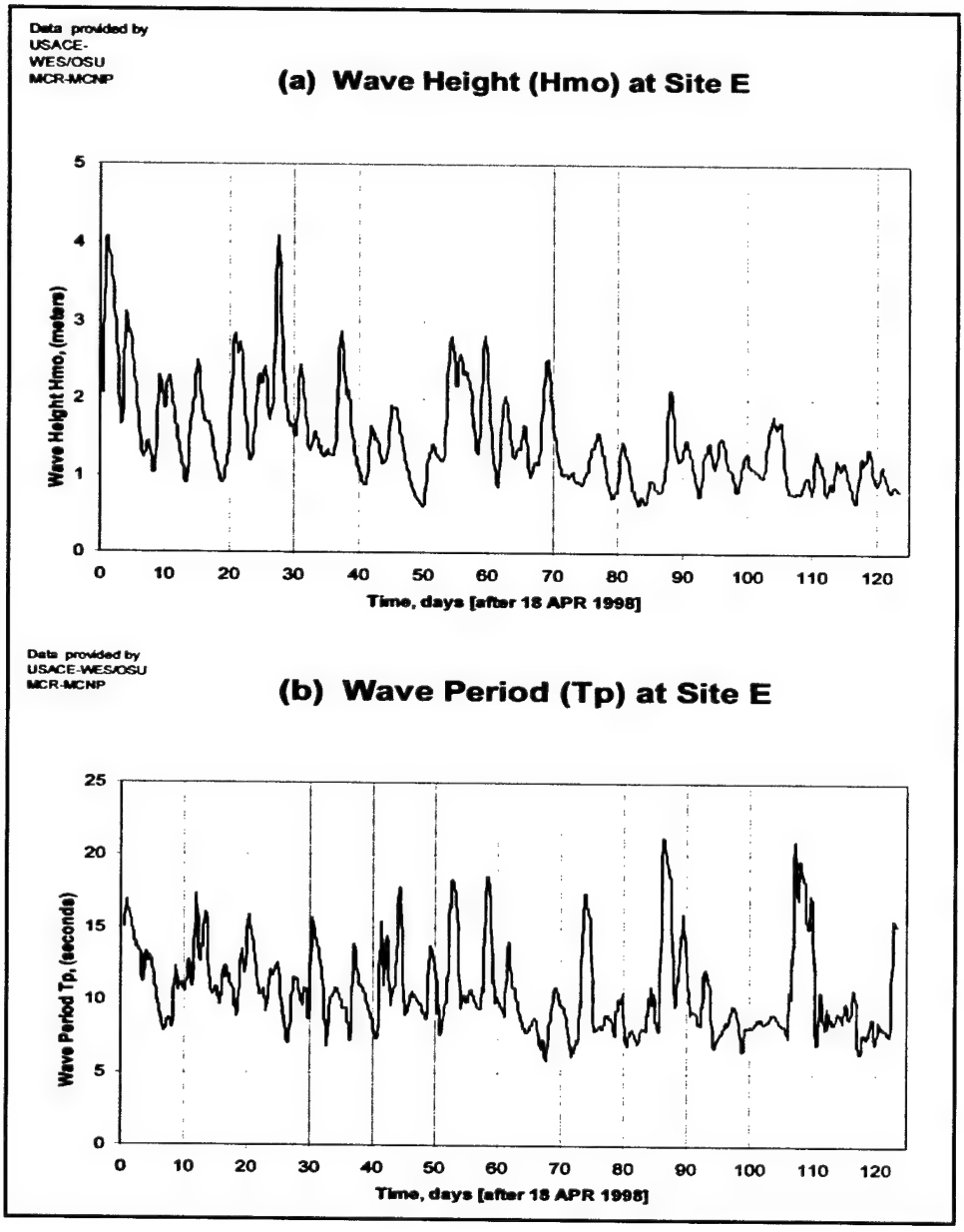

Figure 72. Wave data measurements during 1998 disposal operations (after Moritz, Kraus, and Siipola 1999)

heights during this time ranged from 0.55 to 4.41 m (1.8 to 14.5 ft) with an average height of 1.48 m (4.9 ft). Wave periods ranged from a low of 4.8 sec to a high of 23.3 sec with an average period of 10.7 sec. During the time of dredge disposal at ODMDS E and for the time of sediment transport simulation, the average wave height and wave period were 1.25 m (4.1 ft) and 10.2 sec, respectively.

Measurements of the current throughout the water column were made through the combination of an ADP and an ADV on each of the four data acquisition tripods used in the MCNP monitoring study. The ADV provided current velocities at an approximate depth of 0.45 m (1.5 ft) above the seabed. The ADP collected current velocities representative of 1-m (3.3-ft) bins throughout the water column to a depth of 17.7 m (58 ft) above the seabed. Figure 73 provides the average, maximum, and minimum current velocities throughout the water column for the east/west and the north/south components. Figure 74 illustrates the results from three of the bins at depths above the seabed of (a) 13.7 m (45 ft), (b) 7.7 m (25 ft), and (c) 3 m (10 ft). The very strong east-west component of the velocity near the water surface in this environment is illustrated with the east/west component ranging from a maximum easterly component of +68 cm per sec (+2.2 ft per sec) to a maximum westerly component of -341 cm per sec (-11.2 ft per sec) at 13.7 m (45 ft).

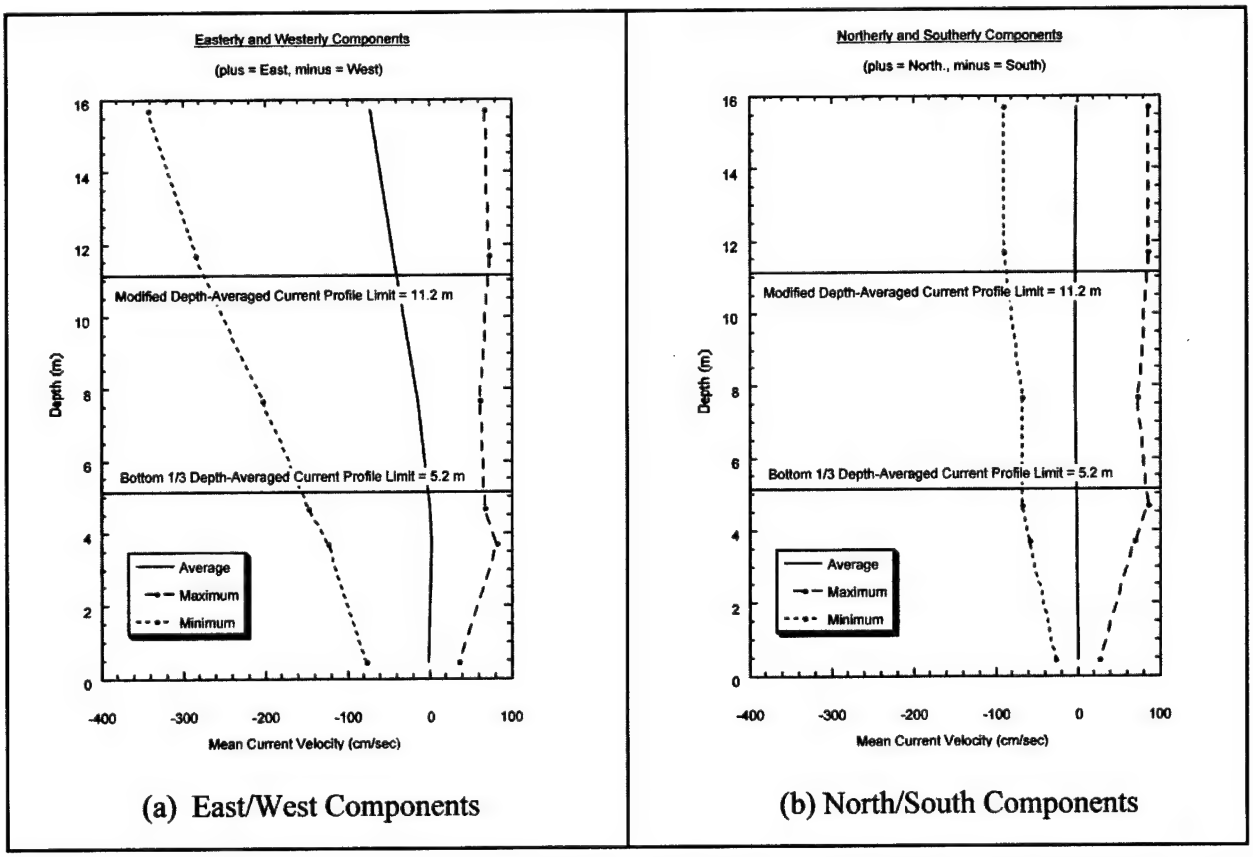

Figure 73. ADP and ADV current velocities through water column during 1998 disposal operations (after Moritz, Kraus, and Siipola 1999)

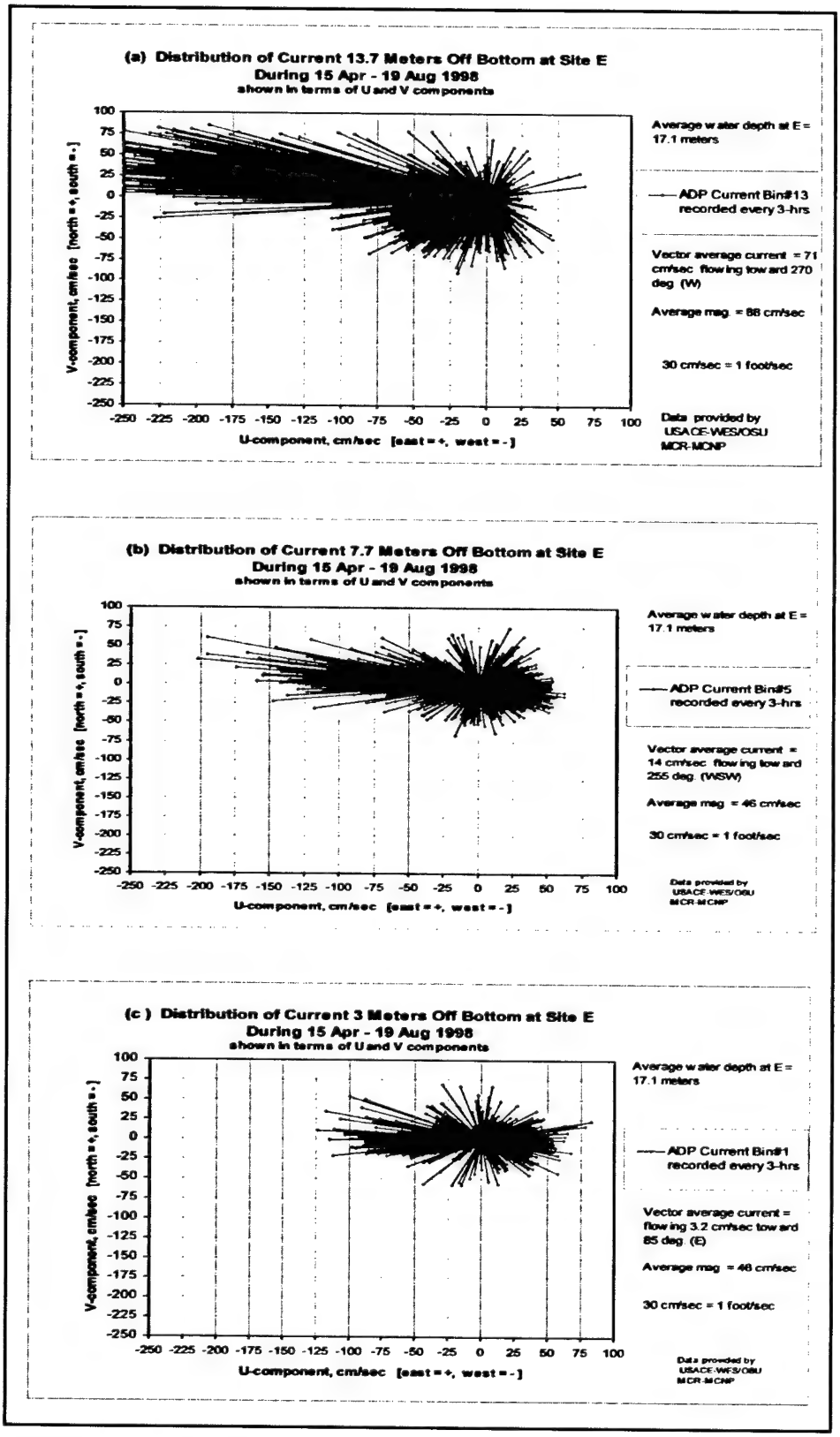

Figure 74. ADP measured current velocities at three locations in water column during 1998 disposal operations (after Moritz, Kraus, and Siipola 1999)

Sediment transport issues

The collection of critical environmental data coincident with a dredged material disposal operation at ODMDS E provided an opportunity to evaluate the robustness of the FATE model application in an energetic current-dominated environment. Key questions raised prior to the application were as follows:

a. Does the magnitude of the currents experienced preclude use of the FATE models?

b. Which physical processes have the greatest impact on short- and long-term sediment transport? Are these processes being correctly simulated in the FATE models?

c. Is some other characteristic current profile more useful in this environment than a depth-averaged current profile, which is typically used in the MDFATE and LTFATE models?

d. Is sediment accumulation and mounding being correctly represented?

e. Is the assumption of no ambient sediment movement into the site valid for an environment where high riverine discharges may generate significant sediment transport? Does the assumption of no-change for the ambient bathymetry impact model results?

f. Do model parameters particularly sensitive to high current velocities (i.e., stripping, critical shear stress, turbulent diffusion parameter, collapse entrainment parameter) need to be reevaluated for this type of environment?

Dredging disposal operations

The disposal site shown in Figure 75 is a trapezoidal area 3,050 m (10,000 ft) long by maximum width of 1,100 m (3,600 ft). The long axis of the site is oriented parallel to the navigation channel at a distance of 400 m (1,310 ft) from the channel. The dredging disposal operation modeled in this analysis at ODMDS E was carried out from 13 June to 11 August 1998. Fine-to-medium sand (D_{50} = 0.15 to 0.25 mm) was dredged from the MCR during two separate dredging operations and transported approximately 1.6 km (1 mile) to ODMDS E.

During the study period, two dredges placed material at ODMDS E. The U.S. Government dredge *Essayons* (multiple bottom-door hopper dredge) placed 1.49 million cu m (1.9 million cu yd) in the western half of ODMDS E from 13 June through 23 July. The contractor dredge *Newport* (split-hull dredge) placed 0.77 million cu m (1 million cu yd) of material in the eastern half of ODMDS E from 11 July to 11 August. The total volume placed at ODMDS E during this period was 2.26 million cu m (3 million cu yd). To maintain safe distance between the two hopper dredges and to avoid overlapping disposal, the middle part of the site was not used.

To avert excessive mounding of placed dredged material within ODMDS E, material was distributed uniformly throughout the site in a series of grid-cells to control the release point for each disposal event. The goal was to prevent

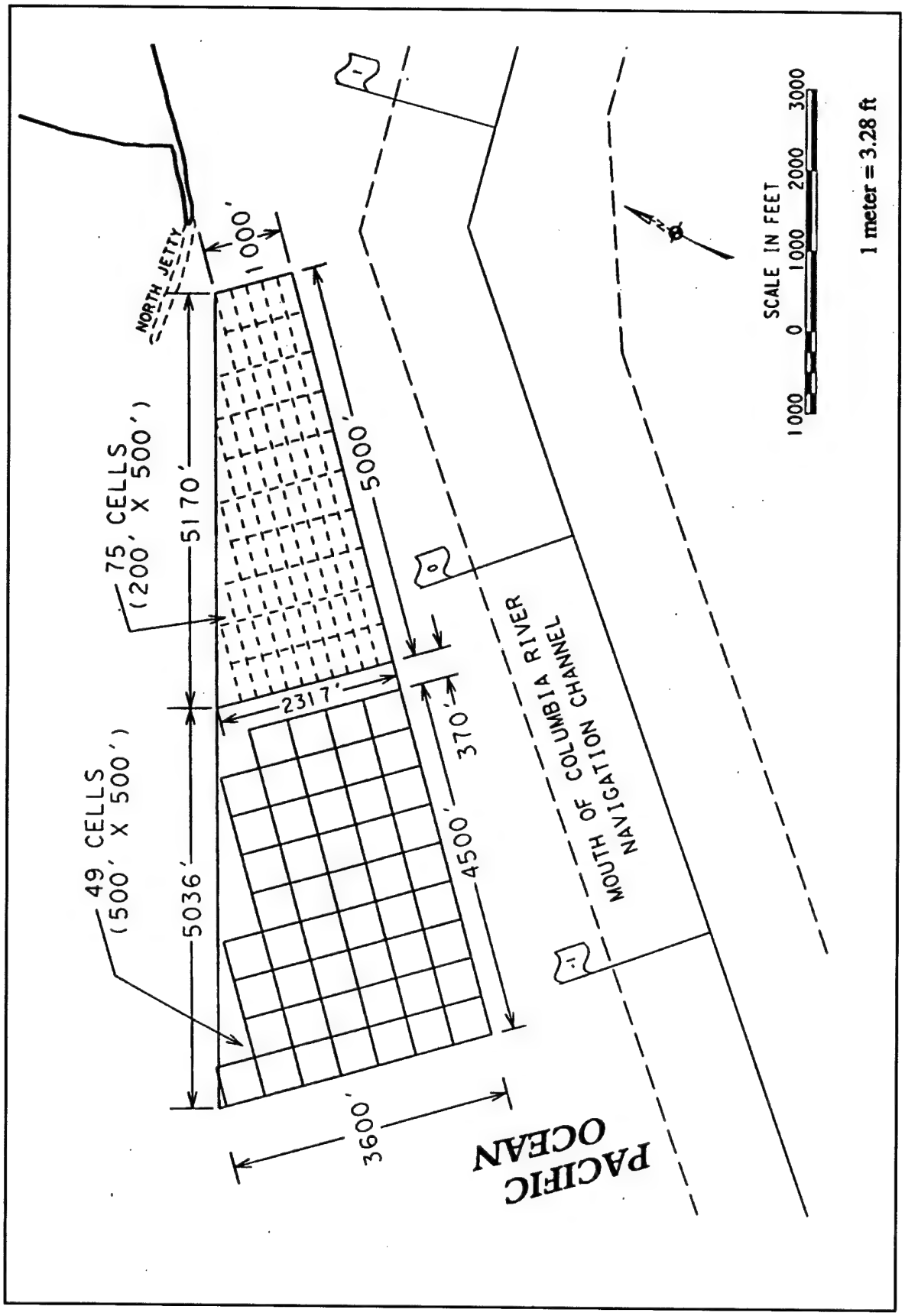

Figure 75. ODMDS E disposal site layout (after Moritz, Kraus, and Siipola 1999)

mound-induced wave amplification at or near the site by limiting the vertical accumulation of placed dredged material to 1.8 m (5.9 ft), with respect to the baseline bathymetry of ODMDS E. Figure 75 shows the distribution of grid cells used to guide the placement of dredged material within ODMDS E during 1998. The 1998 disposal operation, which was simulated by the FATE models, placed 381 loads by the *Essayons* in 49 152-m × 152-m (500-ft × 500-ft) cells and 362 loads by the *Newport* in 75 152-m × 61-m (500-ft × 200-ft) cells.

A key aspect of the proactive cell-management approach to disposal is the capability to model the disposal sequence both for verification of that disposal activity and for prediction and management of future disposal sequence planning. This requires that the operating dredges record their beginning and ending coordinates as well as time of dumping for each dump event.

Input parameters to FATE models

The disposal operation was divided into two sections; (a) *Essayons* disposal cycle (June through July) and (b) *Newport* disposal cycle (July through August). Each disposal operation was simulated using both STFATE, LTFATE, and MDFATE during the disposal. In addition, LTFATE processes were applied to the *Essayons*-placed material during the *Newport* disposal cycle.

The 19 May 1998 bathymetric survey served as the predisposal baseline for the *Essayons* disposal cycle. The output bathymetry from the *Essayons* model application served as the predisposal baseline for the *Newport* disposal cycle. The difference plot between the 19 May and 11 August 1998 surveys was used to compare with the full disposal operation modeling results. The dredged material parameters used in the FATE modeling included:

a. Dredged material type = fine sand, medium sand.

b. D_{50} = material dredged from the MCR = 0.15 mm, 0.25 mm.

c. Fines content (D<0.0625 mm) = 4 percent (silt).

d. Specific gravity of dredged material solids = 2.70.

e. C_s (disposal) = concentration of solids by volume in the disposal vessel = 0.485.

f. ed = depositional void ratio = 1.05.

g. φ_s = subaqueous shearing angle = 2.0 deg.

h. φ_{ps} = subaqueous postshearing angle = 1.9 deg.

i. Critical shear stress = 1.4 to 96 Pa (0.03 to 2.0 lb per ft^2).

Disposal coordinates were supplied to the model by separate data files for each disposal operation. Files included beginning and ending coordinates for each dump. The vessel speed during disposal, and the duration of placement, were calculated from the disposal coordinate file. Wave and current data input to the model in 3-hr intervals were obtained by the data acquisition instruments placed at the seaward end of ODMDS E.

Modeling approach

Initially, the FATE models were run in the same manner as they would in an open-ocean environment. All input data were consistent with an open-ocean application, including full depth-averaged currents for the entire water column. A modified value of 20 percent stripping of the material was applied in the STFATE application to represent losses of material through the water column. The time-step was reduced from 100 sec to 50 sec to accommodate the shallow-water depths with respect to the grid size at the site.

Evaluation of the FATE model performance was based on the following factors in comparison with the actual bathymetric change documented in the difference plot between the 19 May and 11 August 1998 survey:

a. Areal extent of disposal footprint.

b. Approximate location of centroid of disposal feature.

c. Maximum height of disposal feature.

d. Total volume of material on seabed.

The maximum areal extent of the disposal footprint is important with respect to the accurate placement of material within the ODMDS-designated boundaries. The location of the centroid and the distribution of the material throughout the site provide information on the interaction of the disposal activity with the environmental forcing in the area and the correct simulation of those processes. The maximum height of the disposal feature is an important parameter because the ODMDS design limits the maximum allowable feature height so as not to impact navigation in the area. Total volume of material on the seabed provides a measure of the correct modeling of the dispersion of material in a highly energetic site.

The actual change measured in the disposal site from 19 May to 11 August (Figure 76a) is compared with the results of the FATE modeling including both the *Essayons* and *Newport* disposal activities using the full depth-averaged current profile (Figure 76b). The areal extent and location of the footprint of the disposal operation for this application of the FATE models were found to differ significantly from the measured bathymetric change. The *Essayons* disposal material in particular was simulated as moving outside of the ODMDS E boundaries. The maximum mound height for the *Essayons* disposal was simulated to be 2.4 m (8 ft) in comparison to the measured height of 1.8 m (6 ft). The *Newport* disposal also exhibited a fairly dispersed disposal footprint and, in this case, the simulated mound height of predominantly 0.6 m (2 ft) was somewhat less than the measured mound height of 0.6 m (4 ft).

Because of the strong currents in the upper part of the water column (Figures 73 and 74), it was determined that application of the FATE models in a current-dominated environment such as ODMDS E may require modification of the representative current profile. The results of the full depth-averaged application seem to indicate that the strong velocities in the upper one-third of the water column were exerting too much influence on ultimate dredged material placement on the seabed. An assessment was made of the appropriate reduced

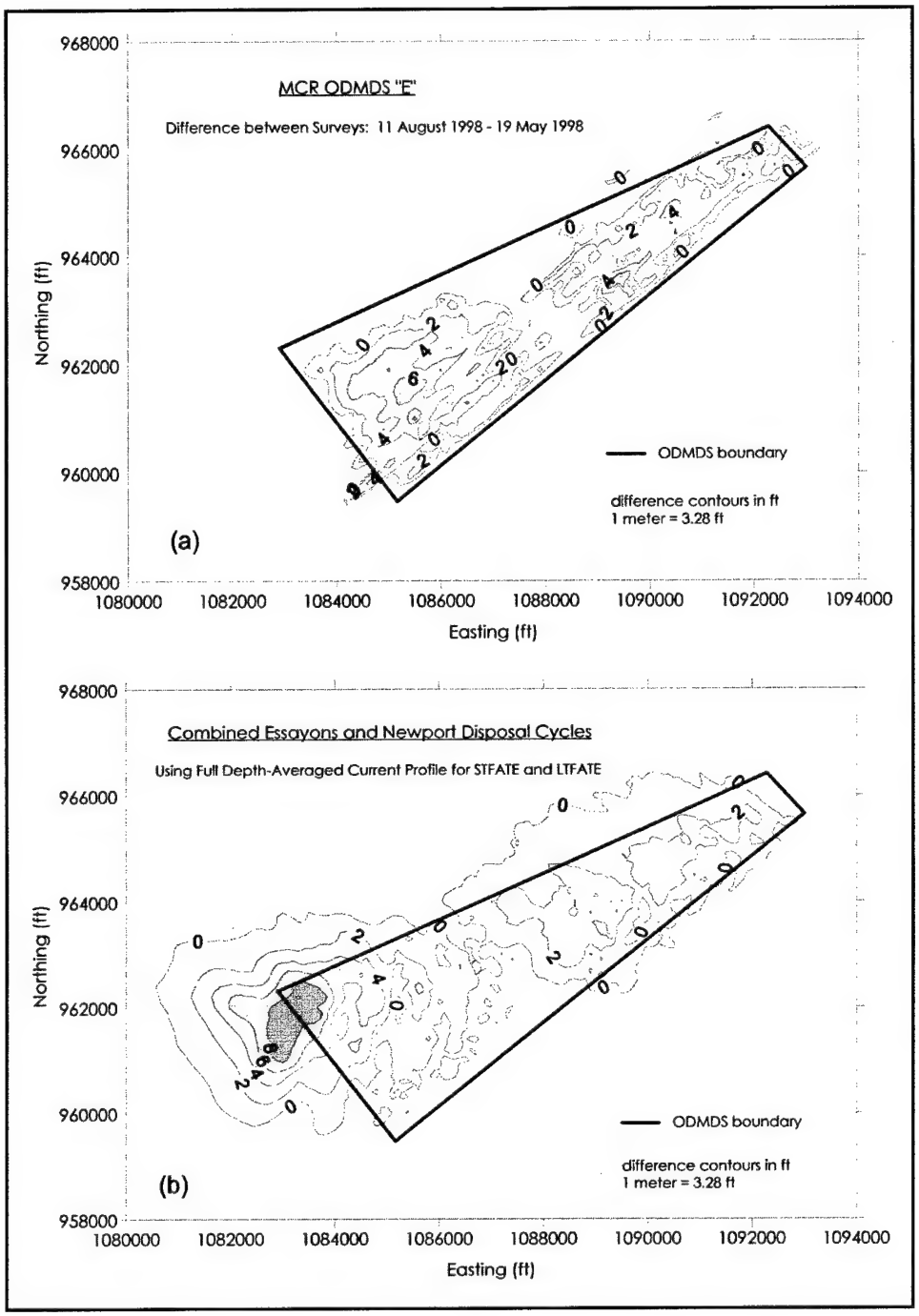

Figure 76. FATE modeling results using full depth-averaged current profile (after Moritz, Kraus, and Siipola 1999)

current profile to develop for this site. STFATE models the sediment dispersion and convection as the material falls from the dredge to the seabed. The average of the loaded/unloaded drafts of the *Essayons* and the *Newport* is 5.5 m (18 ft). Depths in ODMDS E range from 14.3 to 19.8 m (47 to 65 ft), with an average depth of 17.1 m (56 ft). The average water column depth below the average of the loaded/unloaded drafts of the two dredges was calculated to be approximately

11.6 m (38 ft). The highest ADP bin that was completely included in that depth was bin 8 at a median depth of 10.7 m (35 ft). That bin represents a 1-m (3.3-ft) vertical depth from 10.2 to 11.2 m (33.4 to 36.7 ft). Therefore, the modified depth-averaged current profile utilized bins 1 through 8, and averaged the current over a total depth of 11.2 m (36.7 ft), as shown in Figure 73.

The FATE models were rerun using the modified depth-averaged current profile with all other parameters held the same. The results for that application are shown in Figure 77a. When Figure 77a is compared to Figure 76a, it is seen that both the areal footprint and centroid of the overall disposal are better simulated after removing the strong velocities of the top portion of the water column. The mound height for the *Essayons* disposal remained approximately the same at 2.4 m (8 ft) whereas the *Newport* disposal mound height better simulated the 1.2 m (4 ft) mounds of the actual bathymetric change.

The final FATE run incorporated two modifications. The first modification adjusted the critical shear stress at which material would not be deposited on the seabed. Because this parameter has the potential to significantly impact total volume placed on the seabed and the majority of the operational checks require a conservative estimate of disposal material placement (including maximum mound height and areal footprint coverage), the critical shear stress can be a fairly sensitive parameter. For this reason, the critical shear stress applied in initial runs of the disposal sequence was 96 Pa (2.0 lb per ft^2). To more correctly simulate the high-energy environment and the apparent reduction in total material reaching the seabed, the critical shear stresses used were 1.4 to 1.9 Pa (0.03 to 0.04 lb per ft^2).

The second modification to the final FATE model run was the introduction of a separate depth-averaged current profile for the LTFATE portion of the application. The modified depth-averaged profile was utilized for the STFATE portion of the application; however, again the stratification throughout the water column of the current velocities was expected to influence the LTFATE results adversely. In Figure 73, it can be noted that at approximately 5 m (16 ft) above the seabed, the current profile changes in magnitude significantly. The LTFATE depth-averaged profile was developed using ADP data from bins 1 and 2 to cover a depth of 5.2 m (17 ft), as illustrated in Figure 73. Results from the final FATE run incorporating the two modifications are shown in Figure 77b. This run produced the best results for all runs evaluated. The areal footprints for both disposal cycles are well simulated, and the centroids of the disposal areas match the surveyed difference. Additionally, the magnitude of the mound heights for both areas at 1.8 m (6 ft) and 1.2 m (4 ft) reflect the measured bathymetric change.

FATE model comparison to measured data

Bathymetric response data were used to determine the accumulation of dredged material on the seabed during the dredging operation. Table 10 summarizes the total volumes placed on the seabed during the FATE model simulations of ODMDS E. Monitoring results indicate that only 62 percent of all dredged material placed at ODMDS E during the disposal operation accumulated on the seabed.

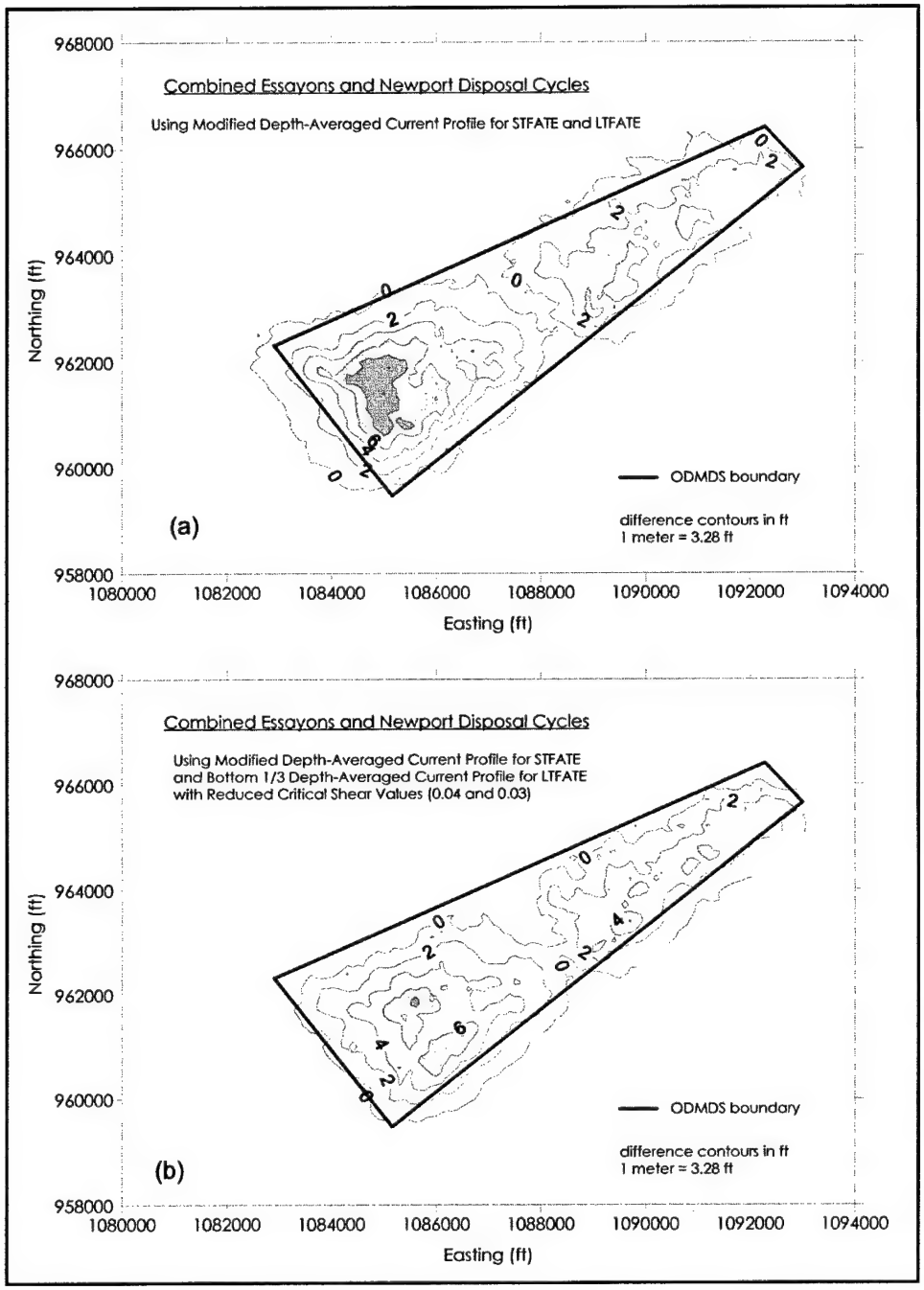

Figure 77. (a) Modified depth-averaged current; (b) Modified depth-averaged and bottom one-third depth-averaged current profiles and reduced critical shear stress (after Moritz, Kraus, and Siipola 1999)

Conclusions

The DRP FATE models (STFATE, LTFATE, and MDFATE) were all found to be applicable at a high energy, current-dominated site. To correctly simulate the sediment deposition on the seabed, the current profile for both the STFATE and LTFATE model applications required modifications from the full

Table 10
FATE Model Simulation of Material Deposited on Seabed (million cu m)

Method of Simulation	*Essayons* Disposal	*Newport* Disposal
Full Depth-Averaged Current Profile for STFATE and LTFATE	1.43	0.69
Modified Depth-Averaged Current Profile for STFATE and LTFATE	1.46	0.73
Modified Depth-Averaged Current Profile for STFATE and Bottom 1/3 Depth-Averaged Current Profile for LTFATE with Reduced Critical Shear Stress (0.04 and 0.03)	1.14	0.58
Actual Volume *Measured* on Seabed	1.03	0.38
Actual Volume *Placed* on Seabed	1.49	0.70

depth-averaged current profile typically used. Although it was possible to simulate the general footprint and centroid of sediment distribution, the total volume reaching the seabed was simulated to be higher than actual measurements indicated. Further research into model parameters and input data that control dispersion and final deposition of material on the seabed is recommended. Those parameters should include percent stripping, critical shear stress, turbulent diffusion parameter, and the collapse entrainment parameter.

6 Analysis of Sediment Transport Processes at ODMDS B, E, and Proposed M[1]

Objectives

Predictive techniques for determining environmental conditions and sediment transport processes under both waves and currents have been developed to assess the movement of disposed material at the MCR ODMDS B and E (Figures 3 and 78). (The location of instrumentation Sites E, B1 and B2 on a profile across the MCR ebb-tidal shoal is shown in Figure 4.) These techniques assist in determining crucial information for the management of dredged materials at navigation channels and harbors, such as mound dispersal, channel infilling, and protective cap erosion. The potential transport climate at a proposed ODMDS M was also analyzed. Processes controlling the transport of sands at ODMDS are complex, and potentially include widely variable environmental conditions and both temporal and spatial variations in the characteristics of sediments.

Three methods of estimating sediment transport by waves and currents (van Rijn, Wikramanayake and Madsen, and Ackers and White methods, to be described later) were applied at MCR ODMDS locations to evaluate the capabilities of available sediment modeling technologies. As an extension of these analyses, an estimate of 12 years of wave and current conditions was developed at each site for determining longer-term transport distributions and trends. Methods verified with the MCR data can be applied with greater confidence to other ODMDS that have similar sediment characteristics and environmental conditions.

ODMDS B and E exhibit significant differences in dispersion of dredged material. Understanding the sediment transport processes that influence these differences is important in developing management strategies for future disposal at the two sites. Sediments dredged from the MCR have been placed at both sites for decades. Even though the sediment characteristics of dredged material are similar, the long-term behavior of sediments at each site has been considerably

[1] Chapter 6 was written by Joseph Z. Gailani and S. Jarrell Smith, U.S. Army Engineer Research and Development Center, Vicksburg, MS (Gailani and Smith, op. cit., p. 101).

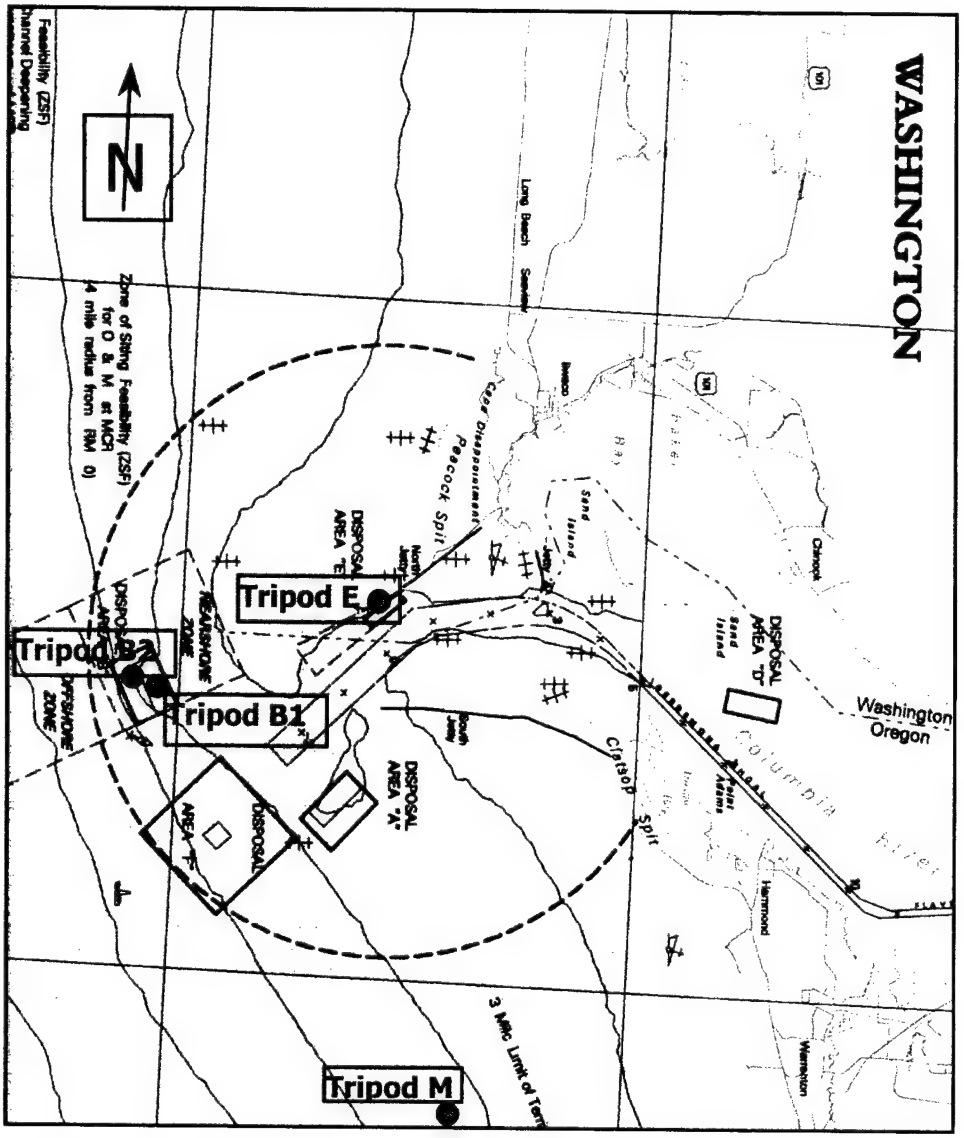

Figure 78. MCR tripod sensor locations at ODMDS B (Sites B1 and B2), ODMDS E, and proposed ODMDS at Site M (after Gailani and Smith, op. cit., p. 101)

different. Bathymetric surveys at ODMDS B indicated the location to be moderately dispersive, and that sediment accumulation occurred during greater than 70 years of disposal. During periods without sediment disposal at the site, bathymetric surveys indicated that the top of the mound at ODMDS B behaved in a dispersive manner. ODMDS E is highly dispersive with little or no disposed sediment remaining at the site on an annual basis. Physical processes that cause the two sites to behave differently have been identified. Longer- term environmental conditions were developed at each site to estimate the sediment transport climate.

Prior to the present study, near-bottom sediment transport conditions and processes had not been measured at the disposal sites. Previous field studies of conditions at ODMDS B and E included annual bathymetric surveys since 1981,

analysis of the wave climate, and local current measurements (USAED, Portland, 1998). No data were available on the short-term sediment transport processes and their association with environmental conditions such as tidal currents, wind-generated currents, and wave action. The recent data collected at the ODMDS (described in Chapter 4, "Field Data Collection and Analysis") provides a detailed data set for near-bed sediment transport processes and the conditions that drive this transport. Data were collected at high frequency, which permits description of the transport processes on time scales ranging from individual waves to several months. These data will assist not only in defining the transport climate, but also in analyzing and developing tools to predict transport processes under a wide range of conditions.

Chapter 6 is composed of five sections. In the first section ("Analysis of Measurements"), the tripod data are analyzed, and a description of the measured data and general interpretation of environmental conditions and resulting transport processes are developed over a range of time scales for Site B1 and ODMDS E. In the second section ("Sediment Transport Methods"), predictive methods are introduced, calibrated, and verified with near-bottom measurements for Site B1 and ODMDS E. The third section ("Modeling Sediment Transport at ODMDS") describes the application of historical measurements and large-domain wave and circulation models to define long-term wave and current climates for Site B1 and ODMDS E. Section four ("Sediment Transport Climate") describes the development of sediment transport climates from the environmental climate at Site B1 and ODMDS E. Section five ("Analysis of Site M") compares waves, currents, and suspended sediments at Sites B2 and M.

Analysis of Measurements

Measurements of suspended sediment concentration, waves, and currents were collected to better understand environmental conditions and sediment transport processes at the ODMDS, and to assist in verification of the numerical methods of estimating sediment transport. Tripod-mounted sensors were deployed during the periods 19 August through 09 October 1997, 15 April through 24 August 1998, and 27 October 1998 through 01 March 1999.

Environmental conditions during data collection

Observations of sediment transport during the monitoring period were compared to results from numerical methods of estimating sediment transport in an effort to verify present and recently developed methods. The three data-collection deployments include all seasons at the MCR, but cannot represent annual variability in seasonal conditions. General observations of the meteorological conditions along the Pacific Northwest coast suggest that significant variation exists in the hydrodynamic conditions, both seasonally and annually. Therefore, to assess the longer-term climate of sediment transport, environmental conditions and resulting sediment transport for the monitoring period are presented in light of longer-term environmental measurements available from offshore buoys.

Deployment 1 (19 August – 09 October 1997). The average wave heights (H_{mo}) at Site B1 and ODMDS E during Deployment 1 were 1.45 m (4.8 ft) and 1.57 m (5.1 ft), respectively (Table 11).

Table 11
Wave Conditions, Deployment 1

Site	H_{mo}, m	T_p, sec	θ_p, deg
B1	1.45	10.4	256
E	1.57	10.7	254
44029	1.66	10.4	270
44029_12*	1.49	9.5	266

* 12-year average for 19 August – 09 October.

Average wave heights at the NDBC buoy 46029 during Deployment 1 were 1.66 m (5.4 ft), slightly larger than the 12-year average of 1.49 m (4.9 ft) for the calendar dates of Deployment 1 (19 August – 09 October). A frequency analysis of wave heights also indicated a greater frequency of occurrence for wave heights greater than 2.0 m (6.6 ft). Wave periods at the buoy were on average 1 sec longer than the 12-year average for the dates of Deployment 1. No significant differences are noted in the average wave direction, but comparison of the angular distribution of incident waves indicates that a significantly greater proportion of waves approach from the NNW octant than for the 12-year average for the calendar dates of Deployment 1. A frequency analysis of wind data collected at the buoy indicated that a greater frequency of higher wind speeds occurred during Deployment 1 than for the 12-year record of winds recorded during the dates of Deployment 1. Not only were higher winds more frequent than average during Deployment 1, but the distribution of wind energy was significantly more concentrated from the south than indicated by the 12-year distribution. The greater distribution of wind energy from the south may have contributed to increased wind-generated currents to the north during Deployment 1. Comparisons of the distribution of wave height, wave period, wave direction, wind speed, wind direction and wind power are presented in Chapter 4 ("Analysis of Collected Data").

Deployment 2 (15 April – 24 August 1998). A summary of the Deployment 2 statistics at Site B1, ODMDS E, the NDBC Buoy 46029, and a 12-year summary of waves at the NDBC buoy for the calendar dates of Deployment 2 (15 April – 24 August) are compared in Table 12.

Table 12
Wave Conditions, Deployment 2

Site	H_{mo}, m	T_p, sec	θ_p, deg
B1	1.65	11.8	276
E	1.77	11.2	259
44029	1.97	10.0	284
44029_12*	1.84	10.2	262

* 12-year average for 15 April – 24 August.

Mean wave height at the buoy during Deployment 2 is slightly higher than the 12-year average wave height for the same calendar dates. A frequency analysis indicated an increased frequency of occurrence for wave heights greater than 1.5 m (4.9 ft) during Deployment 2 compared to the 12-year record. The distribution of wave periods is consistent with the 12-year distribution, but the distribution of wave direction indicated that a greater frequency of waves approached from the WNW octant during Deployment 2. Frequency distributions of wind speed, wind direction, and wind power from Deployment 2 are consistent with those of the 12-year data record.

Deployment 3 (27 November 1998 – 01 March 1999). At the time of this writing, tripods at Site B1 and ODMDS E had not been recovered from Deployment 3. However, data collected at tripods B2 and M, and the NDBC

Buoy 46029, indicated that the third deployment period was much more energetic than normal. Distributions of wave period and wave directions at NDBC Buoy 46029 do not differ significantly from the 12-year distributions, but the distribution of wave heights during the period of Deployment 3 are significantly greater than the 12-year distributions (27 November – 01 March). Comparison of wave height distributions indicated that 50 percent of waves during Deployment 3 were greater than 4.0 m compared to 19 percent for the same calendar dates for the period from 1987-1999. A summary of conditions at the NDBC Buoy 46029 is presented in Table 13.

Table 13
Wave Conditions, Deployment 3

Site	H_{mo}, m	T_p, sec	θ_p, deg
B1	--	--	--
E	--	--	--
44029	3.99	12.7	
44029_12*	2.87	12.2	

* 12-year average for 27 November – 01 March.

Suspended sediment analysis

The wave, current, and suspended sediment concentration data collected during the three deployments at the MCR presents an opportunity to better understand the behavior of sand, and to verify numerical methods of estimating sand transport with combined waves and currents. Observations of sand suspension and transport at ODMDS B and E are presented with comparisons to numerical estimates of sand transport.

Prior to analysis of the measured data and verification of the sediment transport estimation methods, quality control checks were performed on the field data. All data with exception of the OBS data required little supplemental processing. The OBS records the level of emitted radiation reflected back to the instrument, regardless of the source of reflection (fine sediments, suspended organic material, aquatic life, etc.). To extract the portion of the reflected signal contributed by sands, a data processing procedure was developed and applied to the sampled data.

Deployment 1 (19 August – 09 October 1997). The time series of measurements from Site B1 and ODMDS E are presented in Figure 79. Wave conditions during the early portions of the deployment were relatively calm, being on the order of wave heights of 1-2 m (3.3-6.6 ft), but storms began to occur in mid-September. Storm passages were evident in the record of wave conditions (26 August, 16 September, and 19 September). Measurements at ODMDS E continued into early October and indicated additional storms during 27 September and 2 October.

The maximum time-averaged bottom velocities measured at Site B1 and ODMDS E were 61 and 88 cm per sec (2.0 and 2.9 ft per sec), respectively, and corresponded to wind-generated currents during storms. Comparisons of tide- and storm-generated current profiles at Site B1 indicated that although the tidal currents have stronger velocities in the upper portions of the water column, up to 300 cm per sec (9.8 ft per sec), the wind-generated currents generally produce the strongest bottom velocities. Figure 80 compares typical tidal current profiles and wind-generated current profiles at Site B1. The implications of stronger bottom currents from wind-generated currents during storms on sediment transport suggested that the neglect of wind-generated currents in forecasting mound stability at the MCR was not warranted.

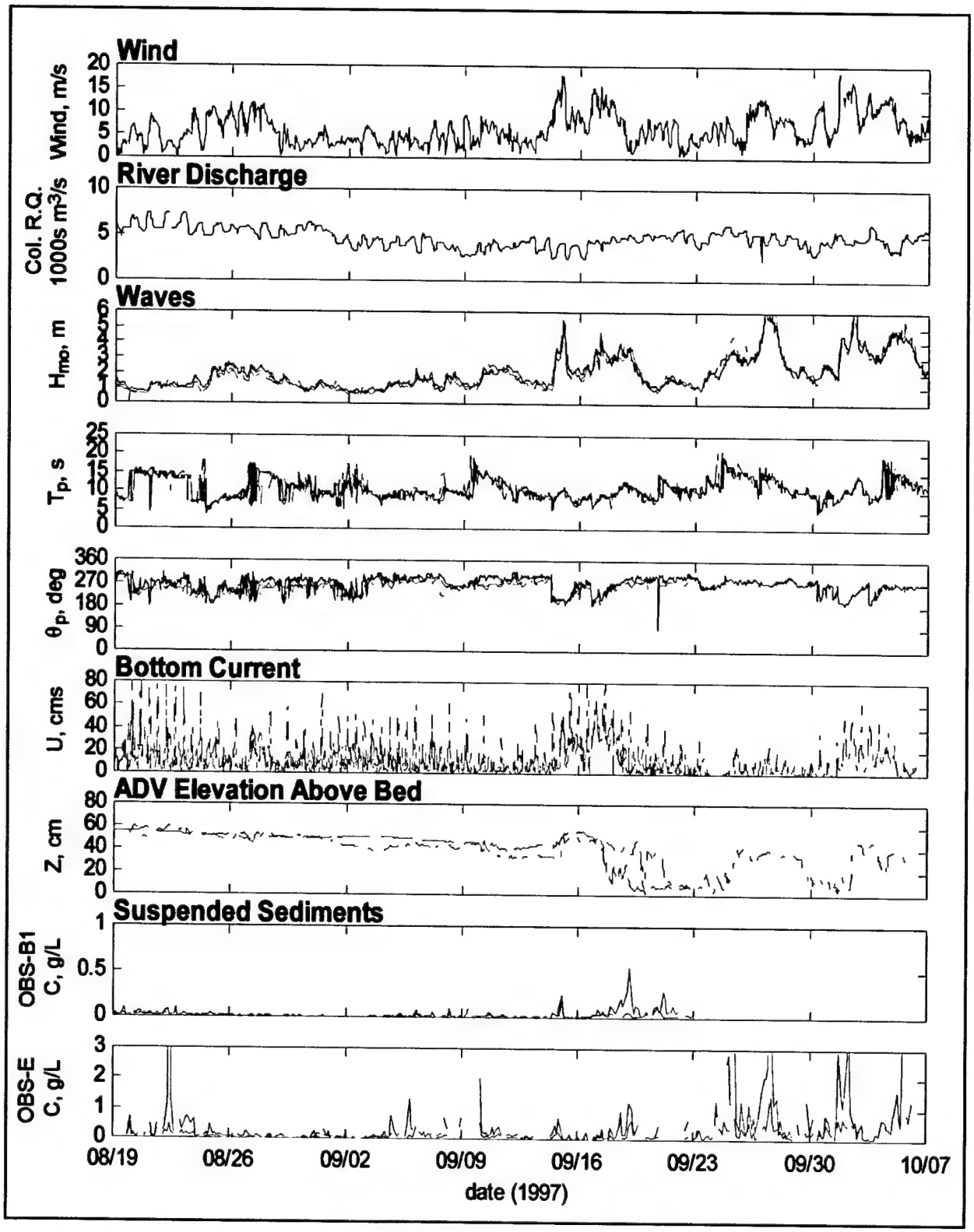

Figure 79. Deployment 1 environmental conditions for Site B1 and ODMDS E (after Gailani and Smith, op. cit., p. 101)

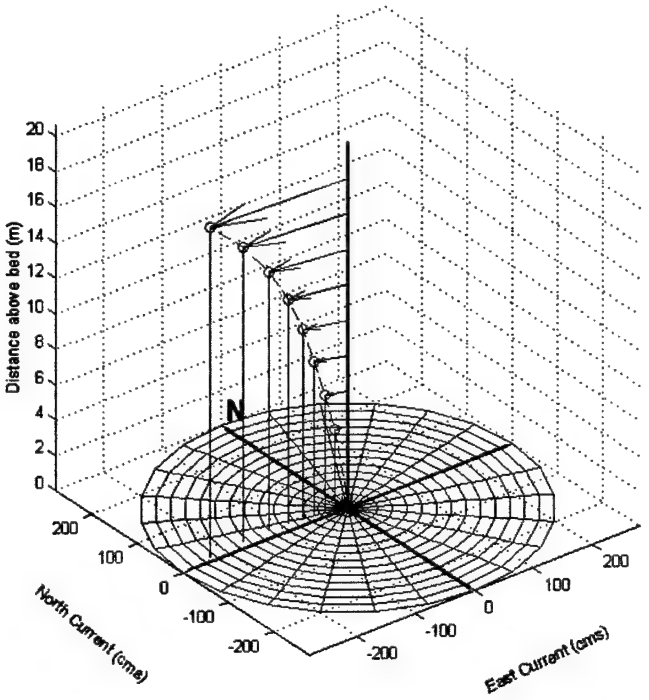

a. Current profile for ebb-tidal current at Site B1, 20 September 1997, 03:00:00

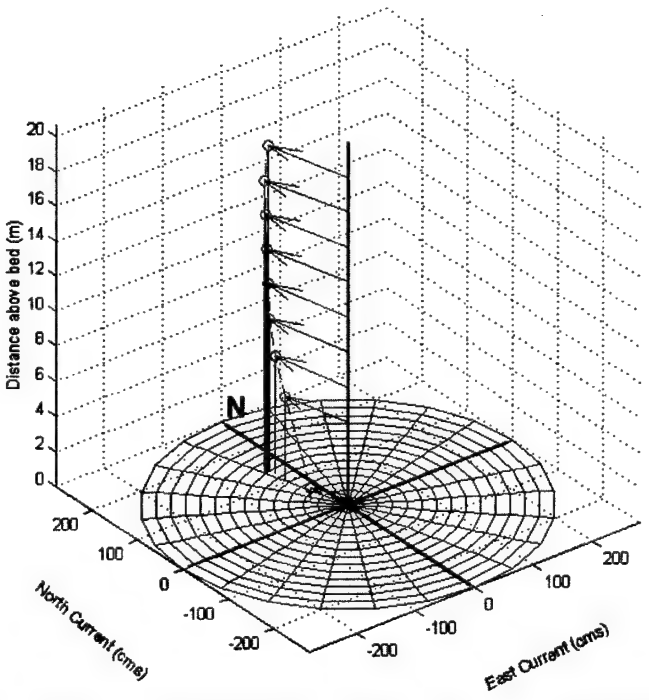

b. Current profile for wind-generated current at Site B1, 17 September 1997, 11:00:00

Figure 80. Comparison of ebb-tidal and wind-generated current profiles (after Gailani and Smith, op. cit., p. 101)

Tidal currents at ODMDS E were significantly stronger than the tidal currents at Site B1. Because of Columbia River freshwater discharge, tidal currents at ODMDS E were ebb-dominant. At Site B1, only the ebb current was evident in the current measurements, and near-zero currents were measured during the flood portion of the tidal cycle. Discharge of the Columbia River at Bonneville Dam was relatively low during the time of Deployment 1, on the order of 5,000 cu m per sec (177,000 cu ft per sec); therefore, the measurements of Deployment 1 are not representative of coastal dynamics associated with periods of high river discharge.

Between 14 September and 20 September 1997 a trough of low pressure developed offshore of the Washington and Oregon coast, resulting in sustained winds greater than 15 m per sec (50 ft per sec) that increased wave heights and bottom currents as indicated in Figure 81. Wave heights peaked during the storm at 4.6 and 4.7 m (15.1 and 15.4 ft) with wave periods of approximately 10 sec. Bottom currents during the storm were directed to the north with a magnitude of 30-60 cm per sec (1.0-2.0 ft per sec). During this period of high bottom shear stress, suspension of sands was detected by the OBS as shown in Figure 82. The suspension of sands during this portion of the data collection appeared to be well correlated to the passing of wave groups.

Deployment 2 (15 April – 24 August 1998). The time series of measurements for Site B1 and ODMDS E during Deployment 2 are presented in Figure 83. Because Deployment 2 measured conditions during the late spring and summer months, wave and current conditions during Deployment 2 were generally less severe than those present during Deployment 1. Storms with higher waves (approximately 4 m (13.1 ft) wave heights and 10-15 sec wave periods) were evident early in the time series, but storms generally decreased in frequency and intensity with the progression from spring into summer.

Peak Columbia River discharges of 21,000 cu m per sec (740,000 cu ft per sec) generally occurred during the months of May and June from snowmelt within the Columbia River basin (Neal 1972). Peak river discharge at Bonneville Dam during Deployment 2 was 10,000 cu m per sec (350,000 cu ft per sec). Near-bottom velocities at Site B1 and ODMDS E were not significantly influenced by the higher river discharge. Peak velocities measured by the bottom ADV at Site B1 were approximately 20 cm per sec (0.7 ft per sec) and correlated to wind-generated currents, whereas the peak near-bottom velocities at ODMDS E were approximately 75 cm per sec (2.5 ft per sec) and corresponded to spring tides.

Suspended sand concentrations during Deployment 2 correlated well with storms at Site B1. However, suspended sand signals at ODMDS E appeared to be contaminated by plumes of turbid water, the nearby disposal of dredged material, or other sources of signal contamination. Regardless, both OBS mounted on the tripod at ODMDS E did not consistently indicate signals indicative of the suspension of sandy material by waves and currents.

Deployment 3 (27 November 1998 – 01 March 1999). Because tripods at Site B1 and ODMDS E had not been recovered from Deployment 3 at the time of this writing, no measurements analysis for Deployment 3 is presented.

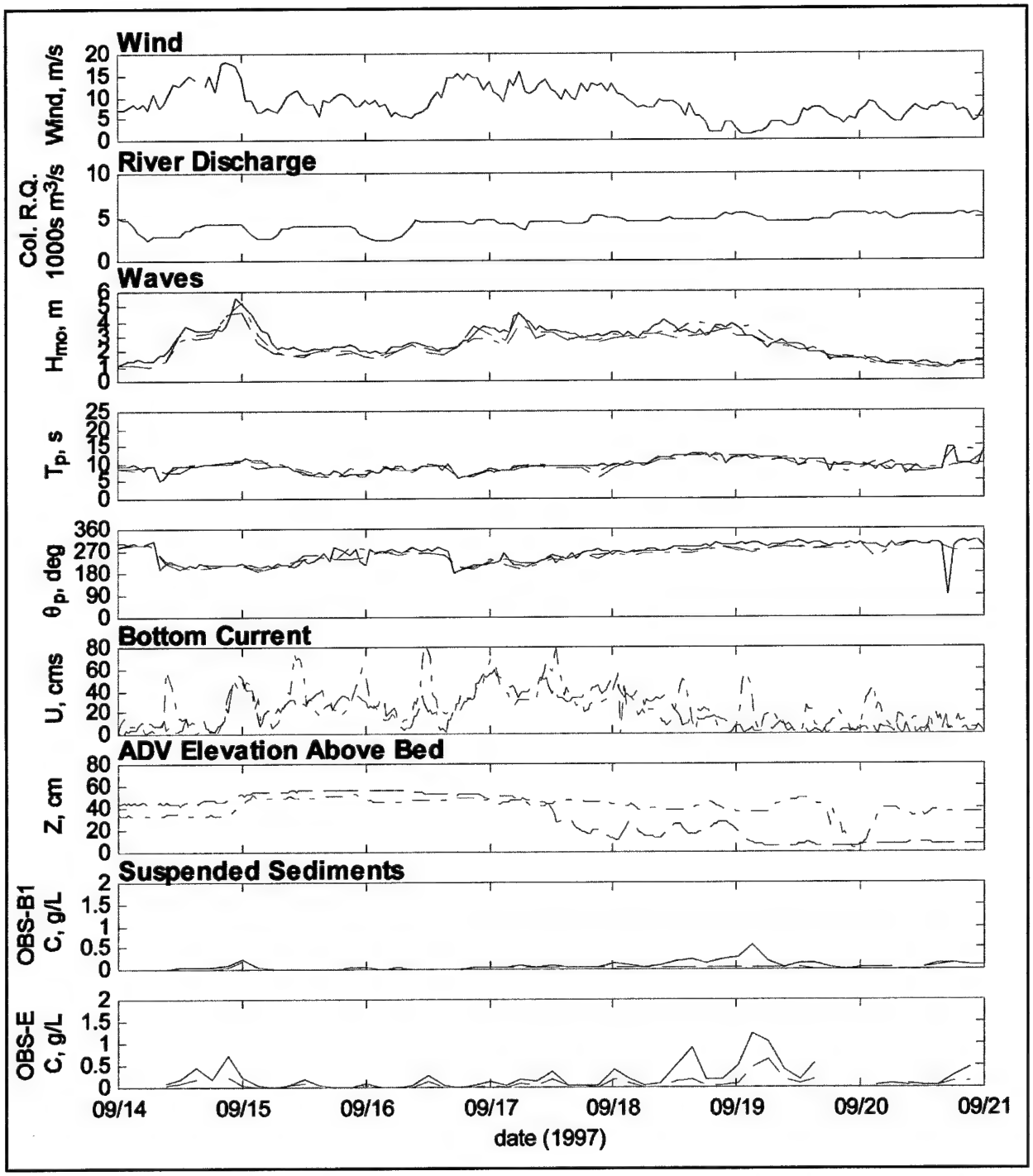

Figure 81. Deployment 1 environmental conditions for Site B1 and ODMDS E, 14 – 20 September 1997 (after Gailani and Smith, op. cit., p. 101)

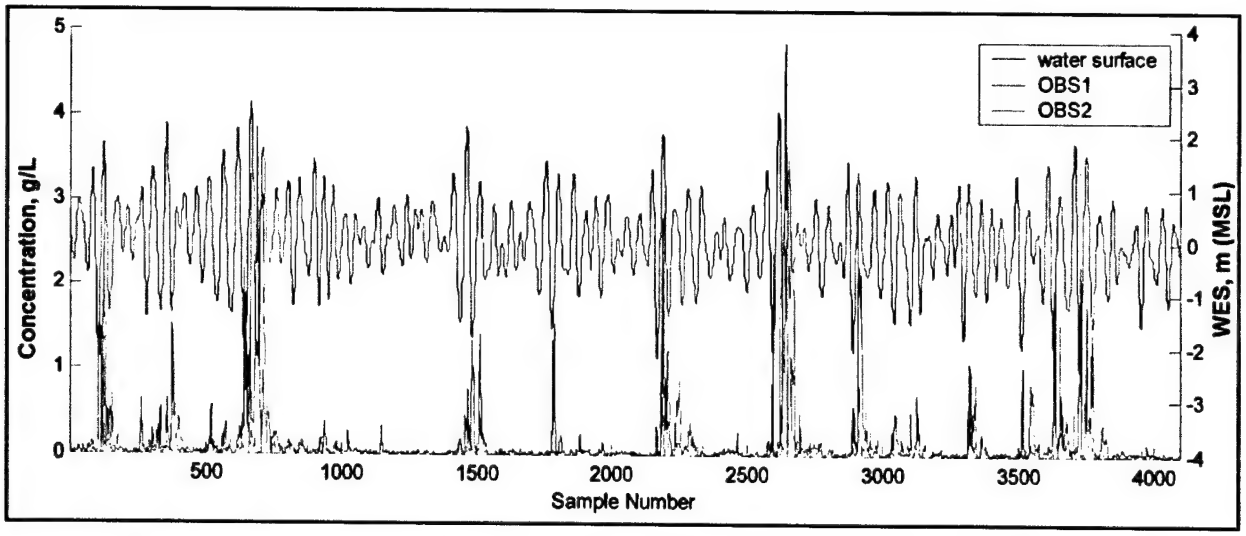

Figure 82. Deployment 1 sand suspension at Site B1, 18 September 1997 (after Gailani and Smith, op. cit., p. 101)

Sediment Transport Methods

Defining sediment dispersion at the two sites requires methods for predicting sediment transport as a function of the current and wave climate. Three methods were selected for analysis of MCR-dredged material transport at Site B1 and ODMDS E, based on well-documented and studied methods that have been verified to field and/or laboratory data sets. The methods selected for analysis include (a) a method developed at Delft Hydraulics Laboratory (van Rijn 1989a, 1989b; van Rijn 1993) (hereafter referred to as the VR method), (b) a method developed under the USACE DRP by researchers at Massachusetts Institute of Technology (Wikramanayake and Madsen 1994) (hereafter referred to as the WM method), and (c) a method developed at HR Wallingford Hydraulic Research Laboratory, England (Ackers and White 1973) (hereafter referred to as the AW method) which has been modified for combined current/wave environments for application in the DRP-developed MDFATE and LTFATE models (Scheffner 1996).

Each method estimates transport magnitude and direction, the combined current and wave related shear stresses at the sediment-water interface, and current available to transport the sediment. Wind-induced currents, tidal currents, and wave orbital velocities can contribute to the bottom shear stresses that mobilize sediments.

van Rijn method

The method developed by van Rijn (1989a, 1989b; 1993) of Delft Hydraulics Laboratory is time-averaged over a wave cycle for suspended load and time varying for bed load. This method was developed for waves outside the surf zone with waves and currents at arbitrary angle. This method requires a near-bed reference concentration for computing suspended load. This near-bed concentration, c_a (kg per m^3), is estimated as:

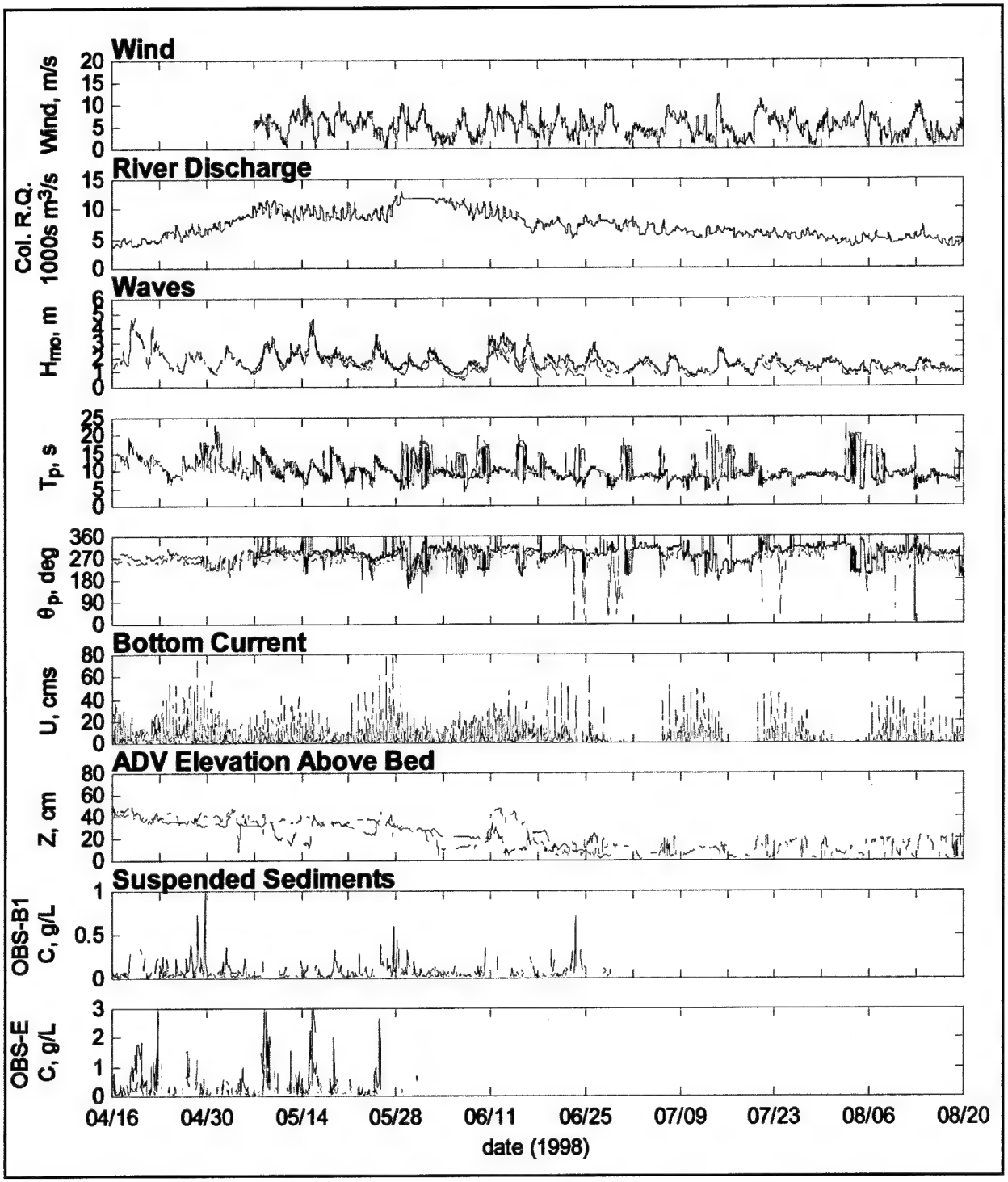

Figure 83. Deployment 2 environmental conditions for Site B1 and ODMDS E (after Gailani and Smith, op. cit., p. 101)

$$c_a = 0.015 \rho_s \frac{d_{50}}{a} \frac{T_a^{1.5}}{D_*^{0.3}} \quad (1)$$

where ρ_s is the sediment density, a is the reference elevation, T_a is the bed shear stress parameter at the reference elevation, and D_* is the particle parameter. T_a and D_* (which are both dimensionless) are estimated by:

$$T_a = \frac{(\alpha_{cw}\mu_c\tau_c + \mu_{w,a}\tau_w) - \tau_{cr}}{\tau_{cr}} \quad (2)$$

$$D_* = d_{50}[(s-1)g/\nu^2]^{1/3} \quad (3)$$

where α_{cw}, the wave-current interaction coefficient, is a function of bed roughness, wave boundary layer thickness, and water depth; μ_c, the current efficiency factor, is a function of bed roughness and grain size distribution; and $\mu_{w,a}$, the wave efficiency factor, is a function of the grain size distribution and wave conditions. The methods for estimating these three parameters are complex and the reader is referred to the original text for details concerning their derivation. In addition, τ_c is the current related bed shear stress, τ_w is the wave related bed shear stress, τ_{cr} is the critical shear stress for the initiation of sediment resuspension, and υ is the kinematic viscosity.

The vertically varying suspended solids concentration, c, is then estimated as a function of a current and wave related mixing coefficient $\varepsilon_{s,cw}$ (which in turn are a function of the kinetic energy, see van Rijn 1993) using the equation:

$$\frac{dc}{dz} = \frac{-(1-c)^5 c\, w_s}{\varepsilon_{s,cw}[1 + (c/c_a)^{0.8} - 2(c/c_a)^{0.4}]} \quad (4)$$

where w_s is the sediment settling velocity.

The time-varying bed load (m^3 per m per s) is estimated as:

$$\bar{q}_b(t) = 0.25\,\alpha\, d_{50} D_*^{-0.3} \left[\frac{\vec{\tau}'_{b,cw}}{\rho}\right]^{0.5} \quad (5)$$

where $\alpha = 1 - (H_s/h)^{0.5}$, h is the water depth, H_s is the significant wave height, ρ is the water density, and $\vec{\tau}'_{b,cw}$ is the grain-related bed shear stress due to currents and waves.

The method as coded by the author (van Rijn 1993) requires input of water depth, depth-averaged current velocity, wave information, grain size distribution, angle between wave and current direction, bed roughness, fluid temperature, and salinity.

van Rijn (1993) compared this method to those of Nielsen (1985) and Bijker (1971) for data from a flume with a steady current superimposed on irregular waves. The van Rijn (1993) method compared most favorably for these data. All data were for rippled beds. No comparison of the method to field data was available.

Wikramanayake and Madsen method

Under contract with the USACE DRP, researchers at the Massachusetts Institute of Technology (MIT) developed combined current-wave environment noncohesive sediment transport algorithms. The algorithms include the effects of variation between current and wave directions. The methods are outlined in DRP reports (Madsen and Wikramanayake 1991; Wikramanayake and Madsen 1994a) and are specifically designed for transport outside the breaker zone. A time-invariant turbulent eddy viscosity model and a time-varying near bottom concentration model are used to estimate suspended sediment transport fluxes. The method first calculates the bed roughness using methods outlined by Wikramanayake and Madsen (1994b). Then, based on bed shear forces, bed load and suspended sediment concentrations are calculated separately. All estimates of vertical variation in the sediment concentration used in suspended load estimates are based on a nondimensional time-varying reference concentration, $c_r(t)$, near the bottom. The authors stress that accurate prediction of this value is critical to accurate transport calculations. This concentration can be estimated as:

$$c_r(t) = \frac{c_b \gamma_o (|\Psi^*(t)| - \Psi_{cr})}{\Psi_{cr}} \tag{6}$$

where c_b is the volume fraction of sediment in the bed and γ_o is a resuspension coefficient. Other parameters in Equation 6 include $\Psi^*(t)$, the Shield's parameter based on instantaneous skin friction shear stress, and Ψ_{cr}, the critical Shield's parameter. These parameters are defined by:

$$\Psi^*(t) = \frac{u_*^2(t)}{(s-1)gd_{50}} \tag{7}$$

$$\Psi_{cr} = \alpha_1 \tan(\phi) \tag{8}$$

where $u_*(t)$ is the bed shear velocity, d_{50} is the median grain size in the bed, s is the sediment specific gravity, g is the acceleration of gravity, α_1 is a coefficient dependent on the local Reynolds number, and ϕ is the angle of repose of the sediment grains. The reference concentration is used to estimate vertically varying concentrations in the water column due to steady currents and oscillatory currents. Coupled with the vertically varying velocities, the total suspended sediment flux is then estimated.

The authors developed a method for estimating the instantaneous bed load flux based on the Meyer-Peter and Müller (1948) formula. This instantaneous bed-load flux, Q_b (cm^3 per cm per sec), is estimated by:

$$\vec{Q}_b(t) = \frac{d_{50}\sqrt{(s-1)gd_{50}}}{2\pi} \frac{8(|\Psi^*(t)| - \Psi_{cr})}{1 + \tan\beta \frac{\cos(\Phi_t - \Phi_{sw})}{\tan\Phi_f}} \frac{\vec{\tau}'_b(t)}{|\vec{\tau}'_b(t)|} \quad (9)$$

where $\beta = h/6\delta$, h is the water depth, δ is the boundary layer length scale, Φ_t is the angle between the current and the wave direction, Φ_{sw} is the angle between the wave direction and bottom slope, Φ_f is the angle of repose for sediment grains (~36 deg), and $\vec{\tau}'_b(t)$ is the instantaneous skin friction shear stress.

The wave-current model was originally developed for a single sinusoidal wave component. The method is extended to include irregular waves by linearly superimposing two or more sinusoidal waves. This method does not account for wave asymmetry in the present form. Other than a constant in the bed-load calculation (incorporated into α_1 in Equation 8) and the resuspension coefficient, the model is completely deterministic. Available data, most of it from the laboratory, are used to estimate the bed-load concentration constants for both rippled and flat beds. Finally, the velocity profile, suspended sediment concentration profile, and bed-load calculations are used to estimate the transport rates.

The authors ran several tests to compare their results to field measurements in wave/current environments. Specifically, two data sets were used for sediment concentration profile verification; (a) Vincent and Green (1990) measured at Holkham, UK, and (b) Vincent and Osborne (unpublished) measured at Cornwall, UK. Additional laboratory data sets were used for verification of the bed roughness model and determination of γ_0. The results of these tests indicated that the model accurately predicted the mean (or current-related) and wave-related fluxes and their distributions in the water column. No verification was offered for the bed-load model estimates.

Ackers and White method

The method developed by Ackers and White (1973) is a total load formula. It does not differentiate between bed and suspended load. The method was also developed for current-only regimes, although it has been modified for combined current-wave regions using methods developed by Bijker (1971) and Swart (1976) by estimating an equivalent stress that can be related to a higher current speed. Application of these methods to the Ackers and White formula is described by Scheffner (1996). The method does not account for differences between wave and current direction. In comparison to the other methods, the Ackers and White method does have some benefits. One benefit is that it does not require estimation of parameters that are difficult to acquire from field data or synthetic databases. In current-only laboratory and field (predominately small creeks) experiments it tends to perform as well as or better than many of the other conventional sediment transport methods available such as Englund and

Fredsoe (1976), Einstein (1950), or Bagnold (1966). A detailed comparison is offered by Brownlie (1981). The Ackers and White for combined wave and current environment was applied to a sand mound in Mobile Harbor (Scheffner 1996). In that application it simulated the migration of the mound footprint with reasonable accuracy.

The Ackers-White transport equations relate sediment transport to three dimensionless quantities. The first, a nondimensional grain size D_{gr}, is defined as a function of the ratio of the immersed particle weight to the viscous forces acting on the grain. The value is defined as:

$$D_{gr} = D\left[\frac{g(s-1)}{\nu^2}\right]^{1/3} \tag{10}$$

where D is the median grain size, g is acceleration of gravity, s is the sediment specific gravity, and ν is the fluid kinematic viscosity. The second nondimensional parameter, F_{gr}, represents particle mobility defined as the ratio of shear forces to the immersed sediment weight. The general form of the relationship is

$$F_{gr} = \frac{v_*^n}{\sqrt{gD(s-1)}}\left[\frac{V_{wc}}{\sqrt{32}\log(10\frac{d}{D})}\right]^{1-n} \tag{11}$$

where V_{wc} is the velocity which is modified (increased) to account for the effect of waves, d is the mean depth of flow, v_* is the shear velocity (ft per sec), and n is an empirical variable related to grain size.

The third nondimensional parameter, G_{gr}, defines a sediment transport rate as a ratio of shear forces to the immersed weight multiplied by the efficiency of transport. The efficiency term is based on work needed to move the material per unit time and the total fluid power. G_{gr} can also be related to F_{gr}. The transport rate is written as:

$$G_{gr} = \frac{Xd}{sD}\left[\frac{v_*}{V_{wc}}\right]^n = C\left[\frac{F_{gr}}{A} - 1.0\right]^m \tag{12}$$

where X is a nondimensional sediment transport function in the form of mass flux per unit mass flow rate. C, A, and m are empirical variables related to grain size (i.e., they are a function of D_{gr}). The preceding equation is then used to solve for X, which can be converted to a dimensional sediment load transport rate Q_b, defined in cu ft of sediment (solids) per sec per unit width by $Q_b = Xvd$ where v is the current velocity.

Modeling Sediment Transport at ODMDS

The three methods estimate transport differently. The VR and WM methods predict bed-load and suspended-load transport separately, adding them to get total transport. AW is a total load formula and does not differentiate between bed and suspended load. The VR method goes one step further, predicting a concentration profile through the entire water column. The WM method only estimates near bed concentrations and the AW method does not predict concentrations. These differences have implications when comparing model results to field data. The OBS data at the sites provide an excellent record of the time-histories of suspended solids concentrations. They do not, however, supply any record of total transport. First, the OBS are located high enough in the water column where they would miss recording data concerning the most significant portion of transport, which occurs near bottom just above the sediment bed. Second, more than two OBS are required to estimate suspended load transport from OBS data because of the significant variation in concentration through the water column. Since only the VR method estimates concentrations throughout the water column, and because transport amounts cannot be derived from the field data, the only direct comparison between field data and models can be the VR method predictions of concentration and the OBS data at known heights above the sediment-water interface. These comparisons will constitute a significant portion of this chapter but this should not be considered as an endorsement of the VR method over the other two methods.

Calibration and verification

To estimate parameters required by each method (bed roughness, median suspended grain size, etc), calibration of the methods to measured sand suspension was performed where possible. Several assumptions were made to develop forcing conditions for the three methods. First, measurements indicate that the current profile typically varies in both magnitude and direction through the water column. The WM and AW methods were developed for regions where the current is relatively constant through the water column (except within the boundary layer) or in nearshore regions. The methods were not designed for regions where flow is stratified due to, for example, density differences or wind-driven currents. This limitation does not, however, negate the usefulness of these methods in stratified flow regions as long as appropriate application of data to model input is undertaken.

Most transport of sand occurs near the bed, and the shear stresses on the bed from the overlying fluid flow can be described better by using current measurements near the bottom (but outside the boundary layer) than it can by using vertically averaged velocities in a stratified regime. Therefore, ADV measurements of current velocity were used as input velocity for all simulations. In comparing OBS data to model estimates of concentration, the elevation of the OBS above the bed was specified by the information from the ADV bottom altimeter. The heights of model-estimated total suspended solids (TSS) were adjusted for consistency with the height of the OBS above bottom.

The VR method estimates the concentration gradient through the water column. Model results were compared to tripod OBS data collected at the sites to determine if the model reasonably estimated sand suspension concentrations. The AW and WM methods do not estimate concentration higher than a few centimeters above the sediment-water interface and were not directly comparable to the OBS data. The VR method was calibrated to the OBS data for Deployment 1, and then partially verified to OBS data from Deployment 2. The first data set simulated was Site B1, Deployment 1. A median grain size of 0.22 mm was specified based on known properties of MCR dredged material.

In addition, the median suspended particle size was calibrated to the field data and a value of 85 percent of the median grain size from the bed (this method will be referred to as VR1). This fit was considered reasonable by visual comparison to field data and no quantitative method was used to determine best fit. To assess model sensitivity to suspended solids median grain size, a second set of simulations was performed assuming that the median grain size of suspended sand was the same as the bed median grain size (this method will be referred to as VR2). Equating the bed and suspended median grain sizes is recommended by model documentation for situations in which TSS grain size distributions are not available. Bed roughness was assumed to be 0.06 m (0.2 ft) for all simulations. The effects of varying grain size and roughness will be discussed later.

Figure 84 shows a time-history of the OBS measured concentrations along with the VR1 and VR2 model estimates at each OBS height for Site B1, Deployment 1. Initially, heights of the OBS were set at 0.55 m (1.8 ft) and 1.25 m (4.1 ft) above bottom, but these heights decreased as the tripod became buried in the sand. Gaps in the OBS data record indicate times when the data were determined not to be clearly characteristic of sand signals. Concentrations predicted by the VR1 method compare favorably to measurements during both storm and most calm periods (no sand in suspension), although the predicted concentrations are generally higher than the measured concentrations. In addition, the method misses some small, early suspension events, but these may be background noise or surficial fine sediment suspension and were not attributable to any corresponding forcing. The comparison of predicted and measured concentration profiles is somewhat more favorable for the VR2 method. Although reasonable comparisons between predicted and measured concentration profiles indicate that the model is qualitatively simulating transport processes, the height above the bottom where concentration was measured is considerably above the near-bottom region where the majority of transport occurs. Therefore, these comparisons can only provide partial verification that the models are accurately simulating total transport at the site.

Figure 85 presents the calibrated VR1 and VR2 methods with comparison to Site B1 tripod data for Deployment 2. Measured suspended solids concentrations during Deployment 2 are much greater than during Deployment 1. The reason for the magnitude of difference in concentration between Deployments 1 and 2 is unknown and not substantiated by the wave and current data. Model simulations predict greater concentrations for Deployment 2, but they underestimate the suspended solids measurements, particularly at OBS 1. Interestingly, the OBS 1 signal during this deployment shows significant activity, without a corresponding increase in concentration at OBS 2. Although several of the spikes in

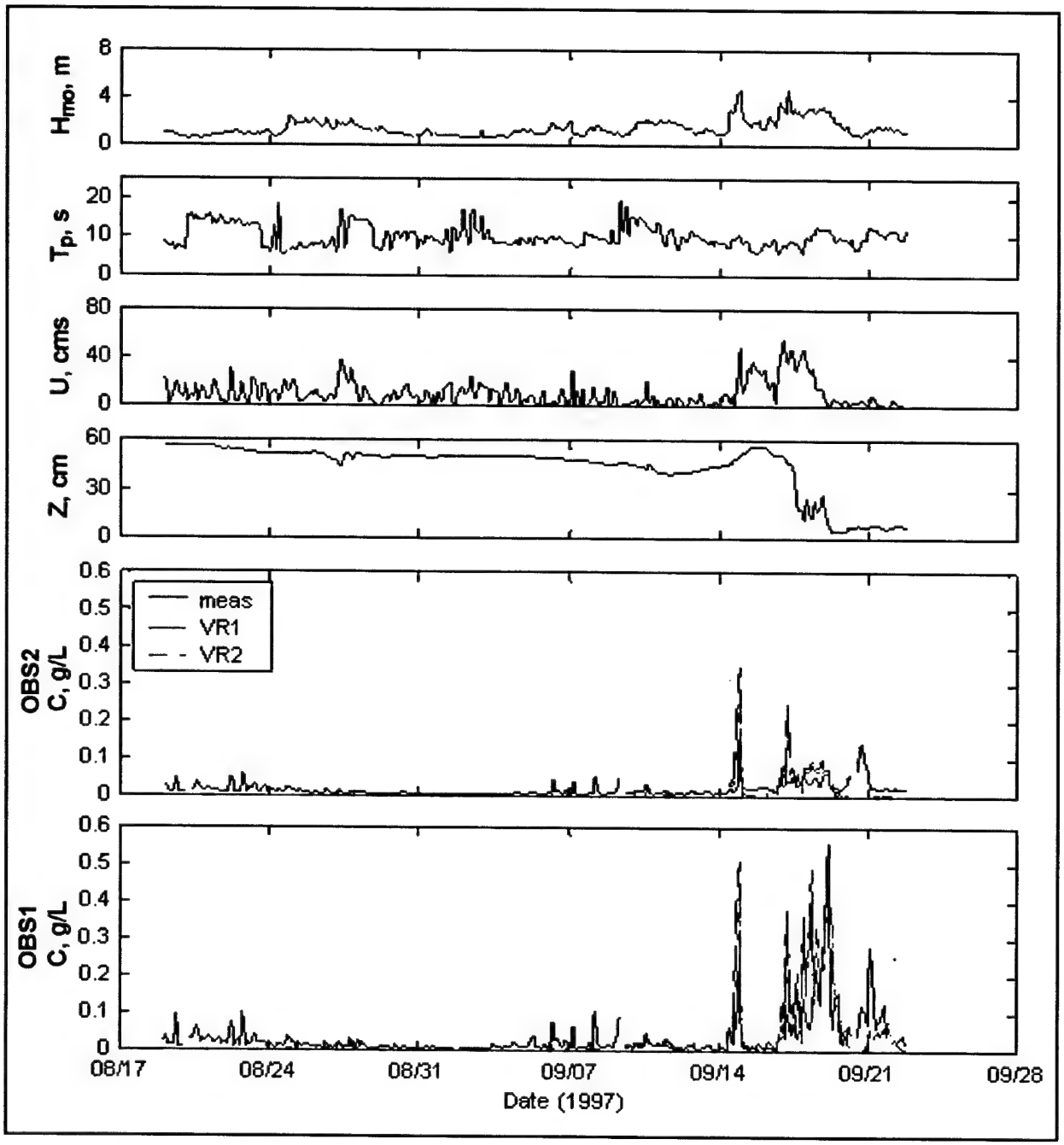

Figure 84. Concentration at Site B1 Deployment 1 simulation with 0.22-mm sand (after Gailani and Smith, op. cit., p. 101)

concentration at OBS correlate to increased wave height (for examples, on April 17 and May 15), other peaks in the OBS signal do not correlate to the wave and current signals. Analysis of the data indicated that these signals behaved like signals from suspended sand and therefore they were not eliminated from the database.

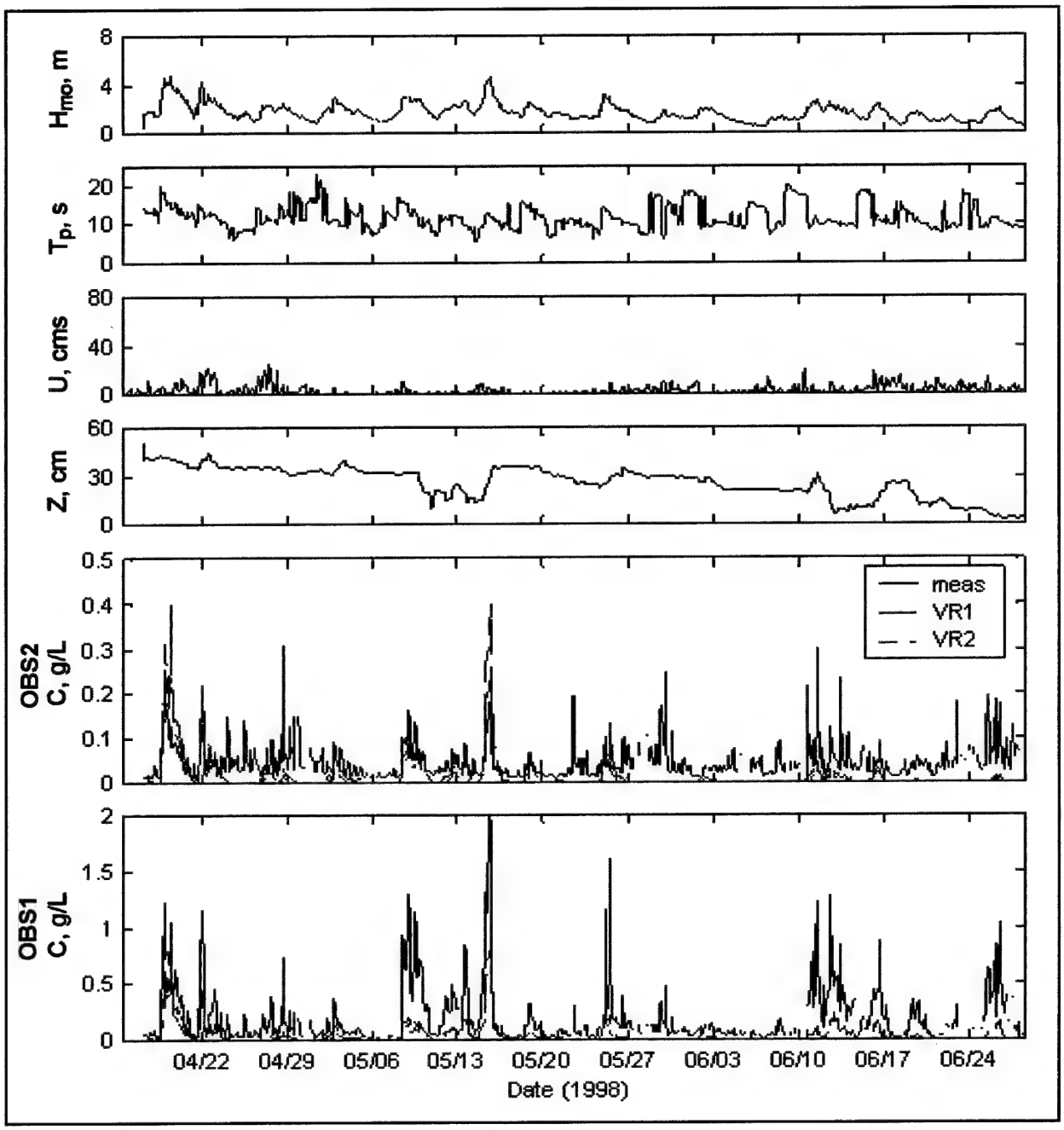

Figure 85. Concentration at Site B1 Deployment 2 simulation with 0.22-mm sand (after Gailani and Smith, op. cit., p. 101)

The difference in behavior of the measured sand signals between Deployments 1 and 2 may be attributable to parameters to which suspended sediment concentration and transport are highly sensitive, but are only known within a broad range for the site. In addition, these parameters can change both spatially over the mound and temporally. One of these parameters is median grain size and grain size distribution. The dredged material is not homogeneous, so the mound can be expected to include patches or layers of varying grain size and/or constituency. As will be demonstrated later in this chapter, modest changes in

grain size will affect suspension and transport rates. Also, the second deployment location was not exactly the same as the first and the sediment characteristics may differ. Another parameter that may be different during each deployment (and may change significantly during a deployment) is total bed roughness, which includes roughnesses due to grain size and bed forms. The implications of the possible variation in these parameters are evident when comparing the OBS signals from Deployments 1 and 2. All transport estimates must be viewed within the context of the limitations of the present understanding of parameter values at the site and how they may vary across the site. For example, although the VR1 and VR2 methods appear to modestly overestimate concentration (and thus transport) during Deployment 1, they underestimate concentrations during Deployment 2. Therefore, it is not reasonable, from viewing field and model data during Deployment 1, to assume that the model is universally overestimating transport. It is reasonable, however, to state that model is reasonably reflecting trends in sediment suspension and transport. It is also reasonable to state, after viewing both deployments, that the concentration magnitudes are generally simulated within the uncertainty of the measurements.

A comparison of ODMDS E, Deployment 1 OBS data and VR method predictions is presented in Figure 86. Parameter values were not changed from the values used in Site B1. Measured and predicted suspended solids concentrations are much greater than at Site B1 due to greater currents and shallower depth. Model estimates of sand concentration at the heights of the OBS agree reasonably well with the measured data. The peaks in mean concentration correspond to the two peaks of the storm and are well represented by the VR method. There appears to be little difference between the VR1 and VR2 methods at the OBS1 position, but the VR2 concentration estimates during the storm peaks at the OBS2 position are of lower concentration and tend to agree better with the measured concentrations.

Figure 87 compares Deployment 2 OBS data to VR1 and VR2 model estimates at ODMDS E. Significant portions of the data at ODMDS E were corrupted or inconsistent with sand signals during this deployment, as evidenced by the large gaps in measured OBS data. Part of the signal contamination for this case was caused by disposal of dredged material at the site from July through August. The large amount of contaminated data left only small amounts of data for model comparison. Simulations that assumed a 0.22-mm diameter sand at ODMDS E significantly underestimated TSS concentrations. The underestimation by the simulations may be explained by the rapid transport of the dredged material from this site. By spring (the time of Deployment 2), most material disposed at the site the previous summer-fall may be removed and the OBS would be measuring suspension of the finer native sediments. Assuming that the OBS was measuring suspension of the finer native sediments, the VR1 method was resimulated with a sediment grain size equivalent to the native sediment, 0.1 mm (USAED, Portland, 1998). Model estimates are presented in Figure 88. With the bed sediment grain size set to the native sediment size, model predictions of TSS concentrations are improved.

Comparisons between calibrated sediment transport methods are presented in Figures 89 and 90 for Site B1, Deployments 1 and 2, respectively. The AW and WM methods tend to predict less transport than VR methods when conditions

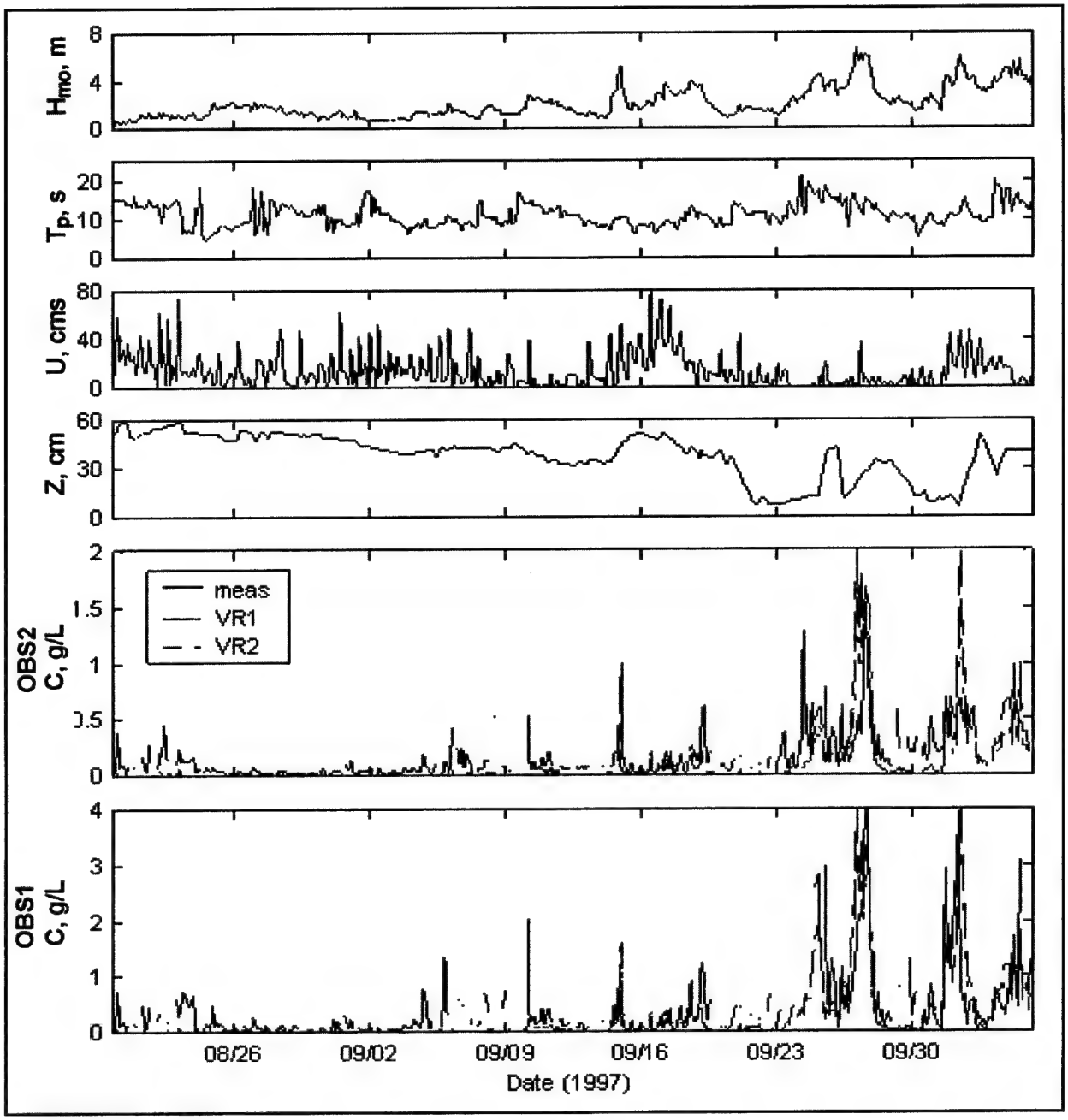

Figure 86. Concentration at ODMDS E Deployment 1 simulation with 0.22-mm sand (after Gailani and Smith, op. cit., p. 101)

include large waves combined with small mean current such as the 15 May 1998 event. The WM and AW methods also predict less transport for modest magnitude events like those in early May 1998 (see Figure 90). The comparisons for ODMDS E Deployment 1 and 2 are presented in Figure 91 and Figure 92, respectively. Again, as at Site B1, the AW and WM methods predict less transport for high-wave/low-current events such as the 27 September storm (Figure 91). The WM method actually predicts significantly more transport

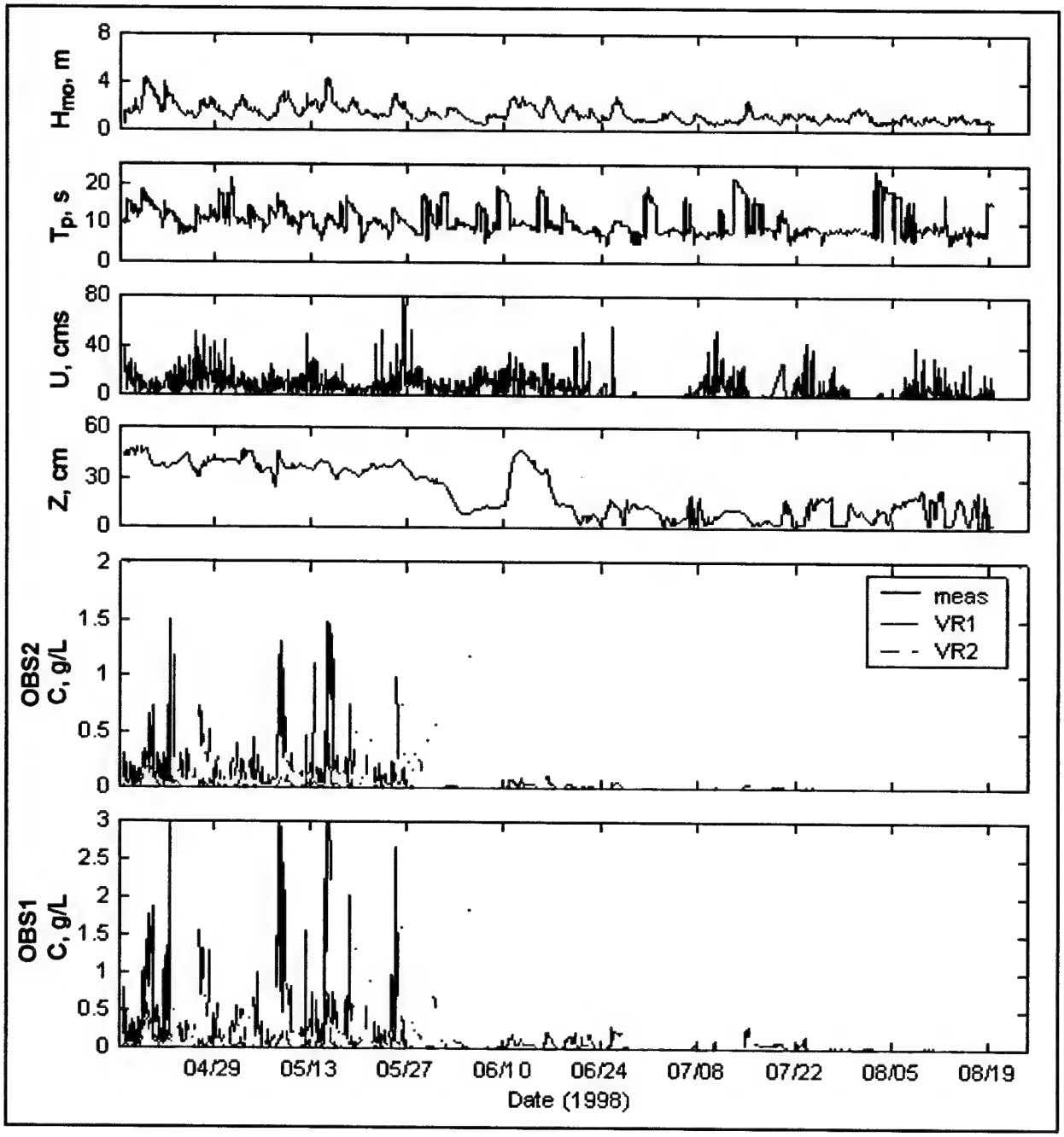

Figure 87. Concentration at ODMDS E Deployment 2 simulation with 0.22-mm sand (after Gailani and Smith, op. cit., p. 101)

when currents are very strong, as demonstrated by the 16 September storm in Figure 91 and the late April storm in Figure 92.

It should be emphasized that no data are available which can be directly used to suggest that one model provides better estimates of transport at the sites. Analysis of the individual methods can, however, provide insight into which methods are more applicable to ODMDS. The VR and WM methods were both

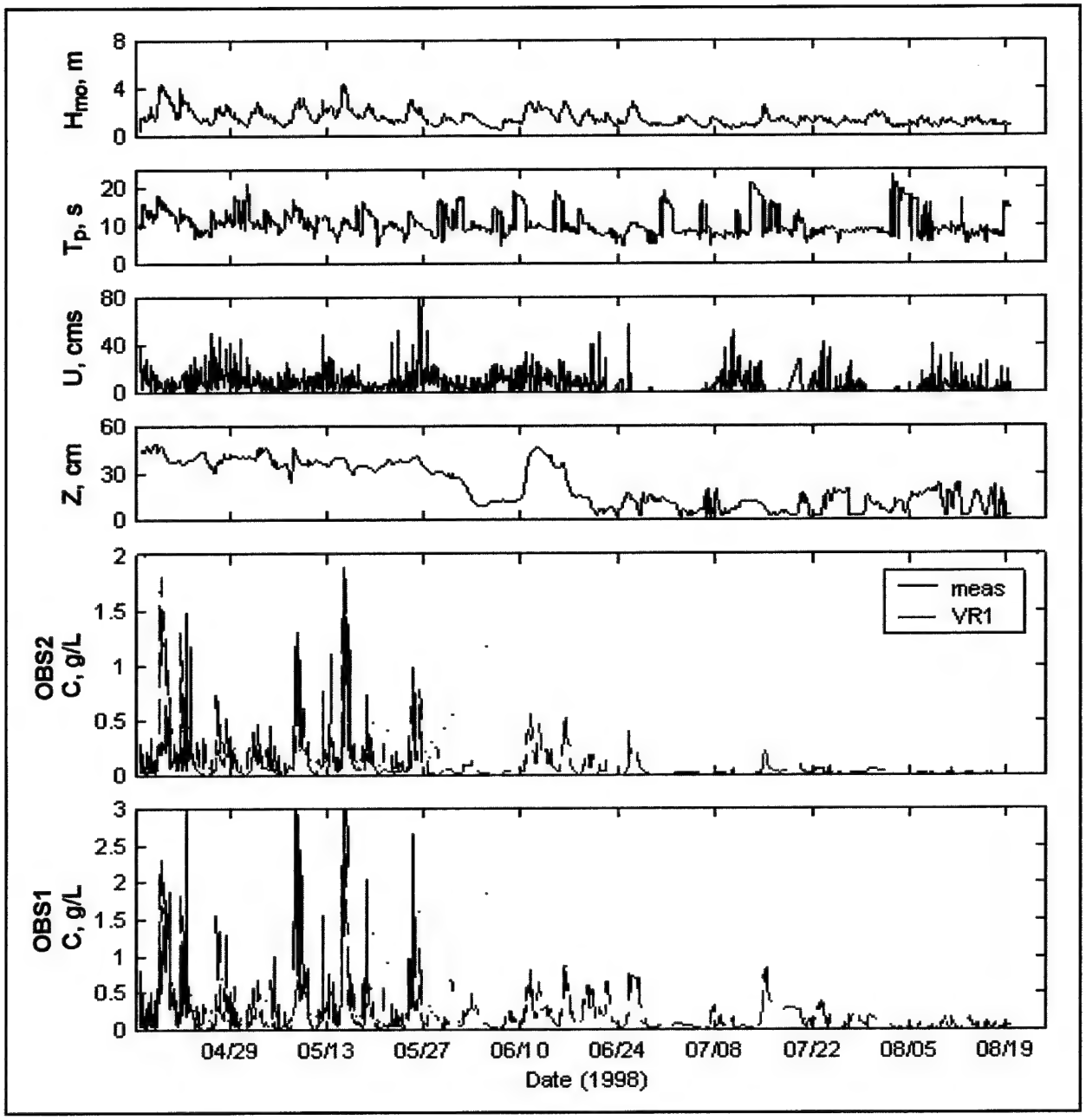

Figure 88. Concentration at ODMDS E Deployment 2 simulation with 0.10-mm sand (after Gailani and Smith, op. cit., p. 101)

designed for open-ocean application. They include processes such as wave asymmetry that under some conditions will affect transport, particularly in shallow water or regions with long-period waves. The AW method was originally applied to and verified for streamflow transport. It was later modified for open-ocean application but does not presently account for some processes that are significant under certain conditions. However, despite the limitations, the AW method under most conditions estimates magnitudes of erosion similar to the other two, more complex methods. It does not appear to accurately predict

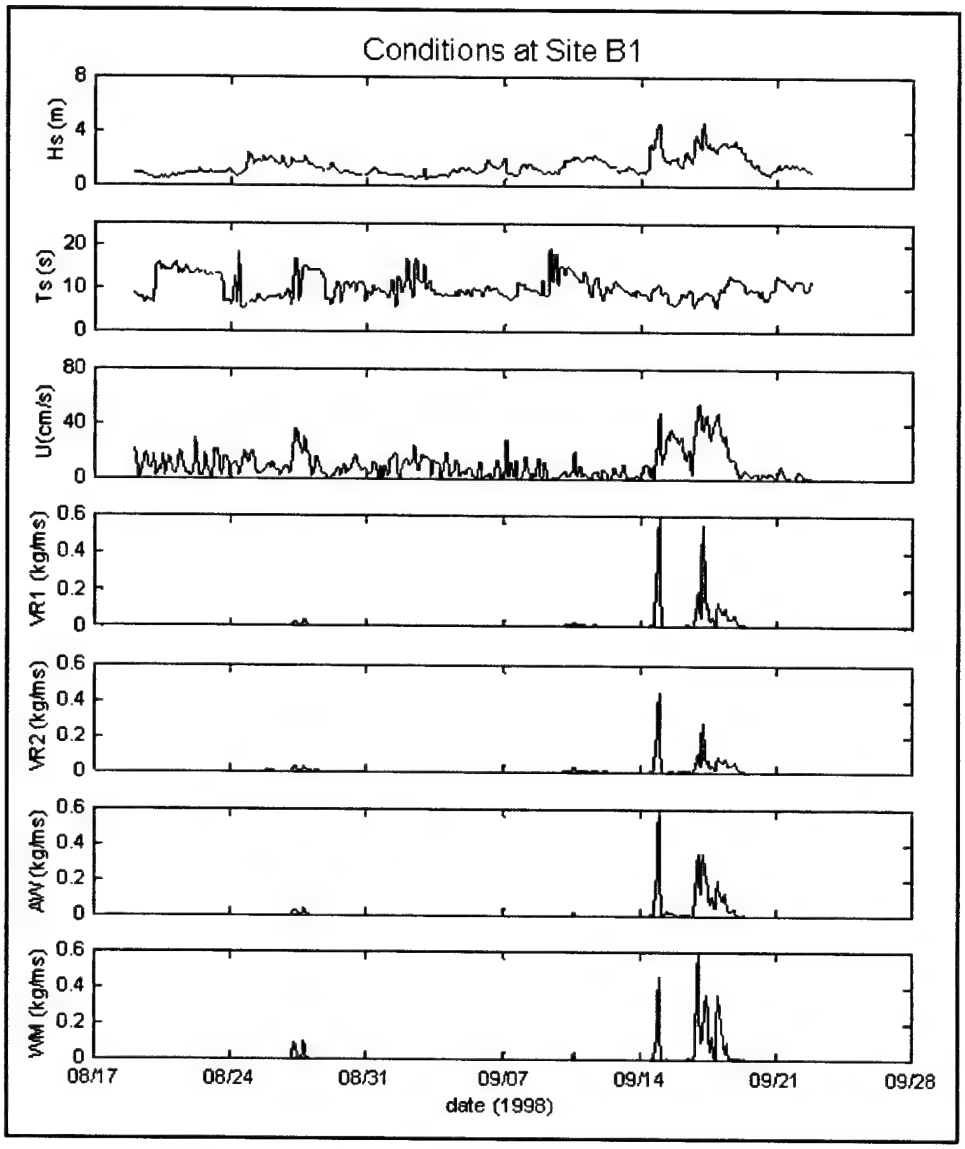

Figure 89. Transport at Site B1 Deployment 1 simulation with 0.22-mm sand (after Gailani and Smith, op. cit., p. 101)

transport under high wave/low current conditions where wave asymmetry significantly influences transport. For application to various ODMDS scenarios, it appears that the AW method represented in the FATE models will predict similar magnitudes of transport to the other more complex models, but it may not be applicable under certain conditions in its present form. An enhanced version of LTFATE completed in 2001 includes wave asymmetry.

Sensitivity analysis

Several parameters, including the roughness coefficient and median grain size were selected based upon knowledge of the site. Uncertainty exists in the selection of these two parameters, and variations of these two parameters within the

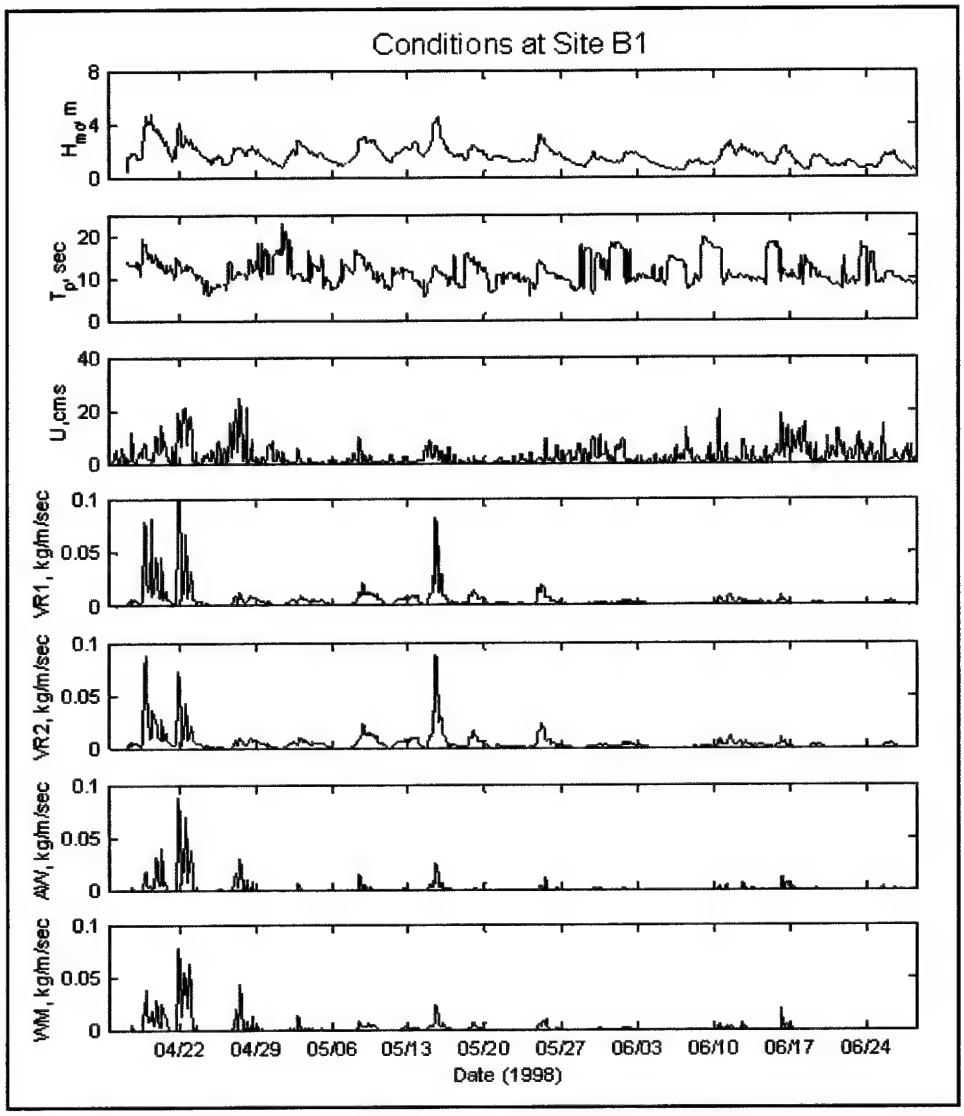

Figure 90. Transport at Site B1 Deployment 2 simulation with 0.22-mm sand (after Gailani and Smith, op. cit., p. 101)

range of reasonable values will influence the transport estimates. To estimate the influence of the uncertainty in selection of the roughness coefficient and the median grain size on sediment flux, a sensitivity analysis of each parameter was conducted with the VR1 method. Although the grain-related roughness is easily estimated from grain size, the roughness related to bed forms (such as ripples) is not known for the sites and fluctuates significantly with wave/current conditions. The sensitivity of sediment flux to roughness was evaluated for bed roughness coefficients of 0.02 m (0.07 ft), 0.06 m (0.20 ft), and 0.10 m (0.33 ft), and displayed for each site and deployment in Table 14. Gross transport estimates from the sensitivity analysis to bed roughness vary by as much as 20 percent from the selected value of 0.06 m (0.20 ft) used in calibration. Sensitivity of transport to median grain size was evaluated by estimating transport for median grain sizes of 0.19 mm, 0.22 mm, and 0.25 mm. The results of this analysis are shown in Table 15. Uncertainty in median grain size results in as much as 70 percent

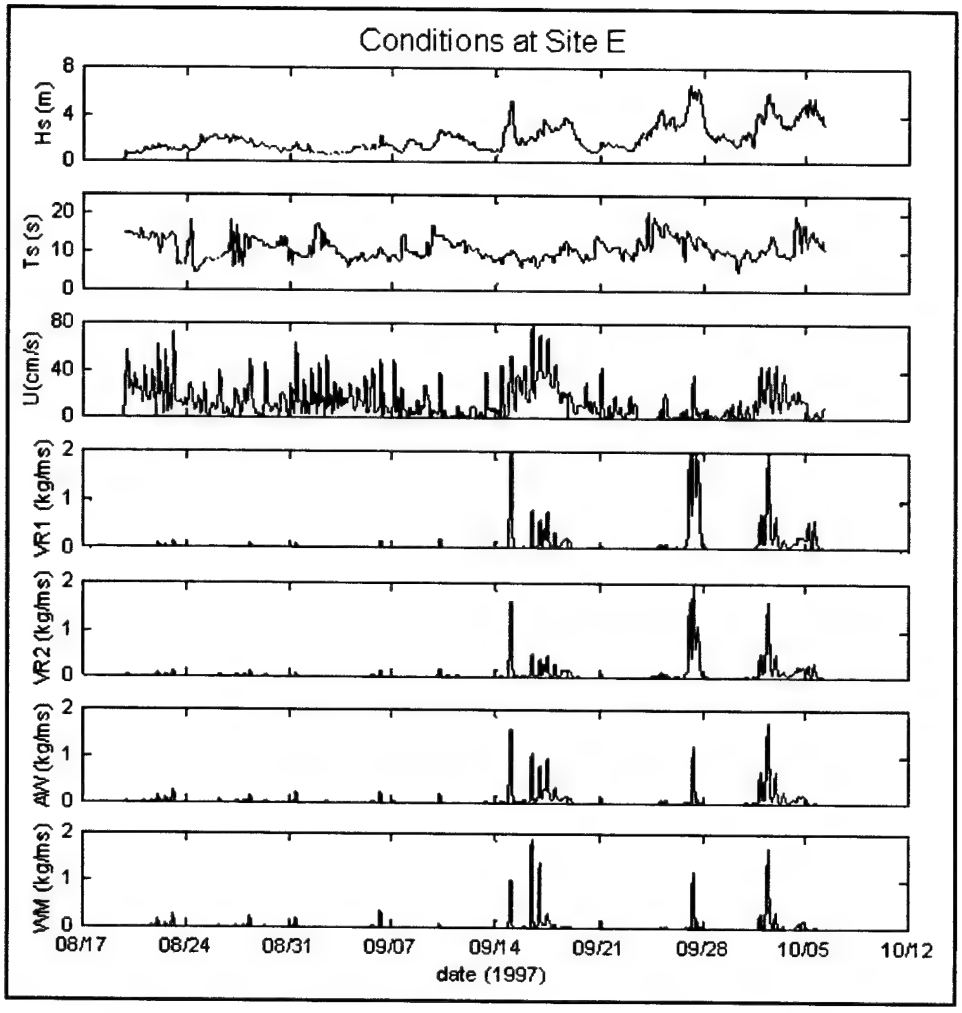

Figure 91. Transport at ODMDS E Deployment 1 simulation with 0.22-mm sand (after Gailani and Smith, op. cit., p. 101)

difference in estimated sand transport. This sensitivity is much greater than the sensitivity of estimated transport from the range of bottom roughness.

The calibrated transport methods applied at Site B1 and ODMDS E confirm the general observation that ODMDS E is considerably more dispersive than ODMDS B, although both behave in a dispersive manner. Two observations from the measurements qualitatively explain the larger rates of sediment dispersion at ODMDS E. Shallower water depths at ODMDS E increase bottom orbital velocities that contribute to greater shear stresses and sediment suspension at ODMDS E. Also, tidal currents at ODMDS E are much stronger than those found at Site B1, increasing suspended sediment transport.

To evaluate the individual roles that differences in current and depth play in increasing sediment transport at ODMDS E, Site B1 and ODMDS E water depths and currents were applied at the alternate site for an 840-hr period during Deployment 1 from 18 August 1997 to 22 September 1997. This period included

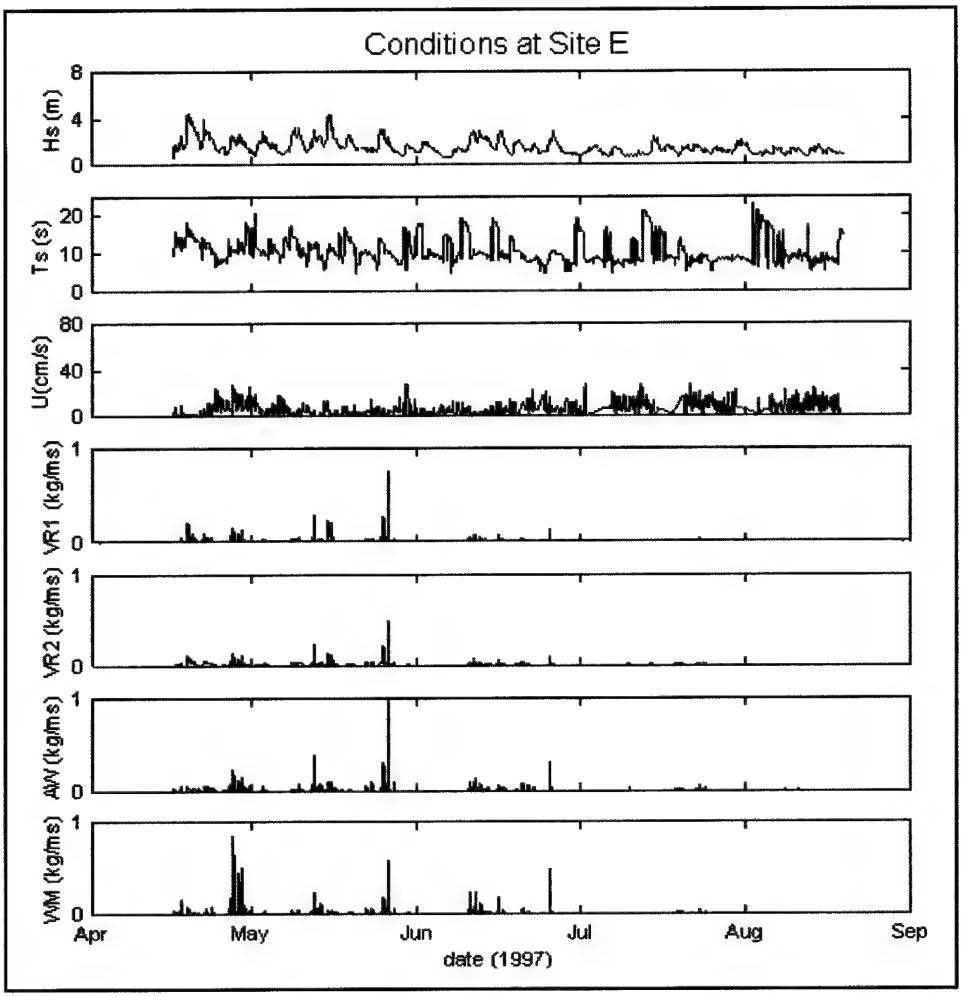

Figure 92. Transport at ODMDS E Deployment 2 simulation with 0.22-mm sand (after Gailani and Smith, op. cit., p. 101)

Table 14
Effects of Roughness on Transport

Location/ Deployment	Roughness Coefficient (m)	Flux (kg/m)
B1-1	0.02	41,600
	0.06	39,300
	0.10	43,400
B1-2	0.02	31,000
	0.06	30,400
	0.10	29,700
E-1	0.02	457,400
	0.06	380,600
	0.10	375,400
E-2	0.02	101,200
	0.06	90,900
	0.10	92,900

Table 15
Effects of Grain Size on Transport

Location/ Deployment	Median Grain Size (mm)	Flux (kg/m)
B1-1	0.19	66,700
	0.22	39,300
	0.25	28,700
B1-2	0.19	38,300
	0.22	30,400
	0.25	29,300
E-1	0.19	630,200
	0.22	380,600
	0.25	269,100
E-2	0.19	128,900
	0.22	90,900
	0.25	79,100

one event with wave heights greater than 4 m. The resulting sand transport rates are presented in Table 16. Decreasing the water depth at Site B1 from 20.7 to 17.1 m (68 to 56 ft) (the depth at ODMDS E) doubles transport rate. Conversely, changing the applied current to that from ODMDS E approximately doubles the transport. If both depth and current fields from ODMDS E are applied to the Site B1 wave field, the transport increases by a factor of three. Shallower water and increased mean currents contribute significantly to the greater transport at ODMDS E. Wave height is also seen to influence transport by an approximate 20 percent increase in transport with application of the larger wave heights from ODMDS E.

Table 16
Influence of Depth, Waves, and Currents on Net Flux

Depth	Waves	Currents	Flux (kg/m)
B1 (20.73 m)	B1	B1	29,300
B1 (20.73 m)	B1	E	60,000
E (17.07 m)	B1	B1	64,600
E (17.07 m)	B1	E	94,000
B1 (20.73 m)	E	B1	47,900
B1 (20.73 m)	E	E	74,800
E (17.07 m)	E	B1	75,900
E (17.07 m)	E	E	113,800

Decreased sediment transport with increased water depth leads one to expect that transport rates at ODMDS B will decrease as the crest elevation at Site B1 is reduced by erosion. To analyze the impact of reduced mound height on sediment transport, Site B1 Deployment 1 was simulated for water depths ranging from 15 to 50 m (50 to 165 ft). Current and wave inputs were not adjusted to account for changes in bathymetry. Figure 93 indicates that the effects of mound height on transport rate at Site B1 are significant. The transport rate at 15-m (50-ft) water depth is approximately two orders of magnitude greater than the rate for depth at mound crest of 50 m (165 ft). The modeling results indicate that as the crest height of a mound decreases, the rate of mound erosion will significantly decrease and the lower portion of the mound will remain as a quasi-permanent feature.

Sediment Transport Climate

The environmental climate of the Pacific Northwest coast varies significantly, both seasonally and annually. The data collected during tripod deployment can, at best, represent the environmental conditions and sediment transport for a single year. To reliably estimate long-term trends in ODMDS migration and dispersion, a longer-term estimate of sediment transport must be developed.

Before estimating the sediment transport climate for each site, a climate of environmental forces influencing transport is required. Specifically, tidal currents, Columbia River outflow, wind-driven currents, and wave conditions must be understood for long time periods. Searches of available data indicated that 12 years (1987-1998) of nearly continuous wind and wave conditions were available for the Pacific Northwest from the NDBC. The 12-year period for which NDBC data are available defines the period of development for the environmental forcings database and the transport climate.

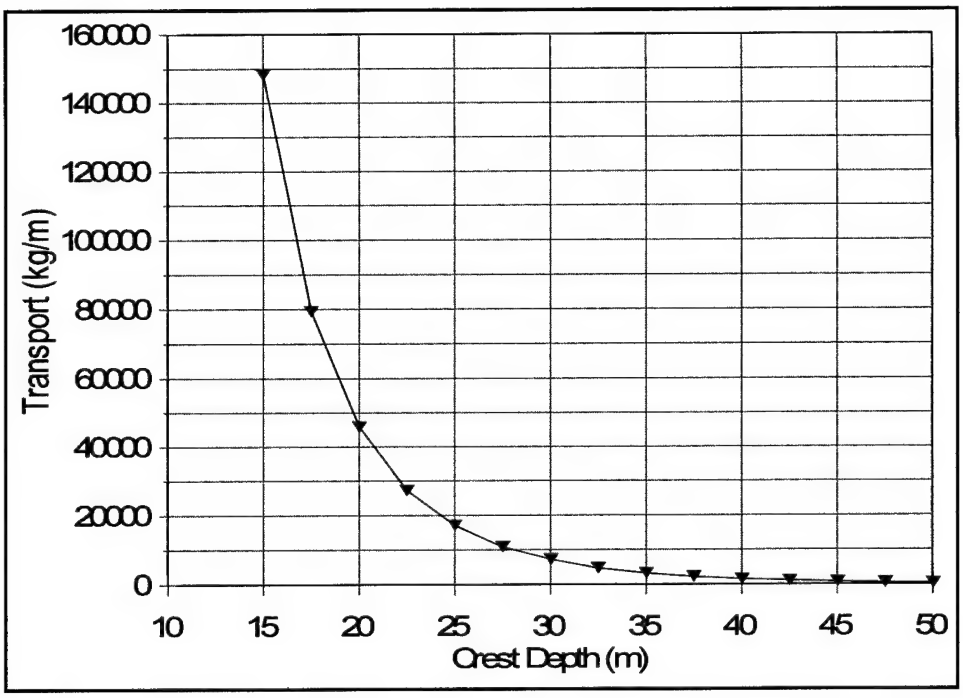

Figure 93. Predicted transport at Site B1 Deployment 1 as a function of depth to crest of mound (after Gailani and Smith, op. cit., p. 101)

12-Year artificial database

Data collected at the NDBC buoy near the MCR are not precisely located at the sites of interest, therefore wave modeling techniques were applied to translate the measurements at the buoy to the positions of Site B1 and ODMDS E. In addition, large-domain circulation models were used to estimate long-term wind-generated current conditions.

Wave condition database. NDBC maintains three buoys in the Pacific Northwest. Buoy 46029 is located just offshore of the MCR in 130-m (425-ft) water depth. The other two buoys are in similar water depths 145 km (90 miles) north of the MCR (NDBC 46041) and 165 km (100 mile) south of the MCR (NDBC 46050). These buoys record significant wave height, wave period, and wave direction, but each buoy did not operate continuously for the 12-year period. Data from buoy 46029 were assigned highest priority in populating the 12-year database. For periods when data from buoy 46029 were unavailable, data from the adjacent buoys populated the database.

Wave conditions at the buoy were transformed to the sites of interest using the spectral wave model STWAVE (Resio 1988a, 1988b; Smith et al. 1999). STWAVE is a steady-state, energy-balance, finite-difference numerical model of spectral wave propagation in the near-coastal zone. The model is capable of accepting arbitrary directional spectra at the offshore boundary. Spectral energy is propagated only in the half-plane directed toward shore and all energy propagating offshore is neglected. Wave propagation within the model is governed by linear theory with energy source/sink terms for wind, steepness-limited and

depth-limited wave breaking, nonlinear wave-wave interactions, and wave-bottom interactions. An 11.5- × 14.6-km (7.1- × 9.1-mile) grid with 100-m (330-ft) grid resolution was developed, and a representative set of 74 wave conditions was transformed from the 130-m (425-ft) depth at buoy 46029 to the tripod locations within the grid. The simulations resulted in a set of wave transformation coefficients and wave directions at each tripod for each of the representative offshore conditions.

Tidal and river currents. Flow from the Columbia River can influence currents at the two ODMDS, particularly ODMDS E. River outflow is controlled by a series of dams on the river and therefore does not vary as significantly as uncontrolled rivers. A 5-year database of flow rates measured at the Bonneville dam 240 km upstream of the mouth indicates variation in river discharge of less than an order of magnitude. In addition, the effects of the river at each site appeared to be consistent throughout each tripod deployment. Therefore, to include combined tidal and river currents at the site, a representative period of mean currents from the tripod deployments was selected and simply repeated throughout the simulations. The period selected for representation of the river currents was 20 April - 19 June 1999, during the higher flow spring freshet. This period represents two lunar cycles during which influences of wind on current were negligible.

Wind generated currents. As previously demonstrated, wind-driven currents can significantly influence bottom currents during storms. The highest rates of transport during tripod deployments frequently corresponded with high wind and wind-generated currents. Therefore, a reasonable estimate of wind-driven current magnitude, direction, and frequency is required for development of a synthetic current database. No long-term current data were available near the MCR, but buoys did provide a database of wind conditions. By applying 12-year database of winds within the ADCIRC global circulation model and neglecting tidal forcing, vertically averaged wind-generated currents were estimated for the 12-year period from 1987-1998.

Analysis of the tripod data indicates that not all wind-generated currents penetrate the entire water column. Light winds typically influence only the upper portion of the water column. Moderate winds generate bottom currents, but not of the same magnitude as in the upper water column. Strong winds develop an approximately uniform current profile through the water column. To represent these differences in wind-generated currents within the sediment transport models, the near-bottom currents were modified as necessary. Bottom currents were assumed to be zero during periods that ADCIRC-calculated, vertically averaged, wind generated currents were less than 20 cm per sec (0.7 ft per sec). Bottom currents were set to one-half the ADCIRC current when calculated values were 20-40 cm per sec (0.7-1.3 ft per sec). Bottom currents were set equal to ADCIRC-calculated, wind-generated, currents were greater than 40 cm per sec (1.3 ft per sec).

Verification of combined database. From the combined simulations and data, a 12-year synthetic database of wave and current conditions at each site was developed. Current fields were estimated by combining the tidal/river outflow database with the wind driven current model predictions. The databases were

then used to simulate 12 years of transport at each site. The sediments were assumed to be similar to MCR dredged material with a median grain size of 0.22 mm. In addition, water depth for the initial simulations was assumed to be the value measured during Deployment 2 (19.8 m (65 ft) at Site B1 and 17.1 m (56 ft) at ODMDS E). Sediment transport for the 12-year period was estimated using the VR1, VR2, AW, and WM methods.

Small errors in the synthetic database can result in significant variations in sand transport because of the nonlinear relationship between environmental conditions and sand transport. To verify correct application of the synthetic database, sand transport was estimated applying both the synthetic database and wave and current tripod measurements for Deployments 1 and 2. Figure 94 presents the VR1 sand transport estimates for Site B1, Deployment 1 for both the synthetic and measured environmental conditions. There is reasonable agreement between transport estimates from the measured and synthetic databases. Transport estimates for Site B1 and ODMDS E during Deployments 1 and 2 are given in Table 17, and suggest that the estimates from the synthetic and measured databases generally agree within 15 percent.

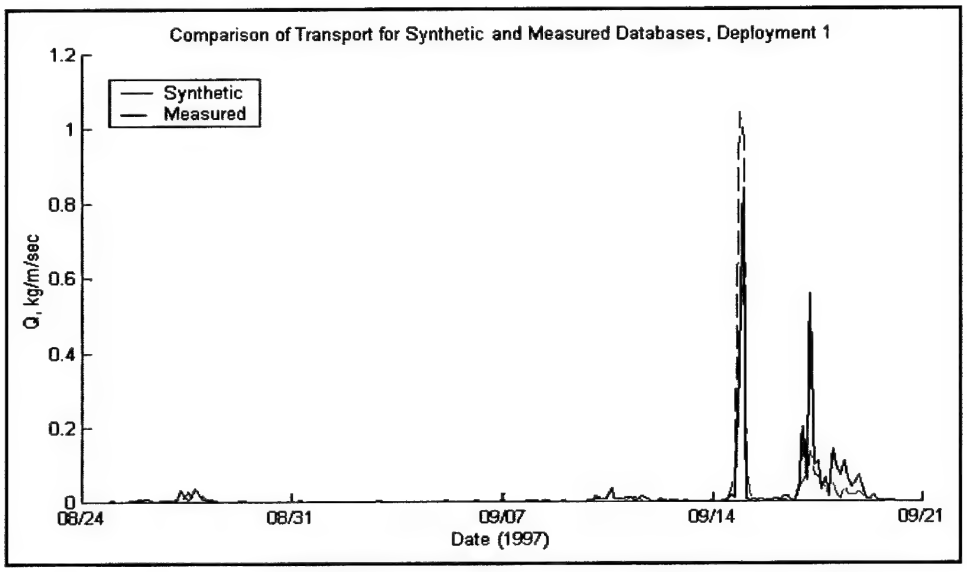

Figure 94. Comparison of sand transport estimates from measured and synthetic databases (after Gailani and Smith, op. cit., p. 101)

Table 17
Verification of Synthetic Databases

Location/ Deployment	Unit Flux, kg/m	
B1-1	Tripod	39,300
	Synthetic Database	37,700
B1-2	Tripod	29,300
	Synthetic Database	32,500
E-1	Tripod	380,600
	Synthetic Database	341,500
E-2	Tripod	90,900
	Synthetic Database	95,500

Further verification of the synthetic database was obtained by simulation of the period between bathymetric surveys. Morphology of the mound at Site B1 and directional distribution of sand transport were compared to assess whether the models correctly simulate transport direction. The period of time between summer 1997 and summer 1998 was established as the period of comparison because of available survey data and no disposal activity. The bathymetry change at Site B1, shown in Figure 95, indicates that the crest of the mound eroded as much as one meter or more and sediment appears to have been transported north and west, depositing in deeper water on the north slope of the mound. After applying the synthetic database to the four methods for estimating transport for the evaluation period, each method estimated dominant northward transport, with a smaller component of transport toward the west as indicated in the transport distribution of Figure 96. These transport directions are consistent with the bathymetric change estimated from surveys (Figure 95).

12-Year sediment transport climate

Each sediment transport method was applied to the 12-year environmental conditions developed for each site. Gross annual transport for the 12-year simulations for Site B1 and ODMDS E are shown in Figures 97 and 98, respectively. For any given year, transport estimates by the four methods can vary by as much as a factor of six, but usually the factor is three or less. As stated previously, data are not available to verify one model as being more accurate than another. The VR methods consistently predict greater transport than the WM and AW methods, with the VR1 method producing the greatest rate of transport. On an individual storm basis, the WM method often predicts transport magnitudes similar to the VR method, but both the WM and AW methods predict significantly less transport than VR during periods of combined high waves and low currents. Examples of this observation are given in Figure 90 during the 15 May 1998 storm at Site B1 and the 27 September 1997 storm at ODMDS E (Figure 14). During strong-current conditions, the AW and WM methods produce similar results as evidenced during the 17 September 1997 storm at Site E (Figure 91). As anticipated, each method estimates greater total transport at ODMDS E than at Site B1 by a factor of two or more.

Figures 99 and 100 indicate the direction of transport for the 12-year simulations for Site B1 and ODMDS E, respectively. The dominant direction of transport for each simulation method is to the north for ODMDS B and north-northeast for ODMDS E. At ODMDS E, this indicated that most of the disposed sediment will move into the littoral transport regime that nourishes beaches to the north. However, each model also predicted a modest transport to the southwest at ODMDS E, which may contribute to channel infilling. This result should be viewed in the context of seasonal changes in transport direction. Most south-directed transport occurs in late spring/early summer, after winter storms have moved most of the dredged material north of the ODMDS. At Site B1, the northward transport predictions are supported by surveys which indicated that the top of the mound is eroding, the area to the north and west of the mound is experiencing net accretion, and the area to the south is experiencing little change.

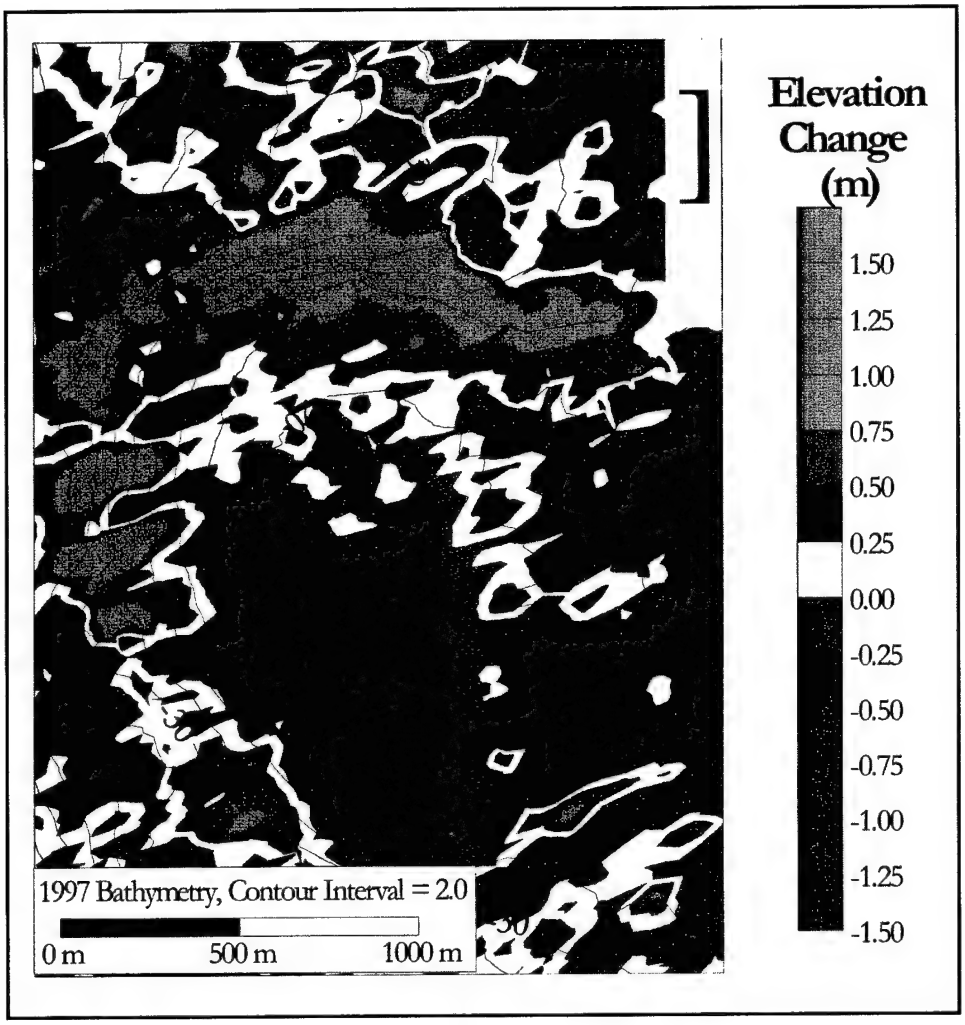

Figure 95. Bathymetry change at Site B1, summer 1997 – summer 1998 (after Gailani and Smith, op. cit., p. 101)

Analysis of Site M

Site M, a potential location for an additional ODMDS, is located southwest of the MCR in 35-m water depth (Figures 3 and 78). There is interest in estimating the dispersion of sediment placed at this location. Potential dispersion of sediments at Site M is estimated by comparing environmental conditions at tripod M to conditions at a location with known transport characteristics. Waves, currents, and suspended sediments were measured at similar water depths during Deployment 2 at tripod M (at Site M) and tripod B2 (at the seaward foot of the mound at ODMDS B, Figures 3 and 78). Assuming that the measurements at tripod B2 represent conditions at ODMDS B without the mound, the conditions at tripods B2 and Site M can be compared to determine if a mound constructed Site M will behave like the mound at ODMDS B.

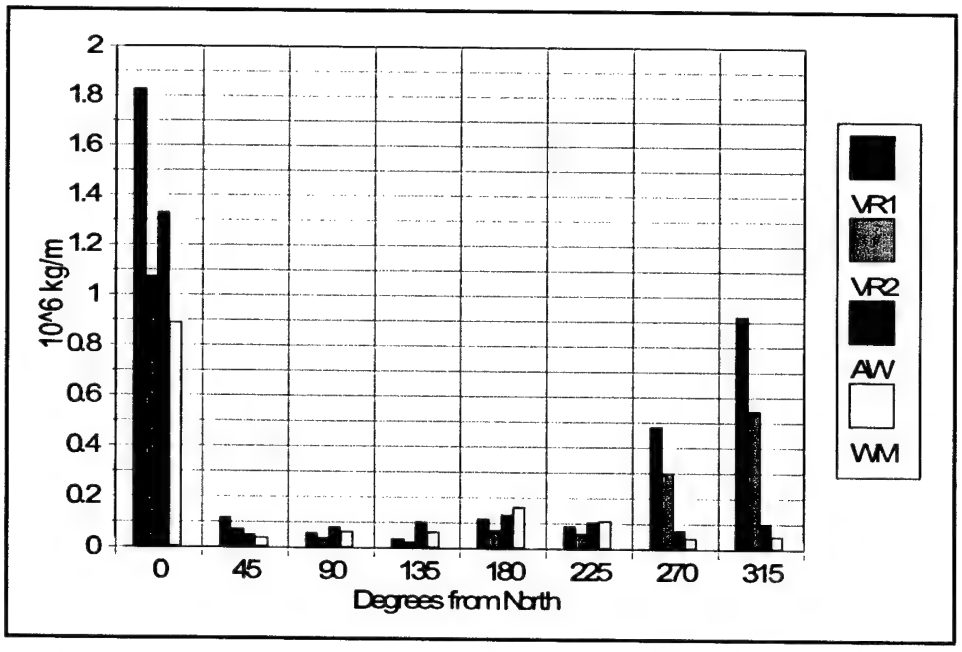

Figure 96. Predicted transport magnitude and direction, 1997-1998 (after Gailani and Smith, op. cit., p. 101)

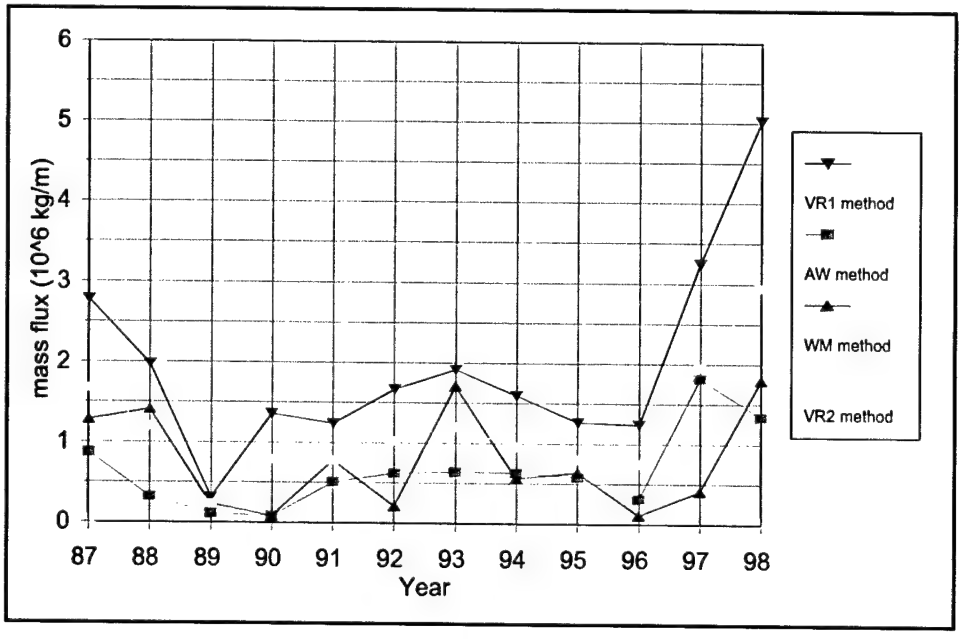

Figure 97. Predicted transport by each method for Site B1, 1987-1998 (after Gailani and Smith, op. cit., p. 101)

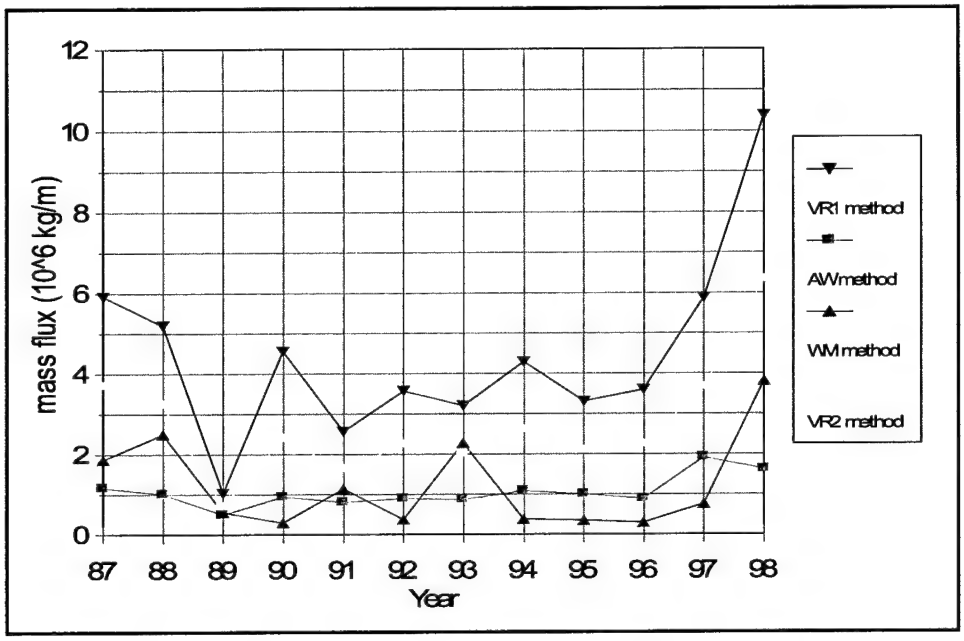

Figure 98. Predicted transport by each method for ODMDS E, 1987-1998 (after Gailani and Smith, op. cit., p. 101)

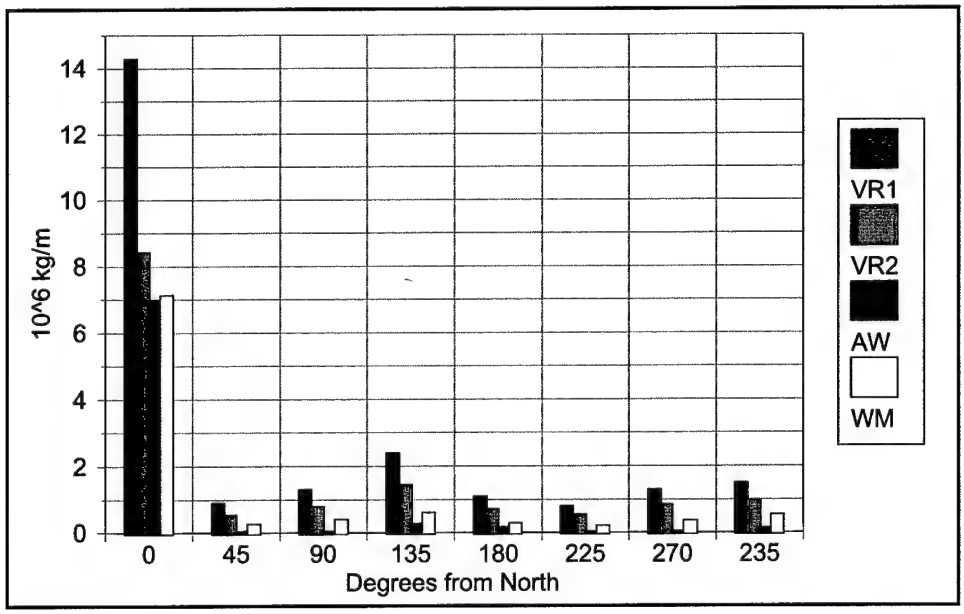

Figure 99. Predicted transport magnitude and direction from Site B1 for 12 years (after Gailani and Smith, op. cit., p. 101)

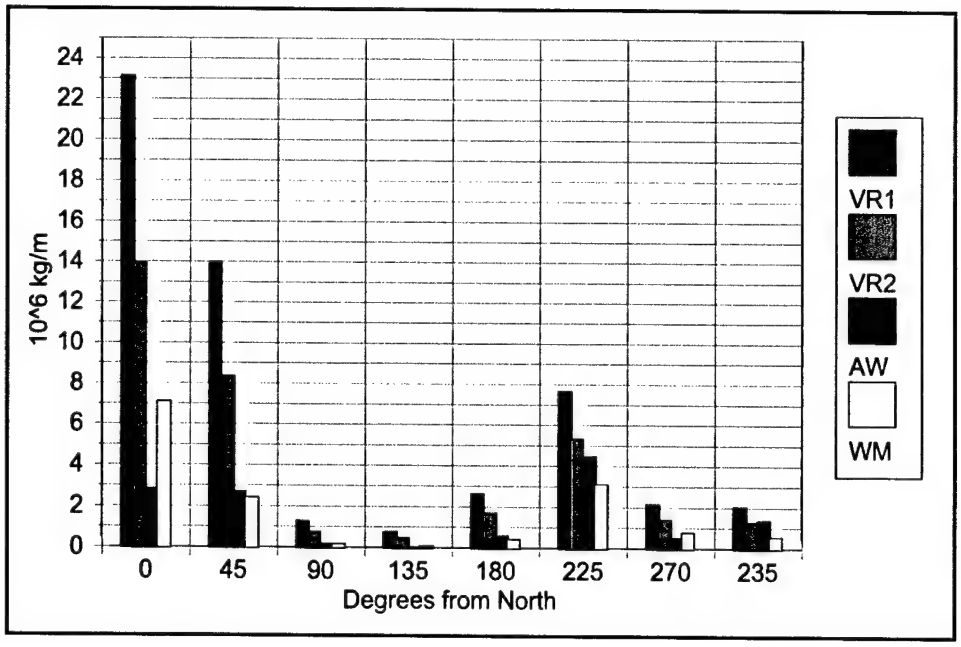

Figure 100. Predicted transport magnitude and direction from ODMDS E for 12 years (after Gailani and Smith, op. cit., p. 101)

Figure 101 compares wave and current conditions for tripods B2 and M. Wave conditions are nearly identical, but the currents at tripod M are consistently smaller than the currents at tripod B2. From this observation, the total transport at Site M is assumed less than transport from the mound at ODMDS B. Therefore, a mound constructed at Site M is expected to be less dispersive than the mound at ODMDS B.

To quantify transport at Site M, sediment transport for the period April - August 1998 was estimated from the Deployment 2 wave and current measurements collected at tripod M for a range of mound heights. Near-bottom current magnitudes were adjusted to account for reduced depth. The resulting transport estimates are shown in Figure 102. The sediment transport for a Site M mound crest depth of 20 m (65 ft) is approximately 15,000 kg per m (10,000 lb per ft), or one-half of the estimated 30,300 kg per m (20,100 lb per ft) (see Table 17) at ODMDS B during the same period. The differences in estimated transport suggest that a mound at Site M would disperse at approximately one-half the rate of a similar mound at ODMDS B.

Summary and Conclusions

Pressure, current, and suspended sediment data were collected during three deployments of instrumented tripods at the MCR ODMDS. These data collected during autumn 1997 and spring 1998 offer a unique and detailed record of wave, current, and suspended sediment processes. The data indicate that transport processes at ODMDS E are more active than at ODMDS B, which supports observations from surveys indicating ODMDS E is more dispersive.

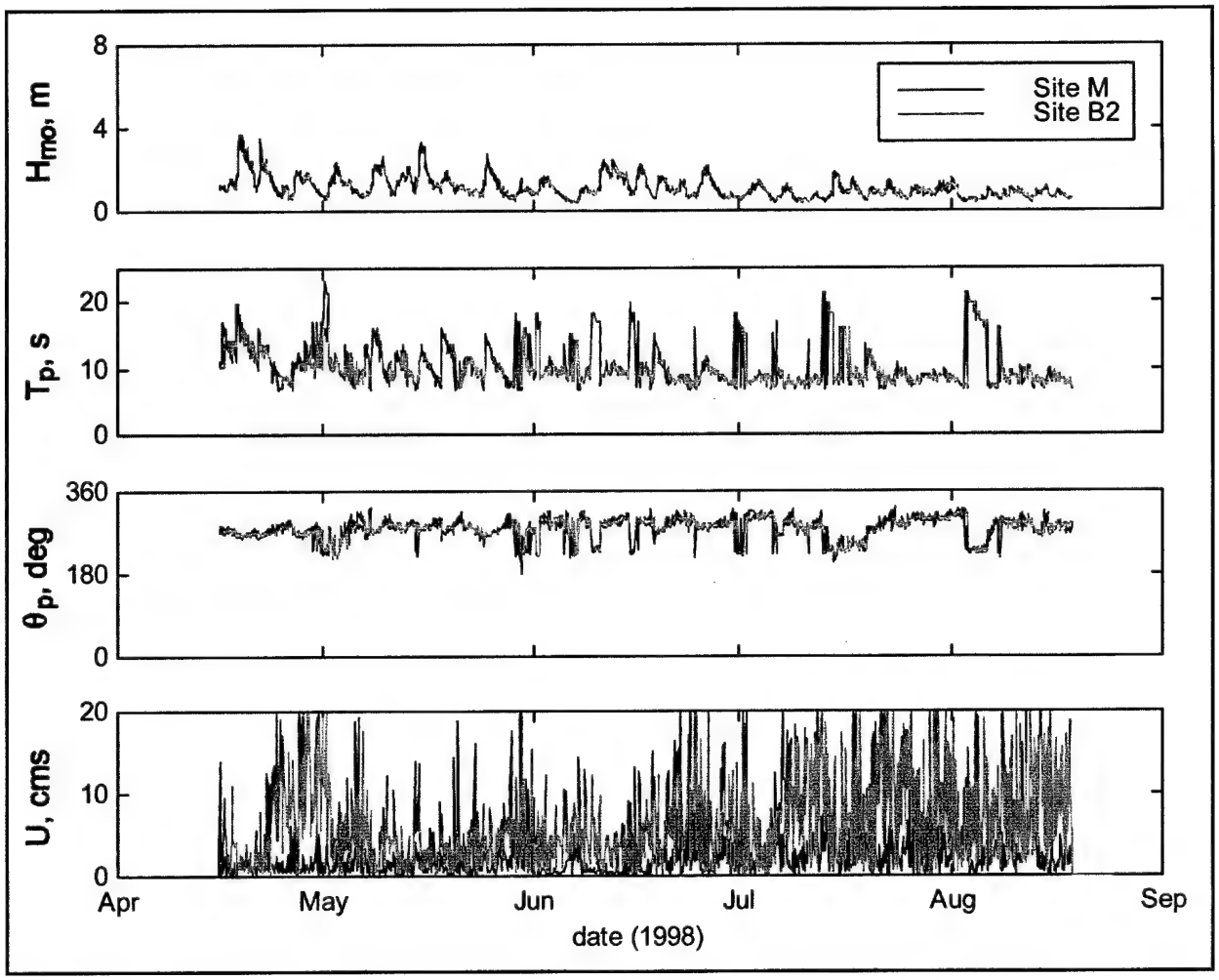

Figure 101. Environmental conditions at tripods B2 and M (after Gailani and Smith, op. cit., p. 101)

Three sediment transport methods were applied to simulate the periods of data collection. The methods applied were those of van Rijn (1993), Wikramanayake and Madsen (1994), and Ackers and White (1973). All methods performed reasonably well under most conditions and detailed conclusions are presented in the following paragraphs. Environmental conditions at the MCR have been observed to vary significantly both seasonally and annually. To estimate the long-term sediment transport climate, a 12-year synthetic database of wave and current conditions was developed from combined field measurements and numerical modeling. The sediment transport methods were then applied to the 12-year period of the developed database. The estimated sediment transport indicated significant variability in annual transport and a predominant transport direction to the north at ODMDS B and E.

Conclusions from this work can be separated into three categories: (a) management of ODMDS, (b) observations from data collection, and (c) indications from sediment transport modeling. Findings are summarized in the following sections.

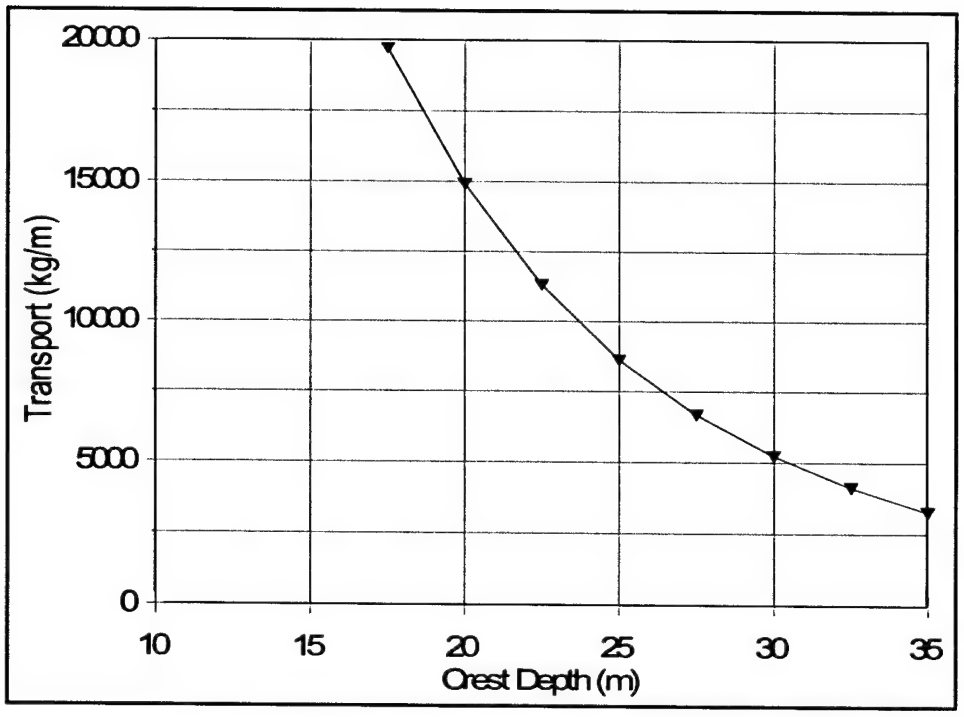

Figure 102. Predicted transport at Site M for Deployment 2 as a function of depth to crest of mound (after Gailani and Smith, op. cit., p. 101)

Management of ODMDS

a. Stronger currents and shallower water depths result in significantly greater transport at ODMDS E (and greater dispersion of sediments) compared to ODMDS B. Both ODMDS B and Site E are dispersive, but disposal rates greater than the dispersal rate will result in mound growth.

b. Transport modeling and general observation indicate that the environmental conditions and resulting sediment transport vary significantly on an annual basis. This variability must be recognized when managing annual volume of disposal for an ODMDS.

c. Modeling indicates that most sand transport at ODMDS E is directed to the north, away from the navigation channel. Most south-directed transport occurred during spring/summer, after the disposed dredging material is transported northward by winter storms.

d. Modeling and field data at ODMDS B indicate that transport at ODMDS B is north and north-northwest directed.

e. Screening-level evaluation at Site M suggests that dredged material placed at Site M will disperse at one-half the rate of ODMDS B.

Observations from data collection

a. The suspension of sand was well correlated to the passing of wave groups.

b. Although the data set provides an opportunity to identify conditions for sand suspension, a greater vertical density of measurements near the bed is required to estimate sediment transport rates.

c. Near bottom velocities at ODMDS B were not significantly influenced by increased river discharge. The strongest bottom currents at ODMDS B occur during storms as wind-generated currents, typically directed to the north.

d. Peak bottom velocities at ODMDS E corresponded to spring tides and were almost four times greater than peak bottom velocities at ODMDS B, which corresponded to strong-wind events.

e. Under similar environmental conditions, Deployment 2 suspended sediment concentrations were observed to be significantly larger than those of Deployment 1. This observation may imply temporal variation in sediment size at the site as the coarser dredged material is transported north during the winter season exposing the finer (and more easily suspended) native sediments.

f. The data set provides an excellent opportunity for further study of the influence of various forcings on noncohesive sediment suspension and transport processes. The data should be analyzed further and used for continued model development and validation.

Indications from sediment transport modeling

a. The models indicate that as the mound crest at ODMDS B continues to erode, transport of material from the mound will be reduced significantly. Long-term simulations of transport predicted by the methods were supported by field data, including bathymetric surveys.

b. In general, during strong-current events, the three methods predicted similar transport magnitudes. During high-wave events, the VR methods predicted greater transport than AW or WM.

c. The AW method incorporated into the DRP-developed FATE models is at least an order-of-magnitude more accurate than the other methods for the analyzed conditions.

d. Shallower depths and increased mean currents contribute significantly to greater transport rates at ODMDS E compared to ODMDS B.

e. Analysis of possible sediment disposal at Site M indicated that sediment placed at this site will disperse at approximately one-half the rate of ODMDS B and if used for significant disposal, mound accumulation can be expected.

f. The DRP-developed AW method performs reasonably well compared to the more complex methods for some storm conditions, but can miss transport under combined high wave and low current conditions. An indication of this method's shortcoming is the incorrect indication of net transport direction.

g. The AW method used in the FATE models estimated the least transport under most conditions simulated (Figure 97). However, under

strong-current conditions at the MCR, it predicted magnitudes of transport similar to the other methods. In addition, other studies have indicated that the FATE models were able to reasonably simulate mound migration in a moderate-wave environment (Scheffner 1996). The concern still exists that the FATE models may be underpredicting sand transport under certain conditions. It is reasonable to assume that under moderate wave and moderate-to-strong current conditions, the FATE models are providing reasonable estimates of transport, but under high wave conditions with low currents, the FATE models may provide transport estimates that are significantly lower than actual transport. One possible reason for these underestimations may be that transport due to wave asymmetry is not included in the AW formulation, implying that including this process in the FATE models would be beneficial.

7 Summary and Conclusions

Problem Statement

The entrance channel at the MCR requires annual dredging of 3 to 5 million cu m of fine-to-medium sand to maintain the navigation channel at the authorized depth. The sandy dredged material is placed in EPA approved ODMDS. Dredging at the MCR is performed by hopper dredge.

ODMDS A and B have been the primary locations where the MCR dredged material has been placed. The two ODMDS are located on the westward boundary of the ebb-tidal shoal, and are economical (in terms of haul distance) for disposal of sediments dredged from both the outer and inner bars at the MCR. Since 1992, ODMDS B has received most of the MCR dredged material as concerns arose that sediments deposited in ODMDS A were accumulating, creating an adverse wave climate, and might migrate northward back into the entrance channel.

ODMDS E and F have been used as secondary disposal sites for sediments dredged from the entrance channel at the MCR. The use of ODMDS E is partially in response to a 1979 request from the Washington Department of Ecology to enhance sand by-passing and retard erosion of the coastal beaches north of the MCR. Beginning in 1988, the volume of dredged material placed in ODMDS E was restricted to (0.77 million cu yd per year) to prevent dredged material accumulation (mounding) and limit transport of placed dredged material back into the MCR channel. ODMDS F has been used only recently.

Since 1986, dredged material placed within the designated ODMDS boundaries has accumulated at a rate much faster than the Portland District had anticipated when the disposal sites were formally designated. ODMDS, which were intended to be moderately dispersive and have a 20-year life cycle, reached capacity within 10 years of initial operation. ODMDS capacity can roughly be defined as that quantity of material that can be placed within the legally designated disposal site without extending beyond the site boundaries or interfering with navigation.

Exceedence of ODMDS capacity at the MCR creates two operational problems for the Portland District:

a. The overall footprint of disposed dredged material extends beyond the existing ODMDS formally permitted boundaries by as much 915 m (3,000 ft) in some cases.

b. Dredged material within the ODMDS has accumulated to such an areal and vertical extent that adverse sea conditions are created. In some cases, mounds rise 18.3 to 21.4 m (60 to 70 ft) above surrounding bathymetry. Mariners report that the ODMDS mounds cause waves to steepen and/or break in the vicinity of the sites, and that these wave conditions are hazardous to navigation.

Objectives of MCNP Monitoring at MCR

The objectives of the MCNP monitoring at the MCR were to:

a. Analyze existing data to document historic bathymetric response at the MCR entrance and the ODMDS due to anthropogenic and environmental conditions at the MCR.

b. Monitor selected MCR ODMDS locations to observe bathymetric response with respect to dredging disposal operations and the forcing environment.

c. Explain qualitatively and quantitatively the rates of sediment dispersion at the MCR ODMDS, and relate observed sediment dispersion to ODMDS siting and management practice.

d. Assess the suitability of new USACE Dredging Research Program sediment fate models (STFATE, LTFATE, and MDFATE) and RCPWAVE, and synthetically-generated input data from HPDPRE, HPDSIM, and ADCIRC for predicting sediment dispersion in the environment off the MCR.

e. Develop a standardized method for data collection and management that can be used by other Corps District offices using an ODMDS.

Study Approach

The inherent nature of an MCNP monitoring program implies that an extensive observational and data acquisition effort will be sustained for a significant period of time (3 to 5 years) to acquire new knowledge pertaining to the phenomena of interest. New field data were obtained by developing and placing four instrumentation tripods at pertinent locations on the ODMDS for three different critical deployment periods. While these new oceanographic forcing data and new hydrographic surveys were being obtained at the MCR, existing data sets and bathymetric surveys were studied and analyzed to formulate an understanding of the processes that have resulted in the existing condition at the ODMDS. These existing data and surveys provided guidance regarding regional sediment transport dynamics associated with natural processes. They also were used as input to wave and sediment fate numerical simulation models for estimating amplification of wave climate resulting from existing disposal mound geometry, and for deducing the ultimate disposition of material previously placed at the ODMDS.

The FATE models had previously suffered from a lack of quality field data for their calibration and verification. As the new MCNP data were being acquired and processed, enhancements to the FATE models were incorporated to ensure these models would accurately predict the ultimate disposition of future dredged material disposal at such exceedingly energetic locations. Finally, predictive techniques for determining sediment transport process under both waves and currents were developed to assess the movement of disposed material at the MCR for assessing capacity and to determine the useful life of the ODMDS. These techniques will assist in crucial decision-making for the management of dredged materials at navigation channels and harbors, including mound dispersal, channel infilling, and protective cap erosion.

This MCNP MCR study approach consisted of the execution of four fundamental tasks; (a) a regional coastal processes analysis, (b) oceanographic field data collection and analysis, (c) state-of-the-art numerical modeling, and (d) a comprehensive analysis of sediment transport processes.

Regional Processes

Methodology

There are data supporting net northward transport of sediment in the vicinity of the MCR. The erosion of beach and shoreface sand south of the south jetty may be related to blocking by the entrance jetties of southward-directed littoral material. However, this erosion could be related to a combination of factors, including reflection of waves arriving from southwest storms by the south jetty, causing large oblique angles to enhance southward sand movement and produce erosion. Detailed shoreline and bathymetric change analyses for the MCR and adjacent shelf and shoreline environments were conducted. Primary interest was sediment transport associated with wind- and wave-induced currents. Historical data sets included shoreline position from USC&GS maps, and bathymetry data from the USACE and the USC&GS. The analysis time period was from 1868 to 1994. Bathymetric surface models were developed for four historical time periods to evaluate regional sediment transport dynamics. Patterns of deposition and erosion relative to engineering activities were quantified to establish a framework upon which management strategies could be developed for dredged material disposal practices.

Conclusions

Shoreline change data for the periods 1868/74 to 1926 and 1926 to 1950/57 illustrate net shoreline advance throughout the study area. However, significant shoreline retreat zones occur along the northern 5 km (3 miles) of Clatsop Spit being up to 5.6 m per year (18.4 ft per year) and the northern 17 km (10.6 miles) of Long Beach Peninsula 3.6 m per year (11.8 ft per year); 1926 to 1950/57). From 1868/74 to 1950/57, average shoreline change north of the Columbia River entrance was 2.2 m per year (7.2 ft per year). South of the entrance jetty, net shoreline advance is documented at 5.5 m per year (18 ft per year).

Four distinct depositional trends were identified. (a) The modern ebb-tidal delta developed as a result of jetty construction. (b) The depocenter for sedimentation on the ebb shoal is to the north of center, and it migrates to the north with time. (c) Northward-directed sediment transport from the entrance resulted in net accretion along the shoreline and on the continental shelf seaward of Long Beach Peninsula. (d) Erosion south of the south jetty is the result of sediment blocking by the jetty and subsequent transport towards the ebb shoal and onto the continental shelf.

Large quantities of sediment have been deposited on the ebb-tidal delta, and redistribution of sediment from earlier ebb-shoal locations (1926 and 1958) is well-documented. The magnitude of sand transport and accretion north of the entrance supports previous study findings regarding net northward sediment transport from the Columbia River mouth. Two well-defined sediment accumulation zones exist as inshore fine sand deposits seaward of Long Beach Peninsula and an offshore silt deposit trending northwest from the ebb shoal.

Bathymetric comparisons with the 1988/94 surface document accumulation trends at ODMDS A and B. Although ODMDS A exists south of the designated channel, bathymetry and change data indicate that the site is too shallow and may be affecting flow from the entrance channel. The main channel appears to diverge when it encounters the mounds associated with ODMDS A. It is likely that on flooding tide, a substantial amount of sediment dumped at the site is mobilized and transported back into the lower estuary, potentially resulting in channel shoaling problems. Conversely, ODMDS B is in deeper water along the outer margin of the ebb shoal. Between 1958 and 1994, approximately 74 percent of disposal material stayed at the site, the remainder of which dispersed in a wider area around the site and/or is transported to the north to supply the continental shelf and beaches with sediment. ODMDS E has been used since 1973 as a disposal site for supplying beaches to the north of the north jetty with channel sand. Although most material was placed in this site prior to the 1990s, it continues to be used.

Given the dynamics of the area, it is suggested ODMDS E be utilized whenever possible to add sand to the littoral system. Although beaches to the north of the entrance have been experiencing accretion throughout the period of record, a 17-km (10.6-mile) length of coast north of this accretion zone has been expanding to the south with time. The problem is chronic and would be best mitigated with sediment added to the system. Assuming ODMDS E is not overfilled, it would seem cost-effective to dispose of sandy sediment at this site to nourish beaches to the north. Furthermore, because erosion along beaches of Clatsop Spit can be associated with blocking of sediment from the river by the south entrance jetty, it would be reasonable to establish a disposal site in this area to fortify beaches. Assuming the operation to be cost-effective relative to other sites, this disposal practice could reduce the need for ODMDS A.

Field Data Collection and Analysis

Methodology

For some locations such as the MCR, dangerously energetic surf is normal. Here, the USACE contracted with OSU to design, construct, deploy, and retrieve four data collection open frame tripod platforms for the acquisition of necessary environmental data pertaining to conditions at the MCR ODMDS. Each of the four tripod platforms was outfitted with Doppler wave and current sensors, temperature, pressure, and salinity sensors, and OBS that measure suspended sediment concentrations. The three deployment periods were (a) Deployment 1: 19 August – 09 October 1997, (b) Deployment 2: 15 April – 24 August 1998, and (c) Deployment 3: 27 November 1998 – 01 March 1999. The four tripod platforms were located at Sites B1, B2, E, and M.

This MCNP study at the MCR also developed techniques for using helicopters to accomplish the data-collection mission. While not actually used for data acquisition at the MCR, this methodology will be exceedingly useful for future long-term management of ODMDS nationwide.

Conclusions

Frequency distributions of wave and wind conditions were computed to compare the environmental climate of the periods of data collection at the MCR to longer-term averages. All data included in the frequency histograms come from a merged database of conditions from three NDBC buoys located off the Pacific Northwest coast during the 12-year period from January 1987 through April 1999. Distributions for the period of tripod deployment are determined from the buoy data for the specific time of instrument deployment and distributions for the 12-year data are compiled from data with calendar dates corresponding to the deployment of interest.

An evaluation of the current data collected at Sites B1, B2, and E during the 19 August – 09 October 1997 deployment was performed by OSU. Site E was located closest to the terminus of the Columbia River and the north jetty, and was in the shallowest location. Conversely, Site B1 was farther offshore and deeper, and Site B2 was several miles from the jetties and located in water nearly twice as deep as the other two sites.

Site E demonstrates the greatest variability in both velocity magnitude and current direction during this time period, and also the greatest velocity magnitude, being approximately 225 cm per sec (7.38 ft per sec), or 4.3 knots. The normal mean velocity for the record is approximately 50 cm per sec (1.64 ft per sec), or 1 knot during this time period, and the corresponding direction is towards the west-southwest, which corresponds closely to the river channel orientation in that region.

Further offshore at Site B1, a decrease in the variability of current velocity and direction and a decrease in the occurrence of extreme velocity events were observed. In this instance, the median velocity once again appeared to

correspond to approximately 50 cm per sec (1.64 ft per sec). In regards to current direction, there appeared to be a strong westerly current and a strong northerly component. The response at Site B1 follows inferred behavior. The further progression offshore accounts for decreasing velocities due to flow expansion. The current direction, rotating from west-southwest at Site E to west at Site B1 also demonstrates a consistent pattern that could be the result of tidal current interactions with local longshore currents, the latter directed south to north for fall storm conditions.

Site B2 shows a continuing decrease in extreme current velocities and an apparent decrease in the median current at the site, approximately 40 cm per sec (1.31 ft per sec), or 0.75 knots.

OBS measure the reflection of emitted radiation off of solids suspended in the water column, regardless of the source of reflection (sand, fine particles, organic material, biological fouling, aquatic organisms, etc.). Assuming that fine particles that result in turbidity are well-mixed and do not settle rapidly and that sand particles are suspended and settle out intermittently, a defined level of background turbidity can be established and subtracted from the indicated OBS signal. A method was developed to identify OBS signals consistent with the suspension of sand from the orbital velocities of passing waves.

Inspection of the data sets at ODMDS B and E indicated that concentration signals at the two locations were quite different. ODMDS E included numerous high concentration bursts that were less frequent at ODMDS B. This is consistent with bathymetry data described earlier which indicate that ODMDS E is more dispersive. However, there may be other reasons for these high concentrations. The elevation of the dredged material configuration at ODMDS E is only 1-2 m (3.3-6.6 ft) above the finer native sediments. OBS measurements at ODMDS E may therefore include suspension of the finer native sediments. In addition, bathymetry data indicate that dredged material placed at ODMDS E generally disperse within 1 year of placement, so only small quantities of the 0.22-mm dredged sediment may have remained at ODMDS E during portions of the two deployments. At ODMDS B, the OBS is atop a 21-m (70-ft) mound created exclusively of the coarser MCR-dredged material, which isolates the measurements from suspension of the finer native material.

Numerical Modeling

The DRP developed several sediment fate numerical simulation models (STFATE, LTFATE, MDFATE, HPDPRE, HPDSIM, and ADCIRC) to enhance and improve the reliability of long-term site management of ODMDS. The numerical simulation modeling objectives of this MCNP monitoring at the MCR were all accomplished and included: (a) verifying the applicability of the DRP numerical models for the evaluation of ODMDS, (b) assessing the data collection needs for site evaluation by the DRP models; (c) identifying the capabilities and limitations of the DRP models and; (d) developing a systematic methodology for the application of the DRP models at other Corps districts. A wave transformation numerical simulation model (RCPWAVE) was also applied at the MCR to ascertain the extent of wave height amplification and resulting hazards to

navigation by the MCR ODMDS. Numerical model verification significantly contributed to attaining the MCNP study objectives of development of a standardized method for data collection and ODMDS management that can be used by other Corps District offices. The very high quality field data obtained during this MCNP monitoring provided the opportunity to better understand sediment suspension and seabed change under highly energetic oceanographic process of combined waves and currents. Specific studies are summarized in the following paragraphs.

Sediment suspension at MCR

Methodology. Seabed sediment suspension due to the presence of waves and currents at the MCR was investigated. Relevant data were measured at ODMDS B, instrumentation tripod platform Site B1, 6 km (3.7 miles) offshore of the MCR in a water depth of 18.3 m (60 ft) with seabed sediment composed of fine to medium sand. The analyses addressed the effect on bottom sediment (sand) when waves and currents interact along the seabed of an ebb-tidal shoal. Special considerations included (a) assessing the modification of waves by current, (b) describing the spectral relationship between bottom current and peak sediment suspension, and (c) investigating wave group effects.

Conclusions. Laboratory-quality wave, current, and suspended sediment data were acquired at a highly energetic prototype setting on top of an ebb-tidal shoal in 18-m water depth at the MCR. Data collected during August-September 1997 were utilized to investigate how current can affect the quality of wave statistics derived from PUV data, and the frequency domain (spectral) response of a sandy seabed to the processes of waves and currents.

The presence of a strong current greater than 50 cm per sec (1.64 ft per sec) through the water column can affect PUV measurements used to describe short-wave statistics. The effect can be up to 25 percent for H_{mo}. Whenever PUV measurements are proposed for observing waves within the inner shelf where depth = 3-40 m (10-130 ft), concurrent measurement of water column current (via ADP) should be seriously considered. The technological advancement and affordability of ADPs makes their use highly effective.

During August-September 1997, the suspension of seabed sediment at Site B1 was dominated by wave processes and secondarily by processes governed by mean bottom current. Spectral decomposition of measured bottom current and suspended sediment (OBS) indicated a range of suspended sediment response to wave action: Grouping only (47 percent); Grouping + Wave (34 percent); Grouping + Wave + 2nd harmonic (12 percent). At Site B1, the coherence between either ADV-RMS or ADV-"with wave" vs. OBS exceeded 0.5 for about 60 percent of all wave bursts. This indicates that transport of sand suspended by wave action occurred 60 percent of the time during data collection.

Oceanographic processes and seabed change at MCR

Methodology. Oceanographic processes at the MCR were correlated with seabed changes that occurred at ODMDS Sites B1, B2, and E during Deployment 1 (19 August – 22 September 1997). Based on the textural variation of bottom sediment at the MCR, both suspended and bed-load aspects of sediment transport were measured to fully describe sediment response versus environmental forcing.

Conclusions. The magnitude of seabed change was compared via computer correlation to the forcing environment at three MCR monitoring sites during 20 August-10 October 1997. Whether or not observed seabed change was positive (accretion) or negative (erosion) was taken as not relevant; only that there was an observed change was important. The time period of correlation analysis for each site was with respect to 20 August 1998: Site B1 = days 3-27; Site B2 = days 11-50; and Site E = days 3-32.

The cross-correlation of lag 0 for the magnitude of wave action versus seabed response was large (0.46-0.66) indicating that these two parameters were correlated simultaneously in time. Cross-correlations of lags 1 and 2 (for wave magnitude vs. seabed change) were moderate, but the trend decreased rapidly with increasing lag. On the average, there is some effect for the delayed response of seabed change due to wave magnitude. Cross-correlation for the difference in wave action versus seabed change was moderate, with lag 1 being slightly higher than lags 0 or 2 at Sites E and B1. This indicates that a sudden change in wave height (either increase or decrease) may have affected the seabed, and in the case of Sites B1 and E, the seabed response lagged behind the change in wave height. The cross-correlation of lag 0 for the magnitude of bottom current vs. seabed response was low (0.13-0.31), indicating that these two parameters were weakly correlated in time. Correlation of lags greater than 1 quickly decayed toward 0 indicating, that once bottom currents subside, seabed change diminishes. The difference in mean bottom current vs. seabed change did not cross-correlate well, indicating that a sudden change in bottom current speed does not dictate a seabed response.

Although correlation does not prove causation, serial correlation results obtained for Sites B1, B2, and E strongly indicate that during 20 August-10 October 1997, the response of the seabed at these sites was affected primarily by wave processes and secondarily by bottom current processes.

Effect of ODMDS A and B on wave climate (1994 bathymetry)

Methodology. The presence of large underwater mounds at the existing MCR ODMDS exacerbates wave amplification to the point of breaking, and adversely impacts marine safety with resulting hazards to navigation. The numerical simulation wave model RCPWAVE was used to predict behavior of waves as they are shoaled, refracted, and diffracted by the bathymetry that the waves pass over. RCPWAVE was used to compare the MCR wave climate due to the present (1994) ODMDS bathymetry with the wave climate due to past (1985) bathymetry before prominent mounds were formed at the ODMDS.

Conclusions. The existing dredged material mounds at ODMDS A and B increased the height of incident waves within or in proximity to the ODMDS by 30 percent for 6-sec waves, 60 percent for 10-sec waves, and 80 percent for 16-sec waves, compared to 1985. A 10 percent increase in wave height due to shoaling could cause a wave to break. The areas most affected by dredged material mounds at ODMDS A and B are located immediately north and south of the MCR entrance.

Presently, the safest ocean approach to the MCR entrance channel is directly in-line with ODMDS F. The present wave condition at the MCR requires that strict site management measures be implemented to (a) prevent additional mounding at ODMDS A and B, and (b) prevent the formation of new mounds at ODMDS F which could adversely affect incoming waves to the MCR.

FATE model simulations at ODMDS B (1994 bathymetry)

Methodology. To avoid placement of dredged material at ODMDS A and F, approximately 3.3 million cu m (4.3 million cu yd) of sandy dredged material were assumed to be placed at ODMDS B during 1995. STFATE was used to predict the bathymetric distribution (footprint) of dredged material after it passed through the water column, on an individual dump (disposal vessel load) basis. LTFATE and MDFATE were then used to predict the bathymetry at the MCR ODMDS B resulting from a series of dumps and simulate long-term change (sediment transport) of the resultant bathymetry. MDFATE can be used to simulate a disposal operation that could extend over a year and consist of hundreds of dumps. The model accounts for the overall disposal operation and environmental parameters such as waves, tides, and currents. Waves and currents are incorporated to account for the sediment transport processes affecting the short- and long-term fate of the dredged material placed in open water.

Conclusions. For similar operating conditions (vessel speed, water depth, and still water), the larger the disposal vessel capacity, the higher the resultant mound footprint. For average operating conditions in 15 m (50 ft) of water depth, the dredge *Essayons* will produce a deposition mound 0.15 m (0.5 ft) high. The *Padre Island* and *Newport* will produce a mound 0.09 and 0.11 m (0.30 and 0.35 ft) high, respectively.

The most significant parameter affecting mound geometry (length and height) is disposal vessel speed, assuming that the time required to empty a given disposal vessel remains constant. Reducing vessel speed during material release from 3 knots (3.5 mph) to 0 knots (0 mph) increases mound height by a factor of 4 for all the dredges (*Essayons, Newport*, and *Padre Island*).

For dredges that are moving while dumping, increasing the water depth by a factor of 3 from 15 m (50 ft) to 45 m (150 ft) decreases disposal mound height for a single dump by a factor of 0.5 for the dredge *Essayons,* and by a factor of 0.7 for the dredges *Padre Island* and *Newport*.

Mound length is directly related to disposal vessel speed and dump duration. For normal operating conditions, the *Essayons* produces a dump footprint about

855 m (2,800 ft) long, while the *Newport* and *Padre Island* produce a dump footprint about 365 m (1,200 ft) long. For stationary dumps, footprint length is the same as the width, and is directly related to water depth. For a stationary dump in 15-m (50-ft) water depth, the average footprint width and length are about 75 m (250 ft) each. For a 45-m (150-ft) water depth, the footprint width and length are about 150 m (500 ft) each.

For vessels moving while dumping, mound width also is directly related to water depth, but at a decreasing proportionality. Increasing water depth by a factor of 3 from 15 m (50 ft) to 45 m (150 ft) increases footprint width by a factor of 2, from 75m (250 ft) to 150 m (500 ft). Mound width for the split-hull hopper dredges is typically 60-120 m (200-400 ft) wider than for the multiple-bin door hopper dredges. This is primarily due to the larger hull opening for the split-hull dredges and the slower vessel speeds at which the split-hull dredges were modeled at 2 knots (2.3 mph) vs. the multiple bin door hopper dredges of 3 knots (3.5 mph).

The U-turn course of dredges while dumping at the MCR ODMDS should be incorporated into the MDFATE simulation model to accurately account for a shortened disposal lane.

Overall bathymetric impacts to ODMDS B should not be significant due to the proposed disposal operation. The largest increase in bathymetric relief is 7 m (23 ft), near the northwest end of ODMDS B.

Based on the MDFATE results, it was not advisable to continue the proposed disposal operation at ODMDS B for additional years past 1995. Mounding would be rapid and might worsen wave conditions at the site. The problem area (high point) associated with the existing mound at ODMDS B would not be made worse by the proposed disposal operation as long as disposal was limited to the western half of ODMDS B and material was evenly distributed. The existing mound at ODMDS would experience additional increase along the western and northwestern areas due to the 1995 disposal operation.

Disposal direction plays an important role in confining dredged material disposal within the formal site boundaries. The southeast approach direction assumed for this investigation produces the best case for keeping material within ODMDS B. Temporary acquisition of a placement buffer extending 230 m (750 ft) beyond the existing site boundaries would prevent dredged material from being placed outside of ODMDS B.

Dredged material placed in the western half of ODMDS B for 1995 would not experience any significant long-term movement except during severe storm events. What is placed there will essentially stay there. This is due to the significant water depths along the western part of ODMDS B of 43 m (140 ft), compared to the depth at the top of the existing mound of 15-18 m (50-60 ft).

The MDFATE predicted postdisposal bathymetry was compared to the bathymetry resulting from the actual disposal operation conducted in 1994. The maximum mound height for the actual disposal operation (1994) was approximately 3.1-3.7 m (10-12 ft). The maximum mound height for the simulated

MDFATE (1995) run was 7 m (23 ft), which is about twice as high as that of the 1994 post-disposal bathymetry. This would be expected since the 1995 operation was intended to place about twice the volume in ODMDS B than had taken place in 1994. The most significant difference between the predicted and actual cases is the steepness of the post-disposal bathymetry. The bathymetric gradient for the actual post-disposal bathymetry was approximately one-half that of the predicted case. A better estimate is needed for the avalanching angles of dredged material.

FATE Model and RCPWAVE model simulations at ODMDS F (1995 bathymetry)

Methodology. In 1996, the MCR ODMDS A, B, and E could accept only limited amounts of dredged material. Excluding ODMDS F, the total capacity of the MCR ODMDS could decrease to 0.77 million cu m per year (1 million cu yd per year) after 1997. The annual volume of sediment dredged from the MCR project and placed in ODMDS varied from 3.1-3.8 million cu m per year (4-5 million cu yd per year). Given the capacity limitations on the MCR ODMDS, ODMDS F would be expected to receive as much as 3.1 million cu m per year after 1996. To confidently rely on ODMDS F to handle present and future MCR dredging disposal requirements, the capacity of ODMDS F (for 1996 and beyond) was assessed with respect to impacts on navigation. Predicted changes in wave height at ODMDS F in 1996 due to mound formation resulting from disposal since the 1995 baseline condition were evaluated by RCPWAVE.

Conclusions. At the beginning of the 1996 dredging season, the remaining capacity for the southeastern half of ODMDS F was approximately 2.3 million cu m (3 million cu yd). A disposal sequence would fill the southeastern half of ODMDS F. After 1996, the total volume of dredged material placed in the southeastern half of ODMDS F was expected to be 6.8 million cu m (8.9 million cu yd) from 1989-1996, assuming 2.3 million cu m (3 million cu yd) was added in 1996. Conducting dredged material disposal in the southeastern half of ODMDS F in excess of 2.3 million cu m (3 million cu yd) total beginning with 1996 disposal, would likely result in increased wave conditions up to 30 percent for 16-sec period waves (far above the 10 percent criteria), according to RCPWAVE.

Dredged material placed in ambient water depths at ODMDS F at -30 to -55 m (-100 to -180 ft mllw) would not significantly disperse in the long-term time-frame. Material placed within ODMDS F stays there. This was concluded from LTFATE calculations for dredged material behavior at ODMDS F. USACE could not risk negatively impacting navigation at or near ODMDS F. The water depths at that location would preclude any dredge from reworking placed dredged material to mitigate for inadvertent mounding problems caused by dredging disposal.

ODMDS F is in the direct line of approach to the MCR entrance channel. Bar pilots use the area as a staging location for transferring pilots to vessels of commerce. ODMDS A and B have been used to an extent such that safe navigation is presently impaired at or near those ODMDS, due to significant

mounding and related wave conditions. If similar conditions were created at ODMDS F, overall navigation at MCR would be impaired.

FATE model and RCPWAVE model simulations at expanded ODMDS B and E (1996 bathymetry)

Methodology. During site assessment studies in 1966, the only feasible option for providing an additional 2.3-3.1 million cu m per year (3-4 million cu yd per year) disposal capacity for the MCR navigation project was to temporarily expand existing ODMDS. STFATE simulations were conducted for the disposal of dredged material from two types of hopper dredges; (a) a split-hull hopper dredge (*Newport*), and (b) a multiple bottom door hopper dredge (*Essayons*). The long-term fate of dredged material to be placed within the expanded ODMDS B and E was assessed using LTFATE and MDFATE. Transport of sediment off the dredged material mounds was simulated for a period of 1 year. Changes in wave height at the MCR due to bathymetric changes mounding) at the expanded ODMDS B and E were estimated using RCPWAVE. The mounded configuration accounts for 15.3 million cu m (20 million cu yd) of dredged material placed within the expanded ODMDS B and E. To permit disposal of this volume of material without negatively affecting the wave environment due to mounding, it was recommended that the site's boundaries be significantly expanded beyond the initially proposed configuration.

Conclusions: Results of LTFATE and MDFATE modeling at expanded ODMDS B. LTFATE simulation results for the expanded ODMDS B indicate that the spring and summer seasons produce little sediment transport 13,000 cu m (17,000 cu yd) or mound movement (less than 0.02 m (0.5 ft) mound height reduction). The winter storm season produces appreciable sediment transport of 1.12 million cu m (1.47 million cu yd) or 8 percent of the total mound volume on dredged material mounds at ODMDS B. The largest changes in mound geometry apply to the shallow water area of the ODMDS where mound height erosion was 1.8 m (6 ft) while the entire mound was initially 2.4 m (8 ft) in some locations. Based on the simulation results, the shallow water area of expanded ODMDS B had favorable potential for dispersing placed dredged material and reintroducing dredged sediments into the littoral zone.

Conclusions: Results of LTFATE and MDFATE modeling at expanded ODMDS E. Long-term fate results for expanded ODMDS E clearly indicate that this site is dispersive in terms of transport of dredged material placed on the seabed. For July-October, movement of sediment of 122,400 cu m (160,000 cu yd) of the 0.77 million cu m (1 million cu yd simulated) was to the southwest, mound height erosion was 0.6 m (2 ft) for the 1.2-m- (4-ft-) high mound, and net aggregate mound movement was 305 m (1,000 ft) toward the southwest. For November-June, significant sediment movement of 0.5 million cu m (0.66 million cu yd) of the 0.77 million cu m (1 million cu yd) simulated was to the north, mound height erosion was 1.1 m (3.5 ft), and net aggregate mound movement was 215 m (700 ft) toward the north. Given the amount of sediment transport predicted for 1 year, it appears that 0.77 million cu m (1 million cu yd)

of dredged material could be dispersed annually at ODMDS E. The direction of sediment transport during the summer is toward the southwest.

A southwest transport direction would disperse placed dredged material back into the navigation channel. Dredged material is not placed at ODMDS E during early to later summer, due to migration of the material back into the MCR navigation channel. During the winter and spring season, a 1.2-m- (4-ft-) high dredged material mound at ODMDS E would be dispersed toward the north, away from the navigation channel and onto Peacock Spit.

The increase in wave height (amplification) from the baseline bathymetric condition to the mounded condition was determined by RCPWAVE. Amplification of wave height greater than 10 percent over the baseline bathymetric condition was considered unacceptable. For both 10- and 16-sec period waves, the 10 percent criterion will be exceeded within the expanded ODMDS B by the mounded bathymetry. Both the deepwater and shallow-water mounds of 4.9-m- (16-ft-) and 2.4-m- (8-ft-) high, respectively, within ODMDS B contribute to exceedence of the wave criterion. The 1.2-m- (4-ft-) high mound within ODMDS E does not significantly affect the wave environment at the MCR.

Based on the previous wave analysis results, it is recommended that 15.3 million cu m (20 million cu yd) of dredged material not be placed (over a 5-year time span) within the expanded boundaries of ODMDS B as initially proposed.

Conclusions: Recommended revised expansions of ODMDS B and E. To permit disposal of 15.3 million cu m (20 million cu yd) of dredged material in ODMDS B without negatively affecting the wave environment due to mounding, the site's boundaries must be expanded beyond the initially proposed configuration. The optimal configuration for ODMDS B would be to additionally expand the site seaward in the same manner as was initially proposed for the landward expansion. The revised expanded ODMDS B would be composed of two distinct zones; (a) an offshore zone situated in water depth 50-67 m (160-220 ft) and (b) a nearshore zone situated in water depth 15-50 m (50-160 ft).

FATE model simulations at expanded ODMDS E (1998 bathymetry)

Methodology. FATE model simulations of dredged material deposited at ODMDS E that is located near the north jetty and adjacent to the navigation channel were conducted using 1998 bathymetry. Environmental data from Deployment 2 (15 April-24 August 1998) was utilized. Since one of the governing parameters in an efficient dredging disposal program is minimization of the haul distance for the dredge, disposal sites such as ODMDS E can be very advantageous. In contrast to the more oceanward sites, ODMDS E is believed to be current- rather than wave-dominated and has been very dispersive in past disposal operations. The energetic dispersiveness of the site, however, also represented an extreme test of the robustness of the DRP FATE models. This study addressed a predictive 2-month application of the FATE models at ODMDS E using oceanographic data that were collected at the same time as the dredge disposal operation.

Conclusions. The DRP FATE models (STFATE, LTFATE, and MDFATE) were all found to be applicable at a high energy, current-dominated site. To correctly simulate the sediment deposition on the seabed, the current profile for both the STFATE and LTFATE model applications required modifications from the full depth-averaged current profile typically used. Although it was possible to simulate the general footprint and centroid of sediment distribution, the total volume reaching the seabed was simulated to be higher than actual measurements indicated. Further research into model parameters and input data that control dispersion and final deposition of material on the seabed is recommended. Those parameters should include percent stripping, critical shear stress, turbulent diffusion parameter, and the collapse entrainment parameter.

Analysis of Sediment Transport Processes, ODMDS B, E, and M

Methodology

Predictive techniques for determining environmental conditions and sediment transport processes under both waves and currents were developed to assess the movement of disposed material at the MCR ODMDS B and E. These techniques assist in determining crucial information for the management of dredged materials at navigation channels and harbors, with implications pertaining to mound dispersal, channel infilling, and protective cap erosion. The potential transport climate at proposed ODMDS M was also analyzed. The data indicate that transport processes at ODMDS E are more active than at ODMDS B, which supports observations from surveys indicating ODMDS E is more dispersive.

Three sediment transport methods were applied to simulate the time periods of data collection. The methods applied to simulate sediment transport by both waves and currents were those of van Rijn (VR, 1993), Wikramanayake and Madsen (WM, 1994), and Ackers and White (AW, 1973). All methods performed reasonably well under most conditions. Environmental conditions at the MCR vary significantly both seasonally and annually. To estimate the long-term sediment transport climate, a 12-year synthetic database of wave and current conditions was developed from combined field measurements and numerical modeling. The sediment transport methods were then applied to the 12-year period of the developed database. The estimated sediment transport indicated significant variability in annual transport and a predominant transport direction to the north at ODMDS B and E.

Conclusions

Conclusions from this work can be separated into three categories, (a) management of ODMDS, (b) observations from data collection, and (c) indications from sediment transport modeling.

Management of ODMDS. Stronger currents and shallower water depths result in significantly greater transport at ODMDS E (and greater dispersion of

sediments) compared to ODMDS B. Both ODMDS B and Site E are dispersive, but disposal rates greater than the dispersal rate will result in mound growth. Transport modeling and general observation indicates that the environmental conditions and resulting sediment transport vary significantly on an annual basis. This variability must be recognized when managing annual volume of disposal for an ODMDS.

Modeling indicates that most sand transport at ODMDS E is directed to the north, away from the navigation channel. Most south-directed transport occurred during spring and summer, after the disposed dredging material is transported northward by winter storms. Modeling and field data at ODMDS B indicate that transport at ODMDS B is north and north-northwest directed. Screening-level evaluation at Site M suggests that dredged material placed here will disperse at one-half the rate of ODMDS B.

Observations from data collection. The suspension of sand was well correlated to the passing of wave groups. A greater vertical density of measurements near the bed is required to estimate sediment transport rates.

Near bottom velocities at ODMDS B were not significantly influenced by increased river discharge. The strongest bottom currents at ODMDS B occur during storms as wind-generated currents, typically directed to the north. Peak bottom velocities at ODMDS E corresponded to spring tides and were almost four times greater than peak bottom velocities at ODMDS B, which corresponded to strong-wind events.

Under similar environmental conditions, Deployment 2 suspended sediment concentrations were observed to be significantly larger than those of Deployment 1. This observation may imply temporal variation in sediment size at the site as the coarser dredged material is transported north during the winter season exposing the finer (and more easily suspended) native sediments. The data set provides an excellent opportunity for further study of the influence of various forcings on noncohesive sediment suspension and transport processes.

Indications from sediment transport modeling. The models indicate that as the mound crest at ODMDS B continues to erode, transport of material from the mound will be reduced significantly. Long-term simulations of transport predicted by the methods were supported by field data, including bathymetric surveys.

In general, during strong-current events, the three methods predicted similar transport magnitudes. During high-wave events, the VR methods predicted greater transport than AW or WM. The AW method is at least an order-of-magnitude more accurate than the other methods for the analyzed conditions. The AW method performs reasonably well compared to the more complex methods for some storm conditions, but can miss transport under combined high wave and low current conditions.

Shallower depths and increased mean currents contribute significantly to greater transport rates at ODMDS E compared to ODMDS B. Analysis of possible sediment disposal at Site M indicated that sediment placed at this site

will disperse at approximately one-half the rate of ODMDS B and if used for significant disposal, mound accumulation can be expected.

The AW method used in the FATE models estimated the least transport under most conditions simulated. However, under strong-current conditions at the MCR, it predicted magnitudes of transport similar to the other methods. Other studies have indicated that the FATE models were able to reasonably simulate mound migration in a moderate-wave environment. Concern still exists that the FATE models may be underpredicting sand transport under certain conditions. It is reasonable to assume that under moderate wave and moderate-to-strong current conditions, the FATE models are providing reasonable estimates of transport, but under high wave conditions with low currents, the FATE models may provide transport estimates that are significantly lower than actual transport. One possible reason for these underestimations may be that transport due to wave asymmetry is not included in the AW formulation. Including this process in the FATE models would probably be beneficial.

References

Ackers, P., and White, W. R. (1973). "Sediment transport, new approach and analysis," *Journal of the Hydraulics Division,* American Society of Civil Engineers 99(HY11), 2041-2060.

Adams, K. T. (1942). *Hydrographic manual.* U.S. Department of Commerce, Coast and Geodetic Survey, Special Publication 143, 940 pages.

Anders, F. J., and Byrnes, M. R. (1991). "Accuracy of shoreline change rates as determined from maps and aerial photographs," *Shore and Beach* 59(1), 17-26.

Bagnold, R. A. (1966). "An approach to the sediment transport problem from general physics," U.S. Geological Survey Professional Paper 422-I, Washington, DC.

Ballard, R. L. (1964). "Distribution of beach sediment near the Columbia River," Technical Report No. 98, University of Washington, Department of Oceanography, Seattle, WA.

Barnes, C. A., Duxbury, A. C., and Morse, B. A. (1972). "Circulation and selected properties of Columbia River effluent at sea." *The Columbia River estuary and adjacent waters, bioenvironmental studies.* A. T. Pruter and D. L. Alverson, eds., 41-80, University of Washington Press, Seattle, WA.

Beach, R. A., and Sternberg, R. W. (1988). "Suspended sediment transport in the surf zone, response to cross-shore infragravity motion," *Marine Geology* 80, 61-79.

Bijker, E. W. (1971). "Longshore transport computations," *Journal of the Waterway, Harbors, and Coastal Engineering* ASCE, 99(WW4), 88-97.

Bokuniewicz, H., Gilbert, J., Gordon, R. B., Higgins, J. L., Kaminsky, P., Pilbeam, C. C., Reed, M., and Tuttle, C. (1978). "Field study of the mechanics of the placement of dredged material at open-water disposal sites," Technical Report D-78-7, U.S. Army Engineer Waterways Experiment Station, Vicksburg, MS.

Borgeld, J. C. (1978). "A geological investigation of the sedimentary environment at sites E, G, and H, near the Mouth of the Columbia River," Department of Oceanography, University of Washington, Seattle, WA. Final Report to U.S. Army Engineer District, Portland, Portland, OR.

Borgman, L. E., and Scheffner, N. W. (1991). "Simulation of time sequences of wave height, period, and direction," Technical Report DRP-91-2, U.S. Army Engineer Waterways Experiment Station, Vicksburg, MS.

Bourke, R. H., and Glenne, B. (1971). "The nearshore physical oceanographic environment of the Pacific Northwest coast," Report 71-45, Oregon State University, Corvallis, OR.

Brownlie, W. R. (1981). "Prediction of flow depth and sediment discharge in open channels," Report KH-R-43A, W. M. Keck Laboratory of Hydraulics and Water Resources, California Institute of Technology, Pasadena, CA.

Byrnes, M. R., and Hiland, M. W. (1994a). "Shoreline position and nearshore bathymetric change," "Kings Bay coastal and estuarine monitoring and evaluation program; Coastal studies," N. C. Kraus, L. T. Gorman, and J. Pope, eds. Technical Report CERC-94-09, Coastal Engineering Research Center, Vicksburg, MS.

_____. (1994b). "Compilation and analysis of shoreline and bathymetry data (Appendix B)," "Kings Bay coastal and estuarine monitoring and evaluation program: Coastal studies," N. C. Kraus, L. T. Gorman, and J. Pope, eds., Technical Report CERC-94-09, Coastal Engineering Research Center, Vicksburg, MS.

Byrnes, M. R., and Li, F. (2001). "Regional analysis of sediment transport and dredged material dispersal patterns, Columbia River mouth, Washington/ Oregon, and adjacent shores," Final Report, Applied Coastal Research and Engineering, Inc. Prepared for U.S. Army Engineer Research and Development Center, Vicksburg, MS.

Crowell, M., Leatherman, S. P., and Buckley, M. K. (1991). "Historical shoreline change: Error analysis and mapping accuracy," *Journal of Coastal Research* 7(3), 839-852.

Ebersole, B. A. (1984). "Refraction-diffraction model for linear water waves," *Journal of Waterway, Port, Coastal, and Ocean Engineering,* American Society of Civil Engineers.

Ebersole, B. A., Cialone, M. A., and Prater, M. D. (1986). "Regional coastal processes numerical modeling system; Report 1: RCPWAVE, a linear wave propagation model for engineering use," Technical Report CERC-86-4, U.S. Army Engineer Waterways Experiment Station, Vicksburg, MS.

Einstein, H. S. (1950). "Estimating quantities of sediment supplied by streams to a coast," *Proceedings of the International Conference on Coastal Engineering.* 137-139.

Ellis, M. Y. (1978). *Coastal mapping handbook.* U.S. Department of the Interior, Geological Survey, U.S. Department of Commerce, National Ocean Service, Washington, DC.

Englund, F., and Fredsoe, J. (1976). "A sediment transport model for straight alluvial channels," *Nordic Hydrology* 7, 293-306.

Graig, R., and Team, W. (1985). "Surfzone and nearshore surveying with helicopter and a total station," *Proceedings, U.S. Army Corps of Engineers Survey Conference.* U.S. Army Engineer Waterways Experiment Station, Vicksburg, MS.

Gross, M. G., and Nelson, J. L. (1966). "Sediment movement on the continental shelf near Washington and Oregon," *Science* 154, 879-880.

Hallermeier, R. J. (1981). "Terminal settling velocity of commonly occurring sands," *Sedimentology* 28, 859-865.

Hayes, M. O., and Kana, T. W. (1976). "Terrigenous clastic depositional environments," Technical Report CRD-11, Department of Geology, University of South Carolina, Columbia, SC.

Headquarters, U.S. Army Corps of Engineers. (1977). Monitoring completed navigation projects; engineer and design, ER 1110-2-8151, Washington DC.

Hench, J. L., Luettich, R. A., Westerink, J. J., and Scheffner, N. W. (1994). "ADCIRC, an advanced three-dimensional circulation model for shelves, coasts, and estuaries; Report 6: Development of a tidal constituent database for the eastern North Pacific," Technical Report DRP-92-6, U.S. Army Engineer Waterways Experiment Station, Vicksburg, MS.

Hubbell, D. W., and Glenn, J. L. (1973). "Distribution of radionuclides in bottom sediments of the Columbia River estuary," Professional Paper 433-L, U.S. Geological Survey, Washington DC.

Huyer, A., and Smith, R. L. (1977). "Physical characteristics of Pacific Northwest coastal waters," *The Marine and Plant Biomass of the Pacific Northwest Coast,* R. W. Krauss, ed., Oregon State University, Corvallis, OR.

Jensen, R., and Hubertz, J. (1989). "Pacific coast hindcast phase III wave information," WIS Report No. 17, U.S. Army Engineer Waterways Experiment Station, Vicksburg, MS.

Johnson, B. H. (1992). "Numerical disposal modeling," Dredging Research Technical Notes DRP-1-02, U.S. Army Engineer Waterways Experiment Station, Vicksburg, MS.

Johnson, B. H., and Fong, M. T. (1995). "Development and verification of numerical models for predicting the initial fate of dredged material disposed in open water; Report 2: Theoretical developments and verification," Technical Report DRP-93-1, U.S. Army Engineer Waterways Experiment Station, Vicksburg, MS.

Johnson, B. H., McComas, D. N., McVan, D. C., and Trawle, M. J. (1993). "Development and verification of numerical models for predicting the initial fate of dredged material disposed in open water; Report 1: Physical model tests of dredged material disposal from a split-hull barge and a multiple bin vessel," Technical Report DRP-93-1, U.S. Army Engineer Waterways Experiment Station, Vicksburg, MS.

Karlin, R. (1980). "Sediment sources and clay mineral distribution off the Oregon coast," *Journal of Sedimentary Petrology* 50(2), 543-560.

Koh, R. C. Y. and Chang, Y. C. (1973). "Mathematical model for barged ocean disposal of waste," Technical Series EPA 660/2-73-029, U.S. Environmental Protection Agency, Washington, DC.

Komar, P. D., and Li, M. Z. (1991). "Beach placers at the Mouth of the Columbia River, Oregon and Washington," *Marine mining* 10(2), 171-187.

_____. (1986). "Pivoting analyses of selective entrainment of sediments by shape and size with application to gravel threshold," *Sedimentology* 33, 425-436.

Lee, B. W. (1990). "Wave-current interaction, the equivalent uniform current," M.S. thesis, University of Liverpool, Liverpool, U.K.

Lockett, J. B. (1967). "Sediment transport and diffusion, Columbia River estuary and entrance," *Journal of the Waterways and Harbors Division,* ASCE, 93(WW4), 167-175.

Luettich, R. A., Jr., Westerink, J. J., and Scheffner, N. W. (1992). "ADCIRC, an advanced three-dimensional circulation model for shelves, coasts, and estuaries; Report 1, Theory and methodology for ADCIRC-2DDI and ADCIRC-3DL," Technical Report DRP-92-6, U.S. Army Engineer Waterways Experiment Station, Vicksburg, MS.

Lund, C. R., Sollitt, C. K., Dibble, T. L., Hollings, W. H., and Standley, D. R. (1999). "Analysis of currents at the mouth of the Columbia River dredged material disposal sites, Oregon State University, Corvallis, OR," Prepared for U.S. Army Engineer Waterways Experiment Station, Vicksburg, MS, and U.S. Army Engineer District, Portland, Portland, OR.

Madsen, O. S., and Wikramanayake, P. N. (1991). "Simple models for turbulent wave/current bottom boundary layer flow," Contract Report DRP-91-1, U.S. Army Engineer Waterways Experiment Station, Vicksburg, MS.

McGehee, D. D., and Mayers, C. J. (2000). "Deploying and recovering marine instruments with a helicopter," Technical Note ERDC/CHL CETN-VI-34, U.S. Army Engineer Research and Development Center, Vicksburg, MS.

McGehee, D. D., and Welp, T. L. (1994). "Helicopter deployment of oceanographic instruments," Video File No. 94039, U.S. Army Engineer Waterways Experiment Station, Vicksburg, MS.

McManus, D. A. (1972). "Bottom topography and sediment texture near the Columbia River mouth." *The Columbia River estuary and adjacent waters, bioenvironmental studies.* A. T. Pruter, and D. L. Alverson, ed., University of Washington Press, Seattle, WA.

Moritz, H. R. (1994). "User's guide for the multiple dump fate model," Final Report to U.S. Army Engineer Waterways Experiment Station, Vicksburg, MS.

Moritz, H. P., Kraus, N. C., and Siipola, M. D. (1999). "Simulating the fate of dredged material, Columbia River, USA," *Coastal Sediments '99. Proceedings of the 4th International Symposium on Coastal Engineering and Science of Coastal Sediment Processes.* Long Island, NY.

Moritz, H. R., Kraus, N. C., Hands, E. B., and Slocum, D. B. (1999). "Correlating oceanographic processes with seabed change, Mouth of the Columbia River, USA," *Coastal Sediments '99. Proceedings of the 4th International Symposium on Coastal Engineering and Science of Coastal Sediment Processes.* Long Island, NY.

Moritz, H. R., and Randall, R. E. (1995). "Simulating dredged material placement at open water disposal sites," *Journal of Waterway, Port, Coastal, and Ocean Engineering* 121(1).

Moritz, H. R., Smith, J. W., Kraus, N. C., and Gailani, J. Z. (2000). "Bottom sediment suspension due to wave-current effects at the Mouth of the Columbia River, USA," *Coastal Engineering 2000. Proceedings of the 27th International Conference on Coastal Engineering.* Sydney, Australia.

Morse, B. A., Gross, M. G., and Barnes, C. A. (1968). "Movement of seabed drifters near the Columbia River," *Proceedings of the American Society of Civil Engineers. Journal of Waterways and Harbors* 99(WW1), 91-103.

Neal, V. T. (1972). "Physical aspects of the Columbia River and its estuary." *The Columbia River estuary and adjacent waters, bioenvironmental studies.* A. T. Pruter, and D. L. Alverson, ed., University of Washington Press, Seattle, WA.

Nielsen, P. (1985). *Coastal bottom boundary layers and sediment transport.* World Scientific Publishing, River Edge, NJ.

Paroscientific Web Site. (1998). *http://www.paroscientific.com/*, Redmond, WA.

Poindexter-Rollins, M. E. (1990). "Methodology for analysis of subaqueous mounds," Technical Report D-90-2, U.S. Army Engineer Waterways Experiment Station, Vicksburg, MS.

Pollock, C.E. (1995). "Effectiveness of spur jetties at Siuslaw River, Oregon; Report 2: Localized current patterns by spur jetties, airborne current measurement system, and prototype/physical model correlation," Technical Report CERC-95-14, U.S. Army Engineer Waterways Experiment Station, Vicksburg, MS.

Reinson, G. E. (1992). "Transgressive barrier islands and estuarine systems." *Facies models, response to sea level change.* R. G. Walker and N. P. James, ed., Geological Association of Canada, 179-194.

Resio, D. T. (1988a). "A steady-state wave model for coastal applications," *Proceedings of the 21st Coastal Engineering Conference.* ASCE, New York, NY.

_____. (1988b). "Shallow water waves II—Data Comparisons," *Journal of the Waterway, Port, Coastal, and Ocean Engineering*, ASCE, 114, 50-65.

Roy, E. H., Creager, J. S., Gelfenbaum, G. R., Sherwood, C. R., and Stewart, R. J. (1982). "An investigation to determine the sedimentary environments near the entrance to the Columbia River," Final Report, U.S. Army Engineer District, Portland, Portland, OR.

Roy, E. H., Creager, J. S., Walter, S. R., and Borgeld, J. C. (1979). "An investigation to determine the bedload and suspended sediment transport over the outer tidal delta and moniter the sediment environment at sites E and D near the mouth of the Columbia River entrance," Final Report, U.S. Army Engineer District, Portland, Portland, OR.

Scheffner, N. W. (1996). "Systematic analysis of long-term fate of disposed dredged material." *Journal of the Waterways, Harbors, and Coastal Engineering Division,* ASCE, 122(3), 127-133.

Scheffner, N. W., Thevenot, M. M., Tallent, J. R., and Mason, J. M. (1995). "LTFATE, a model to investigate the long-term fate and stability of dredged material disposal sites: User's guide," Instruction Report DRP-95-1, U.S. Army Engineer Waterways Experiment Station, Vicksburg, MS.

Shalowitz, A. L. (1964). *Shoreline and sea boundaries, Volume 2.* U.S. Department of Commerce, Publication 10-1, U.S. Coast and Geodetic Survey, Washington, DC.

Sherwood, C. R. (1989). "Use of sediment transport calculations in dredged material disposal site selection," Battelle Marine Sciences Laboratory, Sequim, WA.

Sippola, M. D. (1992). "Reconnaissance level benthic infaunal, sediment, and fish study, offshore from the Columbia River, July 1992," U.S. Army Engineer District, Portland, Portland, OR, and U.S. Environmental Protection Agency, Region 10, Seattle, WA.

Siipola, M. D., and Braun, E. P. (1995). "Management/monitoring program for the ocean dredged material disposal sites of the U.S. Army Corps of Engineers, Portland District," U.S. Army Engineer District, Portland, Portland, OR.

Siipola, M. D., Emmett, R. L., and Hinton, S. A. (1993). "Tongue Point monitoring program 1989-1992," Final Report, U.S. Army Corps of Engineers, Portland District/National Oceanic and Atmospheric Administration, National Marine Fisheries Service, Northwest Fisheries Science Center, Coastal Zone and Estuarine Studies Division, Seattle, WA.

Smith, J. M., Resio, D. T., and Zundel, A. K. (1999). "STWAVE, steady-state spectral wave model; Report 1: User's manual for STWAVE version 2.0," Instruction Report CHL-99-1, U.S. Army Engineer Waterways Experiment Station, Vicksburg, MS.

Sobey, E. J. B. (1977). "The response of Oregon shelf waters to wind fluctuations, differences and the transition between winter and summer," Ph.D. diss., Oregon State University, Corvallis, OR.

SonTek. (1997a). "Acoustic doppler profiler operation manual," San Diego, CA.

_____. (1997b). "Acoustic doppler velocimeter operation manual," San Diego, CA.

Sternberg, R. W. (1986). "Transport and accumulation of river-derived sediment on the Washington continental shelf, USA," *Journal of the Geological Society of London* 143(6), 945-956.

Sternberg, R. W., Creager, J. S., Glassley, W., and Johnson, J. (1977). "Aquatic disposal field investigations at the Columbia River disposal site, Oregon; Appendix A: Investigation of the hydraulic regime and physical nature of bottom sedimentation," Technical Report D-77-30, U.S. Army Engineer Waterways Experiment Station, Vicksburg, MS.

Sternberg, R. W., Creager, J. S., Johnson, J., and Glassley, W. (1979). "Stability of dredged material deposited seaward of the Columbia River mouth." Palmer, H. D. and Gross, M. G., eds., *Ocean Dumping and Marine Pollution; Geological Aspects of Waste Disposal*, 17-49.

Stevenson, M. R., Gravine, R. W., and Wyatt, B. (1974). "Lagrangian measurements in a coastal upwelling zone off Oregon," *Journal of Physical Oceanography* 4(3), 321-336.

Swart, D. H. (1976). "Predictive equations regarding coastal transports," *Proceedings of the International Conference on Coastal Engineering.* 1,431-1,456.

Teeter, A. M., and Pankow, V. W. (1989). "Schematic numerical modeling of harbor deepening effects on sedimentation, Charleston, SC," Miscellaneous Paper HL-89-7, U.S. Army Engineer Waterways Experiment Station, Vicksburg, MS.

U.S. Army Engineer District, Portland. (1960). "Summary of interim report on 1959 current measurement program, Columbia River mouth at Oregon and Washington," Portland, OR.

_____. (1995a). "Ocean dredged material disposal at the Mouth of the Columbia River, Year 1, Monitoring of Completed Coastal Projects," Portland, OR.

_____. (1995b). "Simulation of dredged material disposal at Coos Bay ocean dredged material disposal site "*F*", Portland, OR.

_____. (1998). "Integrated feasibility report for channel improvements and environmental impact statement, Columbia River and Lower Willamette River Federal navigation channel; Vol. 1, Appendix H," Portland, OR.

U.S. Army Engineer District, Portland/U.S. Environmental Protection Agency. (1997). "Utilization of existing MCR ODMDS and proposed expansion of sites "B" and "E"," Final Report, USAED, Portland, and U.S. Environmental Protection Agency, Region 10, Portland, OR.

van Rijn, L. C. (1989a). "Sediment transport: Part I, Bed load transport," *Journal of Hydraulic Engineering* 110(10), 1431-1456.

_____. (1989b). "Sediment transport: Part II, Suspended load transport," *Journal of Hydraulic Engineering* 110(11), 1613-1641.

_____. (1993). *Principles of sediment transport in rivers, estuaries and coastal seas*. Aqua Publications, Amsterdam, The Netherlands.

Vincent, C. W., and Green, M. O. (1990). "Field measurements of suspended sand concentration profiles and fluxes, and of the resuspension coefficient over a rippled bed," *Journal of Geophysical Research* 95(C7), 11,591-11,601.

Westerink, J. J., Blain, C. A., and Scheffner, N. W. (1994). "ADCIRC, An advanced three-dimensional circulation model for shelves, coasts, and estuaries; Report 2, User's manual for ADCIRC-2DDI," Technical Report DRP-92-6, U.S. Army Engineer Waterways Experiment Station, Vicksburg, MS.

Whetten, J. T., Kelly, J. C., and Hanson, L. G. (1969). Characteristics of Columbia River sediment and sediment transport, *Journal of Sedimentary Petrology* 39, 1149-1166.

Wikramanayake, P. N., and Madsen, O. S. (1994a). "Calculation of suspended sediment transport by combined wave-current flows," Contract Report DRP-94-7, U.S. Army Engineer Waterways Experiment Station, Vicksburg, MS.

_____. (1994b). "Calculation of movable bed friction factors," Contract Report DRP-94-5, U.S. Army Engineer Waterways Experiment Station, Vicksburg, MS.

_____. (1994). "Calculation of suspended sediment transport by combined wave-current flows," Contract Report DRP-94-7, U.S. Army Engineer Waterways Experiment Station, Vicksburg, MS.

REPORT DOCUMENTATION PAGE

Form Approved
OMB No. 0704-0188

1. REPORT DATE *(DD-MM-YYYY)*	2. REPORT TYPE	3. DATES COVERED *(From - To)*
July 2003	Final report	

4. TITLE AND SUBTITLE

Monitoring Dredged Material Disposal at Mouth of Columbia River, Washington/Oregon, USA

5a. CONTRACT NUMBER

5b. GRANT NUMBER

5c. PROGRAM ELEMENT NUMBER

6. AUTHOR(S)

Joseph Z. Gailani, Jarrell W. Smith, Nicholas C. Kraus, David D. McGee, Edward B. Hands, Charles J. Mayers, Hans R. Moritz, Heidi P. Moritz, Mark D. Siipola, Daryl B. Slocum, Mark R. Byrnes, Feng Li, Terence L. Dibble, William H. Hollings, Christian R. Lund, Charles K. Sollitt, David R. Standley

5d. PROJECT NUMBER

5e. TASK NUMBER

5f. WORK UNIT NUMBER
11M12

7. PERFORMING ORGANIZATION NAME(S) AND ADDRESS(ES)

See reverse.

8. PERFORMING ORGANIZATION REPORT NUMBER

ERDC/CHL TR-03-5

9. SPONSORING / MONITORING AGENCY NAME(S) AND ADDRESS(ES)

U.S. Army Corps of Engineers
Washington, DC 20314-1000

10. SPONSOR/MONITOR'S ACRONYM(S)

11. SPONSOR/MONITOR'S REPORT NUMBER(S)

12. DISTRIBUTION / AVAILABILITY STATEMENT

Approved for public release; distribution is unlimited.

13. SUPPLEMENTARY NOTES

14. ABSTRACT

The entrance channel at the Mouth of the Columbia River requires annual dredging of 3 to 5 million cu m (3.9 to 6.5 million cu yd) of fine-to-medium sand to maintain the navigation channel at the authorized depth. The sandy dredged material is placed in EPA-approved Ocean Dredged Material Disposal Sites (ODMDS). Exceedance of ODMDS capacity at the Mouth of the Columbia River creates two operational problems for the Portland District: (a) The overall footprint of disposed dredged material extends beyond the existing ODMDS formally permitted boundaries by as much as 915 m (3,000 ft) in some cases, and (b) dredged material within the ODMDS has accumulated to such an aerial and vertical extent that adverse sea conditions are created. In some cases, mounds rise 18.3 to 21.4 m (60 to 70 ft) above surrounding bathymetry. Mariners report that the ODMDS mounds cause waves to steepen and/or break in the vicinity of the sites, and that these waves conditions are hazardous to navigation.

The objectives of the MCNP monitoring at the Mouth of the Columbia River were to: (a) analyze existing data to document historic bathymetric response at the Mouth of the Columbia River entrance and the ODMDS due to anthropogenic and environmental conditions at the Mouth of the Columbia River; (b) monitor selected Mouth of the Columbia River ODMDS locations to observe bathymetric response with respect to dredging disposal operations and the forcing environment; (c) explain qualitatively and quantitatively the rates

(Continued)

15. SUBJECT TERMS
See reverse.

16. SECURITY CLASSIFICATION OF:			17. LIMITATION OF ABSTRACT	18. NUMBER OF PAGES	19a. NAME OF RESPONSIBLE PERSON
a. REPORT	b. ABSTRACT	c. THIS PAGE			19b. TELEPHONE NUMBER *(include area code)*
UNCLASSIFIED	UNCLASSIFIED	UNCLASSIFIED		254	

7. (Concluded)

Coastal and Hydraulics Laboratory
U.S. Army Engineer Research and Development Center
3909 Halls Ferry Road
Vicksburg, MS 39180-6199;
U.S. Army Engineer District, Portland
P. O. Box 2946
Portland, OR 97208-2946;
SonTek, Inc.
6937 Nancy Ridge Drive, No. A
San Diego, CA 92121;
Applied Coastal Research and Engineering, Inc.
766 Falmouth Road, Suite A-1
Mashpee, MA 02649;
O. H. Hinsdale Wave Research Laboratory
Oregon State University
Corvallis, OR 97330

14. (Concluded)

of sediment dispersion at the Mouth of the Columbia River ODMDS, and relate observed sediment dispersion of ODMDS citing and management practice; (d) Assess the suitability of new USACE Dredging Research Program sediment fate models (STFATE, LTFATE, and MDFATE) and RCPWAVE, and synthetically-generated input data from HPDPRE, HPDSIM, and ADCIRC for predicting sediment dispersion in the environment off the Mouth of the Columbia River; and (e) Develop a standardized method for data collection and management that can be used by other Corps District offices using as ODMDS.

The FATE models had previously suffered from a lack of quality field data for their calibration and verification. As the new MCNP data were being acquired and processed, enhancements to the FATE models were incorporated to ensure these models would accurately predict the ultimate disposition of future dredged material disposal at such exceedingly energic locations. Finally, predictive techniques for determining sediment transport processes under both waves and currents were developed to assess the movement of disposed material at the Mouth of the Columbia River for assessing capacity and to determine the useful life of the ODMDS.

The MCNP Mouth of the Columbia River study approach consisted of the execution of four fundamental tasks: (a) a regional coastal processes analysis, (b) oceanographic field data collection and analysis, (c) state-of-the-art numerical modeling, and (d) a comprehensive analysis of sediment transport processes.

15. (Concluded)

Columbia River mouth
Currents
Dredged material disposal
Dredged material FATE models
Dredging
Hazardous waves
Numerical modeling
Ocean dredged material disposal sites (ODMDS)
Ocean data collection
Predictive techniques
Sediment dispersion
Site capacity of ODMDS